THE UNIVERSITY
of EDINBURGH

This thesis has been submitted in fulfilment of the requirements for a postgraduate degree (e.g. PhD, MPhil, DClinPsychol) at the University of Edinburgh. Please note the following terms and conditions of use:

This work is protected by copyright and other intellectual property rights, which are retained by the thesis author, unless otherwise stated.
A copy can be downloaded for personal non-commercial research or study, without prior permission or charge.
This thesis cannot be reproduced or quoted extensively from without first obtaining permission in writing from the author.
The content must not be changed in any way or sold commercially in any format or medium without the formal permission of the author.
When referring to this work, full bibliographic details including the author, title, awarding institution and date of the thesis must be given.

Exploring Mechanisms of Acquired Taxane Resistance in Breast Cancer

Karen Taylor

THE UNIVERSITY *of* EDINBURGH

Doctor of Philosophy

The University of Edinburgh

2021

Declaration

This thesis presents my own work and has not been submitted in fulfilment of any other degree or professional qualification. Where results have been obtained in collaboration with others, I have clearly stated it in the text. Any information derived from the published work of others has been cited in the text, and a complete list of references can be found in the bibliography.

Karen Taylor, 2021

Abstract

Breast cancer is the most commonly diagnosed cancer globally and, despite advances in detection and improved treatment, it remains the leading cause of cancer death among women. Chemotherapy regimens include taxanes in combination, or in sequence, with anthracyclines as first-line treatment with proven survival benefits. However, the development of chemoresistance is a major clinical challenge in the treatment of breast cancer with limited treatment options available thereafter. Identification of mechanisms driving taxane resistance is therefore critical to developing new treatment strategies to improve patient survival. The primary aim of this thesis was to model acquired taxane resistance and identify actionable pathways associated with the progression to a chemoresistant phenotype.

Isogenic models of acquired taxane resistance were developed from the breast cancer cell lines MDA-MB-231 and MCF7 by continuous exposure to either paclitaxel or docetaxel. STR profiling confirmed the parental lineage of the derived taxane resistant isogenic cell lines and assessment of biomarkers by western blotting confirmed retention of the triple negative phenotype of MDA-MB-231. MCF7 25PACR cells exhibited a slight decrease in ERα expression but otherwise retained the protein expression profile of its parent. The resistant cell lines exhibited the ability to proliferate and progress through the cell cycle in the presence of taxanes, unlike the parental cell lines which arrested at the G2/M phase. This was reflected in the absence of apoptosis in the resistant cell lines when exposed to concentrations of taxanes which induced cell death in the parental counterpart. Low level cross resistance was observed to anthracyclines and other commonly used chemotherapeutic agents. Expression of p-gyp protein encoded by MDR1 was assessed by western blotting and shown to be slightly elevated in both MCF7 25PACR and MDA-MB-231 25DOCR cell lines. However knockdown of MDR1 by siRNA did not result in reversion to the same level of taxane sensitivity as observed in the parental cell lines, suggesting other mechanisms are involved in the resistance observed in the isogenic cell lines derived for this study.

To gain insight in to the pathways driving taxane resistance in the cell line models, a multi-omic approach was taken. Targeted exome sequencing of the isogenic taxane resistant cell lines revealed few resistance-associated genomic changes. Transcriptomic analysis of the parental and isogenic taxane resistant cell lies was performed by Nanostring®. Bioinformatic analysis revealed deregulation of the PI3-Akt, MAPK, and transcriptional regulation pathways in the isogenic cell lines, suggesting that inhibition of these pathways may be an effective treatment strategy for taxane resistant breast cancer. RPPA and Western blotting confirmed these findings and a small molecule kinase screen identified several clinically relevant inhibitors with nanomolar potency in the resistant cell line models. The PI3K inhibitors, PIK75 and BKM120, and the CDK inhibitors, dinaciclib and alvocidib, were selected for further investigation via a combination of *in vitro* techniques. Confirmation of their potency against all taxane resistant cell line models was established and combination assays to assess synergy with other chemotherapeutics performed.

Together, these results extend our knowledge of the drivers of taxane resistance in breast cancer and support the use of PI3K and CDK inhibition as candidate therapeutics in taxane resistant breast cancer.

Lay Summary

Breast cancer remains the most common cancer in woman worldwide with an estimated 2.3 million new cases in 2020. Chemotherapy treatment for early breast cancer typically includes the use of taxanes in combination with anthracyclines, along with other drugs targeted to proteins expressed by the tumour cells themselves. Cancer is characterised by a loss of tightly regulated mechanisms where cell division occurs unchecked and results in an abnormal growth of cells to form a tumour. The taxanes (paclitaxel and docetaxel) act by 'arresting' cells at a particular point in the cell cycle which controls division ultimately resulting in cell death. However, approximately 30% of early breast cancer patients' progress to metastatic breast cancer due to the development of drug resistance and treatment options thereafter are limited. To be able to identify new chemotherapy options it is necessary to understand the mechanisms which drive resistance but there are few preclinical models available to facilitate investigation.

In this study models of acquired resistance were established by exposing breast cancer cell lines to increasing doses of taxanes until a population remained that continued to grow even when exposed to high concentrations of the drugs. By developing resistance models in this way, it is possible to compare the sensitive 'parental' cell line with the resistant 'daughter' line to determine what is different between them. Initial investigations concentrated on characterising these novel taxane resistant cell lines. It was found that, unlike the parental lines when treated with taxanes, the resistant cell lines continued to progress through the cell cycle and cell death (apoptosis) did not occur. Although a low level of cross resistance to other commonly used chemotherapy drugs was noted, this was not driven by a protein that regulates multi-drug resistance and it was hypothesised that other mechanisms were responsible.

To identify other mechanisms which might be driving resistance in the model cell lines, comparative gene expression analysis was performed which helped identified disruption of a series of proteins involved in the cell cycle, PI3K-Akt and MAPK

pathways. Alterations in the pathways were confirmed by a variety of proteomic approaches. This suggested that inhibition of these pathways may be effective as targets for novel treatment strategies for taxane resistant breast cancer. A drug screen of inhibitors targeting proteins in these pathways identified compounds which were potently active against the cell cycle and PI3K-Akt pathways. Selected compounds were tested further and found to be equally efficient at inhibiting cell growth and promoting cell death in the resistant 'daughter' cell lines as the sensitive 'parent' cell lines.

In conclusion successful generation of models of taxane resistance in breast cancer cell lines allowed the identification of signalling pathways which are believed to be crucial to the development of chemoresistance. New drugs effective against taxane resistant breast cancer were also identified which may offer promise for patients who no longer respond to first-line treatment options.

Acknowledgements

Firstly, I would like to thank my supervisors, Profs. Charlie Gourley and David Cameron, along with Prof. John Bartlett for their support and guidance throughout my PhD, and for allowing me the opportunity to achieve a long-held goal. Special thanks to Dr Melanie Spears who, although not officially my supervisor, has gone above and beyond, both as a colleague and friend. I am so grateful for the faith you've shown in me, and for your incredible support and enthusiasm throughout this project.

I consider myself extremely lucky to work alongside a great group of colleagues and I would like to thank John, Rich, Becka, Ash, Jan, Tammy, Carrie and Monika for the laughter and conversation. To Alison, Kenny, Jayne and Catherine – thank you for being such wonderful friends and personal cheerleaders. Each of you has contributed to this thesis in ways too many to mention, and I am grateful to you all.

Most importantly, I would like to thank my family. To my Mum and late Dad, thank you for the constant love and support, and always encouraging me to try and achieve my dreams. How I wish you were here to see this Dad; you were right, I could do it. Finally, to the three most important people in my life - Martin, Euan and Calum - thank you for your endless patience and love. I couldn't have done any of this without you.

Contents

Declaration ii

Abstract iii

Lay Summary v

Acknowledgements vii

List of Figures xii

List of Tables xv

1. INTRODUCTION 1

1.1 Overview of cancer 1

1.2 Hallmarks of cancer 1

1.3 Breast cancer 3

1.3.1 Overview 3

1.3.2 UK breast cancer statistics 6

1.3.3 Risk factors 8

1.3.4 Breast cancer histology and subtypes 9

1.3.4.1 Histopathological classification of breast cancer 9

1.3.4.2 Histological grading and staging of breast cancer 10

1.3.5 Molecular classification 12

1.3.5.1 Expression of hormone receptors 12

1.3.5.2 Molecular subtypes 12

1.3.6 Treatment of breast cancer 15

1.3.6.1 Surgery 15

1.3.6.2 Radiotherapy 15

1.3.6.3 Endocrine therapy 16

1.3.6.4 Targeted Therapy 18

1.3.6.5 Chemotherapy 24

1.4 Taxanes in breast cancer 28

1.4.1 Mechanism of action 28
1.4.2 Taxane chemoresistance 29
1.4.2.1 Drug efflux 29
1.4.2.2 Drug metabolism 30
1.4.2.3 Alteration of microtubule associated proteins 30
1.4.2.4 Alterations in apoptosis, cell cycle and signalling pathways 32
1.5 Overview and aims of this thesis 33
2. MATERIALS AND METHODS 35
2.1 Materials 35
2.1.1 Common Buffers and Reagents 35
2.1.2 Compounds 36
2.1.3 Antibodies 38
2.2 Methods 40
2.2.1 Cell culture 40
2.2.1.1 Cell culture maintenance 40
2.2.1.2 Cell line authentication 41
2.2.1.3 Cell harvesting and counting 42
2.2.1.4 Cryopreservation and recovery from liquid nitrogen storage 42
2.2.2 Generation of taxane resistant isogenic cell lines 43
2.2.3 Cell doubling times 44
2.2.4 Cell viability assays 44
2.2.5 Small Molecule Kinase Screen 45
2.2.6 Drug combination synergy assays 51
2.2.7 Cell cycle assays 52
2.2.8 Apoptosis and cell death assays 53
2.2.9 Transient transfection of small interfering RNA (siRNA) 53
2.2.10 Nucleic Acid Analysis 54
2.2.10.1 DNA Extraction 54

2.2.10.2 RNA Extraction 55
2.2.10.3 Mutational Profiling of cell lines by MSK-IMPACT 56
2.2.10.4 Nanostring Gene Expression 56
2.2.11 Protein Methods 59
2.2.11.1 Protein lysate preparation 59
2.2.11.2 SDS-Polyacrylamide Gels and Western Blotting 60
2.2.11.3 Reverse Phase Protein Array 62
2.2.12 Data Analysis 73
3. GENERATION AND CHARACTERISATION OF ISOGENIC CELL LINE MODELS WITH ACQUIRED RESISTANCE TO TAXANES 75
3.1 Introduction 75
3.2 Results 76
3.2.1 Sensitivity of breast cancer cell lines to taxanes 76
3.2.2 Establishment of taxane resistant cell lines 77
3.2.3 STR profiling of taxane resistant cell lines confirms parental lineage 81
3.2.4 Confirmation of taxane resistance 84
3.2.5 Expression of common breast cancer biomarkers 89
3.2.6 Stability of acquired taxane resistance in isogenic cell lines. 91
3.2.7 Cellular proliferation and doubling rates of taxane resistant cell lines 92
3.2.8 Effects of resistance on the cell cycle 95
3.2.9 Cell death and apoptosis 97
3.2.10 MDR does not drive the chemoresistant phenotype of the taxane resistant isogenic cell lines 101
3.3 Discussion 104
4. THE EFFECT OF TAXANE RESISTANCE UPON DOWNSTREAM SIGNALLING IN BREAST CANCER CELL LINES 109
4.1 Introduction 109

4.2 Results 110
4.2.1 Proteomic analysis by Reverse Phase Protein Array (RPPA)..... 110
4.2.2 Targeted exome sequencing of the isogenic taxane-resistant cell lines 118
4.2.3 Transcriptomic profiling of taxane resistant cell lines using Nanostring® technology..... 134
4.2.4 Validation of the dysregulated pathways as identified by RPPA and Nanostring..... 153
4.3 Discussion..... 155
5. IDENTIFICATION OF SMALL MOLECULE KINASE INHIBITORS TARGETING DYSREGULATED TAXANE RESISTANCE ASSOCIATED PATHWAYS 162
5.1 Introduction 162
5.2 Results 164
5.2.1 OICR Small Molecule Kinase Screen..... 164
5.2.2 Validation of small molecule kinase hits..... 170
5.2.2.1 PI3K inhibitors 171
5.2.2.1 Validation of CDK Inhibitors..... 177
5.2.3 Dinaciclib induces deregulation of the cell cycle 179
5.2.4 Assessment of combinatorial effect of dinaciclib with select chemotherapy agents..... 184
5.3 Discussion..... 187
6. DISCUSSION AND CONCLUSION 192
6.1 Introduction 192
6.2 Summary of findings 193
6.3 Future studies..... 196
6.4 Conclusion 199

List of Figures

Figure 1.1: Hallmarks of Cancer 2
Figure 1.2: Global incidence and mortality rates of different cancer types 5
Figure 1.3: UK breast cancer incidence and mortality. 7
Figure 1.4: Schematic representation of the Class I PI3K-Akt pathway. 20
Figure 1.5: Simplified diagram of eukaryotic cell cycle. 23
Figure 2.1: Combination matrix layout for assessment of synergistic drug activity. . 51
Figure 2.2: Summary of Nanostring nCounter® technology 57
Figure 3.1: Half maximum inhibitory concentrations (IC50) for docetaxel and paclitaxel of parental breast cancer cell lines. 77
Figure 3.2: Development of taxane resistant isogenic breast cancer cell lines 78
Figure 3.3: Representative phase contrast images of native and taxane resistant isogenic cell lines 80
Figure 3.4: Half maximum inhibitory concentrations (IC50) for docetaxel and paclitaxel of taxane resistant isogenic cell line series 85
Figure 3.5: Common biomarker expression is largely unchanged in taxane resistant isogenic cell lines compared to the native parental cell line. 90
Figure 3.6: Half maximum inhibitory concentrations (IC50) for docetaxel and paclitaxel of (A) MDA-MB-231 25DOCR and (B) MCF7 25PACR after taxane withdrawal 92
Figure 3.7: Representative phase contrast and masked images from the Incucyte® Zoom 93
Figure 3.8: Doubling times of native and isogenic taxane resistant cell lines 94
Figure 3.9: Cell cycle distribution in MDA-MB231 and MCF7 parental and resistant isogenic cell lines upon exposure to 25 nM paclitaxel or docetaxel. 97
Figure 3.10: Taxane resistant MDA-MB-231 isogenic cell lines reduces the apoptotic response to (A) paclitaxel and (B) docetaxel. reagent 99
Figure 3.11: Fold change induction of apoptosis upon taxane treatment. 100

Figure 3.12: Expression of P-gp in the isogenic taxane resistant cell lines and sensitive native parental cell lines.. 102
Figure 3.13: Half maximum inhibitory concentrations (IC50) for docetaxel and paclitaxel of MDA-MB-231 25DOCR and MCF7 25PACR after MDR1 knockdown by siRNA transient transfection. 103
Figure 4.1: Hierarchical clustering analysis of changes in protein and phosphoprotein levels upon acquirement of taxane resistance. 113
Figure 4.2: Functional annotation analysis of differentially expressed proteins identified via comparison of MDA-MB-231 25PACR and parental MDA-MB-231... 114
Figure 4.3: Reverse Protein Phase Array (RPPA) analysis results.. 115
Figure 4.4: Schematic representation of pathway changes identified by RPPA..... 118
Figure 4.5: Copy number alterations in taxane resistant isogenic cell lines..... 121
Figure 4.6: Summary of observed gene mutations in the taxane resistant isogenic cell line series 122
Figure 4.7: Functional interaction network of mutated genes identified by MSK-IMPACT analysis of MDA-MB-231 and MCF7 taxane resistant cell line models. 123
Figure 4.8: Expression of cancer associated pathway mRNAs are altered in taxane resistant cell lines compared to native parental lines.. 135
Figure 4.9: Differential gene expression associated with taxane resistance..... 138
Figure 4.10: Supervised hierarchical clustering of genes from the Nanostring PanCancer Pathway codeset in taxane resistant isogenic cell lines 139
Figure 4.11; Enrichment analysis of DEGs from both MDA-MB-231 taxane resistant cell line models..... 142
Figure 4.12: Enrichment analysis of DEGs from MCF7 25PACR taxane resistant cell line model. Functional interaction (FI) networks for 161 target genes was visualised using Cytosape Reacomte FIViz.. 147
Figure 4.13: Enrichment analysis of commonly dysregulated taxane resistance associated DEGs from Nanostring PanCancer pathway code set. 152
Figure 4.14: EGFR and PI3K-Akt signalling pathway proteins in MCF7 and MDA-MB-231 parental and taxane resistant isogenic cell lines. 154

Figure 5.1: Small molecule kinase inhibitors of the PI3K-Akt pathway and cell cycle selected for screen 164
Figure 5.2: Dose response curves for small molecule kinase screen compounds with potency of <5 µM in MDA-MB-231 taxane resistant cells 167
Figure 5.3: Half maximum inhibitory concentrations (IC50) for selected PI3K inhibitors. 172
Figure 5.4: Unsupervised hierarchical clustering of changes in protein and phosphoproteins associated with BKM120 treatment 175
Figure 5.5: Western blot analysis of PI3-Akt pathway associated proteins and phoshoproteins in MDA-MB-231 and MDA-MB-231 25PACR cells treated with BKM120 176
Figure 5.6: Half maximum inhibitory concentrations (IC50) for selected CDK inhibitors 178
Figure 5.7: Dinaciclib induces caspase 3/7 activity in the MDA-MB-231 isogenic cell lines 180
Figure 5.8: Cell cycle distribution in (A) MDA-MB-231 parental, (B) MDA-MB-231 25PACR (C) MDA-MB-231 25DOCR (D) MCF7 parental and (E) MCF7 25PACR upon exposure to dinaciclib. 181
Figure 5.9: Assessment of downstream targets of dinaciclib. 183
Figure 5.10: Combination of taxanes and dinaciclib induce an additive effect which reduces cell viability 185
Figure 5.11: Combination of epirubicin and dinaciclib induce an additive effect in MDA-MB-231 taxane resistant cell lines and synergy in MCF7 25PACR. 186

List of Tables

Table 1.1: Simplified description of TNM staging 11
Table 1.2: Molecular subtypes of invasive ductal carcinoma 13
Table 2.1: Common buffers and reagents 35
Table 2.2: Chemotherapy and small molecule kinase compounds 37
Table 2.3: Antibody list 38
Table 2.4: Human breast cancer cell lines used in this study 41
Table 2.5: Inhibitors and targets of small molecule kinase screen 46
Table 2.6: Volumes of solutions required for two mini-Protean SDS-PAGE 61
Table 2.7: Primary antibodies used for RPPA 64
Table 3.1: STR profile analysis of MDA-MB-231 and MCF7 isogenic cell lines. 81
Table 3.2: Summary of IC50 values of taxanes for all parental and isogenic resistant cell line models 86
Table 3.3: Summary of IC50 values of chemotherapeutic agents in the isogenic breast cancer cell line models. 88
Table 3.4: Cell doubling times of native and taxane resistant cell lines 95
Table 4.1: MSK-Impact™ assay for human cancer genes for MDA-MB-231 parental and isogenic taxane resistant cell lines 124
Table 4.2: MSK-Impact™ assay for human cancer genes for MCF7 parental and MCF7 25PACR taxane resistant cell lines 130
Table 4.3: Differentially expressed genes from PanCancer Pathway codeset in taxane resistant cell lines 137
Table 4.4: List of the common statistically significant differentially expressed genes derived from the Nanostring PanCancer Pathway codeset in the taxane resistant cell lines. 149
Table 5.1: Small molecule kinase inhibitors with activity against MDA-MB-231 taxane resistant isogenic cell line series of <5 μM. 168

Table 5.2: Half-maximal inhibitory concentration (IC50) values of selected PI3K inhibitors 173
Table 5.3: Half-maximal inhibitory concentration (IC50) values of selected CDK inhibitors 179

Abbreviations

5-FU	5-Fluorouracil
ABC	ATP-binding cassette
AI	Aromatase inhibitor
AMPS	Ammonium persulphate
ANOVA	Analysis of variance
BAD	BCL2-associated death promoter
BAK	BCL2 antagonist/killer
BAX	BCL2-associated X
BCA	Bicinchoninic acid
BCS	Breast conserving surgery
BCL2	B-cell lymphoma 2
BCL-XL	BCL -extra large
BIM	BCL2-like protein 11
BRCA	Breast cancer type 1 susceptibility protein
BSA	Bovine serum albumin
CCK8	Cell counting kit-8
CCN	Cyclin
CDC	Cell division cycle-associated protein
CDK	Cyclin dependent kinase
CST	Cell Signalling Technology
CYP3A4	Cytochrome P450 enzyme
DAVID	Database for Annotation, Visualisation and Integrated Discovery
DCIS	Ductal carcinoma in situ
DMEM	Dulbecco's Modified Eagle's Medium
DMSO	Dimethyl sulfoxide
EDTA	Ethyl Diamine Tetra Acetic Acid
EGFR	Epidermal Growth Factor Receptor
EMT	Epithelial to mesenchymal transition
ER	Oestrogen Receptor
FAK	Focal adhesion kinase
FCS	Foetal calf serum
FISH	Fluorescent in situ hybridisation
GAPDH	Glyceraldehyde-3-phosphodehydrogenase
GO	Gene ontology
HIF	Hypoxia-inducible factor
HK	Hexokinase
HR-	Hormone receptor
HER	Human Epidermal Growth Factor
IHC	Immunohistochemistry
IDC	Invasive ductal carcinoma

ILC	Invasive lobular carcinoma
MAP	Microtubule associated protein
MAPK	Mitogen activated protein kinase
MDR	Multidrug resistance
mTOR	Mammalian targe of rapamycin
NF-κB	Nuclear factor kappa B
PBS	Phosphate buffered saline
PDX	Patient derived xenograft
P-gp	P glycoprotein
PI3K	PI3 kinase
PKC	Protein kinase C
PKM	Pyruvate kinase isoenzyme
PLK	Polo-like kinase
PR	Progesterone receptor
PTEN	Phosphatase and Tensin Homologue
RFI	Relative fluorescence intensity
RIPA	Radioimmunoprecipitation assay
RPPA	Reverse phase protein array
RTK	Receptor tyrosine kinase
SAC	Spindle assembly checkpoint
SDS	Sodium dodecyl sulphate
SDS-PAGE	SDS- polyacrylamide gel electrophoresis
SEM-	Standard error of the mean
SERD	Selective oestrogen receptor down-regulators
STAT3	Signal transducer and activator of transcription 3
STR	Short tandem repeat
TEMED	Tetramethylethylenediamine
TNBC	Triple negative breast cancer
XIAP	X linked inhibitor of apoptosis
WHO	World Health Organisation

1. INTRODUCTION

1.1 Overview of cancer

Cancer remains among the leading causes of death worldwide, with approximately 19.3 million new cancer cases diagnosed globally in 2020 and 10 million cancer-associated deaths. By 2040, the global cancer burden is predicted to grow to almost 28 million new cancer cases, simply due to an aging and growing worldwide population (1). This is likely to grow further due to increases in the prevalence of risk factors associated with cancer.

The term 'cancer' encompasses a large heterogeneous group of diseases characterised by uncontrolled cell proliferation and the ability to invade other tissues. Cell division in a healthy cell is tightly controlled by a number of regulatory mechanisms. However, these are bypassed by cancer cells resulting in aberrant growth and division of cells. In solid cancers this leads to the formation of a primary mass, and disseminated disease throughout the body (2).

1.2 Hallmarks of cancer

Cancer represents a diverse collection of diseases. More than 100 different cancer types have been identified, of which many have additional subtypes. Intra-tumour heterogeneity adds further complexity to the landscape of tumorigenesis. In an effort to rationalise the complexity of neoplastic disease, Hanahan and Weinberg proposed the 'Hallmarks of Cancer' to describe essential cellular events acquired by all cancer cells which enable tumour development (3).

These ‘hallmarks’ include self-sufficiency in growth signals, insensitivity to growth suppressors, evasion of apoptosis, limitless replicative potential, increased angiogenesis and tissue invasion and metastasis. This landmark review was later updated to include reprogramming of energy metabolism and evasion of immune system destruction. The acquisition of the hallmarks rely on two enabling characteristics: genome instability and mutation which drive tumour formation and, tumour promoting inflammation which enables tumour progression (4) (Figure 1.1). Together these factors describe a critical framework for how cancer cells survive, proliferate and invade.

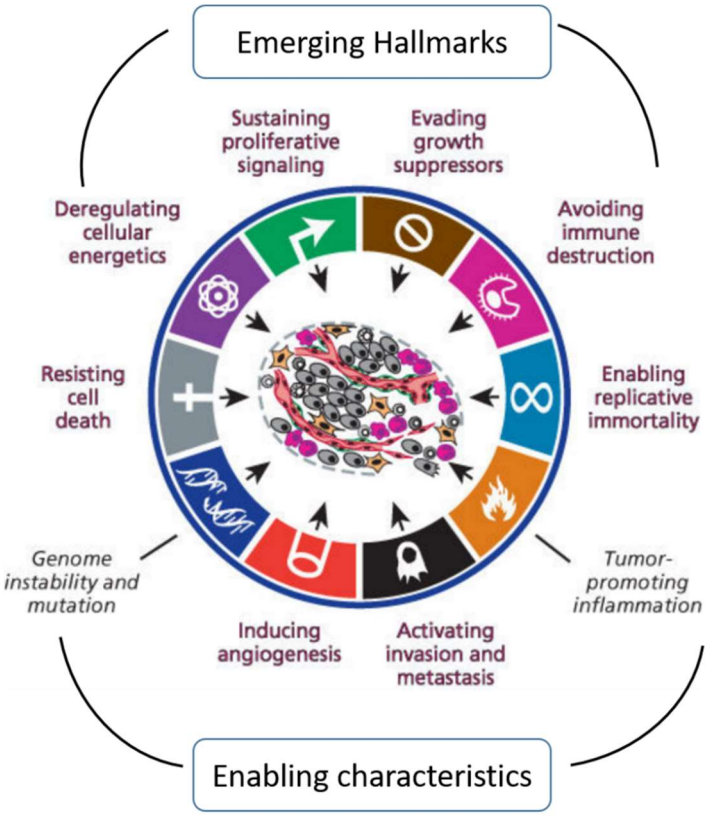

Figure 1.1: Hallmarks of Cancer. Illustration of the defining ‘Hallmarks of cancer as defined by Hanahan and Weinberg (2011)

The development and progression of cancer is influenced by genetics and environmental factors. However it is generally believed that tumorigenesis is a multistep process which is initiated by the accumulation of a succession of genetic changes which alter the genome, leading to the eventual transformation of normal cells into malignant ones (3, 5, 6). The accrual of somatic, germline or epigenetic mutations are a result of the inability of cells to maintain DNA integrity. Contributing factors of DNA instability include environmental exposure, such as from tobacco smoke or UV radiation, viruses such as HPV, and changes to normal DNA replication which become more common with aging. Mutations in cell cycle checkpoint and DNA repair genes cause damage to accumulate, accelerating tumorigenesis (7). The sequential development of mutations alters fundamental regulatory mechanisms of the cell resulting in a malignant phenotype, while also rewiring their microenvironment to sustain tumorigenesis (8).

1.3 Breast cancer

1.3.1 Overview

In 2020 it was reported that breast cancer had surpassed lung cancer as the most commonly diagnosed cancer globally, with an estimated 2.3 million cases worldwide (Figure 1.2A) and represents the 5th leading cause of cancer mortality (Figure 1.2B). It remains the most common cancer in women (Figure 1.2C) and, despite advances in early detection and treatment, the leading cause of death in females (Figure 1.2D) (1, 9).

A

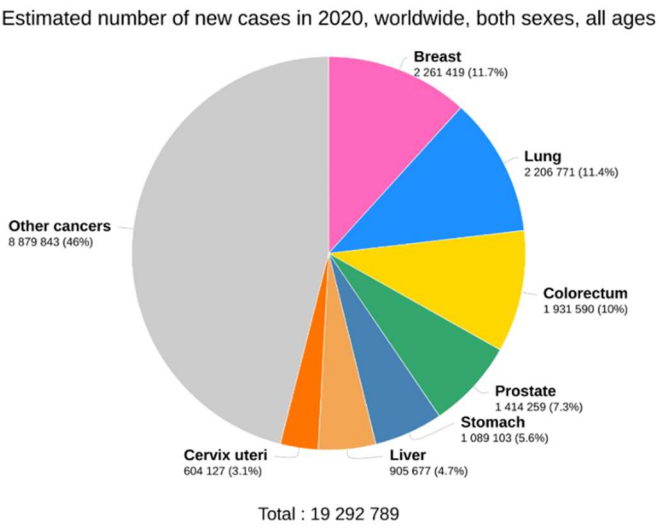
Estimated number of new cases in 2020, worldwide, both sexes, all ages
Breast
2 261 419 (11.7%)
Lung
2 206 771 (11.4%)
Colorectum
1 931 590 (10%)
Prostate
1 414 259 (7.3%)
Stomach
1 089 103 (5.6%)
Liver
905 677 (4.7%)
Cervix uteri
604 127 (3.1%)
Other cancers
8 879 843 (46%)
Total : 19 292 789

B

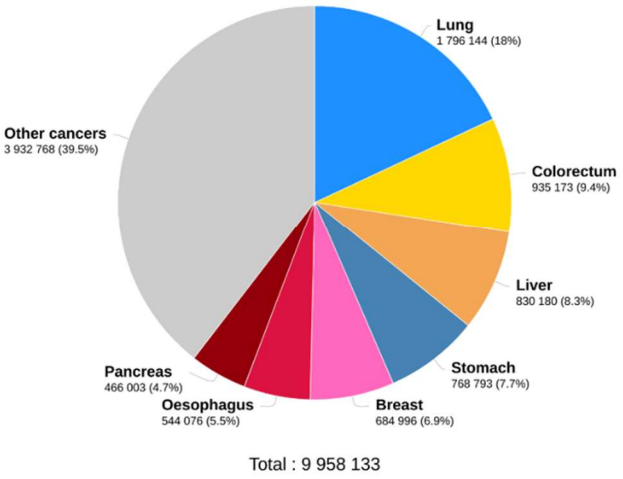
Estimated number of deaths in 2020, worldwide, both sexes, all ages
Lung
1 796 144 (18%)
Colorectum
935 173 (9.4%)
Liver
830 180 (8.3%)
Stomach
768 793 (7.7%)
Breast
684 996 (6.9%)
Oesophagus
544 076 (5.5%)
Pancreas
466 003 (4.7%)
Other cancers
3 932 768 (39.5%)
Total : 9 958 133

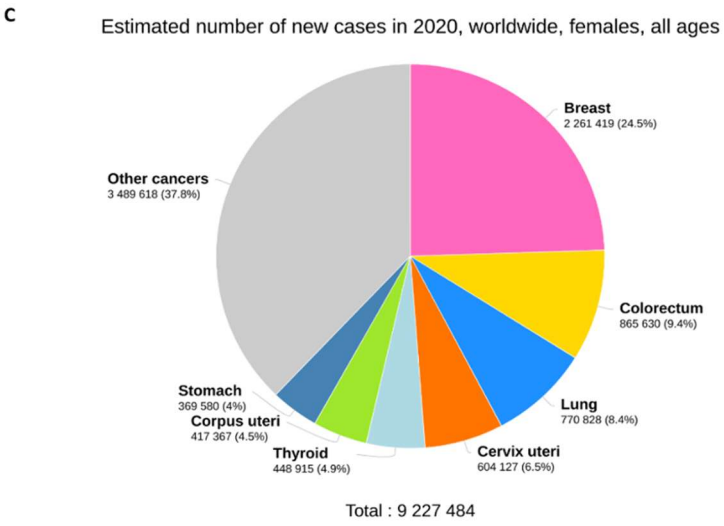

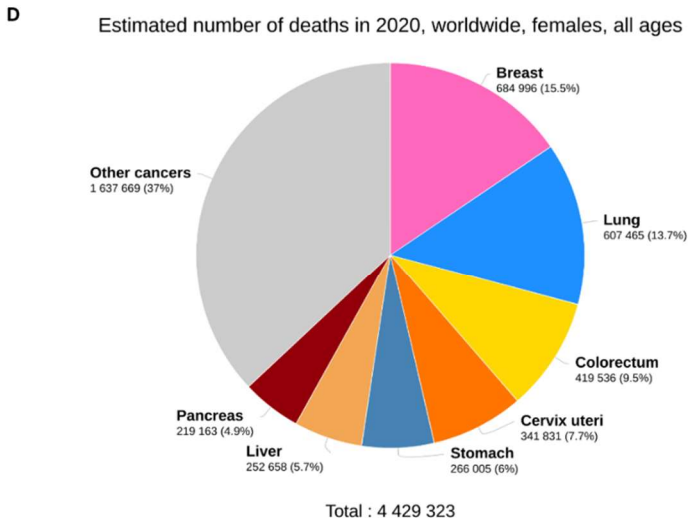

Figure 1.2: Global incidence and mortality rates of different cancer types: (A) and (B) for both sexes and (C) and (D) for females, according to WHO reports 2020 (1)

1.3.2 UK breast cancer statistics

In the UK, breast cancer accounts for approximately 25% of all diagnosed cancers in women, with an estimate of almost 55,000 new cases in 2020 (Figure 1.3A), and is the second leading cause of cancer death (10). Due to advances in treatments and effective screening programmes, the mortality rate of patients with breast cancer under the age of 70 has declined steadily over the last 30 years (11). However, the incidence of breast cancer has continued to rise (Figure 1.3) (12). This increase may in part be due to earlier diagnosis as a result of improved surveillance in women invited for breast cancer screening, but also the positive effects of improved treatments on patient survival.

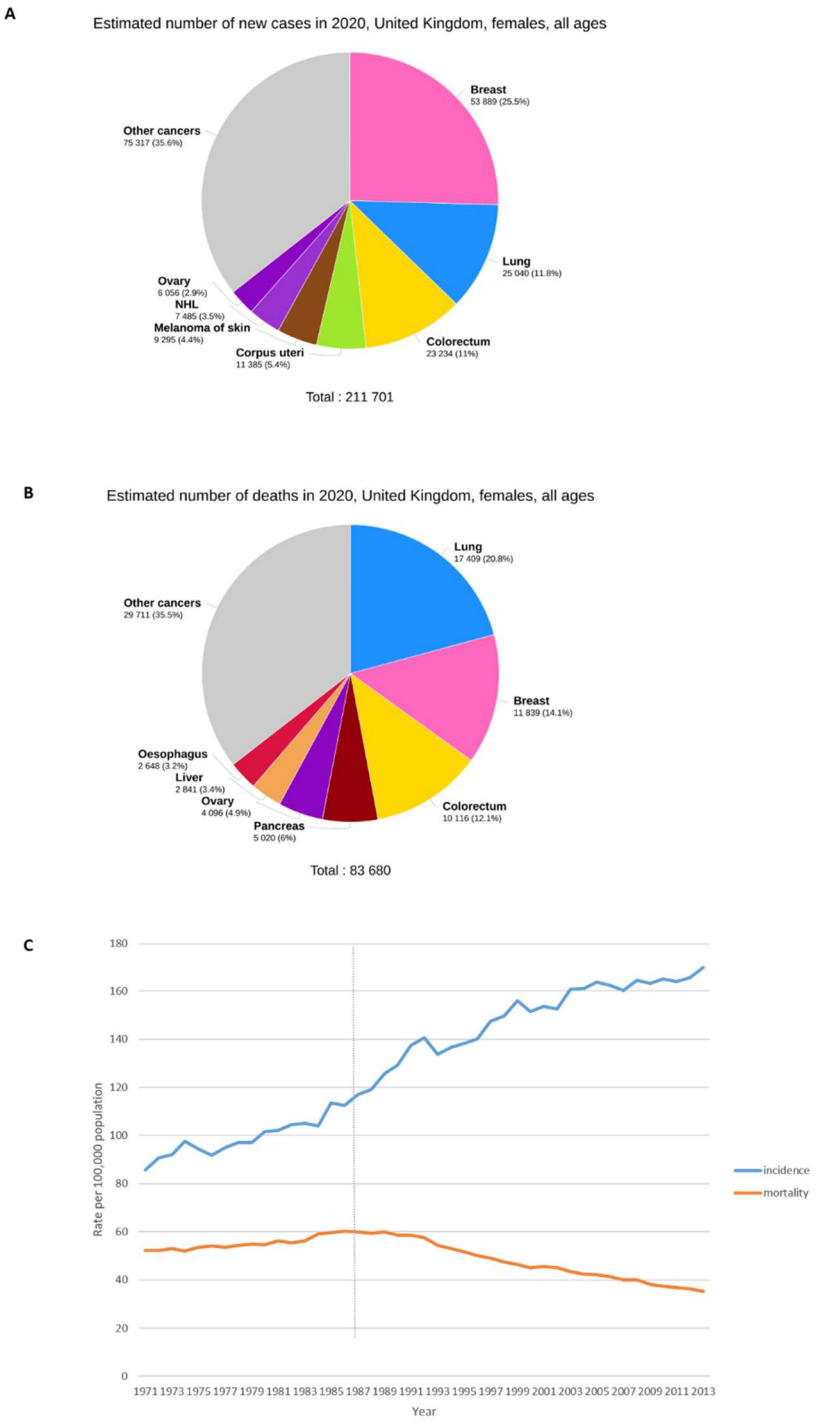

Figure 1.3: UK breast cancer incidence and mortality. Pie charts representing the UK (A) incidence and (B) mortality rates of the most common cancer types in females. Source: GLOBOCAN, 2020.(1) (C) Graph illustrating the decrease in mortality rate and increase in incidence rate of breast cancer in the last 4 decades in the UK. Dotted vertical line represents the introduction of the breast cancer screening program in 1987. Source: Office for National Statistics.

1.3.3 Risk factors

A number of factors can contribute to the development of breast cancer. The two greatest risk factors for breast cancer are non-modifiable; gender and age. Breast cancer can occur in both men and women. However, in men, breast cancer is considered a rare disease and accounts for less than 1% of all diagnosed cases. The comparative lifetime risk of developing breast cancer for men is less than 1 in 1000 compared to 1 in 7 for women (10).

The close association between risk of developing breast cancer and age has long been acknowledged, with the highest incident rate in older people. Approximately 24% of all new cases in the UK are in those aged 75 and over. Age-specific incidence rises steadily from the age of 25 and effectively doubles every 10 years until menopause when it starts to slow (13). The highest incidence of new cases is detected in women aged 65-69 years (10).

A strong family history of breast cancer also increases the risk of developing the disease. The risk is approximately doubled in women with a first-degree relative with breast cancer, and increases still with a larger number of affected first-degree relatives (14, 15). The majority of hereditary breast cancer cases are associated with mutations in breast cancer type 1 susceptibility protein (BRCA1) and breast cancer susceptibility protein 2 (BRCA2) (16, 17). Women with a BRCA1 or BRCA2 mutation have a 45-65% risk of developing breast cancer before they are 70 years old (18).

Finally, as with most cancers, the impact of what can be termed as modifiable risk – smoking, alcohol consumption, and sedentary lifestyle – is significant, with 23% of cases attributed to lifestyle and environmental factors (19).

1.3.4 Breast cancer histology and subtypes

Breast cancer is a highly heterogeneous disease, with distinctive clinical presentation, histopathological and molecular features, therapeutic response, and outcomes. This heterogeneity is observed both between tumours (intertumoral) and within the same tumour (intratumoral). Classification systems of breast cancer have been developed which aid diagnosis and inform treatment choices for patients. Broadly, breast cancer is classified according to histopathology, which defines type and grade, and molecular classification, based on expression of cellular markers.

1.3.4.1 Histopathological classification of breast cancer

Breast cancer tumours originate from the epithelia lining of the mammary gland cells and present with a range of clinical, biological and morphological characteristics (20, 21). The World Health Organisation (WHO) classification defines 21 distinct histological subtypes on the basis of cell morphology and patterns of growth (22). Breast cancer can be broadly categorised as either *in situ* carcinoma (stage 0, pre-cancer) or invasive carcinoma (stages I-IV). The most common subtype of *in situ* carcinoma is ductal carcinoma *in situ* (DCIS) which accounts for approximately 90% of all stage 0 cases diagnosed (23). An increase in diagnosis of *in situ* carcinomas in recent years, particularly in pre-menopausal women, is likely a result of improved screening strategies. While classified as stage 0 disease, DCIS are considered as pre-malignant and have an associated 2 to 8-fold increased risk of developing invasive breast cancer(24-26).

Invasive carcinoma is the most common type of breast cancer. It is highly heterogeneous group of tumours and can be subdivided in to 7 different histological groups: invasive ductal carcinoma (IDC), invasive lobular carcinoma (ILC), ductal/lobular, tubular, mucinous (colloid), medullary and papillary carcinomas. Of these the most common histological type is invasive ductal carcinoma of no special type (IDC-NST), which accounts for between 70-80% of all cases, followed by ILC with

10-15% of cases (10, 27-29). IDC is a diagnosis of exclusion referring to those tumours which lack specific differentiating morphological or cytological features necessary to classify the tumour as a special type. IDC may be further classified as well-differentiated (grade 1), moderately differentiated (grade 2) and poorly differentiated (grade 3) (30).

1.3.4.2 Histological grading and staging of breast cancer

All breast cancers are traditionally graded according to histological grade which is reported using the "Bloom Richardson Scale" or "Nottingham Scale" histological system (31, 32). First developed in the 1950s by Bloom and Richardson, the grading system considers nuclear pleomorphism, glandular/tubular formation and mitotic index. Each factor is graded between 1 and 3 and added to obtain an overall grade: non-tumour (score <3), grade 1 (score 3-5), grade 2 (score 6-7) or grade 3 (score 8-9). Tumours with high grades are typically poorly differentiated and indicate advanced disease and poor prognosis.

Once breast cancer is diagnosed, it is important that the cancer is staged to define how advanced the disease is and inform treatment strategies. Staging of breast cancer is based on a system known as TNM classification (Table 1.1) which takes into account tumour size (T), invasion of lymph nodes (N) and presence of metastasis (M). These scores can be combined to assign an overall stage of disease from stage 0 (in situ), through stage I (early cancer) to stage IV (advanced, metastatic cancer which has spread to other parts of the body) (33, 34) .

Table 1.1: Simplified description of TNM staging

Tumour size (T)	**Tx**	**Primary tumour cannot be assessed**
	T0	No evidence of tumour
	Tis	Carcinoma in situ
	T1-T4	Size of the tumour
Invasion of lymph nodes (N)	Nx	Regional lymph nodes cannot be assessed
	N0	No regional lymph node involvement
	N1-N3	Involvement of regional lymph nodes (score based on number of nodes involved)
Metastasis (M)	M0	No distant metastasis
	M1	Distant metastasis

1.3.5 Molecular classification

Increasingly molecular biomarkers have been employed as valuable tools for breast cancer classification. Together with grading, staging and histological subtyping, the hormone receptor status of a breast cancer can be used to guide targeted therapeutic strategies for the treatment of patients (12, 30, 35).

1.3.5.1 Expression of hormone receptors

Following a diagnosis of breast cancer, the expression of the nuclear receptors, oestrogen receptor α (ERα) and progesterone receptor (PR), and of human epidermal growth factor receptor 2 (HER2) which is expressed on the cell membrane, are determined by immunohistochemical (IHC) assessment. The expression levels of ERα and PR are assessed using the Allred score, which accounts for the abundance and intensity of positively stained cells (36). A scoring system ranging from 0 to 3+ is applied to assess HER2 expression by IHC. For those cases where a score of 2+ is recorded, further assessment of HER2 gene copy number by fluorescent *in situ* hybridisation (FISH) is performed (37-39).

1.3.5.2 Molecular subtypes

Breast cancers exhibit a wide degree of heterogeneity and diversity at both a morphological and molecular level. Advances in molecular profiling based on transcriptomic profiling have furthered our understanding of the genes and pathways involved with breast cancer development and progression. A pivotal study by Perou *et al* (40) compared the heterogeneity of a cohort of breast cancers by gene expression analysis. This led to the identification of four distinct intrinsic subtypes which corresponded with clinical outcomes, namely luminal, basal-like, normal-like and HER2 enriched. Follow up studies further refined the subtypes resulting in the molecular characterisation of five intrinsic breast cancer subtypes which are defined

in Table 1.2 (41, 42). These studies were the first to provide evidence of heterogeneity within ER+ tumours and suggested at least two subtypes of luminal breast cancer. More recently an additional subtype named claudin-low has been described which has a similar profile to basal/TNBC but characterised by enrichment of epithelial to mesenchymal (EMT) markers, immune response genes and cancer stem cell-like features (43, 44).

Table 1.2: Molecular subtypes of invasive ductal carcinoma

Subtype	**Protein Expression Profile**
Luminal A	ER+ and/or PR+, HER2-, $Ki67^{low}$
Luminal B	ER^{low} and/or PR+, HER2+/-, $Ki67^{high}$
Basal/Triple negative (TNBC)	ER-, PR-, HER2-; basal cytokeratins and EGFR
Claudin-low	ER-, PR-, HER2-; low Claudin 3, 4 and 7, E-cadherin
HER2	ER-, PR- HER2+
Normal-like (similar to normal breast tissue)	ER+/-, PR-, HER2-

Luminal tumours are ER+ and/or PR+ and can be further subdivided into luminal A and luminal B depending on expression of the proliferation marker, Ki67. Luminal A tumours represent the most commonly diagnosed subgroup of breast cancers, and have a better prognosis presenting at a lower stage compared to luminal B tumours.

HER2 tumours are characterised by amplification of HER2 and account for approximately 15-30% of all breast cancers (45). HER2 is a member of the Epidermal Growth Factor Receptor (EGFR) family, and is an important component of cell signalling pathways, driving pathways such as mitogen-activated protein kinase (MAPK), and phosphatidylinositol-4,5-bisphosphate 3-kinase (PI3K) which play pivotal roles in the activation of cell proliferation, migration and invasion (46).

TNBC account for 10-20% of all breast cancers (47). It is a highly heterogeneous group of tumours that can be classified into distinct molecular subtypes by further gene expression stratification (48, 49). They do not express ER, PR or HER2 and present as highly aggressive tumours, with a poor prognosis and higher incidence in young women (50, 51). Loss of function mutations in TP53 and gain of function mutations in the PI3K signalling pathways are common in TNBC and thought to contribute to this aggressive phenotype (52, 53). Alterations in MAPK signalling genes and cell-cycle regulators are also frequently observed. Due to the lack of classically targeted receptors TNBC do not respond to commonly used treatments such as endocrine therapy or HER2 targeted treatment. Systemic chemotherapy remains the most effective treatment for TNBC. However, despite initially responding well to treatment, TNBC has a high rate of metastasis and distant recurrence or death compared to other breast cancer subtypes (54, 55).

The molecular stratification of breast cancers has now been translated in to the clinical setting with the design of gene-expression diagnostic tests. Tests such as EndoPredict (56), OncotypeDX (57), MammaPrint (58) and Prosignia (59) have been developed based on a minimised gene set with the purpose of predicting risk of recurrence and relative response to chemotherapy in patients with early breast cancer. The results from the tests are used along with other clinical risk factors, such as nodal status and tumour size, to predict the risk of disease recurrence and aid decision making about adjuvant chemotherapy use.

1.3.6 Treatment of breast cancer

Breast cancer is a heterogeneous disease with specific properties. The molecular and histopathological classification of breast cancer is therefore critical for determining prognosis and selecting appropriate treatment strategies for patients following diagnosis. Therapeutic strategies typically include a combination of treatments and may include surgery, radiotherapy, endocrine therapy and targeted biological therapy.

1.3.6.1 Surgery

Surgery, with or without radiotherapy, remains the mainstay of early breast cancer treatment. Most women with stage I, II or III breast cancer are offered surgery, with the intention of achieving local control, preventing locoregional recurrence and improving survival. Surgery may be performed to remove only part of the breast tissue (lumpectomy or breast conservation surgery (BCS)) or the whole breast (mastectomy) (60, 61). The choice of surgery approach depends on tumour size or evidence of metastasis. Preoperative or neoadjuvant chemotherapy is offered in cases where the tumour size exceeds that recommended for BCS to allow subsequent surgery (62). Patients who have presented as lymph node positive will also have their affected lymph nodes surgically removed (63). Women with a high susceptibility to developing breast cancer due to germline BRCA1/2 mutations or a strong family history are offered preventative prophylactic mastectomy, significantly reducing the risk of developing disease (64).

1.3.6.2 Radiotherapy

Radiotherapy is widely used for the management of breast cancer typically in the adjuvant setting after lumpectomy or mastectomy in an effort to reduce local recurrence (65). The most common method for radiotherapy delivery is via external

beam radiation. The ionising radiation, given in focused beams to the site of the tumour mass, targets rapidly dividing cancer cells which are particularly sensitive to radiotherapy. Successful radiotherapy causes DNA damage to such an extent that cells are unable to undergo DNA repair resulting in cell death by apoptosis (66).

Adjuvant radiotherapy to reduce local recurrence is the standard of care after BCS for the majority of early breast cancer patients and has been shown to reduce the risk of recurrence and mortality (67-69). Radiation therapy may also be given in a neoadjuvant setting, along with chemotherapy, to reduce tumour size prior to surgery, or to control symptoms in cases of terminal cancer.

1.3.6.3 Endocrine therapy

Oestrogen and progesterone play an important role in the development and progression of breast cancer and are primary regulators of breast tissue growth and differentiation (70). They induce their cellular effects by binding to and activating their respective nuclear receptors, ER and PR (71). Activation of the receptors on breast cancer cells can promote cell proliferation, while also inhibiting apoptosis by regulating expression of key molecules controlling the cell cycle, such as c-myc and cyclin D1 (72, 73). As the majority of breast cancers are ER+ and hormone dependent, anti-endocrine therapies have become some of the most powerful tools currently available for their treatment in the adjuvant and metastatic setting. Effective disruption of oestrogenic signalling can be achieved through direct inhibition of the oestrogen receptor or by inhibiting the production of oestrogen or progesterone (73).

1.3.6.3.1 SERMs and SERDs

Selective oestrogen receptor modulators (SERM) such as tamoxifen and raloxifene, act by competitively binding to ER, and inducing down-regulation of the transcription of oestrogen-regulated genes (74-76). Tamoxifen is widely used to treat both early

and late-stage breast cancer in pre- and post-menopausal ER+ women (77). Use of tamoxifen in the adjuvant setting for 5 years confers a reduction in relative risk and mortality, with benefits still present up to 15 years after diagnosis (78, 79). Two recent studies have shown further benefit of extending tamoxifen use to 10 years. The aTTom and ATLAS trials compared 10 years of adjuvant tamoxifen to 5 years and showed an absolute reduction of recurrence by 3.7% and mortality by 2.8% with extended use (80, 81). Selective oestrogen receptor down-regulators (SERDS), such as fulvestrant, are a similar class of endocrine therapy used to treat hormone receptor positive metastatic breast cancer. Fulvestrant acts by downregulating and degrading ER through competitive binding to ER dimers (82).

1.3.6.3.2 Aromatase inhibitors

Aromatase inhibitors act by inhibiting the oestrogen biosynthesis, specifically the conversion by aromatase of androgen precursors into oestrone or oestradiol (83). The use of aromatase inhibitors, such as exemestane, letrozole and anastrazole, is mostly limited to postmenopausal women. Their use in advanced breast cancer have demonstrated a better response when compared to tamoxifen in terms of clinical response rates and time to progression treatment (84, 85).

1.3.6.4 Targeted Therapy

As our knowledge of the molecular biology of breast cancer has expanded over recent years it has become evident that optimal therapy is driven by subtype. This has led to the development of targeted therapies, such as monoclonal antibodies or small molecule kinase inhibitors, which now forms one of the major modalities of treatment (86). A common strategy of targeted therapies is to exploit molecular targets which discriminate normal from cancer cells, and which selectively target the malignant phenotype.

1.3.6.4.1 HER2 targeted therapy

Several tumour types depend on the continuous activation of oncogenic signalling for their survival. In the context of breast cancer, HER2 is probably the most important. HER2 is a member of the human epidermal growth factor receptor (EGFR) family which are key regulators of proliferation, growth and survival (87). Activation of HER2 occurs by formation of homo-dimers, or hetero-dimers with other members of the EGFR family, resulting in the initiation of signalling pathways such as PI3K, MAPK and protein kinase C (PKC) which drive cell proliferation, survival, differentiation, angiogenesis, and invasion. Overexpression of HER2 occurs in 15-30% of invasive breast cancers, conferring a more aggressive clinical phenotype (39). Amplification of the gene *ERBB2* results in ligand-independent homo-dimerization and constitutive signalling primarily through the PI3K cascade (45, 88).

Numerous clinical trials investigating the use of HER2 targeted therapies in both the neoadjuvant and adjuvant settings have indicated significant benefits in terms of disease free survival and overall survival (89, 90). Trastuzumab and pertuzumab are monoclonal antibodies against HER2 which act by inhibiting dimerization of the receptors, preventing activation of the HER2 signalling pathways and tumour growth (91, 92). Trastuzumab was the first HER2-targeted therapy and is used in combination with systemic chemotherapy to treat both early and late stage HER2+ breast cancer

(93). Treatment of early stage HER2+ breast cancer with trastuzumab as adjuvant chemotherapy has been shown to reduce recurrence and mortality by a third (94).

Lapatinib and neratinib are small molecule tyrosine kinase inhibitors which directly inhibit kinase activity of EGFR family members (95). They are used to treat early HER2+ ER+ breast cancer in patients who have completed trastuzumab therapy, and in advanced HER2+ cancer that has progressed after previous treatment (96, 97).

1.3.6.4.2 Other targeted therapies – PI3K-Akt and Cyclin Dependent Kinases

Multiple protein kinases have been found to play an important role during tumorigenesis and cancer progression, making them valid candidates for the development of new targeted therapies. Uncontrolled kinase activity, as a result of loss of inhibitory mediators or gain of function mutations are common in cancer, and lead to increased kinase activity. Constitutive activation of signalling pathways may then be induced which render them essential for cell proliferation, differentiation and inhibition of apoptosis (98).

The PI3K-Akt pathway is the most commonly altered pathway in cancer, and frequently dysregulated in breast cancer driving cell growth, survival, and motility (99). The PI3K family of enzymes can by subdivided in to three main classes (I, II and III). Class I PI3K is comprised of two classes, class IA and IB, with class IA most often associated with cancer (100). In the normal cell, class IA exist as heterodimers consisting of a catalytic subunit (p110α/β/γ/δ) and a regulatory subunit (p85β). Class I of the PI3K enzymes are primarily activated by the binding of hormones, cytokines or growth factors (101, 102). Receptor activation occurs by recruitment of PI3K to the plasma membrane where it catalyses the conversion of membrane phosphoinositide 4,5- bisphosphate (PIP2) to phosphatidylinositol-3,4,5-trispho-sphate (PIP3). Kinases such as PDK1 and Akt bind to PIP3, confining them at the plasma membrane where PDK1 activates Akt by phosphorylation at its threonine 308 residue (103). To be fully activated Akt must also be phosphorylated at serine 473 residue. The pathway is

regulated by phosphatase and tensin homologue, encoded by the tumour suppressor gene *PTEN*, which acts to dephosphorylate PIP3 to PIP2 and therefore prevents Akt activation (104). Activation of Akt leads to a number of downstream processes which are crucial for cell proliferation and survival including the inhibition of pro-apoptotic factors, such as Bad and procaspase-9, the stimulation of cell growth and proliferation by inhibiting beta-catenin antagonist GSK3β and an increase in protein synthesis through regulation of mTOR(105) (Figure 1.4).

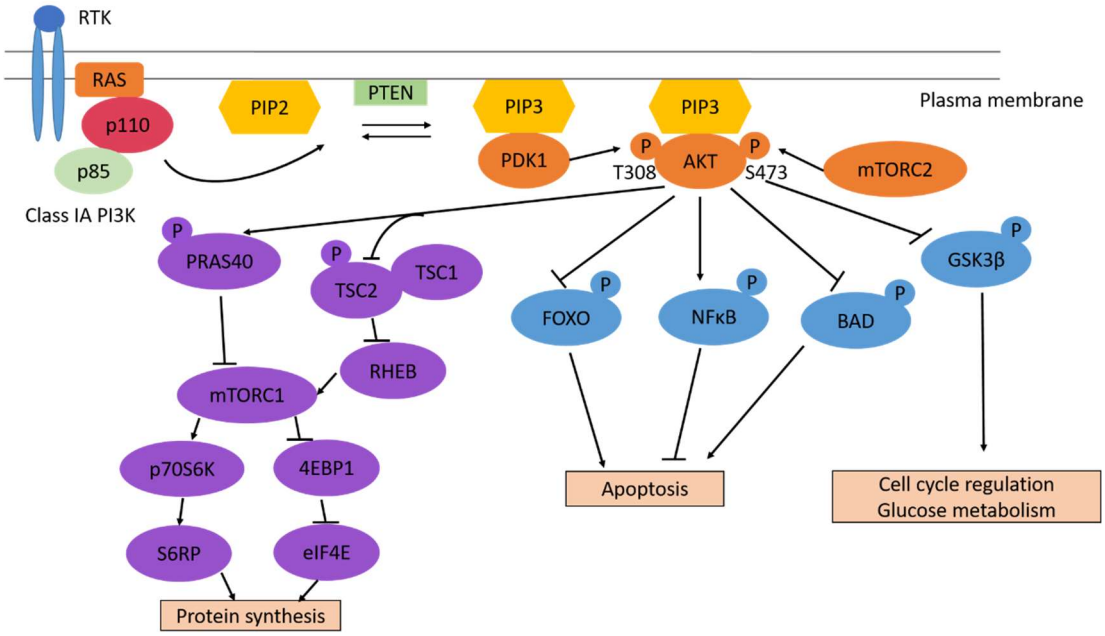

Figure 1.4: Schematic representation of the Class I PI3K-Akt pathway. Upon growth factor stimulation and activation of receptor tyrosine kinases (RTKs), class I PI3Ks are recruited to the plasma membrane. Activated p110 converts phosphatidylinositol-4,5-bisphosphaste (PIP2) to phosphatidylinositol-3,4,5-bisphosphaste (PIP3) providing docking sites for phosphoinositide-dependent kinase 1 (PDK1) and AKT. PDK1 activates AKT which results in a downstream cascade of signalling events. Arrows represent positive regulation and block-headed arrows represent negative regulation. Image adapted from Liu et al., 2009 (106).

Activating mutations of PI3KCA, the gene encoding the p110a catalytic subunit of PI3K, are frequently observed across numerous cancers, including breast cancer (107, 108). PI3KCa mutations are one of the most common events in HR+ breast cancers, occurring in approximately 35% of cases. PI3KCA mutations are also observed in the other cancer subtypes but to a lesser extent; 20-25% of HER2+ and 8% of TNBC (109). The mutations cluster in the helical and kinase domain, including three hot-spot mutations (E545K, E542K and H1047R) which activate the enzymatic activity of PI3K, and results in constitutive activation of Akt and its downstream effectors (110, 111). Amplification of PI3KCA and loss of PTEN activity have been associated with PI3K-Akt pathway activation in TNBC (109).

As a consequence of these observations, efforts have been made in the development of inhibitors of this pathway, many of which are now in clinical trial l (112, 113). The PI3K inhibitors can be classified into pan-PI3Ki such as buparlisib (BKM120) and pictilisib (GDC-0941), isoform specific such as alpelisib (BYL719) and dual mTOR/pan PI3K, such as BEZ235. The pan-PI3K inhibitor, buparlisib, targets all isoforms of class I PI3K (114). Most recently, the p110α-specific phosphatidylinositol-3-kinase (PI3K) inhibitor, alpelisib, was approved for use in combination with fulvestrant in women with HR+/HER2- PI3KCA-mutated advanced breast cancer (115, 116). The isoform specific PI3K inhibitors have proved to show improved tolerability and increased efficacy compared to pan-PI3K inhibitors (117). It is therefore anticipated that selective PI3K inhibitors continues to be an area of interest for the treatment of breast cancer.

A second strategy of targeted therapy is the inhibition of kinases which are necessary for sustained proliferation and survival of cancer cells despite genetic alterations. Deregulation of the cell cycle through inactivation of tumour suppressors (eg RB1) and aberrant activation of cyclin-dependent kinases (CDKs) is a defining characteristic of breast cancer, with different subtypes displaying differing dependencies (118). Due to the essential role of the cell cycle for sustaining cancer cell proliferation, inhibition

of selected kinases represents a promising therapeutic opportunity, and in recent years a large number of CDK inhibitors have entered clinical trial (119, 120).

The cell cycle is an ordered series of events, involving cell growth, DNA replication and cell division to produce two daughter cells (121). The cell cycle can be divided into four sequential phases referred to as Gap_1 (G1), synthesis (S), Gap_2 (G2) and mitosis (M). A cell enters the G0 resting phase from G1 when fully differentiated or in the presence of DNA damage, which impedes movement through the cell cycle. Progression through the phases is strictly controlled by surveillance mechanisms known as checkpoints which ensure the order, integrity and fidelity of the major events of the cell cycle (122) (Figure1.5).

Advancement through the cell cycle is controlled by two classes of regulatory proteins: cyclin-dependent kinases (CDK) and their activators, cyclins. The overall rate of cell cycle progression is determined by the relative activity of the Cyclin-CDK complexes and their inhibitory proteins, the INK4 and the WAF/CIP families (123, 124).

CDK4, CDK6 and CDK2 cooperate to drive cells through G1 into S phase. CDK4 and CDK6 are thought to be involved in early G1, forming complexes with D-type cyclins (cyclin D1, D2 and D3). CDK2 is required to complete G1 and initiate the S phase, and is activated by the E-type cyclins (cyclin E1 and cyclin E2). Finally, during S phase, CDK2 is activated by the A-type cyclins – cyclin A1 and cyclin A2. CDK1 is a key mediator of mitotic progression, with activity levels peaking during G2/M phase of the cell cycle (121).

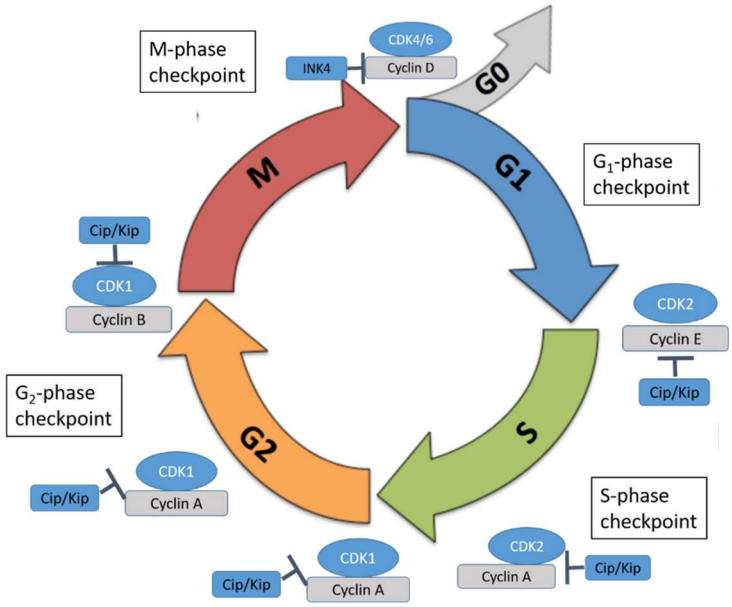

Figure 1.5: Simplified diagram of eukaryotic cell cycle. The cell cycle is comprised of four sequential phases regulated by cyclin-dependent kinases (CDKs) and their cyclin regulatory subunits. During G1 cells respond to extrinsic signals and decide to either exit cell cycle, or to pass the restriction point (G1 checkpoint) and complete cell division. Activation of the Cyclin E-CDK2 complex initiates transition into S phase where DNA replication takes place. Progression through the S phase is regulated by Cyclin A-CDK2 complex formation. At the end of S phase Cyclin A complexes with CDK1 and cells enter the G2 phase in preparation for mitosis (M). Mitosis is initiated by Cyclin B-CDK1 complex. Checkpoints occur during the cell cycle to ensure effective completion of key events.

Cell-cycle regulators are frequently mutated in human cancers. Alterations include amplification of cyclins, such as cyclin D1 and cyclin E1, and of CDKs, mainly CDK4 and CDK6 (125-127). Additionally, loss of cyclin kinase inhibitors, such as INK4A and INK4B, or downregulation of Rb expression are also observed. CDK2 is rarely altered in human tumours although loss of *CDKN1B* expression and overexpression of cyclin E1 correlates with poor prognosis. Down regulation of $p27^{KIP1}$ has been found to be predictive of breast cancer tumour resistance to radiotherapy and HER2 target therapy (128, 129).

Due to the central role of CDKs in cell cycle progression, small molecule kinase inhibitors are actively being pursued as novel therapeutic targets. First generation cell cycle inhibitors included multi-CDK inhibitors such as alvocidib, dinaciclib and seliciclib. However, the success of early generation cell cycle targeting agents were limited due to lack of target specificity and dose-limiting toxicities as monotherapies. Concerted efforts to explore their use in combination with other therapies are ongoing, but it is likely that further stratification of patients is required to ensure successful treatment. Preclinical studies have also identified opportunities for repurposing some of these compounds, although these mechanisms are based on inhibition of transcription rather than the cell cycle (130, 131).

The most successful CDK inhibitor to date is undoubtedly palbociclib, which specifically targets CDK4/6. CDK4 and CDK6 are activated by cyclin D1 (CCND1) and initiate the phosphorylation of retinoblastoma tumour suppressor protein (pRb). Dysregulation of the CDK4/6 pathway has been implicated in breast cancer, with overexpression of *CCND1* observed in up to 45% of breast cancers (132, 133). As CCND1 is a transcriptional target of ER, CDK4/6 is a logical target for ER+ breast cancer. This approach has proven particularly successful with palbociclib, an inhibitor of cyclin dependent kinase 4/6 (CDK4/6), approved for use in combination with endocrine therapy for the treatment of locally advanced ER+ HER2- breast cancer (134, 135).

1.3.6.5 Chemotherapy

Chemotherapy refers to the cyclical systemic administration of cytotoxic drugs which provide an effective broad acting therapy for all tumour types. Their mode of action is to inhibit cell proliferation and induce cell death in highly proliferating cancer cells. They are used in the management of both early and metastatic breast cancer, and represents the main treatment option for TNBC.

Systemic chemotherapy was originally used as a way to downstage patients with inoperable or locally advanced breast cancer, and remains the backbone of chemotherapy regimes in metastatic disease. Its use in the adjuvant setting for the treatment of early breast cancer has demonstrated efficacy in randomised studies and is primarily used to reduce the risk of recurrence and improve overall survival by eradicating micrometastatic disease (136). Neoadjuvant chemotherapy is now extensively used in the treatment of early-stage breast cancer (137). A range of chemotherapeutic agents are used for the treatment of breast cancer and are often given in combination as poly-chemotherapy treatment regimens which have been shown to be superior to single agents in terms of efficacy and safety (138).

Alkylating agents, such as cyclophosphamide, are DNA damaging agents which inhibit DNA replication by forming covalent bonds between strands. This results in double strand DNA breaks and cell death (139). The platinum analogues (cisplatin and carboplatin) are considered to be alkylating-like agents, which also act by introducing inter-and intra-strand crosslinks in DNA which require repair (140). They are used in the treatment of metastatic breast cancer and triple negative breast cancer. Methotrexate and 5-fluorouracil (5-FU) are anti-metabolites, and are commonly used along with cyclophosphamide, as poly-chemotherapy in both the adjuvant and neoadjuvant settings. Typically this also includes an anthracycline, followed by a taxane (141).

Anthracyclines and taxanes are the most effective and widely used cytotoxic agents in the treatment of cancer, and are the preferred first line treatment for all stages of early breast cancer (142-144). Anthracyclines, such as epirubicin and doxorubicin, are DNA damaging agents which inhibit topoisomerase -II activity thereby accelerating the rate of insertion of double-strand breaks in DNA strands (145). Simultaneously, anthracyclines intercalate with DNA and induce the formation of reactive oxygen species (ROS), as well as activating ataxia telangiectasia mutated kinase (ATM), resulting in cell cycle arrest and apoptosis (146). The taxanes (paclitaxel and docetaxel) belong to the microtubule-stabilising class of antimitotic cancer drugs

(147), which act by interfering with the normal functions of microtubules during cell division (148, 149). In clinical practice, taxanes remain a first line treatment for metastatic breast cancer in both the adjuvant and neoadjuvant settings, but have increasingly formed part of the polychemotherapy regimen for the treatment of early breast cancer. A recent review of the use of taxanes for adjuvant treatment for early breast cancer showed improvement in overall survival and disease-free survival, and recommended their continued use in this setting (150).

1.3.6.5.1 Limitations of chemotherapeutic agents

Systemic chemotherapeutic agents act by targeting highly proliferative cells, a characteristic of cancer cells. The assumption therefore is that cancer cells, which divide more frequently than normal cells, will be affected more than healthy cells. However, other cells within the body such as of the gastrointestinal tract, bone marrow and hair follicles, are also rapidly dividing, resulting in the characteristic side-effects associated with chemotherapy such as nausea, diarrhoea or neutropenia (151). Extended use of cyclophosphamides, a component of almost all polychemotherapy regimens for breast cancer, is commonly associated with nausea and vomiting, as well as reversible hair loss (152). The side-effects of taxanes, which include neurotoxicity and haematological suppression, are often considered to be dose-limiting factors leading to treatment disruption (153, 154). Long term side-effects have also been identified, such as the cardiotoxicity observed in some patients treated with anthracyclines or trastuzumab (155). These side-effects can be a significant barrier to completing chemotherapy regimens. The current approach to limiting such complications are to lower the dose of chemotherapy administered, postpone treatment until the immediate effects subside, or treat effects with other drugs. However these practices can also risk the patient's benefit from treatment, compromise disease control, or have their own associated side-effects which limit use.

Resistance to chemotherapy and to targeted therapies, remains the biggest challenge to the treatment and long-term control of breast cancer. Patients who present with recurrent cancers are frequently found to have chemoresistant tumours presenting a significant challenge to clinicians. Therapy options for these patients are often limited and most patients die as a result of metastatic disease. Despite advances in our understanding of cancer biology and treatment, the mechanisms of drug resistance remain poorly understood.

Drug resistance may be either innate or acquired. Innate resistance indicates that a tumour presents with an inherent lack of sensitivity to the drug meaning it is unresponsive to treatment. Acquired resistance develops over the course of drug treatment, resulting in tumour cells which are no longer responsive to treatment (156). Initially many tumours appear to respond to treatment but, as not all neoplastic cells are killed, a residual resistant population allows regrowth that is no longer responsive to drugs (157). The development of acquired resistance cannot be explained by one single event. Instead, it is likely to be in response to a combination of treatment-induced somatic mutations and non-genetic changes, such as expression changes in genes or alterations in protein phosphorylation (158).

With the increased popularity for use of taxanes as part of the treatment regimens of early breast cancer, many patients will become resistant to their action. Subsequent therapeutic options for metastatic disease are limited if resistance occurs, and represents a significant problem for the clinician. However, an increased understanding of the mechanisms driving resistance to taxanes has the potential to improve therapeutic strategies benefiting patient management. The following sections discuss more fully taxanes and mechanisms which drive resistance.

1.4 Taxanes in breast cancer

1.4.1 Mechanism of action

Taxanes are naturally occurring compounds derived from the *Taxoidaceae* tree family(159). Paclitaxel was developed first but due to solubility and availability issues, a semi-synthetic analogue, docetaxel, was developed (160-162). Taxanes are potent anti-mitotic drugs, which selectively and reversibly bind to β-tubulin that have previously been incorporated into microtubules (148, 161). This stabilises the structure of the microtubule by inducing the formation of stable microtubule bundles which prevent corrects spindle formation, ultimately blocking the cell cycle and inducing apoptosis.

Microtubules are long, hollow dynamic structures which are involved in a number of cellular functions, but, in particular, play a critical role during cell division (163). Microtubules comprise heterodimers of α and β-tubulin and are dynamic structures which undergo continual assembly and disassembly within the cell. The microtubules in most cells radiate out from the centrosome, a microtubule organising centre in which the microtubules are anchored. During mitosis, the microtubules extend outward from the duplicated centrosomes to form the mitotic spindle assembly checkpoint (SAC). As the cell enters mitosis, the turnover of spindle microtubules increases dramatically. Stabilisation of microtubules and cell polarity is maintained by microtubule associated proteins (MAPs) and microtubule interacting proteins.

Microtubule-targeting drugs function by suppressing microtubule dynamics, binding to the inner surface of the microtubule (164, 165). This binding promotes microtubule stability by increasing tubulin assembly independently of MAPs and GTP, which are normally necessary for the assembly process (161, 166). This results in arrest of the cell cycle at the G2/M phase, which inhibits mitosis and induces apoptosis through downregulation of Bcl2 and upregulation of p53 and p21/WAF1 (167, 168). Cell cycle arrest can occur at different phases depending on the dose of taxane used.

Interruption of the cell cycle at G0/G1 has also been observed in some cell lines when low doses of taxane were given, resulting in downregulation of c-myc (169).

1.4.2 Taxane chemoresistance

Resistance to chemotherapy is a well-known phenomenon where tumours become tolerant to the effects to pharmaceutical agents. Taxanes have been found to be highly effective chemotherapeutic agents, offering benefit in terms of overall survival and disease free survival (150). However many patients develop progressive disease over time and no longer respond to treatment. An increased understanding of the mechanisms driving resistance to taxanes has the potential to identify predictive biomarkers of taxane response and promising targets for new therapeutic strategies.

1.4.2.1 Drug efflux

Alterations in drug transport, particularly in drug efflux, are a common resistance mechanism in cancer. Resistance can occur by specific resistance to a single drug or resistance to a wide variety of compounds, so called multi-drug resistance. The ATP-binding cassette (ABC) transporter family are drug efflux pumps which are key regulators of multidrug resistance. Paclitaxel and docetaxel are both substrates of P-glycoprotein (P-gyp), which is encoded by the MDR1 gene (170). Overexpression of MDR1 is frequently observed in cell lines but has not consistently been observed in primary breast cancer samples (171). Other members of the ABC family have been associated with resistance to taxanes, including ABCB4 (MDR2/3) for which paclitaxel is a substrate and ABCC2 (MRP2), ABCC10 (MRP7) for which both taxanes are substrates (172, 173).

1.4.2.2 Drug metabolism

Alterations in drug metabolism and detoxification, resulting in reduced intracellular drug concentrations, are key resistance mechanisms in many cancers. Cytochrome p450 is a family of metabolising enzymes, which includes CYP3A4 the enzyme responsible for metabolism of paclitaxel and docetaxel into inactive precursors (174). The CYP enzymes are expressed predominantly in the liver but are also found in other extrahepatic tissues including the digestive tract (175). Expression has also been observed in malignant tissue including breast, colon and oesophageal tumours (176). Overexpression of CYP3A4 in tumours may contribute to chemoresistance by limiting efficacy or influencing intracellular drug concentrations (177). As a strategy of overcoming resistance, inhibition of CYP3A4 activity has been shown to decrease tumour volume in an *in vivo* model of breast cancer when given with docetaxel (178). However given the role of the CYP enzymes in the metabolism of more than 50% of medicines (179), inhibition may prove clinically challenging. CYP3A4 expression in breast cancer tumours from patients treated with docetaxel has been found to correlate with clinical outcome, with overexpression of CYP34A observed in patients who respond poorly to docetaxel (180-182). This suggests that CYP3A4 assessment may be a valid predictive marker for therapeutic response to taxanes.

1.4.2.3 Alteration of microtubule associated proteins

The functional target of the taxanes is the microtubule, acting exclusively with tubulin to inhibit the dynamic changes normally seen during cell division. It is therefore plausible to anticipate that an on-target resistance mechanism may limit the activity of taxanes. There are multiple isotypes of tubulin with evidence indicating that βIII-tubulin is most frequently associated with taxane resistance (183). Over expression of βIII-tubulin has been shown in several human cancer cell lines with associations with taxane sensitivity (184). This finding was validated by the observation of high expression levels of *TUBB3* correlating with low response rates in patients treated

with taxane-containing regimens (185, 186). Additionally several mutations carried by beta-tubulin have been identified which are associated with taxane resistance (187). However the clinical significance of these mutations remains unclear (188).

The assembly and dynamics of the mitotic spindle are tightly regulated by a family of microtubule-associated proteins (MAPs) and mitotic kinases proteins (189). Alterations in their expression or function in breast cancer may therefore regulate their sensitivity to taxanes. As such MAPs have long been considered as potential predictive biomarkers of taxane response (190). One such protein, MAP4, stabilises microtubules playing a critical role in mitotic dynamics (191). *In vitro*, MAP4 overexpression has been associated with paclitaxel resistance (192). However this observation has not been confirmed in patient samples. MAPT/Tau, which functions primarily be enabling tubulin assembly and promoting microtubule stabilisation, has also been observed as being upregulated in breast tumours and it was therefore suggested that its expression could serve as a predictor of response. However, a study in ER+ early breast cancer failed to show an association between Tau and taxane benefit (193). A recent *in silico* analysis of 280 microtubule associated genes identified increased expression of MTUS1, a gene encoding a stabilising MAP, as being associated with resistance to taxanes in breast cancer and therefore of interest as potential biomarker of response (194). Stathmin, a microtubule destabiliser and regulator of the G2/M phase of the cell cycle, may also play a role in taxane resistance. It is found to be overexpressed in breast cancer and its expression is associated with poor prognosis (195). RNA interference knockdown of stathmin was found to reverse taxane resistance *in vitro* and it is postulated that overexpression of stathmin may therefore modulate paclitaxel efficacy by decreasing microtubule sensitivity to taxanes (196).

The spindle assembly checkpoint is activated by taxanes when the attachment of microtubules to the kinetochores is interrupted. Maintenance of this checkpoint is tightly regulated by proteins such as MAD2 and BUBR1 which ensure correct microtubule attachment. Sustained activation of these checkpoint proteins by

taxanes increases activity of cyclin B1-CDK1 leading to cell cycle arrest at the M phase (197). Polo-like kinase 1 (PLK1) promotes mitotic progression by phosphorylating CDC25C, which also activates cyclin B1-CDK1 complexes(198). Studies have shown that suppression of the SAC checkpoint genes in the MCF7 breast cancer cell line results in paclitaxel resistance with associated downregulation of CDK1 (199), a protein which is essential for the regulation of mitosis. In addition, inhibition of cyclin dependent kinases by overexpression of p21 are associated with paclitaxel treatment (167).

1.4.2.4 Alterations in apoptosis, cell cycle and signalling pathways

A common resistance mechanism is to increase cell pro-survival signalling, and reduce signalling through pathways, which result in apoptosis. A primary function of taxanes, and other chemotherapy agents, is to induce programmed cell death and it has been proposed that perturbations in the pathway may induce chemoresistance (168). Several apoptosis-related or survival signalling genes have been shown to be activated by taxanes for example c-Jun N-terminal kinase (JNK), nuclear-kappa B (NFκB) and Bcl-2 proteins (200, 201).

The Bcl-2 family of proteins consists of both anti-apoptotic (Bcl-2, Bcl-X_L, and Mcl-1), and pro-apoptotic proteins (Bax, Bak, Bim). Inhibition of the anti-apoptotic effects of Bcl-2 is thought to be induced through its phosphorylation, allowing pro-apoptotic proteins such as Bax and Bak to become activated (202). Changes in expression levels or posttranslational modifications of Bcl-2 family members have been associated with taxane resistance. The relative concentrations of pro-apoptotic and anti-apoptotic Bcl2 proteins may therefore be involved in resistance to taxane-induced cell death.

Resistance to systemic therapies can also be conferred indirectly by altered activity of molecular pathways. As discussed previously the activation of the pro-survival PI3K-Akt pathway is associated with chemoresistance by driving cell survival, cell

growth and cell cycle progression (105) . Akt has been shown to phosphorylate a number of key apoptotic proteins including Bad, and NFκB transcription factors. Akt is involved in the phosphorylation of the pro-apoptotic protein Bad, which becomes bound to 14-3-3, inhibiting its pro-apoptotic activity (203). Activation of NFκB an inhibit apoptosis through induction of anti-apoptotic proteins such as Bcl-2 and Bcl-xL (204). Cell line studies have demonstrated upregulation of NFκB in response to treatment with paclitaxel, resulting in reduced apoptosis suggesting a role in taxane resistance (205, 206).

Increased activity of the mitogen-activated protein kinases (MAPK) pathway, has also been implicated in resistance to numerous systemic therapies. JNK is a subfamily of mitogen-activated protein kinases (MAPK), which regulates important cellular activities, including cell proliferation, differentiation, and apoptosis (207). The JNK pathway is activated by taxanes via the apoptosis signal-regulating kinase (ASK1) as well as by Ras, and phosphorylates and inactivates Bcl-2 at the G2/M phase of the cell cycle (208). The Raf/MEK/ERK pathway is a pro-survival pathway playing an important role in apoptosis, by phosphorylating both pro- and anti-apoptotic proteins (Bax, Bad, and Bcl-2, Bcl-xL respectively) (209). Inhibition of ERK signalling has been shown to increase the sensitivity of cells to taxane suggesting it may also play a role in taxane resistance (210).

1.5 Overview and aims of this thesis

The challenge of acquired chemoresistance in breast cancer remains the major cause of treatment failure, with limited treatment options available to patients thereafter contributing to a poor prognosis. With the growing use of taxanes as a first-line treatment for early breast cancer, resistance to these chemotherapy agents is becoming an increasing challenge for the clinician. An appropriate second line therapy is required after resistance to taxanes has occurred, which remains an unmet need. Understanding the mechanisms which drive acquired taxane resistance in

breast cancer could potentially improve the outcomes for patients by identifying pathway changes which are predictive of resistance, and which could then be exploited as novel therapies to treat chemorefractory disease.

The main objective of this thesis was therefore to generate a series of well-characterised isogenic taxane-resistant breast cancer cell lines as a model system. It is hypothesised that isogenic taxane-resistant cell line models will undergo phenotypic and transcriptomic changes when compared to their parental cell lines which can be attributed to acquired taxane resistance. I theorised that differences in signalling pathways could therefore be used to identify biomarkers associated with response to taxanes, and that the isogenic cell lines could be employed as pre-clinical models to identify novel therapeutic targets with activity against taxane resistant breast cancer.

Aims and objectives:

a. To develop a panel of isogenic taxane-resistant breast cancer cell line models representing different molecular breast cancer subtypes.
b. To characterise the isogenic cell lines through a variety of *in vitro* assays.
c. To identify signalling pathways altered in the resistant cell lines through comprehensive transcriptomic and proteomic characterisation of the sensitive and taxane-resistant breast cancer cells.
d. To identify novel strategies for the treatment of taxane resistance by performing a pathway-focussed small molecule kinase screen to detect inhibitors with activity in the isogenic breast cancer cell lines.

2. MATERIALS AND METHODS

2.1 Materials

2.1.1 Common Buffers and Reagents

The compositions of common buffers are listed in Table 2.1. Buffers were prepared in Milli-Q water unless otherwise stated.

Table 2.1: Common buffers and reagents

Buffer	Composition
Blocking buffer	5% w/v milk powder added to TBS-T
Phosphate buffered saline (PBS)	137 mM NaCl, 2.7 mM KCl, 10 mM Na_2HPO_4, 1.8 mM KH_2PO_4, pH 7.4.
PBS with Tween (PBS-T)	0.1% (v/v) Tween® 20 to PBS
Radioimmunoprecipitation assay (RIPA) buffer	50 mM Tris pH 8.0, 150 mM NaCl, 1% (v/v) NP-40, 0.5% (w/v) sodium deoxycholate, 0.1% (v/v) SDS. cOmplete™ mini-Protease Inhibitor Cocktail tablets (Roche, #4693159001) and PhosSTOP™ tablets (Roche, #4906845001) were added directly before use.
RPPA lysis buffer	1% (v/v) Triton X-100, 50 mM HEPES (pH 7.4), 150 mM NaCl, 1.5 mM $MgCl_2$, 1 mM EGTA, 100 mM NaF, 10 mM $Na_4P_2O_7$, 1 mM Na_3VO_4, 10% glycerol

RPPA sample buffer 4 X	250 mM Tris, pH 6.8, 8% (w/v) SDS, 40% (v/v) glycerol. Before use, 2-mercaptoethanol at 1/10th of the volume was added.
SDS-PAGE sample buffer 3 X	150 mM Tris HCl pH6.8, 3% (w/v) SDS, 30% (v/v) glycerol, 0.03% (w/v) bromophenol blue
Tris buffered saline (TBS)	50 mM Tris, 150 mM NaCl, pH 7.5
TBS with Tween 0.1% (TBS-T)	0.1% v/v Tween®20 to TBS
Tris Glycine SDS Running buffer	25 mM Tris, 192 mM glycine, 0.1% (w/v) SDS, pH 8.3.
Tris Glycine Transfer buffer	25mM Tris, 192 mM glycine, pH 8.3
Trypsin-EDTA	10X Trypsin-EDTA (Sigma, T4174) diluted to 1X in PE (PBS with EDTA) buffer

2.1.2 Compounds

Compounds (Table 2.2) were diluted in DMSO at a stock concentration of 10 mM and stored at -80°C unless otherwise stated. Compound source plates were prepared in v-bottom 96 well plates (Corning #3363) at 1000-fold assay concentration over an 8-point semi-log range and stored at -20°C for short-term use.

Table 2.2: Chemotherapy and small molecule kinase compounds

Compound	Supplier	Catalogue Number	Solvent	Stock concentration	Storage
5-fluorouracil	Sigma	F6627	DMSO	10 mM	-80°C
Alvocidib	Stratech	S1230-SEL	DMSO	10 mM	-80°C
BKM120	Cayman Chemicals	11587	DMSO	10 mM	-80°C
BYL719	Cayman Chemicals	16986	DMSO	10 mM	-80°C
Carboplatin	Cayman Chemicals	13112	H_2O	10 mM	Prepare fresh
Cisplatin	TEVA		PBS	3.3 mM	RT
Dinaciclib	Cayman Chemicals	14707	DMSO	10 mM	-80°C
Docetaxel	Sigma	O1885	DMSO	10 mM	-80°C
Doxorubicin Hydrochloride	MP Biochemicals	215910101	DMSO	10 mM	-80°C
Epirubicin hydrochloride	Cambridge Biosciences	E6235	DMSO	10 mM	-80°C
Paclitaxel	Selleck	S1150	DMSO	10 mM	- 80°C
PIK75 hydrochloride	Cayman Chemicals	10009210	DMSO	10 mM	-80°C
SNS-032	Selleck	S1145	DMSO	10 mM	-80°C

2.1.3 Antibodies

Antibodies for Western blots were diluted in blocking buffer.

Table 2.3: Antibody list

Target	Source	Supplier	Catalogue Number	Dilution
β-actin	Mouse	Calbiochem	CP01	1:100,000
Total Akt	Rabbit	CST	4691	1:1000
Akt1	Mouse	CST	2967	1:1000
Akt S473	Rabbit	CST	9271	1:1000
CCNB1	Mouse	CST	4135	1:1000
EGFR	Rabbit	Santa Cruz	Sc-03	1:2000
ERα	Mouse	Leica	NCL-L-ER-6F11	1:100
FAK	Rabbit	CST	3285	1:1000
FAK (Y397)	Mouse	BD Biosciences	611722	1:1000
GAPDH	Rabbit	CST	2118	1:5000
HER2	Rabbit	CST	2165	1:1000
HER3	Mouse	Fisher/LabVision	MS201	1:1000
MDR1	Mouse	Santa Cruz	Sc-13131	1:1000
P38 MAPK	Rabbit	CST	9212	1:1000
P44/42 MAPK (ERK1/2)	Rabbit	CST	9102	1:1000

P44/42 MAPK (ERK1/2) (Thr202/Tyr204)	Rabbit	CST	9101	1:1000
PgR	Mouse	Leica	NCL-L-PGR-312	1:1000
pS6	Rabbit	CST	2215	1:1000
RB (Ser807/811)	Rabbit	CST	9308	1:1000
Anti-mouse IgM (actin)	Goat	Calbiochem	401225	1:120000
Anti-mouse	Horse	CST	7076	1:5000
Anti-rabbit	Goat	CST	7074	1:5000

2.2 Methods

2.2.1 Cell culture

2.2.1.1 Cell culture maintenance

All cell lines were obtained from the American Type Cancer Collection (LGC Standards, UK). MDA-MB-231 and MCF-7 cells were cultured in Dulbecco's Modified Eagle Medium (DMEM) (Thermo Fisher Scientific; #21969035) supplemented with 10% foetal calf serum (FCS) (Life Technology #16140071) and 2mM L-glutamine (Thermo Fisher Scientific; #A2916801). SK-BR-3 cells were cultured in Rosewell Park Memorial Institute (RPMI) 1640 Medium (Thermo Fisher Scientific; #11875101) supplemented with 10% FCS and 2mM L-glutamine.

All cells in culture were maintained at 37°C in a humidified atmosphere containing 5% CO_2. Cells were routinely tested for mycoplasma using the Venor™GeM Mycoplasma Detection PCR kit (Sigma; #MP0025).

Table 2.4: Human breast cancer cell lines used in this study

Cell line	Origin	Classification	Description
MCF-7	Human breast cancer; pleural effusion from 69 year old woman with metastatic disease originating from luminal mammary adenocarcinoma (211)	Luminal A	ER+/PgR+/HER2-
MDA-MB-231	Human breast cancer; pleural effusion from 51 year old woman with metastatic disease originating from basal mammary adenocarcinoma (212)	Basal B	ER-/PgR-/HER2-
SK-BR-3	Human breast cancer; pleural effusion from 43 year old woman with metastatic disease originating from luminal mammary adenocarcinoma (213)	Luminal	ER+/PgR-/HER2+

ER, oestrogen receptor; PgR progesterone receptor; HER2, human epidermal growth factor receptor 2.

2.2.1.2 Cell line authentication

Cell line authentication was confirmed by short tandem repeat (STR) genotyping. Parental cell lines were genotyped prior to establishment of taxane resistance and

cryopreservation of cell line stocks. The process was repeated for all cell lines at 3 monthly intervals during the development of resistant cell lines, prior to freezing stock aliquots and during the course of this study to confirm integrity of experiments. Genomic DNA from all cell lines were analysed by the DNA Sequencing Facility, Institute of Genetics and Cancer, University of Edinburgh, using the GenePrint® 10 system (Promega; B9510).

2.2.1.3 Cell harvesting and counting

Cells were routinely sub-cultured in 75cm^2 cell culture flasks (Greiner; #658175) according to cell growth, 1-3 times per week. The media was aspirated, and the flasks washed twice with phosphor buffered saline (PBS), pH7.3. Cells were harvested by brief incubation with 0.25% trypsin/1mM EDTA at 37°C. The disaggregated cells were resuspended in 10 ml of the appropriate complete growth media to neutralise the trypsin and centrifuged for 5 min at 250 x g. To ensure a single cell suspension, the cell pellet was resuspended in fresh media before being passed through a 21G needle attached to a 10ml syringe. A proportion of the resulting cell suspension was then transferred to appropriate tissue culture plates and maintained at 37°C and 5% CO_2 in a humidified atmosphere.

Where a fixed number of cells were required for an experiment 10µl of the above cell suspension was transferred to a haemocytometer. The cell count was obtained by manually counting the number of cells in the each of the large 1mm^2 corner squares. The average number of cells per ml was obtained by dividing by the count by four and multiplying by 10^4.

All cell line experiments were performed using sub-confluent cultures in their log-phase of growth.

2.2.1.4 Cryopreservation and recovery from liquid nitrogen storage

Cells from a confluent flask were harvested as outlined above. The cell suspension was centrifuged at 250 x g for 5 minutes to form a pellet. The media was carefully

aspirated and the cell pellet resuspended in freezing medium at a concentration of 1 x 10^6 to 5 x 10^6 cells/ml. The resulting suspension was transferred to cryovials and stored at -80°C for 24 hours before moving to long term storage in liquid nitrogen.

To recover cells from liquid nitrogen, the cryovial was incubated briefly at 37°C to defrost the contents before resuspension in 10ml of complete media. The resuspended cells were pelleted by centrifugation at 250 x g for 5 minutes. The supernatant was aspirated, and the pellet resuspended in complete medium before transferring the contents to appropriate tissue culture flasks.

2.2.2 Generation of taxane resistant isogenic cell lines

Cells were routinely passaged prior to subculture to two 25 cm^2 and two 175 cm^2 cell culture flasks (Greiner; #690175 and #660175 respectively). When 80% confluent, the cells from the 175cm^2 cell culture flasks were harvested and frozen down as master stocks of the parental native cell line. These cells were used as controls for all subsequent experiments.

For the establishment of taxane resistance, working stock solutions at 1µM of paclitaxel and docetaxel were prepared in complete medium and stored, wrapped in foil to protect from light degradation, at 4°C for one week.

After 24 hrs in culture the media was replenished in the 25 cm^2 cell culture flasks with complete media containing either paclitaxel or docetaxel. Cells were initially exposed to 0.5nM taxane, a dose which approximately represented the IC_{80} of each cell line. The media in each flask was replaced twice weekly with fresh taxane. On reaching confluence, the cells were passaged twice before the next increment of drug was introduced. The contents of one flask was harvested and seeded in to two further 25cm^2 cell culture flasks and an incremental dose of taxane added to the media. Increments in taxane dosage was guided by the ability of the cells to tolerate the drug and proliferate in culture. Initially an increase of 0.5 nM of each drug was applied at each stage. The contents of the second 25cm^2 cell culture flask was collected and

frozen down as a representative of that concentration of taxane, ensuring that the full spectrum of doses were available for future experiments if required.

Cells were named according to cell type, dose of drug and taxane e.g. MDA-MB-231 25nM PACR; MDA-MB-231 treated with 25nM paclitaxel. This naming schedule was applied to all cell lines generated for the purpose of this thesis.

2.2.3 Cell doubling times

To quantify any differences in growth rate between the parental and resistant cell lines, live cell imaging using an IncuCyte ZOOM® system was performed. The IncuCyte ZOOM® provides the capability to capture real-time quantitative kinetic data of cellular confluence by periodic imaging over multiple time points and days. MDA-MB-231 and MCF7 parental and taxane resistant isogenic cells were counted and seeded at 6 x 10^{4} cells.ml^{-1} in triplicate in the inner wells of a 96 well cell culture plate (Greiner; #655180) either in the presence or absence of the maintenance dose of 25nM of the relevant taxane. Control wells containing 0.1% (v/v) DMSO were included for each cell line. The outer wells were filled with 100µl PBS. Four images per well in the phase channel using a 10x objective were captured every 3 hours for 72 hours. Mean confluence for each well and time points were obtained using IncuCyte ZOOM® software and data extracted as a csv file. All experiments were performed in triplicate.

2.2.4 Cell viability assays

Cell Counting Kit-8 (CCK-8) assays (Sigma 96992) were used for the determination of cell viability in cell proliferation and cytotoxicity assays. CCK-8, is a sensitive formazan-based colorimetric assay, which is converted to an orange product under reducing conditions of viable cells. The product is measured by absorbance at 450 nm and is directly proportional to the amount of living cells in each well.

Cells were seeded at a density of 0.5 x 10^4 in triplicate in 96-well plates and incubated for 24 hours before treatment. Edge wells were not used due to evaporation effects which may affect cell growth. Each well was then replaced with fresh media containing the compound of interest over an 8 point semi-log concentration range. Stock dilution plates of test compounds were prepared in DMSO. A working-dilution plate was prepared in complete medium. Drug vehicle control wells were included and treated with 0.1% v/v DMSO corresponding to the final concentration of drug diluent. Media only controls were also included. Cells were grown for 72hrs and viability assessed with the addition of CCK-8. All experiments were performed in triplicate. Cell counts were normalised to the DMSO control as a measure of cell viability and concentration response curves plotted using GraphPad Prism v6 and IC_{50}s calculated.

2.2.5 Small Molecule Kinase Screen

All inhibitors described in Table 2.5 were provided by the Drug Discovery group at OICR. Each compound was tested against MDA-MB-231 Native, MDA-MB-231 25PACR and MDA-MB-231 25DOCR.

Table 2.5: Inhibitors and targets of small molecule kinase screen

Inhibitor	Target
(+)-P276, P276-00	CDK1, CDK4
2-Thio(3-iodobenzyl)-5-(1-pyridyl)-[1,3,4]-oxadiazole	GSK3B
6-bromoindirubin-3'-oxime, BIO	GSK3
A 1070722, A-1070722	GSK3
Alsterpaullone	CDK1, CDK2, CDK5, GSK3
Alvocidib, Flavopiridol	CDK1, CDK2, CDK4, CDK63, CDK7, CDK9, Bcl-2, Mcl-1, Survivin, XIAP
AR-A014418	GSK3
Arcyriaflavin A	CDK4, CaMK2b (CaMK2)
AS-252424	PI3K
AS604850, AS-604850	PI3K
AS605240, AS-605240	PI3K
AT-7519 hydrochloride	CDK1, CDK2, CDK3, CDK4, CDK5, CDK6
AZD 7762, AZD-7762 hydrochloride	CHK1, CHK2
AZD5438, AZD-5438	CDK1, CDK2, CDK9
AZD6482, AZD-6482	PI3K
BGT-226, NVP-BGT-226	PI3K, FRAP (MTOR, FRAP1)
BKM120, NVP-BKM-120	PI3K

BS-181 hydrochloride	CDK7
BYL-719, NVP-BYL-719	PI3Ka
CAL-101, GS-1101	PI3Kd
Cdk1/2 Inhibitor III	CDK1, CDK2
CGK 733	ATR, ATM
CGP-74514A hydrochloride	CDK1
CHIR-124	CHK1
CHIR-98014 isomer, CT-98014	GSK3
Chk2 Inhibitor II, 339253	CHK2
Compound 52, NG-52	CDK1
CP466722, CP-466722	ATM
CT-99021, CHIR-99021	GSK3
Dinaciclib, MK-7965, SCH-727965	CDK2, CDK5, CDK1, CDK9
FAK Inhibitor 14	FAK (FAK1)
GDC-0941	PI3K
GDC-0941 bismesylate, RG-7321, Pictilisib	PI3K
GSK-1059615, GSK-615	PI3K
GW8510	CDK2
IC87114, D-030, IC-87114	PI3Kd

Indirubin, NSC-105327	CDK1, CDK2, CDK4, CDK5, GSK3B
Kenpaullone, NSC-664704	CDK1, CDK2, CDK5, GSK3, LCK (p56lck)
KU-55933, KU-0064	ATM, PI3K
KU-60019	ATM
LY2835219, LY-2835219	CDK4, CDK6, PIM1
LY-294002	PI3K
NSC 109555 ditosylate, DDUG	CHK2
NSC 625987	CDK4
NSC 693868	CDK1, CDK5, GSK3
NSC-663284	cdc25
NU-2058	CDK1, CDK2, CDK5, GSK3
NU-6102	CDK1, CDK2
NVP-BEZ235, BEZ235	PI3K
Olomoucine	CDK1, CDK2, CDK5
PD-0332991, PD-332991	CDK4, CDK6
PD-407824	CHK1, WEE1
PF-04691502, PF-502	PI3K, FRAP (MTOR, FRAP1)
PF431396, PF-431396	FAK (FAK1), PYK2 (FAK2, PTK2B, CAKB)
PF562271, PF-562271	FAK (FAK1), PYK2 (FAK2, PTK2B, CAKB)
PF-573228	FAK (FAK1)

PHA690509, PHA-690509	CDK2
PHA-767491 hydrochloride	CDC7, CDK9, MAPKAPK2 (MK2)
PHA-793887	CDK1, CDK2, CDK4, CDK5
PHA-848125, PHA-848125AC	CDK2, CDK7, CDK4, CDK5, CDK1
PI-103	PI3K
PI3-Kinase a Inhibitor 2	PI3K
PI-828	PI3K
PI-93, PIK-93	PI3Ka
PIK-294	PI3Ka
PIK-294	PI3Ka
PIK-75 hydrochloride	PI3K
PIK-90	PI3Ka
Purvalanol A, NG 60	CDK1, CDK2, CDK4, CDK5, DYRK1A (DYRK)
Purvalanol B, NG 95	CDK1, CDK2, CDK5
PV-1019, NSC-744039	CHK2
PX-866, DJM-166, Sonolisib, NSC-722134	PI3K, PTEN inhibitor
Quercetin	PI3K
Roscovitine, CYC202, Seliciclib	CDK1, CDK2, CDK5
Ryuvidine	CDK4

SB 216763	GSK3
SB-218078	CHK1, CDK1, PKC
SB-415286	GSK3
SCH-900776, MK-8776	CHK1, CDK2
SNS-032, BMS-387032	CDK2, CDK7, CDK9
SU-9516	CDK1, CDK2, CDK4
TCS 2312	CHK1
TCS 2312 dihydrochloride	CHK1
TG100-115, TG-100115	PI3K
TGX-221	PI3K
TWS-119	GSK3
VE-821	ATR
Wortmannin, KY 12420	PI3K - Irreversible
WYE-125132, WYE-132	PI3K, FRAP (MTOR, FRAP1), mTORC1, mTORC2
XL-147, , SAR-245408	PI3K
XL765, SAR245409	PI3K, mTORC1, mTORC2
ZSTK474	PI3K

Cells were seeded at 1000 – 1200 cells/well into 384 well cell culture plates (Greiner; #781073). After 24 hrs, resistant cells were exposed to the relevant taxane at the selection doses established then exposed to small molecule kinases dissolved in DMSO in 12 concentrations ranging from 0.0026 to 10 µM using a HP D300 digital

compound dispenser (Tecan). 0.5% v/v DMSO controls were included to reflect the maximum concentration of compound diluent in each well. After 72 hr, the effects of inhibitors were determined using CellTiter-Glo™ Luminescent Cell Viability Assay (Promega; G7570) and the Wallac EnVision 2104 Multilabel Reader. Raw data were normalised to negative (media) and positive (20 µM staurosporine; Selleckchem S1421) controls and analysed using GraphPad Prism v6 software.

2.2.6 Drug combination synergy assays

For drug combination assays, a drug dose combination matrix was applied before assessment of synergistic effects. Briefly, cells were seeded as described above and a working-dilution compound plate prepared in complete medium. After incubation for 24 hours, taxanes (compound A) were added over an 8-point semi-log concentration range down the inner rows of 96 well plates, along with a 5-point semi-log concentration range of compound B along the inner columns. Drug vehicle control wells were included in wells C2-G2 of the 96 well plate. A 'no treatment' well was included with cells in well B2 incubated in complete medium (Figure 2.1). Cells were grown for 72 hours and viability assessed with the addition of CCK-8. Triplicate plates were set up for each experiment, and all experiments performed three times.

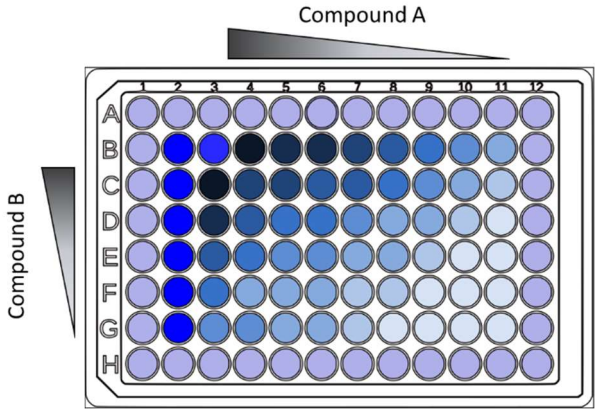

Figure 2.1: Combination matrix layout for assessment of synergistic drug activity

Values normalised to the DMSO controls were analysed using SynergyFinder v2.0 (www.synergyfinder.fimm.fi) (214) a web application for interactive analysis and visualisation of multi-drug combination profiling data. The program calculates separate scores based on four main reference models: Bliss independence, Loewe additivity, Highest Single Agent (HSA) and Zero Interaction Policy (ZIP) models.

2.2.7 Cell cycle assays

Cells were seeded at 2500 cell/well in 100 µl of complete media in 96-well black optical-bottom plates (Fisher Scientific; #10281092) and incubated at 37°C with 5% CO_2 for 24 hours before treatment. Media from each well was aspirated and replaced with fresh medium containing the compound of interest, 0.1% v/v DMSO as a vehicle control or 300nM staurosporine as a positive control. Each treatment was performed in triplicate.

The plates were incubated for a further 24 hours at 37°C before fixation of the cells with 100 µl 8% (v/v) formaldehyde (Fisher Scientific; #11586711)) in PBS at room temperature for 20 mins. The media/formaldehyde was removed, and wells washed three times with 100 µl PBS, and then permeabilised with 0.1% Triton X-100 for 5 mins. Cells were labelled with Hoescht 33342 (2µg.ml^{-1} final concentration; Molecular Probes #H32721) for 30 mins at room temperature, then washed three times with PBS and plates sealed. Images of Hoescht-labelled nuclei were acquired using the ImageXpress® Micro XL System (Molecular Devices), a multi wavelength wide-field fluorescent microscope with a 20x S Plan Fluor objective, and analysed using the Cell Cycle module in the MetaXpress® software. This software enables cell-by-cell cell cycle classification into G0/G1, S phase and early and late mitosis. Briefly, to configure the analysis, an image of stained cell nuclei was used to define the size and intensity thresholds. The integrated intensity of the nuclear stain was then used to quantify DNA content. Image analysis was performed with the assistance of Dr John Dawson, Drug Discovery Group, University of Edinburgh.

2.2.8 Apoptosis and cell death assays

To assess the apoptotic effects of taxanes and inhibitors on the isogenic cell lines, cells were seeded and cultured in 96-well plates as described above for 24 hrs. Cultures were subsequently treated with an 8-point semi-log concentration curve of drug. Negative control wells were treated with vehicle only (0.1% v/v DMSO) and positive control wells with 300nM staurosporine. To allow real time quantification of apoptosis and cell death, Incucyte® Caspase-3/7 reagent (Essen Bioscience; #4440) or DRAQ7™ (Abcam; ab109202) reagent were used. The Incucyte® Caspase-3/7 apoptosis assay reagent couples the activated capase-3/7 recognition motif (DEVD) to a DNA intercalating dye which enables real-time quantification of cells. DRAQ7™ is a membrane-permeable dye that only stains the nuclei of dead or permeabilised cells. Incucyte® Caspase-3/7 or DRAQ7™ were added at the same time as addition of inhibitors at final concentrations of 5 µM or 3µM respectively. Four images per well in the phase and fluorescent channels using a 10x objective were captured every 3 hours for 72 hours. Mean confluence for both phase and fluorescent channels at every timepoint were obtained using IncuCyte ZOOM® software and data extracted as a csv file. Values were normalised to the average of all wells at time zero and apoptosis expressed as a percentage of total confluence. All experiments were performed in triplicate.

2.2.9 Transient transfection of small interfering RNA (siRNA)

Knockdown of target genes was achieved through reverse siRNA transfection according to Lipofectamine® RNAiMAX manual instructions. ON-TARGET*plus* siRNA reagent human SMARTpool targeting MDR1, GAPDH and scrambled siRNA control (GE Healthcare Dharmacon) were reconstituted in distilled H_2O to achieve a stock concentration of 20 µM according to manufacturer's instructions and aliquots stored at -80°C. siRNA targeting GAPDH was included as a positive control for transfection. Negative controls included lipofectamine only and mock transfection with a scrambled non-targeting siRNA.

For each well to be transfected, master mixes of RNAi-Lipofectamine complexes were prepared as follows: 20 µM siRNA was diluted 1:500 in OptiMEM™ I Reduced Serum Medium in give a final volume of 2000 µl. 14.4 µl Lipofectamine® RNAiMAX reagent was added and mixed gently before aliquoting 25 µl of RNAi-Lipofectamine complexes in a 96-well plate. Incubation at room temperature for a further 15 mins allowed complex formation to occur. Cells were prepared at a concentration of 6.7 x 10^4.ml^{-1}. 75 µl of the resulting cell suspension was then added to each well to give a final siRNA concentration of 10 nM and the solutions mixed by gentle agitation. Plates were incubated overnight before the media was replaced with complete growth media. Paclitaxel or docetaxel over an 8 semi-log concentration range was added to triplicate wells per concentration point. 0.1% v/v DMSO controls were included. After a further 72 hrs the proliferation of each well was assessed by CCK-8 assay as previously described.

To confirm knockdown of target protein, RNAi-Lipofectamine complexes were formed by aliquoting 2.5µl siRNA (20 µM) diluted in 250µl OptiMEM I Reduced Serum Medium (Thermo Fisher Scientific; #31985-062) in a 6 well tissue culture plate. 7.5 µl Lipofectamine® RNAiMAX transfection reagent (Thermo Fisher Scientific; #13778075) was then added to each well, gently mixed and complexes allowed to form by incubation for 15 mins at room temperature. A total of 2.5 x 10^5 cells were added to each well and gently mixed by rocking the plate back and forth. After 16 hours, the media was aspirated and replaced with complete growth medium containing maintenance doses of taxane if applicable. After 72 hours, the cells were lysed with RIPA buffer for protein analysis.

2.2.10 Nucleic Acid Analysis

2.2.10.1 DNA Extraction

Cells were cultured in 75cm^3 tissue culture flasks and after 72 hrs, 5 x 10^6 cells collected as a pellet prior to lysis using the DNeasy® Blood and Tissue Kit (Qiagen,

#69514) according to manufacturer's instructions. Briefly, the cell pellet was resuspended in PBS prior to cell lysis with Proteinase K for 10 mins at 56°C. An equivalent volume of ethanol was added to the sample before loading the lysate into a DNeasy mini spin column. The sample was centrifuged for 1 minute at 8000 rpm. After a series of washes, the column was placed in a fresh 1.5ml tube before elution. Extracted DNA quantification was performed using a Nanodrop ND-1000 Spectrophotometer. Samples were aliquoted and stored at 4°C.

2.2.10.2 RNA Extraction

Cells were seeded in 6 well plates at a concentration of 3 x 10^5 cells.ml^{-1} and incubated for 24 hrs before addition of compounds of interest. DMSO only controls were included at a final concentration of 0.1% v/v. Duplicate wells were seeded for each treatment and pooled for nucleic acid extraction.

Cells were cultured for 48hrs before trypsinisation and 5 x 10^6 – 1 x 10^7 cells collected as a pellet prior to lysis using the RNeasy Mini Kit (Qiagen, #74104) according to manufacturer's instructions. Briefly, RLT buffer was added to the pellet to lyse cells and the lysate added to a QIAshredder spin column (Qiagen, #79654) and homogenised by centrifugation for 5 mins at 14,000 rpm. An equivalent volume of ethanol was added to the homogenised lysate before loading into an RNeasy spin column and centrifugation for 15 secs at 14,000 rpm. On-column DNase digestion was carried out before a series of wash steps to remove contaminants. The column was placed in a fresh 1.5ml tube before elution in 30 µl RNase-free water. Extracted RNA quantification was performed using a Nanodrop ND-1000 Spectrophotometer. Samples were aliquoted and stored at - 80°C.

2.2.10.3 Mutational Profiling of cell lines by MSK-IMPACT

This experiment was performed in collaboration with Dr Melanie Spears, OICR, Toronto, Canada.

Briefly, genomic DNA from the parental and taxane resistant cells were sequenced using the MSK-IMPACT platform, a capture-based Next Generation Sequencing (NGS) assay capable of identifying sequence mutations, copy number alterations and select gene fusions. Genomic DNA was sheared and sequencing libraries prepared through several enzymatic steps, including end repair, A-base addition and ligation of Illumina sequence adaptors followed by PCR amplification. Adaptors containing 6-mer unique barcodes corresponding to the Illumina TruSeq barcoding system were used in the library preparation. A mix of blocker oligos synthesized at IDT (Integrated DNA Technologies, Coralville, IA) and compatible with the TruSeq barcodes was also added to the pool to help prevent nonspecific binding and improve target capture specificity. Custom DNA probes targeting exons and selected introns of 341 genes were synthesized using the NimbleGen SeqCap EZ library custom oligo system and were biotinylated to allow for sequence enrichment by capture using streptavidin-conjugated beads. Pooled libraries containing captured DNA fragments were subsequently sequenced on the Illumina HiSeq 2500 system (rapid-run mode) as 2 × 100-bp paired-end reads. Sequence reads are then aligned to the reference human genome. By comparing the identity of bases from the tumour DNA to the matched normal DNA and the reference human genome, somatic alterations are identified in the tumour.

2.2.10.4 Nanostring Gene Expression

Nanostring nCounter® technology directly detects and quantifies individual target sequences in a highly multiplexed single reaction without the need for amplification or library preparation (215). The technology is based on direct molecular barcoding and digital detection of up to 800 target transcripts in one reaction using colour

coded probe pairs. The probe pair consists of two target specific probes; a 50 base reporter probe with a unique fluorescent barcode on the 5' end and a 50 base capture probe with a biotin tag at the 3' end to enable complex immobilisation to a proprietary cartridge prior to quantification.

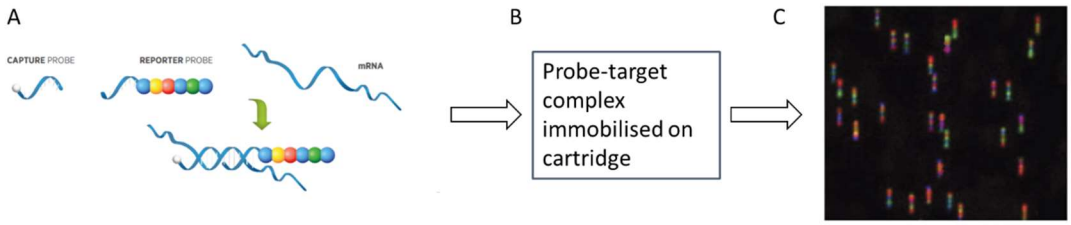

Figure 2.2: Summary of Nanostring nCounter® technology A) Capture and reporter probes are hybridised with mRNA to form probe-target complexes. B) Complexes are immobilised to cartridge C) False colour image of detected digital probes. (Adapted from Nanostring)

2.2.10.4.1 Sample hybridisation and processing

Total RNA extracted from the resistant and parental taxane resistant cell lines were normalised to 20ng.µl^{-1}. Triplicate samples were included in each analysis. Hybridisation was performed according to manufacturer's instructions using the nCounter® PanCancer Pathway panel which covers 770 genes and 13 canonical cancer hallmark pathways including MAPK, STAT, PI3K, RAS, Cell Cycle, Apoptosis, Hedgehog HH, Wnt, APC, DNA Damage, Transcriptional Regulation, Chromatin Modification and TGFβ (XT-CSO-PATH1-1). The panel included housekeeping genes which were used during the normalisation process. Briefly, a hybridisation master mix was prepared by adding 70 µl hybridisation buffer to the Reporter CodeSet and mixed by inversion of the tube. 8 µl of the master mix was aliquoted into each tube of a pre-labelled 12-tube strip. Thereafter 5 µl total RNA (100 ng) and 2 µl Capture ProbeSet were added to each well. Samples were placed in a pre-heated thermocycler at 65°C before incubation at 80°C for 18 hours to allow probe hybridisation to the target sequences.

The following day samples were transferred to the nCounter® Prep Station. This fully automated liquid handling platform uses affinity purification to remove excess probes. Capture probes were bound to magnetic beads and unbound reporter probes washed away. This was followed by a second wash where excess capture probes were removed. Finally the purified Target-Probe complexes were eluted and immobilised onto the nCounter® cartridge for data collection.

For automated imaging and barcode quantification, the cartridge was then moved to the nCounter® digital analyser. Images are collected from the immobilised fluorescent reporter probes with a charge coupled device (CCD) camera through a microscopic objective lens at a resolution of 555 fields of view (FOV). The expression levels of each gene were then evaluated by counting the number of times its unique barcode was detected and data reported in the form of a Reporter Code Count (RCC) file and exported as a csv file for further analysis.

All Nanostring nCounter® reagents were sourced from Nanostring Technologies Inc, Seattle, USA. Sample processing was carried out with the assistance of Nicola Lyttle, OICR, Toronto, Canada.

2.2.10.4.2 Data normalisation and statistical analysis

Data normalisation and analysis was performed by using nSolver 4.0 and advanced analysis 2.0 plug-in which utilises the statistical analysis package R 3.3.2. A reporter library file (RLF) specific to each codeset was uploaded to nSolver 4.0 which identified which probe was associated with each gene. The RCC files were then uploaded to the software. Samples were assigned to studies as groups of native parental cell lines and isogenic taxane resistant cell lines.

For each codeset, internal positive and negative controls were added at the time of manufacture. A series of robust quality control (QC) steps were automatically performed using the controls and internal reference genes. The efficiency of imaging, binding density, positive control linearity or positive control limit of detection QC

were assessed. Background thresholding was set as the mean of the negative controls. Finally, normalisation of samples was performed employing a combination of positive control normalisation and codeset content normalisation. Positive control normalisation adjusted for variation in sample processing (pipetting, scan resolution, lot-to-lot variation in plates etc) while codeset content normalisation accounts for input variability.

Statistically significant, differentially expressed genes (DEGs) were defined as those with fold change expression levels corresponding to log2 ratio ≥0.58 or ≤-0.58 (equivalent to fold change = 1.5) and a p-value ≤ 0.05.

2.2.11 Protein Methods

2.2.11.1 Protein lysate preparation

Cells were seeded in 6 well plates or 10cm^2 plates, with appropriate inhibitor treatments if required, and incubated until 80% confluence was reached. Media was removed and cell monolayers were washed twice with ice cold PBS. The plates were placed on ice and RIPA buffer with phosphatase and protease inhibitors added (100µl per 6 well or 200µl per 10cm^2 plate). Cells were scraped off the surface of the culture vessel, the suspension collected and incubated on ice for 10 mins. Cell lysates were centrifuged at 13, 000 rpm for 10 mins at 4°C and the supernatant transferred to a fresh 1.5ml microcentrifuge tubes. All samples were stored at -20°C.

Protein concentrations were evaluated by bicinchoninic assay (BCA). An 8-point standard curve using protein standard was created (1mg.ml^{-1} bovine serum albumin (BSA) (Sigma Aldrich; #82516). Lysates were diluted 1:10 in RIPA buffer. Fresh BCA solution was prepared by mixing copper (II) sulphate (Sigma Aldrich; C2284) with BCA (Sigma Aldrich; B9643). 1ml of this solution was added to 50 µl of diluted lysates and incubated for 15 mins at 60°C. In a 96 well plate, 200 µl of each sample was added in duplicate to appropriate wells. OD values were obtained by measuring absorbance at

540 nm using a Biorad iMARK plate reader and protein concentrations determined from the standard curve.

2.2.11.2 SDS-Polyacrylamide Gels and Western Blotting

To detect proteins of interest, denatured protein lysates were resolved by SDS-polyacrylamide gel electrophoresis (SDS-PAGE). 10% resolving and 3.6% stacking gels were prepared as outlined in Table 2.3. 10µg protein lysates were prepared in a final volume of 10µl in PBS to which 5µl 3 x SDS-PAGE sample buffer was added. Protein lysates were denatured at 95°C for 5 mins. Samples and SeeBlue™ Plus2 Pre-Stained Standard (Thermo Fisher Scientific; #LC5925) were separated by electrophoresis in a BioRad mini-PROTEAN II gel chamber with the gels run in Tris-Glyicine-SDS running buffer at 100V for 90 mins.

Table 2.6: Volumes of solutions required for two mini-Protean SDS-PAGE

	10% resolving gel (ml)	3.6% stacking gel (ml)
30% (w/v) acrylamide (Severn Biotech; #20-2100-10)	6.7	1.2
1M Tris, pH8.8	7.5	-
0.375M Tris pH6.8	-	3.3
10% (w/v) SDS	0.2	0.1
MilliQ H_2O	5.84	5.3
10% (w/v) Ammonium persulphate (Sigma; A3678)	0.2	0.1
TEMED (Sigma; T9281)	0.02	0.02

Proteins were transferred on to nitrocellulose membranes by wet transfer blotting in Tris-glycine transfer buffer at 100V, constant 350mA for 1.5hrs. Membranes were blocked with blocking buffer for 1 hr at room temperature before incubation with primary antibodies at 4°C overnight on a rocking platform. They were then washed twice with TBS-T (0.1% v/v) for 5 mins before addition of appropriate secondary antibodies and incubation for 1 hour at room temperature on a rocking platform. Membranes were washed 3 times for 5 mins with TBS-T, before a final wash in TBS. Antibodies were detected by chemiluminescence by incubating membranes with BM Chemiluminescence western blotting substrate (Sigma Aldrich; #11500694001) for 1 minute before imaging in the ChemiDoc XRS+ Imaging System (BioRad).

2.2.11.3 Reverse Phase Protein Array

Cell lysates from parental and taxane resistant cells were prepared in 1 x RPPA lysis buffer supplemented with cOmplete™ ULTRA protease inhibitor (Sigma Aldrich; #5892970001) and PhosSTOP™ phosphatase inhibitor cocktails (Sigma Aldrich; #4906845001). After clearing by centrifugation at 13,300 rpm for 10 min at 4°C the protein concentration was determined using a BCA assay. The samples were adjusted to a final concentration of 2 $mg.ml^{-1}$ followed by denaturation upon addition of 4 x RPPA sample buffer at 95˚C for 5 minutes. Samples were stored at -80˚C until required.

A four-step doubling dilution series for each sample was prepared in PBS with 10% v/v glycerol to give final concentrations of 1.5$mg.ml^{-1}$, 0.75 $mg.ml^{-1}$, 0.375 $mg.ml^{-1}$, and 0.1875 $mg.ml^{-1}$. RPPA samples were spotted in technical triplicates in arrays of 12 x 12 spots at a 500µm spot-to-spot distance using the Aushon 1740 Arrayer platform (Quanterix) on to SuperNova Nitrocellulose slides (Grace Bio-Labs; #705278) under conditions of 70% constant humidity. The slides were incubated with the sample for at least one hour to ensure sample capture on the nitrocellulose membrane. After washing, the slides were incubated with Reblot Plus Strong (Merck Millipore; #2504) for 15 minutes. The membrane was then washed twice with deionized water then twice in PBS-T for 15 minutes.

The arrayed slides were blocked using SuperBlock™ T-20 blocking buffer (Thermo Fisher Scientific; #37536), and each sub-array separately incubated with validated primary antibodies (table x) diluted 1:250 in Superblock™ T-20. The slides were washed twice in TBS-T, then blocked for 10 minutes as described above. Bound antibodies were detected by incubation with anti-rabbit or anti-mouse DyLight 800-conjugated secondary antibodies (New England Biolabs; #5151 and #5257 respectively) as appropriate. Slide images were acquired using an InnoScan 710-IR scanner (Innopsys) with laser power and gain settings optimised for highest readout without saturation of the fluorescence signal. The relative fluorescence intensity of each array feature was quantified using Mapix software (Innopsys).

The linear fit of the dilution series of each sample was verified for each primary antibody and the median relative fluorescence intensity from the dilution series was calculated to represent relative abundance of total protein and post-translational epitopes across the sample set. Signal intensities for each sample were normalized to total protein loading on the array slides by using the signal readout from a Fast Green FCF (total protein) stained array (Sigma Aldrich; #F7258) before final global sample median normalisation.

RPPA assay processing was performed by Kenny Macleod from the HTPU facility, Institute of Genetics and Cancer, University of Edinburgh.

Table 2.7: Primary antibodies used for RPPA

Antibody	Supplier	Catalogue Number	Species
4E-BP1 P Ser65	CST	9451	rabbit
4E-BP1 P Thr37, Thr46	CST	2855	rabbit
Akt	CST	9272	rabbit
Akt P Ser473	CST	4060	rabbit
Akt P Thr308	CST	2965	rabbit
AMPK alpha	CST	2532	rabbit
AMPK alpha P Thr172	CST	2535	rabbit
ATM	Merck (Calbiochem)	PC116	rabbit
ATM/ATR Substrate P Ser/Thr	CST	2851	rabbit
Aurora A/B/C P Thr288/Thr232/Thr198	CST	2914	rabbit
Bad P Ser112	CST	9291	rabbit
Bad P Ser136	CST	9295	rabbit
Bak	Epitomics	1542-1	rabbit
Bax	Epitomics	1063	rabbit
Bcl-2	Epitomics	1017-1	rabbit
Bcl-2 P Ser70	CST	2827	rabbit
Bcl-xl	Epitomics	1018	rabbit

beta-actin	CST	4970	rabbit
beta-Catenin	CST	9562	rabbit
beta-Catenin P Ser33, Ser37, Thr41	CST	9561	rabbit
beta-Catenin P Thr41, Ser45	CST	9565	rabbit
beta-Tubulin	Abcam	ab6046	rabbit
Bid	Abcam	ab32060	rabbit
Bim	Epitomics	1036	rabbit
Bim P Ser69	CST	4585	rabbit
BRCA1	CST	9010	rabbit
Calmodulin	CST	NB12	Mouse IgG1
Calpain2	CST	2539	rabbit
Calpastatin	CST	4146	rabbit
CamKII alpha (22B1) P Thr286	Abcam	ab2724	Mouse IgG1
CamKII P Thr286	CST	3361	rabbit
Caspase 3	CST	9662	rabbit
Caspase 3 cleaved	CST	9664	rabbit
cdc25A	CST	3652	rabbit
cdc25c P Ser216	CST	4901	rabbit
CDK1 (cdc2)	CST	9112	rabbit

CDK1 (p34cdc2) P Tyr15	CST	9111	rabbit
CDK2	Abcam	ab32147	rabbit
Chk1 P Ser345	CST	2348	rabbit
Chk2 P Thr68	CST	2661	rabbit
c-Jun N-term	Epitomics	1254-1	rabbit
c-Jun P Ser73	CST	9164	rabbit
c-Myc	CST	5605	rabbit
c-Myc P Thr58, Ser62	Epitomics	1203-1	rabbit
CREB	CST	9197	rabbit
CrkL	CST	3182	Mouse IgG1
CrkL P Tyr207	CST	3181	rabbit
Cyclin D1	CST	2926	Mouse IgG2a
Cyclin D1 P Thr286	CST	3300	rabbit
E-Cadherin	CST	3195	rabbit
EGFR P Tyr1086	ThermoFisher	369700	rabbit
EGFR P Tyr1173	CST	4407	rabbit
ErbB-1/EGFR	CST	4267	rabbit
ErbB-2/Her2/EGFR	Dako	A0485	rabbit
ErbB-2/Her2/EGFR P Tyr1248/Tyr1173	CST	2244	rabbit

ErbB-3/Her3/EGFR	CST	4754	rabbit
ErbB-3/Her3/EGFR P Tyr1289	CST	4791	rabbit
FAK1	CST	3285	rabbit
FAK1 P Y397	CST	3283	rabbit
FLT3 P Tyr591 P Tyr591	CST	3461	rabbit
FRA1 (R20)	Santa Cruz	sc-605	rabbit
GAPDH	Abcam	ab9484	Mouse IgG2b
GFAP	Abcam	ab7260	rabbit
GSK-3-alpha/beta P Ser21/Ser9	CST	9331	rabbit
GSK-3-beta	CST	9315	rabbit
GSK-3-beta P Ser9	CST	9336	rabbit
Hexokinase	CST	2867	rabbit
Histone H2A.X P Ser139	Millipore (Upstate)	05-636	Mouse IgG1
HSP27 (HSPB1)	CST	2402	Mouse IgG1
HSP27 (HSPB1) P Ser78	CST	2405	rabbit
IGF-1R beta	CST	3027	rabbit
IGF-1R beta P Tyr1162, Tyr1163	Invitrogen (Biosource)	44-804G	rabbit
IkB-alpha	CST	4812	rabbit

IkB-alpha P Ser32	CST	2859	rabbit
IKK alpha/beta P Ser176/Ser177	CST	2078	rabbit
IRS-1	CST	2382	rabbit
IRS-1 P S636/639	CST	2388	rabbit
JAK1	CST	3332	rabbit
JAK1 P Tyr1022, Thr1023	Invitrogen (Biosource)	44-422G	rabbit
Ki-67 (Annexin II, p36)	Beckton Dickinson	610968	Mouse IgG1
LKB1	CST	3047	rabbit
MAPKAPK-2	Epitomics	1497-1	rabbit
MAPKAPK-2 P Thr334	CST	3041	rabbit
M-CSF P Tyr723	CST	3155	rabbit
MEK1/2	CST	9122	rabbit
MEK1/2 P Ser217/221	CST	9154	rabbit
Met	CST	4560	rabbit
Met P Tyr1234	Signalway	11227-1	rabbit
Met P Tyr1349	Signalway	11238	rabbit
MNK1 (MKNK) P Thr197, Thr202	CST	2111	rabbit
MSK1 P Ser376	CST	9591	rabbit
mTOR	CST	2972	rabbit

mTOR P Ser2448	CST	2971	rabbit
mTOR P Ser2481	Millipore (Upstate)	09-343SP	rabbit
NFkB p105/p50	GeneTex	GTX110585	rabbit
NFkB p65 Ser536	CST	3033	rabbit
p21 CIP/WAF1	CST	2946	Mouse IgG2a
p21 CIP/WAF1 p Thr145	Santa Cruz	sc-20220-R	rabbit
p38 MAPK	CST	9212	rabbit
p38 MAPK PThr180, Tyr182	CST	9211	rabbit
p44/42 MAPK (ERK1/2)	CST	9102	rabbit
p44/42 MAPK (ERK1/2) P Thr202/Thr185, Tyr204/Tyr187	CST	4370	rabbit
p53	CST	9282	rabbit
p53 P Ser15	CST	9284	rabbit
p70 S6 Kinase	CST	9202	rabbit
p70 S6 Kinase P Thr389	CST	9205S	rabbit
p70 S6 Kinase P Thr421, Ser424	CST	9204	rabbit
p90 S6 kinase (Rsk1-3)	Santa Cruz	sc-231	rabbit
p90 S6 kinase (Rsk1-3) P Thr359, Ser363	CST	9344	rabbit
PARP	CST	9542	rabbit

PARP cleaved Asp214	CST	9541	rabbit
PDGFR P Tyr751	CST	4549	rabbit
PDGFR P Tyr1021	CST	2227	rabbit
PDK-1	CST	3062	rabbit
PDK-1 P Ser241	CST	3061	rabbit
PI3 Kinase p110-alpha	CST	4249	rabbit
PKA	Abcam	ab26322	rabbit
PKA RII P Ser96	Epitomics	1151-1	rabbit
PKC (pan) P Ser660 (beta-2)	CST	9371	rabbit
PKC substrate P (R/K)	CST	2261	rabbit
PKC-alpha	Beckton Dickinson	610108	Mouse IgG2b
PKC-alpha P Thr638	Abcam	ab32502	rabbit
PKC-gamma P Thr514	GeneTex	GTX25778	rabbit
PKC-zeta	CST	9372	rabbit
PKC-zeta/lambda P Thr410/403	CST	9378	rabbit
PKM2 XP(R)	CST	4053	rabbit
PLC-gamma1	CST	2822	rabbit
PLC-gamma1 P Tyr783	CST	2821	rabbit
Prohibitin	Santa Cruz	sc-28259	rabbit

PTEN	CST	9552	rabbit
PTEN P Ser380, Thr382, Thr383	CST	9554	rabbit
Puma	CST	4976	rabbit
Raf P Ser259	CST	9421	rabbit
Raf P Ser338	CST	9427	rabbit
Raf1 (C-12)	Santa Cruz	sc-133	rabbit
Rap1	CST	4938	rabbit
Ras	Beckton Dickinson	610001	Mouse IgG1
Rb	Abcam/Epitomics	ab113074	rabbit
Rb P Ser807, Ser811	CST	9308	rabbit
Rb P Ser780	CST	9307	rabbit
Rsk2 Pser 227	CST	3556	rabbit
S6 Ribosomal Protein	CST	2217	rabbit
S6 Ribosomal protein P Ser235, Ser236	CST	2211	rabbit
S6 Ribosomal protein p Ser240, Ser244	CST	2215	rabbit
SAPK/JNK (JNK2)	CST	9258	rabbit
SAPK/JNK P Thr183, Tyr185	CST	4668	rabbit
SHP2 P Tyr542	CST	3751	rabbit
Smad1/5 P Ser463/Ser465	CST	9516	rabbit

Smad2 P Ser465, Ser467	CST	3108	rabbit
Smad2/3 P Ser465/Ser423, Ser467/Ser425	CST	8828	rabbit
Smad3 P Ser423, Ser425	CST	9520	rabbit
SQSTM1	CST	8025	rabbit
Src	CST	2109	rabbit
Src (family) P Tyr416	CST	2101	rabbit
Stat1	CST	9176	Mouse IgG1
Stat1 P Ser727	Invitrogen (Biosource)	44-382G	rabbit
Stat1 P Tyr701	CST	9171	rabbit
Stat3	CST	12640	rabbit
Stat3 P Tyr705	CST	9138	Mouse IgG1
Stat5	Invitrogen (Biosource)	44-368G	rabbit
Stat5 P Tyr694	CST	9351	rabbit
Stat6	CST	9362	rabbit
Stat6 P Tyr641	CST	9361	rabbit
Survivin	CST	2808	rabbit

Tau	Abcam/Epitomics	ab32057	rabbit
Tau Phospho/non Phos ser 305	Epitomics	2368-1	rabbit
TBK1/NAK	CST	3504	rabbit
Tsc-2 (Tuberin)	CST	3612	rabbit
Tsc-2 (Tuberin) P Thr1462	CST	3617	rabbit
Tuberin P S1387	CST	5584	rabbit
Tyk2 P Tyr1054, Tyr1055	CST	9321	rabbit
Ubiquitin (P4D1)	CST	3936	Mouse IgG1
VEGFR P Tyr1059	CST	3817	rabbit
VEGFR P Tyr1175	CST	2478	rabbit
VEGFR P Tyr951	CST	4991	rabbit
XIAP	CST	2045	rabbit
Zap70	CST	2705	rabbit

CST: Cell Signalling Technologies

2.2.12 Data Analysis

Graphing of results and statistical analysis were performed using GraphPad Prism v6.0 software. Details of statistical tests are provided in figure legends.

Functional interaction network visualisation was achieved through use of Cytoscape 3.9.0 (216) and the Reactome FIViz app (217). Gene Ontology (GO) analysis of

differentially expressed genes, including biological process (BP) and molecular function (MF), and Kyoto encyclopaedia of genes and genomes (KEGG) pathway analysis were enriched using the Database for Annotation, Visualisation and Integrated Discovery (DAVID) (https://david.ncifcrf.gov/tools.jsp).

3. GENERATION AND CHARACTERISATION OF ISOGENIC CELL LINE MODELS WITH ACQUIRED RESISTANCE TO TAXANES

3.1 Introduction

Anthracyclines and taxanes are the most active and widely used adjuvant chemotherapeutics in the treatment of breast cancer in hormone receptor-negative patients, or for those with acquired resistance to endocrine therapy (141). They are commonly used in the adjuvant setting either in combination or sequentially (218). However, upon disease relapse it is often found that the tumours are no longer responsive to these drugs. Despite the importance of taxanes as a treatment option for solid tumours, their use is limited by the development of chemoresistance (acquired or intrinsic) and represents a major clinical obstacle in the treatment of the disease.

Acquired resistance may develop as a result of complex events including changes in signalling pathways, drug metabolising enzymes and drug efflux or through epigenetic changes such as DNA modification or histone acetylation which deregulate expression of normal genes (219). Exploration of the mechanisms driving taxane resistance may lead to the identification of biomarkers and guide effective treatment options for treatment resistant breast cancer. The development and use of preclinical models are therefore key to defining these underlying drivers. In this study acquired resistance models were derived by sustained exposure of the selected breast cancer cell lines to either paclitaxel or docetaxel. Cell lines were chosen to represent the different molecular subtypes of breast cancer. By deriving isogenic models differential analyses can be performed by comparing the paired parental and resistant cell lines. This chapter describes the development and characterisation of isogenic *in vitro* models of acquired taxane resistance in breast cancer.

3.2 Results

3.2.1 Sensitivity of breast cancer cell lines to taxanes

We have previously developed paclitaxel-resistant MDA-MB-231 (MDA-MB-231 PACR) and ZR-75-1 lines which are resistant to paclitaxel (ZR-75-1 PACR) and docetaxel (ZR-75-1 DOCR) respectively (220). The initial aim of this project was to expand the panel of isogenic taxane resistant breast cancer cell lines to include representative examples of the main breast cancer subtypes through exposure to either paclitaxel or docetaxel.

The breast cancer cell lines MDA-MB-231, MCF7 and SKBR3 were identified as representing the different molecular subtypes of breast cancer. MDA-MB-231 represents a triple negative breast cancer, lacking receptors for oestrogen (ER), progesterone (PR) and human epidermal growth factor receptor 2 (HER2). MCF7 is an example of a hormone-dependent breast cancer, expressing ER and PR but not HER2. SKBR3 was included to represent a HER2 over-expressing breast cancer cell line which is negative for ER and PR hormone receptors.

To assess the sensitivity of SKBR3, MDA-MB-231 and MCF7 to taxanes I treated the cell lines with escalating doses of paclitaxel or docetaxel across an 8 semi-log concentration range for 72 hrs before performing a CCK8 assay for proliferation. Each experiment was performed in triplicate and the mean IC_{50} and SEM calculated. It was found that both taxanes inhibited the proliferation of all tested cell lines in a nanomolar range indicating their sensitivity to the drugs. For paclitaxel the mean IC_{50} for MDA-MB-231 was 3.97 nM, for MCF7 2.99 nM and for SKBR3 7.37 nM. Similar ranges of sensitivity was observed upon exposure to docetaxel with a mean IC_{50} was 2.34 nM for MDA-MB-231, 5.46 nM for MCF7 and 1.46 nM for SKBR3 (Figure 3.1).

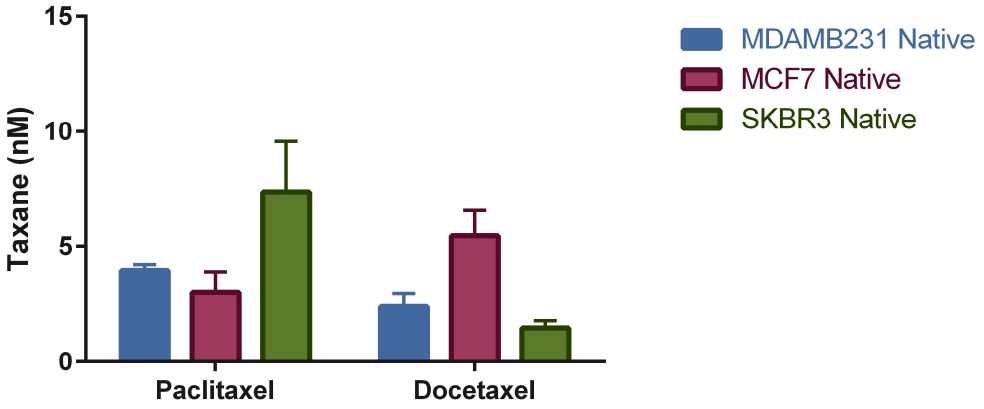

Figure 3.1: Half maximum inhibitory concentrations (IC50) for docetaxel and paclitaxel of parental breast cancer cell lines. 96 well plates were seeded with 5000 cells/well for each cell line and after 24hrs treated with increasing doses of paclitaxel or docetaxel for 72hrs. CCK-8 assays were then performed and data analysed using GraphPad Prism 6 software. Results are expressed as mean IC50 ± SEM of three independent experiments performed in triplicate for each cell line.

3.2.2 Establishment of taxane resistant cell lines

MDA-MB-231, MCF7 and SKBR3 cells were each cultured in two T25 flasks. When the cells were approximately 80% confluent, treatment with paclitaxel or docetaxel was commenced. Two T175 flasks of untreated cells were also grown to 80% confluence and frozen down as master stocks of the parental native cell line to be used as controls in all subsequent experiments.

An incremental dosage schedule was applied, starting at 0.5 nM of each drug and allowing the cells to passage twice before increasing the dose by 0.5 nM at a time until it was clear that the developing cell lines could tolerate a larger increase in taxane concentration. Thereafter increments were typically 2 nM each time, rising to 5 nM as the lines became established. The timing of each increment was guided by the ability of the cell line to adapt to a given concentration of taxane. Media with fresh taxane was replaced twice weekly. When the cells reached 80% confluence, one flask was passaged on while the other flask was frozen down to provide stocks of the full concentration range of taxanes used to establish each line (Figure 3.2).

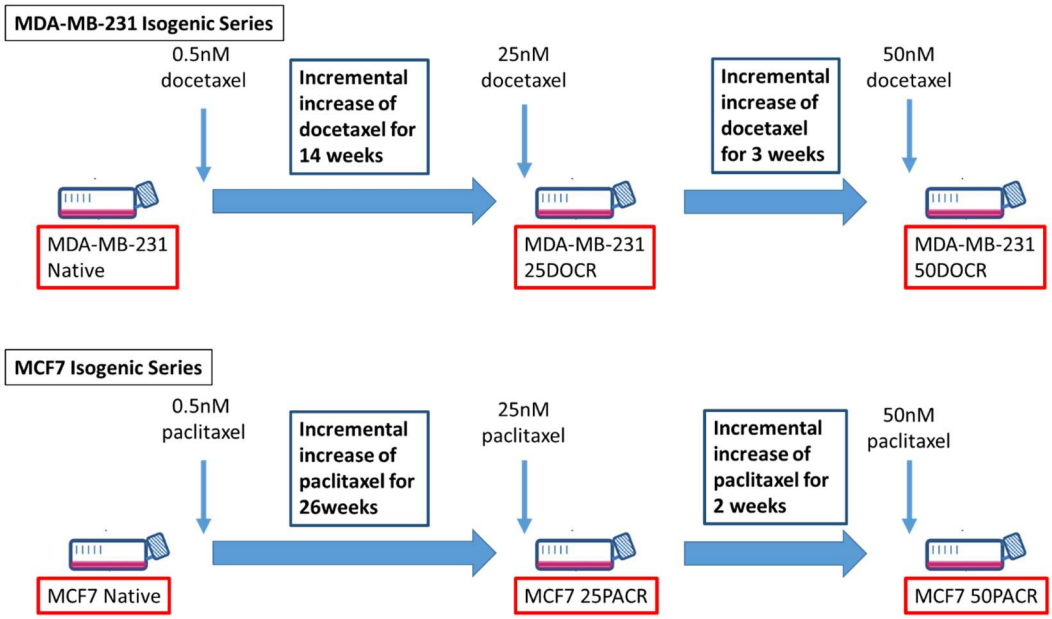

Figure 3.2: Development of taxane resistant isogenic breast cancer cell lines

Incremental and continuous dosage of taxane continued until resistance at 50 nM was reached. At this point it was considered that a resistant phenotype had been achieved as the cell lines continued to proliferate at a taxane concentration that represented a dosage greater than 10 times that of the IC_{50} for each cell line. Established lines were maintained in either paclitaxel or docetaxel throughout culture and all further experiments, unless otherwise stipulated.

Docetaxel-resistant isogenic cell lines were generated for MDA-MB-231 along with paclitaxel-resistant MCF7. A MDA-MB-231 isogenic cell line resistant at 25 nM docetaxel took 14 weeks to establish and resistance to 50nM docetaxel a further three weeks. The development of a paclitaxel resistant MCF7 line took twice as long to establish, with the cells stalling at a paclitaxel concentration of 10 nM. By reducing each dosage increments to 1 nM paclitaxel, establishment of a more robust culture was achieved at 15 nM which could withstand more significant increases in taxane

concentration. A stable line at 25 nM was established after approximately 26 weeks in culture and resistance at 50 nM after another two weeks.

A stable isogenic MCF7 line resistant to docetaxel was not achievable, regardless of several attempts to establish this line. No MCF7 cells survived an increase above 5 nM with total cell death being observed in the flasks. Attempts were made to establish a resistant phenotype by reducing the increments to 0.1 nM at a time but this also failed to produce a population of cells that would survive above the IC_{50} for docetaxel. The decision was therefore made not to pursue the establishment of a docetaxel-resistant line. Likewise, it proved impossible to establish a stable taxane resistant cell line with SKBR3 with either paclitaxel or docetaxel. No cells survived above a concentration of 10nM paclitaxel or docetaxel. Lines established at a lower dose of docetaxel proved unstable and over time reverted to a taxane sensitive phenotype. After repeated attempts the decision was made not to pursue establishment of taxane resistant SK-BR-3 isogenic cell lines.

It was observed that subtle morphological changes had occurred in the gross cell morphology of MDA-MB-231 cells rendered resistant to docetaxel. The native MDA-MB-231 cell line (Figure 3.3A) is typically described as being of an epithelial-like morphology with spindle shaped cells. The paclitaxel resistant MDA-MB-231 25PACR cell line closely resembled the parental cell line, with no gross morphological changes (Figure 3.3B) However, the docetaxel resistant MDA-MB-231 25DOCR cells appeared larger in size, with a more rounded shape (Figure 3.3C). The observed cellular morphology of the native MCF7 cell line (Figure 3.3D) was epithelial-like in nature, which was retained by the paclitaxel resistant MCF7 25PACR cell line (Figure 3.3E).

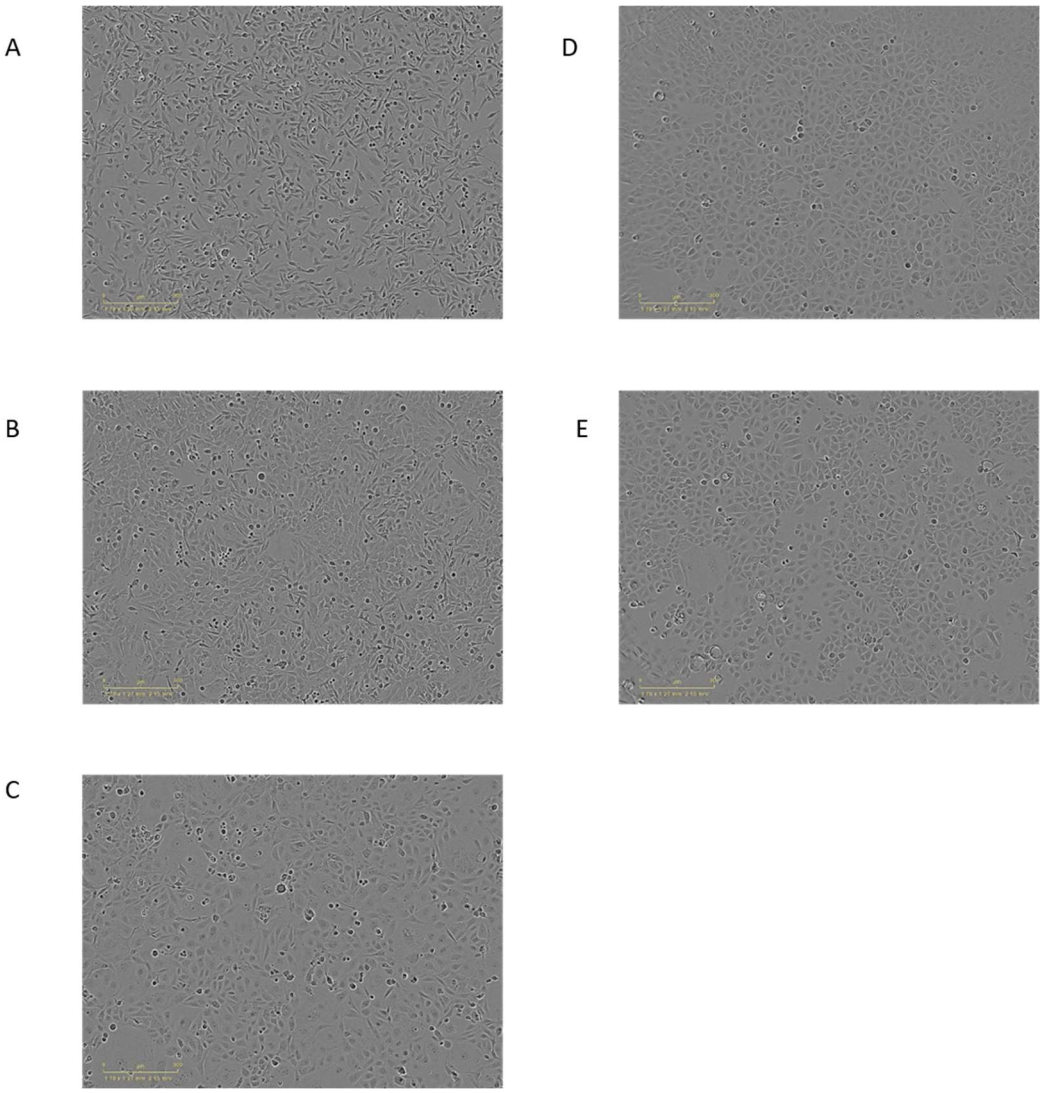

Figure 3.3: Representative phase contrast images of native and taxane resistant isogenic cell lines (A) MDA-MB-231 cells, (B) paclitaxel-resistant MDA-MB-231 25PACR cells, (C) docetaxel-resistant MDA-MB-231 25DOCR cells, (D) MCF7 cells and (E) paclitaxel-resistant MCF7 25PACR cells. Scale bar: 300 µm.

3.2.3 STR profiling of taxane resistant cell lines confirms parental lineage

Authentication of the cell lines was performed using STR (short tandem repeat) profiling to ensure parental lineage of the resistant cell lines. Using markers at 10 different loci (TH01, TPOX, vWA, CSF1PO, D16S539, D7S820, D13S317, D5S818, D21S11 and Amelogenin), it was confirmed that all taxane resistant lines were identical in origin to their respective parent.

Table 3.1: STR profile analysis of MDA-MB-231 and MCF7 isogenic cell lines.

Sample Name	Marker	Allele 1	Allele 2
MDA-MB 231 Native	**AMEL**	**X**	**X**
MDA-MB-231 25PACR	**AMEL**	**X**	**X**
MDA-MB-231 25DOCR	**AMEL**	**X**	**X**
MCF7 Native	**AMEL**	**X**	**X**
MCF7 25PACR	**AMEL**	**X**	**X**
MDA-MB 231 Native	CSF1PO	12	13
MDA-MB-231 25PACR	CSF1PO	12	13
MDA-MB-231 25DOCR	CSF1PO	12	13
MCF7 Native	CSF1PO	10	10
MCF7 25PACR	CSF1PO	10	10
MDA-MB 231 Native	D13S317	13	13
MDA-MB-231 25PACR	D13S317	13	13

MDA-MB-231 25DOCR	D13S317	13	13
MCF7 Native	D13S317	11	11
MCF7 25PACR	D13S317	11	11
MDA-MB 231 Native	D16S539	12	12
MDA-MB-231 25PACR	D16S539	12	12
MDA-MB-231 25DOCR	D16S539	12	13
MCF7 Native	D16S539	11	12
MCF7 25PACR	D16S539	11	12
MDA-MB 231 Native	D21S11	30	33.2
MDA-MB-231 25PACR	D21S11	30	33.2
MDA-MB-231 25DOCR	D21S11	30	33.2
MCF7 Native	D21S11	30	30
MCF7 25PACR	D21S11	30	30
MDA-MB 231 Native	D5S818	12	12
MDA-MB-231 25PACR	D5S818	12	12
MDA-MB-231 25DOCR	D5S818	12	12
MCF7 Native	D5S818	11	12
MCF7 25PACR	D5S818	11	12
MDA-MB 231 Native	D7S820	8	8
MDA-MB-231 25PACR	D7S820	8	8

MDA-MB-231 25DOCR	D7S820	8	8
MCF7 Native	D7S820	8	9
MCF7 25PACR	D7S820	8	9
MDA-MB 231 Native	TH01	7	9.3
MDA-MB-231 25PACR	TH01	7	9.3
MDA-MB-231 25DOCR	TH01	7	9.3
MCF7 Native	TH01	6	6
MCF7 25PACR	TH01	6	6
MDA-MB 231 Native	TPOX	8	9
MDA-MB-231 25PACR	TPOX	8	9
MDA-MB-231 25DOCR	TPOX	8	9
MCF7 Native	TPOX	9	12
MCF7 25PACR	TPOX	9	12
MDA-MB 231 Native	vWA	15	15
MDA-MB-231 25PACR	vWA	15	15
MDA-MB-231 25DOCR	vWA	15	15
MCF7 Native	vWA	14	15
MCF7 25PACR	vWA	14	15

The table shows the results at markers Amelogenin, CSF1PO, D13S317, D16S539, D21S11, D5S818, D7S820, TH01, TPOX and vWA.

3.2.4 Confirmation of taxane resistance

Once cells had been passaged for at least 3 weeks in the maintenance dose of either paclitaxel or docetaxel, sensitivity to taxanes was reassessed. Both parental and established resistant isogenic cell lines were treated with either paclitaxel or docetaxel across an 8 point semi-log concentration curve ranging from 0.3 nM to 1µM for 72hrs before proliferation was assessed by using a CCK8 assay. All experiments were performed in triplicate.

The parental cell lines were found to have IC_{50}s at levels previously reported when testing the sensitivity of the cell lines. The cell lines exposed to incremental dosing of taxanes were found to have significantly increased IC_{50}s and it was necessary to repeat the assessment of taxane sensitivity at a dose range of 3 nM to 10000 nM to produce a sigmoidal IC_{50} curve and accurate estimation of the IC_{50} in GraphPad Prism. The mean IC_{50} of docetaxel for MDA-MB-231 25DOCR was calculated as being 74 nM, representing 31-fold increase in tolerance to docetaxel exposure in the resistant line. An IC_{50} of 769 nM of paclitaxel was observed for MCF7 25PACR, a 183-fold increase in resistance. Due to the significant differences between the IC_{50}s of the parental cell lines and those exposed to taxanes, I concluded that the isogenic MDA-MB-231 and MCF7 lines had indeed been rendered resistant to docetaxel or paclitaxel, respectively.

Prolonged exposure to a single agent can lead to cross-resistance to structurally similar compounds. To address this possibility, resistance to the other taxane was also assessed. MDA-MB-231 25DOCR had an IC_{50} for paclitaxel of 415 nM, representing a 105 – fold increase compared to the sensitive parental cell line. This contrasted with the isogenic line derived from continuous paclitaxel exposure, MDA-MB-231 25PACR, which had an IC_{50} of 17.8 nM with docetaxel when compared to 2.4 nM calculated for the parental line, representing an 8-fold increase in resistance. MCF7 25PACR cells also demonstrated an increase in resistance to docetaxel with an IC_{50} of 43.1 nM, reflecting an 8-fold increase in resistance compared to the parental cell line. A summary of the mean IC_{50}s of both paclitaxel and docetaxel for all cell

lines are shown as a bar graph in Figure 3.4. Table 3.3 summarises the IC_{50} values for all tested cell lines, with resistance factors (the fold difference calculated by dividing the IC_{50} of resistant cells by the IC_{50} of the parental line) in parenthesis.

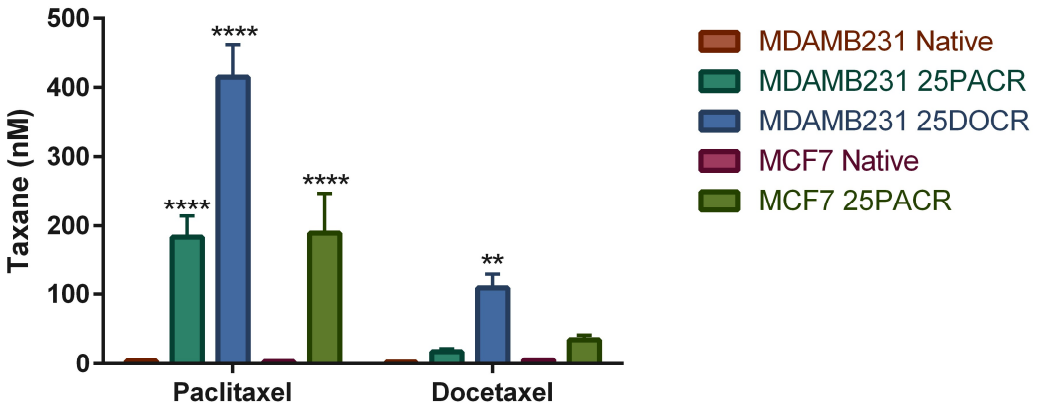

Figure 3.4: Half maximum inhibitory concentrations (IC50) for docetaxel and paclitaxel of taxane resistant isogenic cell line series. 96 well plates were seeded with 5000 cells/well for each cell line and after 24hrs treated with increasing doses of paclitaxel or docetaxel for 72hrs. CCK-8 assays were then performed and data analysed using GraphPad Prism 6 software. Results are expressed as mean IC50 ± SEM of three independent experiments performed in triplicate for each cell line. Statistical significance was determined by one-way ANOVA using the Tukey multiple comparison test. ** $p<0.01$, **** $p<0.0001$

Table 3.2: Summary of IC50 values of taxanes for all parental and isogenic resistant cell line models

Cell line	Paclitaxel (nM ±SEM)	Docetaxel (nM ±SEM)
MDA-MB-231 Native	3.97 ± 0.145	2.38 ± 0.32
MDA-MB-231 25PACR	183.4 ± 17.81 (46.2)	17.79 ± 2.37 (7.5)
MDA-MB-231 25DOCR	414.9 ± 27.39 (104.5)	109.02 ± 12.18 (45.8)
MCF7 Native	2.99 ± 0.521	5.459 ± 0.63
MCF7 25PACR	189.3 ± 33.53 (63.3)	34.96 ± 3.78 (6.4)

Cells were plated at 5000 cells per well in a 96 well plate and exposed to drug concentrations ranging from 0.3 to 3000 nM. Cell viability was determined 72hr later by Cell Counting Kit-8 (CCK-8) assay. Results show the mean of biological replicate experiments (n=3, with 3 technical replicates for each treatment condition). Resistance factors are shown in parentheses and represents resistant IC_{50}/parental IC_{50}.

Chemotherapy options for patients with breast cancer in both the adjuvant and neo-adjuvant settings typically include the use of the anthracyclines (epirubicin or doxorubicin) in combination with or before the use of taxanes. To test whether the resistance observed with both taxanes extend to anthracyclines, sensitivity to epirubicin and doxorubicin was also assessed. Results are summarised in Table 3.4.

Increased resistance to the anthracyclines was observed but at varying levels. MDA-MB-231 25DOCR was found to have an IC_{50} of 1814 nM for epirubicin, representing a statistically significant 24-fold increase in resistance compared to the parental cell line which had an IC_{50} of 76.5 nM. However the paclitaxel resistant MDA-MB-231 25PACR cell line was found to have only a 1.5-fold increase in IC_{50} at 136 nM. Resistance to doxorubicin was also observed in MDA-MB-231 25DOCR with a 5.5-fold

increase in IC_{50} (1526 nM) compared to the native parental cell line (278 nM). The taxane resistant MDA-MB-231 25PACR cell line retained a level of sensitivity comparable to the parental cell line with an IC_{50} of 183 nM.

This variability in anthracycline sensitivity was also observed with the MCF 25PACR cell line. An 8-fold increase in resistance to epirubicin was observed in the taxane resistant cell line, whereas a fold increase of only 1.6 was observed when the MCF 25PACR cell line was exposed to doxorubicin.

To further explore any cross-resistance, the panel was extended to include carboplatin and 5-fluorouracil (5-FU). MDA-MB-231 25DOCR and MDA-MB-231 25PACR demonstrated negligible changes in sensitivity to either carboplatin or 5-FU compared to the observed IC50 of its parental cell line. An IC_{50} of 54 µM was calculated for the native MDA-MB-231 cell line, with comparative concentrations of 49 µM and 69 µM for the paclitaxel and docetaxel resistant isogenic cell lines, respectively. The cell line MCF7 appeared to be more sensitive to carboplatin compared to MDA-MB-231 with an IC_{50} of 11µM. Its paclitaxel-resistant derivative, MCF7 25PACR, had a higher IC_{50} at 34 µM, the equivalent of a 3-fold increase.

There is clear cross-resistance of MDA-MB-231 25DOCR to both anthracyclines. This reduction in sensitivity to eprirubicin and doxorubicin in not, however, observed with the paclitaxel resistant MDA-MB-231 isogenic cell line, which retains an IC_{50} that is similar to the parental cell line. MCF7 25PACR also appears to be cross-resistant to epirubicin but not doxorubicin. The resistance shown by all lines to either carboplatin or 5-FU is at a level where it could be argued that there is no perceptible difference with the parental line and that the taxane resistant cell lines do not exhibit multi-drug resistance.

Table 3.3: Summary of IC50 values of chemotherapeutic agents in the isogenic breast cancer cell line models.

	Epirubicin (nM ±SEM)	Doxorubicin (nM ±SEM)	Carboplatin (µM ± SEM)	5-FU (µM ± SEM)
MDA-MB-231 Native	76.47 ± 4.416	277.7 ±33.02	54.26 ± 3.66	12.45 ± 1.79
MDA-MB-231 25PACR	136.4 ± 11.59 (1.8)	182.8 ± 7.662 (0.66)	49.23 ± 3.24 (0.91)	26.64 ± 11.00 (2.14)
MDA-MB-231 25DOCR	1814 ± 395.6 (23.7)	1526 ± 167.1 (5.5)	69.15 ± 5.55 (1.27)	29.89 ± 1.69 (2.40)
MCF7 Native	387.8 ± 28.9	461.9 ± 60.09	11.40 ± 1.375	19.8 ± 4.19
MCF 25PACR	3081 ± 991.4 (7.9)	734.9 ± 89.42 (1.6)	33.79 ± 2.595 (2.96)	33.79 ± 2.59 (1.71)

Cells were plated at 5000 cells per well in a 96 well plate and exposed to drug concentrations ranging from 0.3 to 3000nM. Cell viability was determined 72hr later by Cell Counting Kit-8 (CCK-8) assay. Results show the mean of biological replicate experiments (n=3, with 3 technical replicates for each treatment condition) in nanomolar concentrations for epirubicin and doxorubicin, and micromolar concentrations for carboplatin and 5-FU. Resistance factors are shown in parentheses and represents resistant IC_{50}/parental IC_{50}.

3.2.5 Expression of common breast cancer biomarkers

The panel of native and taxane resistant isogenic cell lines were initially characterised by their expression of the main tissue-based molecular biomarkers used routinely in the subtyping and treatment of breast cancer. To this end the levels of expression of ERα, HER2 and PgR were assessed by Western blotting, along with other members of the HER family, EGFR and HER3. The cells were grown in complete medium with the appropriate maintenance dose of taxanes where applicable, whole cell lysates prepared when the cells were 80% confluent and levels of proteins assessed by Western blotting (Figure 3.5). While there was no change in the expression of ERα, HER2 or PgR in any of taxane resistant MDA-MB-231 isogenic cell lines, there was a very slight increase in HER3 expression in the docetaxel resistant lines MDA-MB-231 25DOCR and 50DOCR. Elevated levels of EGFR was observed for all of the MDA-MB-231 taxane resistant cell lines. There appeared to be no difference in the expression of HER2 and PgR in the taxane resistant MCF7 isogenic cell lines. However there appeared to be a reduction in EGFR expression in the resistant isogenic cell lines compared to the native parental cell line. No changes were observed in EGFR or HER3 expression between the native and resistant lines.

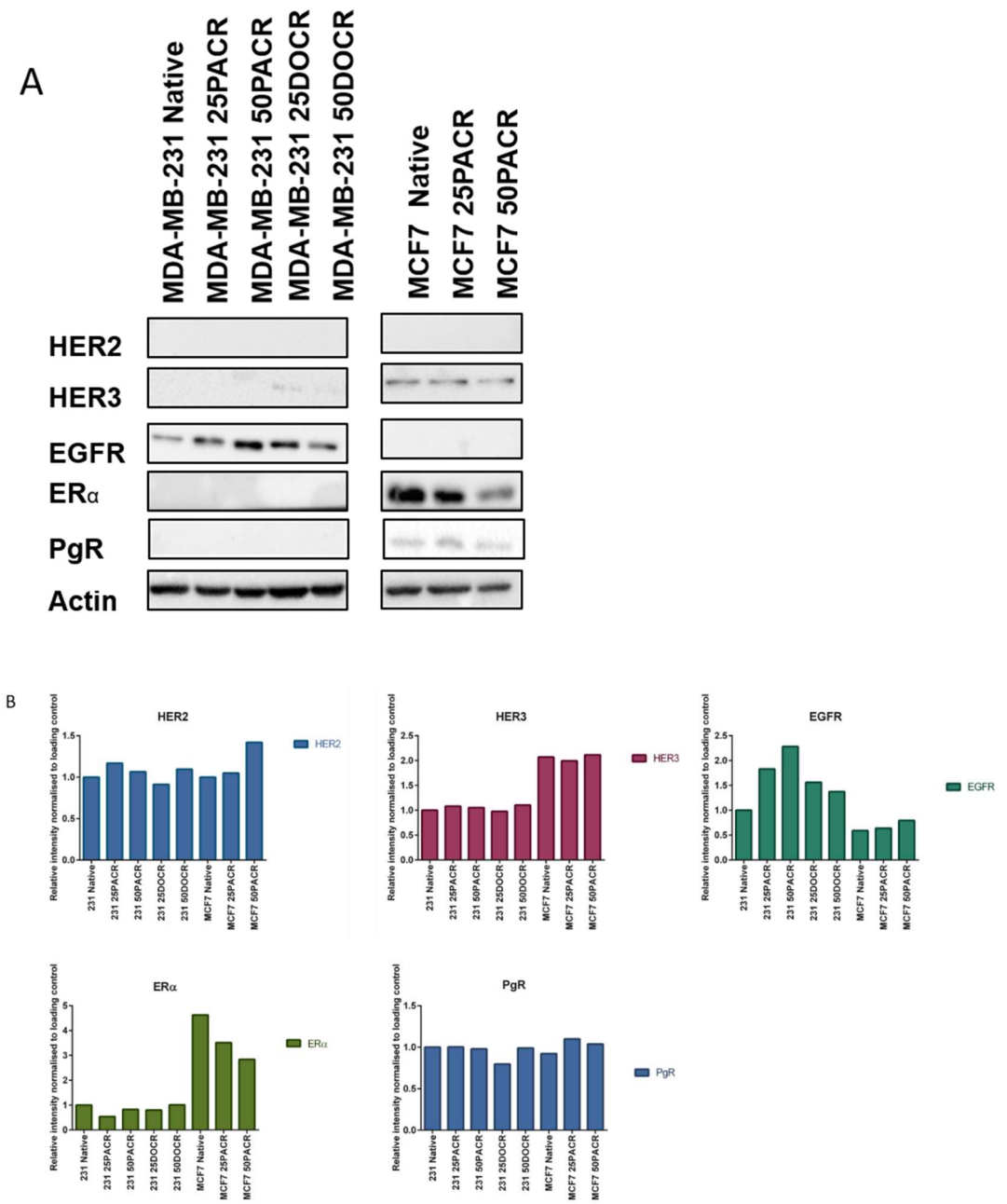

Figure 3.5: Common biomarker expression is largely unchanged in taxane resistant isogenic cell lines compared to the native parental cell line. (A) Whole cell lysates and western blotting as described in Materials and Methods. The proteins were separated by SDS-PAGE and probed for HER2, HER3, EGFR, ERα, PgR and actin. (B) Quantification of expression of biomarkers relative to native parental cell line after normalisation to actin loading control (n=1).

3.2.6 Stability of acquired taxane resistance in isogenic cell lines.

The long-term stability of resistance was determined by withdrawing taxane exposure and culturing all resistant isogenic cell lines over an extended period. Each line was cultured in two T25 flasks, one in complete media without taxane, and the other in the presence of the maintenance dose of 25 nM paclitaxel or docetaxel. After periods of 4 and 20 weeks the sensitivity of the cell lines to taxanes were reassessed.

After 4 weeks continuous culture in the absence of docetaxel, an IC_{50} of 41 nM was calculated for MDA-MB-231 25DOCR which reflects a resistance factor of 17-fold compared to the parental cell line. However when compared to the IC50 of MDA-MB-231 25DOCR this change reflects a statistically significant reduction. After a total of 4 months continuous culture without drug, the IC_{50} of MDA-MB-231 25DOCR dropped further to 3.6 nM, comparable to the taxane sensitive parental MDA-MB-231 cell line (Figure 3.6A). Similarly a reduction in resistance was observed for the paclitaxel-resistant MCF7 isogenic cell line after 4 weeks in continuous culture in the absence of paclitaxel. MCF7 25PACR cells remained resistant to paclitaxel compared to the parental cell line, with an observed IC_{50} of 34 nM and a resistance factor of 11-fold. However after 20 weeks of continuous culture in the absence of paclitaxel, resistance fell further to an IC_{50} of 5.25 nM (Figure 3.6B).

It was therefore concluded that, while it could be said that taxane resistance persisted in the isogenic cell lines after a month of continuous culture in the absence of drug, this was not the case after an extended period without taxane, with resensitisation occurring with both MDA-MB-231 25DOCR and MCF7 25PACR cell lines.

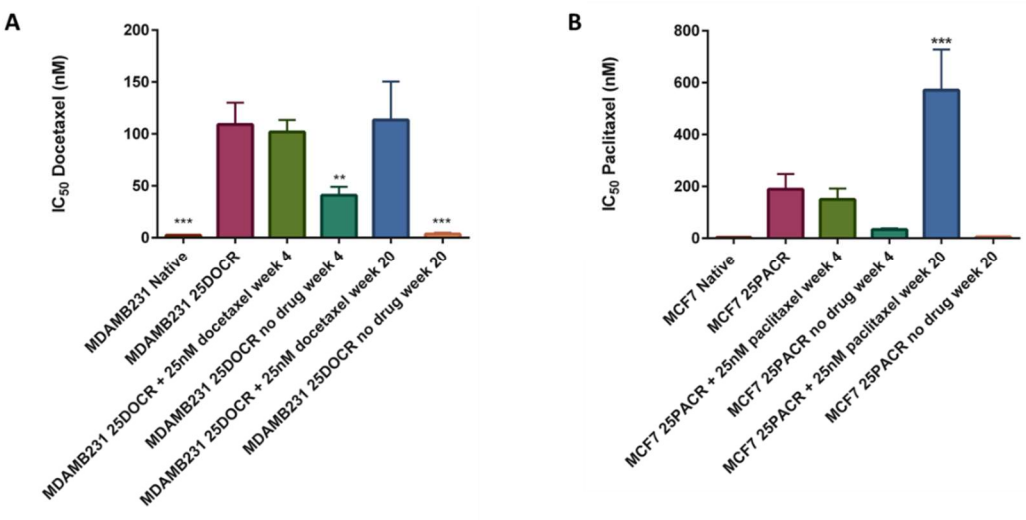

Figure 3.6: Half maximum inhibitory concentrations (IC50) for docetaxel and paclitaxel of (A) MDA-MB-231 25DOCR and (B) MCF7 25PACR after taxane withdrawal. Cell lines were grown in the presence or absence of 25nM taxane for 4 and 20 weeks. At each time point, 96 well plates were seeded with 5000 cells/well for each cell line and after 24hrs treated with increasing doses of paclitaxel or docetaxel for 72hrs. CCK-8 assays were then performed and data analysed using GraphPad Prism 6 software. Results are expressed as mean IC50 ± SEM of three independent experiments performed in triplicate for each cell line. Statistical significance was determined by one-way ANOVA using the Tukey multiple comparison test. ** $p<0.01$, *** $p<0.001$

3.2.7 Cellular proliferation and doubling rates of taxane resistant cell lines

To quantify differences in growth rate between the parental and resistant cell lines, cell counting was performed by live cell imaging using an Incucyte® Zoom system over a period of 72hrs. The Incucyte® provides the capability to capture real-time quantitative kinetic data of cellular confluence by periodic imaging over multiple time points and days. MDA-MB-231 and MCF7 native and isogenic cell lines were cultured in 96 well plates with and without the addition of the 25nM dose of their respective maintenance taxane, and cell proliferation monitored in real time. Four phase contrast images were captured for each well at every time point and masking applied to evaluate confluence (Figure 3.7). The mean confluence for each well and time points were calculated using Incucyte® analysis software, normalised to time 0 values and cell doubling times determined by GraphPad Prism version 6.

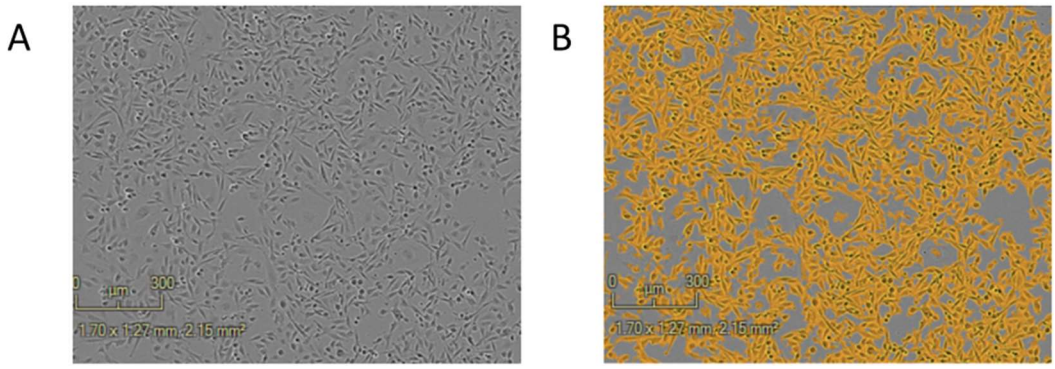

Figure 3.7: Representative phase contrast and masked images from the Incucyte® Zoom. (A) Phase contrast image of MDA-MB-231 native cells (B) MDA-MB-231 native cells with confluence mask applied.

Under standard culturing conditions and in the absence of taxanes, the native parental cell lines, MDA-MB-231 and MCF7, had mean doubling times of 29.9 hours and 36.3 hours respectively. The paclitaxel resistant isogenic cell line, MDA-MB-231 25PACR, demonstrated a near identical doubling time to the native parental cell line of 30.1 hours whereas the docetaxel resistant line, MDA-MB-231 25DOCR, had a statistically significantly longer doubling time of 41.9 hours (p=0.0012). The MCF paclitaxel resistant line, MCF7 25PACR, had a shorter doubling time of 32.8 hours compared to its sensitive parental line (Figure 3.8A).

The doubling times of the native parental cell lines in the presence of 25nM taxane proved impossible to accurately estimate. This dosage of taxane reflects a concentration well in excess of the IC_{50} for both cell lines (Figure 3.1) and it clear that proliferation is inhibited at this dose. There was no significant change in the doubling times of any of the taxane resistant cell lines when cells were cultured in the presence of the maintenance dose of 25nM paclitaxel or docetaxel. However when MDA-MB-231 25PACR cells were cultured in the presence of 25nM docetaxel, the doubling time of the cell line increased to 77.1 hours, a statistically significant increase ($p<0.0001$). Similarly upon culture with docetaxel an increase in doubling time of MCF7 25PACR

(49.7 hours; p=0.0004) compared to the untreated cells was also noted (Figure 3.8B). Cell doubling times for all cell lines are summarised in Table 3.4.

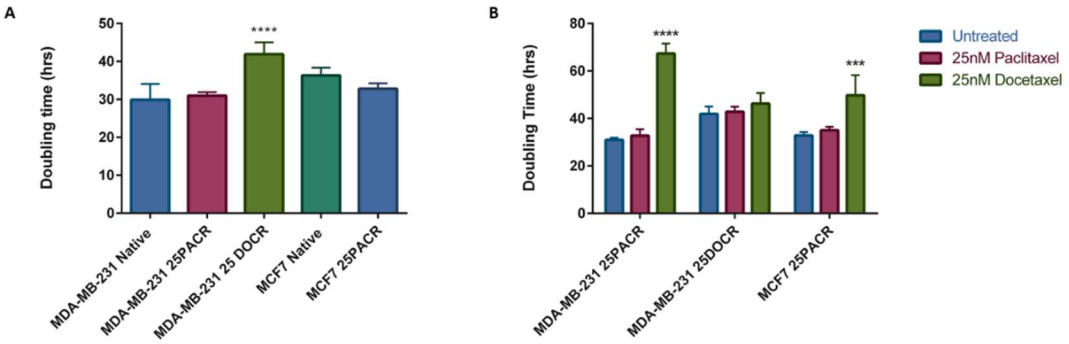

Figure 3.8: Doubling times of native and isogenic taxane resistant cell lines

(A) Doubling times of native and isogenic taxane resistant cell lines under normal culturing conditions (25nM taxane) (B) Doubling times of taxane resistant cell lines in absence or presence of 25nM paclitaxel/docetaxel. Cell lines were seeded in 96 well plates with 5000 cells/well for each cell line. After 24hrs the media was replaced with media containing 25nM paclitaxel, 25nM docetaxel or 0.1% DMSO as appropriate. Plates were imaged in an Incucyte® Zoom for 72 hours, acquiring phase contrast images every 3 hours. Images were analysed by Incucyte® software and results expressed as normalised mean confluence ± SEM of three independent experiments performed in triplicate for each cell line. Statistical significance comparing to (A) the appropriate native cell line and (B) untreated control was determined by two-way ANOVA using the Tukey multiple comparison test (*** $p<0.001$, **** $p<0.0001$).

Table 3.4: Cell doubling times of native and taxane resistant cell lines

	Doubling time (hrs ± SEM) No treatment	Doubling time (hrs ± SEM) + Paclitaxel	Doubling time (hrs ± SEM) + Docetaxel
MDA-MB-231 native	29.91 ± 2.07	-	-
MDA-MB-231 25PACR	30.99 ± 0 .45	32.75 ± 1.55	67.4 ± 2.96
MDA-MB-231 25DOCR	41.89 ± 1.57	42.87 ± 1.47	46.2 ± 2.60
MCF7 native	36.32 ± 1.01	-	-
MCF7 25PACR	32.83 ± 0 .70	33.87 ± 1.33	49.74 ± 6.02

3.2.8 Effects of resistance on the cell cycle

Taxane treatment leads to profound cell-cycle effects, principally arrest at the G2/M phase of the cell cycle due to stabilisation of the microtubules resulting in inhibition of the cell cycle and causing cell death. Paclitaxel prevents progression of mitosis and activates the mitotic checkpoint, initiating the pathway to apoptosis. To gain an insight into the effects of acquired taxane resistance on the cell cycle, the cell cycle distribution of each of the isogenic cell lines in the presence of taxane was assessed by confocal high content imaging. Briefly, taxane-treated cells were fixed and stained with Hoescht 33342 prior to imaging. Images were acquired using an ImageXpress Micro XLS widefield microscope and image analysis was performed using the 'Cell Cycle' module in the MetaXpress software.

Treatment of the native, parental cell lines with either paclitaxel or docetaxel resulted in arrest in the G2/M phase of the cell cycle and failure to return to the G0/G1 phase, along with associated reduction of cells in the G0/G1 and S phases. Upon treatment of MDA-MB-231 native cell lines with paclitaxel, 44.5% of cells were found to accumulate in the G2/M phase compared to 31.6% of the DMSO control. More strikingly, 66% of cells arrested at G2/M upon docetaxel treatment. MCF7 native cells also demonstrated a robust cell cycle arrest upon treatment with taxanes. Paclitaxel exposure resulted in 63.9% of cells accumulating at G2/M compared to 35% in the DMSO control. However, this accumulation in the mitotic phase was not observed in the resistant lines after taxane exposure. Exposure of MDA-MB-231 25DOCR to docetaxel did not result in a noticeable change in cell cycle profiles when compared to the DMSO control. 26.7% of cells were observed in the G2/M phase after docetaxel treatment, a level comparable to the 23.7% of the DMSO control cell population in the G2/M phase. Similarly paclitaxel treatment of MCF7 25PACR cells resulted in 35% of cells accumulating in the G2/M phase of the cell cycle, reflecting a similar percentage of 27% in the DMSO control wells. Exposure of MDA-MB-231 25PACR to 25nM paclitaxel resulted in a decrease of cells in the G2/M phase of the cell cycle and a concomitant increase of cells in the G0/G1 phase of the cell cycle, compared to cells in the DMSO control population. These results confirm that the taxane resistant isogenic cell lines are no longer susceptible to disruption of G2/M phase of the cell cycle by either paclitaxel or docetaxel.

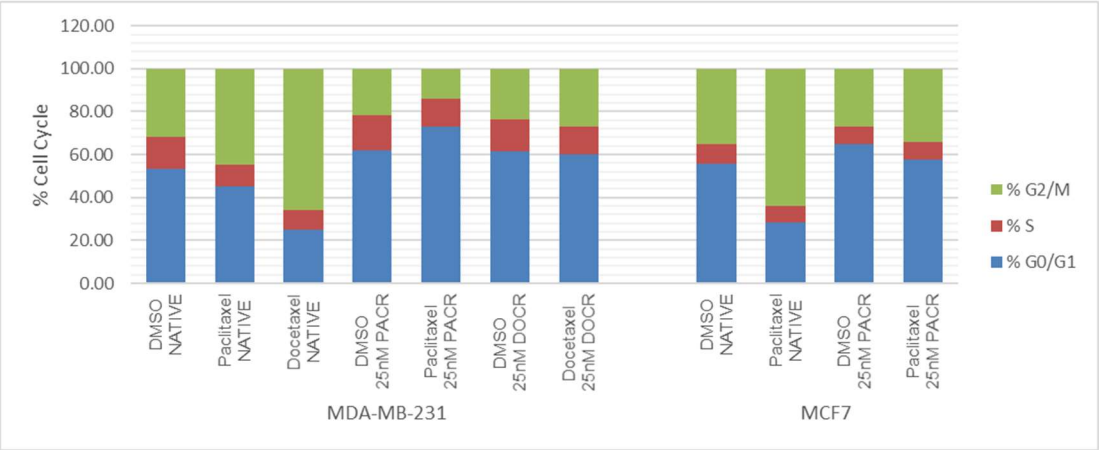

Figure 3.9: Cell cycle distribution in MDA-MB231 and MCF7 parental and resistant isogenic cell lines upon exposure to 25 nM paclitaxel or docetaxel. Cell lines were seeded in optical density 96 well plates with 2500 cells/well for each cell line. After 24hrs the media was replaced with media containing 25nM paclitaxel, 25nM docetaxel or 0.1% DMSO as appropriate and incubated for a further 72hrs. Cells were fixed and stained with Hoescht 3342 before imaging by the ImageXpress. Images were analysed by the cell cycle module of the MetaXpress software.Results are displayed as means (n=3).

3.2.9 Cell death and apoptosis

Taxanes are cytoskeletal targeting drugs which act by stabilising microtubule polymerisation and inducing formation of stable microtubule bundles. The dynamic ability of microtubules to polymerise and depolymerise are of critical importance in cellular functions, particularly in spindle formation during mitosis. Stabilisation of microtubules by taxane binding results in disruption of the mitotic spindle assembly, arrest at the G2/M phase of the cell cycle leading to cell death by apoptosis (221). To examine whether the reason why the taxane resistant cell lines continue to proliferate in the presence of taxanes is due to inhibition of this apoptotic response the effects of paclitaxel and docetaxel exposure on the isogenic resistant cell lines was examined

MDA-MB-231 cells were seeded in 96 well plates with Incucyte®Caspase -3/7 green apoptosis assay reagent and a six semi-log point concentration range of either paclitaxel or docetaxel applied. Staurosporine treated cells were included as a positive control for cell death. Four images per well were captured using the Incucyte

Zoom in both phase and green channels over a 72 hour period. Images were analysed using the inbuilt software to calculate the confluence of fluorescent objects (%) per well as a measure of apoptosis. Counts were normalised to the total cell confluency (%) of the same area of the image (phase) to generate the apoptotic index. Results displayed in Figure 3.10A represent values at the 48hr time point for treatment of the MDA-MB-231 taxane resistant isogenic cell line series with paclitaxel and Figure 3.10B for docetaxel treatment. Figure 3.11 shows the fold change calculated for each taxane concentration normalised to the DMSO control for each cell line.

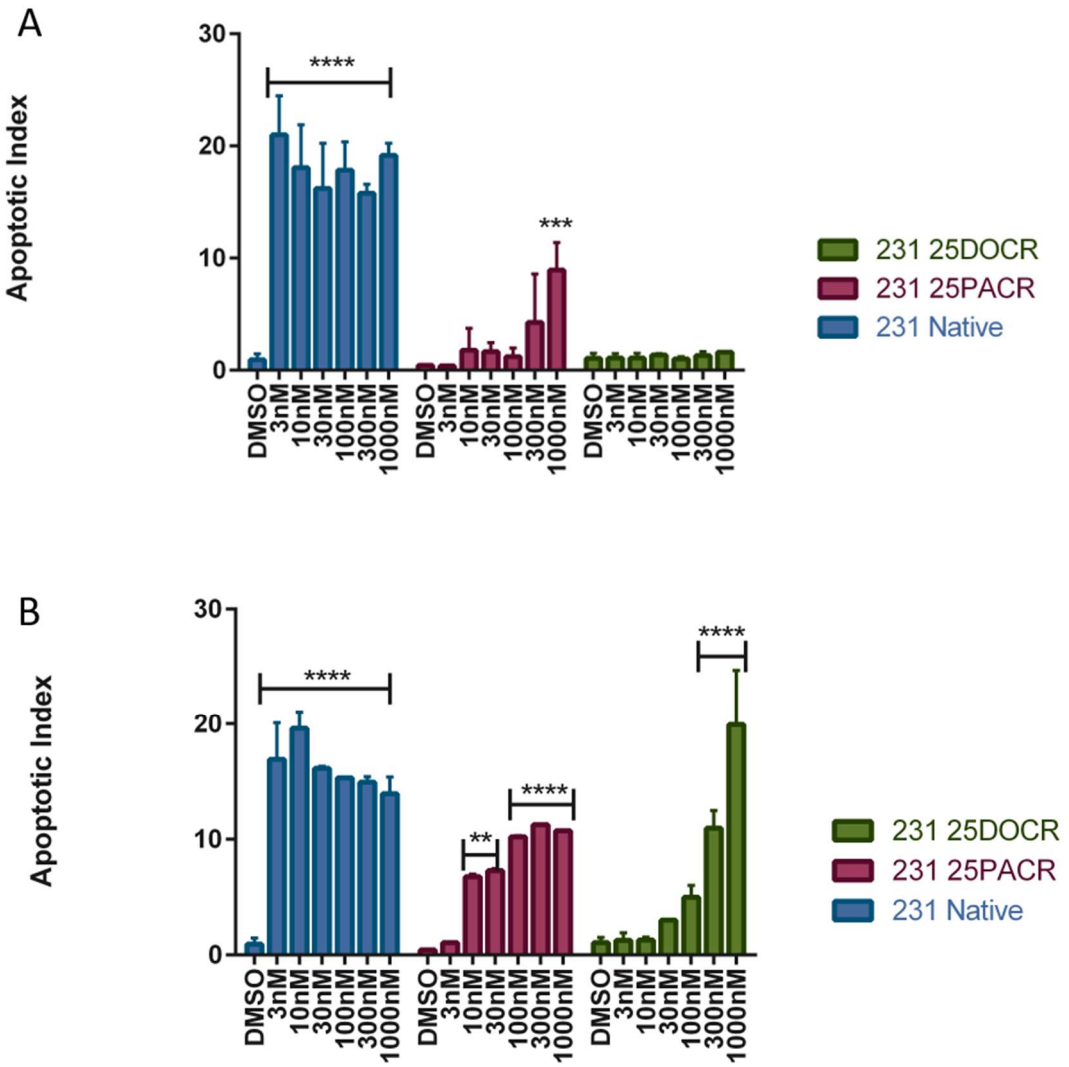

Figure 3.10: Taxane resistant MDA-MB-231 isogenic cell lines reduces the apoptotic response to (A) paclitaxel and (B) docetaxel. Cell lines were seeded in 96 well plates with 5000 cells/well for each cell line. After 24hrs the media was replaced with media containing 25nM paclitaxel, 25nM docetaxel or 0.1% DMSO and 1nM Caspase-3/7 reagent. Plates were imaged in an Incucyte® Zoom for 72 hours, acquiring 4 phase contrast and 'green' channel images per well every 3 hours. Images were analysed by Incucyte® software and results expressed as apoptotic index ± SEM of two independent experiments performed in triplicate for each cell line. Statistical significance was determined by two-way ANOVA using the Tukey multiple comparison test (** $p<0.005$, **** $p<0.0001$).

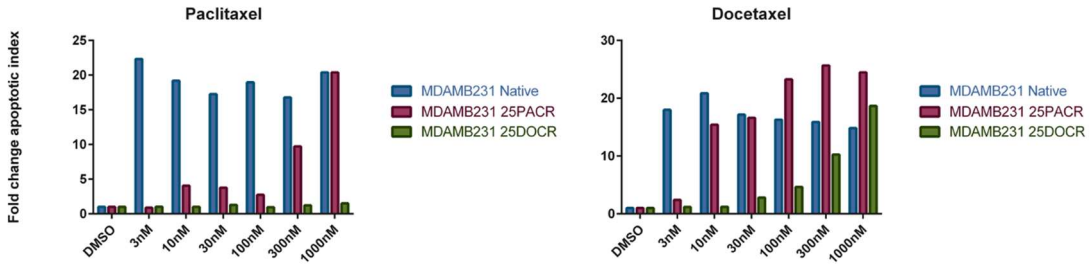

Figure 3.11: Fold change induction of apoptosis upon taxane treatment. Fold change values were calculated by normalising the mean apoptotic index value for each taxane concentration against the mean 0.1% DMSO control of two independent experiments.

Caspase-3/7 activity was found to be consistently increased in the parental MDA-MB-231 cell line upon exposure to both paclitaxel and docetaxel at statistical significance for all tested concentrations. At 3 nM taxane, a concentration comparable to the observed IC_{50} for MDA-MB-231, statistically significant ($p<0.001$) increases in Caspase-3/7 activity was observed after exposure to paclitaxel (22.3-fold) and after docetaxel exposure (18-fold). This contrasted with the negligible changes in activation with MDA-MB-231 25PACR or MDA-MB-231 25DOCR isogenic cell lines at this concentration suggesting that the taxanes did not induce an apoptotic response in the taxane resistant cell lines at IC_{50} of the parental MDA-MB-231 cell line.

It was observed, however, that taxane treatment of MDA-MB-231 25PACR did result in a concentration dependent increase in caspase-3/7 activation although this only became statistically significant at 1000nM paclitaxel ($p<0.001$) and 10nM docetaxel ($p<0.05$), in keeping with the observed IC_{50} for each of the compounds. The docetaxel resistant isogenic cell line, MDA-MB-231 25DOCR, did not demonstrate activation of caspase-3/7 at any of the tested concentrations of paclitaxel. A statistically significant increase in caspase-3/7 activation was observed at 300nM and 1000nM docetaxel.

3.2.10 MDR does not drive the chemoresistant phenotype of the taxane resistant isogenic cell lines

As all isogenic cell lines had been shown to demonstrate resistance to other chemotherapeutics to some level, it was necessary to investigate whether alterations in drug transport, particularly the expression of the P-glycoprotein, MDR1, might be responsible for the observed chemoresistant phenotype. A common mechanism of chemoresistance is alterations in drug transport, particularly drug efflux. Overexpression of P-glycoprotein (P-gp), an ATP-binding cassette (ABC) drug efflux pump encoded by the MDR1 gene, is one the most well-known causes of multidrug resistance in cancers and in particular as a resistance mechanism to taxane and doxorubicin treatment (168, 221-223).

P-gp expression in the taxane sensitive and resistant cell lines was assessed by Western blotting (Figure 3.12). Lysates were prepared as described earlier in the chapter. The taxane sensitive parental cell lines, MDA-MB-231 and MCF7, did not express P-gp as expected. Similarly, absence of expression in the paclitaxel resistant MDA-MB-231 isogenic cell lines (MDA-MB-231 25PACR and MDA-MB-231 50PACR) confirmed previous studies (220). However the docetaxel resistant MDA-MB-231 isogenic cell lines and MCF7 paclitaxel resistant isogenic cell lines were found to express P-gp at low levels.

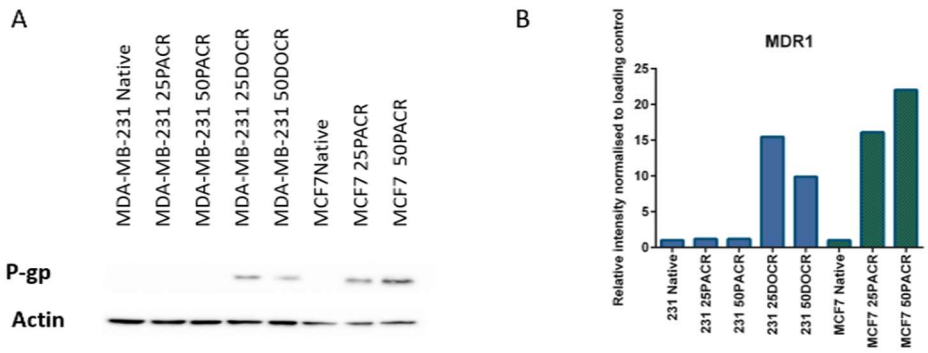

Figure 3.12: Expression of P-gp in the isogenic taxane resistant cell lines and sensitive native parental cell lines. Whole cell lysates and western blotting as described in Materials and Methods. The proteins were separated by SDS-PAGE and probed for P-gp and actin. (B) Relative expression of MDR1 compared to parental cell line after normalisation to loading control (n=1).

The role of P-gp over-expression on the chemoresistance observed in the docetaxel-resistant MDA-MB-231 and the paclitaxel resistant MCF7 cell lines was explored by knockdown of MDR1 and analysing the effects on sensitivity to their respective modulating taxanes.

Transient knockdown of MDR1 was achieved by siRNA reverse transfection using 40 nM of target siRNA. GAPDH was included as a positive control and scrambled siRNA as a negative control as outlined in section 2.2.9 in Materials and Methods. Appropriate controls were also included. To assess resensitisation to taxane upon target knockdown, the IC50's were calculated after treatment with an 8 point semi-log concentration range of either paclitaxel or docetaxel. All experiments were performed in triplicate. Graphs displaying calculated IC50s and confirmation of target knockdown by Western blotting of lysates collected 48 hrs after siRNA transfection are shown in Figure 3.13.

Knockdown of MDR1 in MDA-MB-231 25DOCR induced no effect on the proliferation and no observable change in the docetaxel IC_{50} of the cell line upon transient transfection of target siRNA. An IC_{50} of 109 nM was calculated for paclitaxel in the MCF7 25PACR cell line after MDR1 transient transfection. This represented a 1.7-fold

reduction compared to the observed value for the Optimem media only control and was not statistically significant. It was therefore concluded that MDR1 is not the primary driver of taxane resistance in either MDA-MB-231 25DOCR or MCF7 25PACR cell lines.

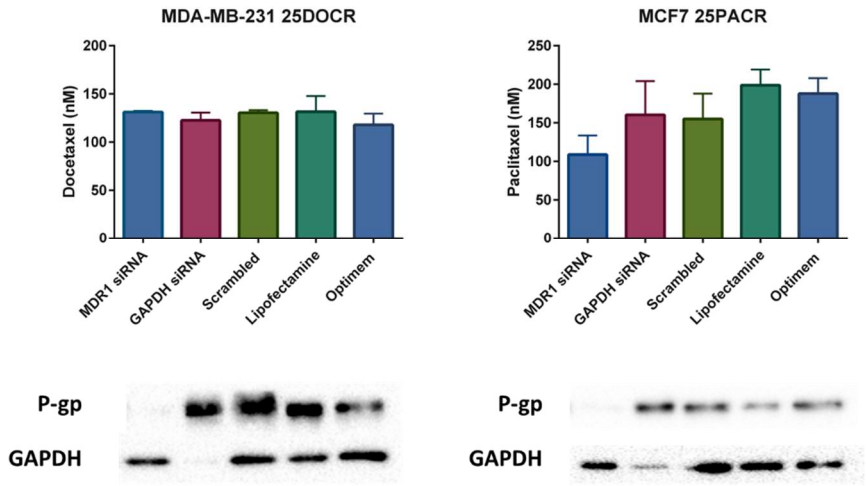

Figure 3.13: Half maximum inhibitory concentrations (IC50) for docetaxel and paclitaxel of MDA-MB-231 25DOCR and MCF7 25PACR after MDR1 knockdown by siRNA transient transfection. siRNA complexes were formed in 96 well plates and seeded with 5000 cells/well for each cell line. After 24hrs the cells were treated with increasing doses of paclitaxel or docetaxel for 72hrs. CCK-8 assays were then performed and data analysed using GraphPad Prism 6 software. Results are expressed as mean IC50 ± SEM of three independent experiments performed in triplicate for each cell line. Statistical significance was determined by one-way ANOVA using Dunnett's multiple comparison test. Western blotting of whole cell lysates after transient transfection with target siRNA were collected as described previously, separated by SDS-PAGE and probed for P-gp and GAPDH.

3.3 Discussion

Breast cancer cells that acquire chemoresistance, or which possess innate resistance, present a challenging scenario for treatment options for patients particularly upon relapse of disease. Treatment failure in these patients contribute to a bleak prognosis due to limited available therapeutic options. The aim of this chapter was to develop *in vitro* breast cancer cell line isogenic models of taxane resistance and characterise them fully prior to further studies. These models would provide a means of studying the mechanisms which drive taxane resistance in breast cancer patients with a view of identifying druggable targets. The cell lines developed as part of this study were designed to complement those previously established which included paclitaxel resistant MDA-MB-231 isogenic cell lines and ZR-75-1 paclitaxel and docetaxel resistant cell lines (220). Characterisation of those cell lines had revealed that taxane resistance observed in paclitaxel- and docetaxel-resistant ZR-75-1 isogenic cell line series was driven by overexpression of the multidrug resistance protein, P-gp. These cell lines were therefore not included here as part of the chemoresistant cell line panel. This chapter describes the development of docetaxel resistant MDA-MB-231 and paclitaxel resistant MCF7 isogenic cell lines and their characterisation.

Historically there are two main methods of deriving *in vitro* models of chemoresistance; clinically relevant and high-level laboratory models. Clinically relevant models are developed by mimicking chemotherapy regimens where drug is delivered in pulses at low doses. Typically these models only achieve a low level of resistance and are unstable. High-level laboratory models are derived through continual escalation of drug concentrations with the aim of developing models which allow the investigation of mechanisms of resistance due to a more stable phenotype. Whilst the levels of resistance found in models derived in this way may be higher than that seen in clinically relevant models and therefore not mimic doses typically used during treatment, the stable phenotype lends itself to experimental investigation. Molecular changes associated with chemoresistance levels of this magnitude tend to be large and therefore easy to identify. Dose-escalation is limited by the solubility of the selecting agent, and consideration should be given to selecting cell lines with a

relatively low baseline IC_{50} to facilitate development of clinically-relevant chemoresistance. As the aim of this study was to identify molecular changes associated with taxane resistance, and to maintain consistency with previous studies, it was decided that the latter method be employed for the establishment of the cell lines described in this chapter.

It was found that the breast cancer cell lines MDA-MB-231, MCF7 and SK-BR-3 were all sensitive to both paclitaxel and docetaxel at nanomolar levels. These cell lines were chosen to broadly reflect the breast cancer subtypes and to complement existing isogenic taxane resistant cell line models already developed by the group. It proved impossible to develop a stable docetaxel resistant MCF7 cell line in the time frame available, nor to establish taxane resistant SK-BR-3 isogenic cell lines with either paclitaxel or docetaxel. Continuous culture of MDA-MB-231 in escalating doses of docetaxel resulted in resistant cell lines after a period of some 16 weeks. Similarly, paclitaxel resistant MCF7 isogenic cell lines were also developed after continuous culture in the presence of taxane. However the establishment of this resistant cell lines took a total of 26 weeks to achieve.

Following the establishment period, resistance to paclitaxel or doctetaxel was confirmed by proliferation assays. STR analysis established that the resistant cell lines corresponded to the parental cell line profile and Western blotting confirmed that there was no alterations in the hormone receptors which define the cells lines. These initial experiments confirmed the isogenic cell lines as appropriate models of *in vitro* taxane resistance suitable for further analysis to elucidate mechanisms of acquired chemoresistance.

While resistance was maintained after 4 weeks in continuous culture in the absence of taxane, resensitisation occurred after prolonged culture in drug free media with the IC_{50} of both MDA-MB-231 25DOCR and MCF7 25PACR dropping to near parental cell line levels. Whilst disappointing that a more stable phenotype wasn't established, for the purposes of the short experiments carried out in this thesis, it was felt that they remained valid chemoresistant cell lines. The significant increase in IC_{50}

recorded for MCF 25PACR after 20 weeks of continuous culture in paclitaxel is likely due to selection over time of cells with a more robust taxane resistant phenotype from what is a heterogeneous cell population. Breast cancer is one of the most heterogeneous solid tumours with well-defined morphological subtypes with distinct molecular signutures (224-227). Intratumour heterogeneity which arises through complex genetic, epigenetic and protein modifications contributes to the adaptability seen in tumours with consequences for treatment and prognosis (228). This heterogeneity is also detected in cancer cell lines (229, 230) and interplay between clones have been found to confer malignant potential (230). Whilst the isogenic taxane resistant cell lines established in this chapter are heterogeneous in nature, it would be possible to clonally select out individual resistant sublines which would likely demonstrate a wider spectrum of resistance and long term stability than observed here.

Alterations in cell cycle progression and apoptosis due to the microtubule modulating action of taxanes is a well-documented effect (160, 231, 232). Taxanes act by stabilising microtubules (161), causing G2/M arrest followed by apoptosis (148). Although they bind poorly to soluble tubulin, taxanes instead bind directly to β-tubulin along the inside length of the microtubule, increasing microtubule polymerisation. Docetaxel, with a greater affinity to β-tubulin, also exerts an effect on the S phase of the cell cycle (233). Results from this study confirm cell cycle arrest and accumulation in the G2/M phase in the native parental cell lines whilst the resistant cell lines treated with the same concentration of taxane appeared to be able to overcome this effect and continued to cycle as normal. The taxane sensitive MDA-MB-231 parental cell line was also found to have a higher rate of apoptosis compared to either of the taxane resistant isogenic cell lines when challenged with paclitaxel or docetaxel, with statistically significant levels observed even at low nanomolar concentrations. This result agreed with the literature where low concentrations of taxanes were found to be sufficient to induce mitotic block and cell death by apoptosis in HeLa cells (234, 235). Challenging MDA-MB-231 25PACR with paclitaxel resulted in a concentration dependent increase in apoptosis although this only

reached a significant level at 1000 nM, a concentration above the observed IC50 for this cell line. A significant increase in apoptotic index was not observed for MDA-MB-231 25DOCR even when exposed to the highest concentration of 1000 nM paclitaxel. However, the apoptotic index did increase commensurate with taxane dose and it was anticipated that future experiments to assess expansion of the concentration range of paclitaxel in this cell line would demonstrate an increase in apoptosis. Exposure to docetaxel resulted in a concentration dependent increase in the apoptotic index for MDA-MB-231 25PACR with statistical significant changes noted at concentrations around that of the observed IC_{50} of 18 nM. Similarly, a significant increase in apoptotic index was only observed in MDA-MB-231 25DOCR at a docetaxel concentration of 300 nM. These results further served to confirm the conferring of taxane resistance in the MDA-MB-231 isogenic cell line in vitro models.

One of the most commonly cited mechanisms of taxane resistance *in vitro* is the over-expression of ATP-binding cassette transport proteins and, in particular, P-gycoprotein (P-gp) which is encoded by the MDR1 gene. These proteins function as drug efflux pumps, removing drug from the intracellular compartment. Paclitaxel is a known substrate of P-gp, causing a conformational change and increasing drug efflux (170). Studies in mammalian cancer cell lines confirmed that there was a correlation between resistance to docetaxel and expression of the P-gp protein (236) and further that MDR1 expression in the NCI-60 drug screening panel correlates with resistance to a wide range of compounds (237). Cross-resistance to the non-selecting taxane was observed in all of the taxane-resistant cell lines. To assess whether the cell lines had developed a multi-drug resistant phenotype, the response to other chemotherapeutic agents was also assessed. While low level resistance was observed for MDA-MB-231 25DOCR and MCF7 25PACR against the anthracyclines, the IC_{50}s for carboplatin and 5-FU were not significantly different to the values reported for the parental cell lines. Over expression of P-gyp was observed in both of these cell lines gave weight to the suggestion that the observed resistance to taxanes was driven by MDR1. However, transient knockdown of the MDR1 gene by siRNA transfection revealed that reversal to a taxane-sensitive phenotype was not observed in either

MDA-MB-231 25DOCR or in MCF7 25PACR. This suggests that the taxane resistant cell line models derived for this thesis are driven by mechanisms of resistance independent of MDR1. Further exploratory studies are therefore merited to identify these mechanisms and assess their clinical relevance as actionable pathways.

This chapter has described the development and characterisation of novel taxane resistant models. Full characterisation of the isogenic cell lines suggests that these are robust models of acquired taxane resistance with significant increases in IC_{50} for taxanes, continued passage through the cell cycle and an absence of apoptosis under conditions which would cause cell death in the parental cell line. Even though some cross-resistance to some chemotherapeutics was observed along with an elevation of P-gp expression, the taxane resistant phenotype was not found to be solely driven by MDR1 with no restoration of sensitivity upon knockdown. The development of isogenic taxane resistant cell lines allowed the comparison with the parental taxane sensitive cell line and provides a robust internal control for subsequent experiments. Establishment of a docetaxel resistant MDA-MB-231 isogenic cell line allows for direct comparison with the paclitaxel resistant MDA-MB-231 25PACR previously characterised, and therefore the potential of identifying whether mechanisms of resistance is specific to either taxane. Further, by developing the MCF7 25PACR cell line, there is the opportunity to assess whether there are differences in the mechanisms of acquired taxane resistance between molecular breast cancer subtypes.

4. THE EFFECT OF TAXANE RESISTANCE UPON DOWNSTREAM SIGNALLING IN BREAST CANCER CELL LINES

4.1 Introduction

In the previous chapter it was demonstrated that the isogenic cell lines developed through continual exposure to either paclitaxel or docetaxel had resulted in a chemoresistant phenotype. The cell lines were no longer sensitive to taxanes and continued to progress through the cell cycle and proliferate. Although an increase in the expression of MDR1 was observed, knockdown of the gene by siRNA did not result in a complete recovery of sensitivity to taxanes. I therefore speculated taxane resistance was driven by mechanisms other than PgP glycoproteins and it was appropriate to identify targetable pathways which are differentially expressed between the parental cell line and resistant isogenic daughter cell line.

Currently breast cancer patients who relapse and become resistant to taxanes have limited treatment options, with the majority dying within 5 years of disease progression (238). As discussed previously multiple factors are associated with the acquisition of taxane resistance, including dysregulation of signalling pathways, altered DNA damage repair mechanisms and the evasion of apoptosis. With the development of *in vitro* isogenic models of taxane resistance it is possible to investigate multiple proteomic and transcriptomic pathways and provide an overview of the processes involved in the development of acquired chemoresistance. The aim of this chapter was therefore to identify those genes and proteins differentially expressed between the taxane sensitive parental cell line and the resistant isogenic derivatives and to identify pathways commonly dysregulated in all taxane resistant cell lines. A multi-omic analysis was performed through transcriptomic analysis utilising Nanostring technology, targeted sequencing through MSK-IMPAKT and the application of reverse phase protein array (RPPA) analysis to identify dysregulated proteins. Together these results were analysed to identify targetable pathways involved in the evolution of taxane resistance in breast cancer cell lines. By identifying those pathways involved, the opportunity to specifically target those pathways or to develop a biomarker based diagnostic test which could inform treatment options might be possible.

4.2 Results

4.2.1 Proteomic analysis by Reverse Phase Protein Array (RPPA)

The development of taxane resistance is multi-faceted, involving multiple pathways involved in proliferation, apoptosis, up-regulation of pro-survival pathways and activation of drug export transporters. To further understand the pathways involved in the mechanisms driving chemoresistance in the isogenic cell lines, RPPA was performed on the parental MDA-MB-231 cell line and its paclitaxel resistant derivative, MDA-MB-231 25PACR. This study was limited to this pair of cell lines as it was performed at the outset of my studies and preceded the stable establishment of the other isogenic taxane resistant cell lines.

RPPA is a highly sensitive and quantitative immunoassay where the cell lysate is immobilised on to a solid phase, in this case nitrocellulose, and then probed with antibodies towards specific targets (239). This high throughput proteomic technique allows the simultaneous quantification of multiple total or phospho-proteins in multiple cell lysates. As a result, RPPA has increasingly become viewed as an efficient method of accurately and efficiently assessing a large number of proteins in a time and cost-effective manner (240). The assay is based on a dot-blot performed in microscale with minute quantities of protein immobilised to a nitrocellulose surface, which are then visualised in a way similar to Western blotting with incubation of primary and fluorescently labelled secondary antibodies, allowing the high-throughput analysis of a multiple proteins at one time.

Denatured protein lysates from the parental MDA-MB-231 cell line and the paclitaxel resistant MDA-MB-231 25PACR cell lines were spotted on to nitrocellulose-coated glass slides. The 150 candidate antibodies chosen for this study were directed towards key cancer associated signalling pathways and their targets, such as cell

cycle, kinase cascades and canonical signalling pathways. The samples were examined in a process outlined in the method section.

The relative fluorescent intensity (RFI) for each target were normalised by global sample mean normalisation, standardised as z scores and then subjected to hierarchical clustering analysis. The heat map in Figure 4.1 display the relative enrichment of proteins and phosphoproteins (red, up-regulated; blue, down-regulated).

Relative expression of each target in the taxane resistant MDA-MB-231 25PACR compared to the native parental cell line were calculated as log2 ratio. Differentially regulated proteins and phosphoproteins were compared using a Student's t-test with Holm-Sidak correction, and a cut off of $p \leq 0.05$ applied. Of the 150 antibodies tested, 97 showed a statistically significant change in expression when comparing the taxane resistant MDA-MB-231 25PACR with its parental MDA-MB-231 cell line. Overall, the fold changes observed in the paclitaxel resistant cell line were modest. The triple negative MDA-MB-231 cell line and the isogenic paclitaxel-resistant cell line MDA-MB-231 25PACR exhibited characteristic lack of HER2 expression as expected.

Due to the large number of antibodies included in the proteomic analysis by RPPA, differential expression of proteins can be interpreted as an indicator of alterations within pathways, rather than simply the identification of changes in specific proteins. Visualisation of the functional interaction and gene enrichment was therefore performed using Cytoscape 3.8.2 and the Reactome FIViz app, clustering the differentially regulated proteins into modules. The analysis is based on overrepresentation analysis where a hypergeometric distribution test was employed to identify which curated KEGG pathways are enriched in the protein list submitted. The Reactome FIViz app was also used to retrieve associated gene ontology (GO) biological processes annotations and independently verified by using DAVID online resource (Database for Annotation, Visualisation and Integration Discovery)(241). Linker genes were applied to facilitate FI network visualisation. However, these were

excluded in the subsequent enrichment analysis, with analysis performed only on those proteins identified as being dysregulated in the taxane resistant cell lines.

The analysis of the statistically dysregulated proteins revealed four interconnected modules associated with distinct pathways and biological processes (Figure 4.2A & B). The modules were primarily associated with cell signalling pathways including mTOR, PI3K-Akt and ErbB. GO biological pathway analysis indicated alterations in response to DNA damage and cell cycle, which could also rationally be linked with a drug response phenotype.

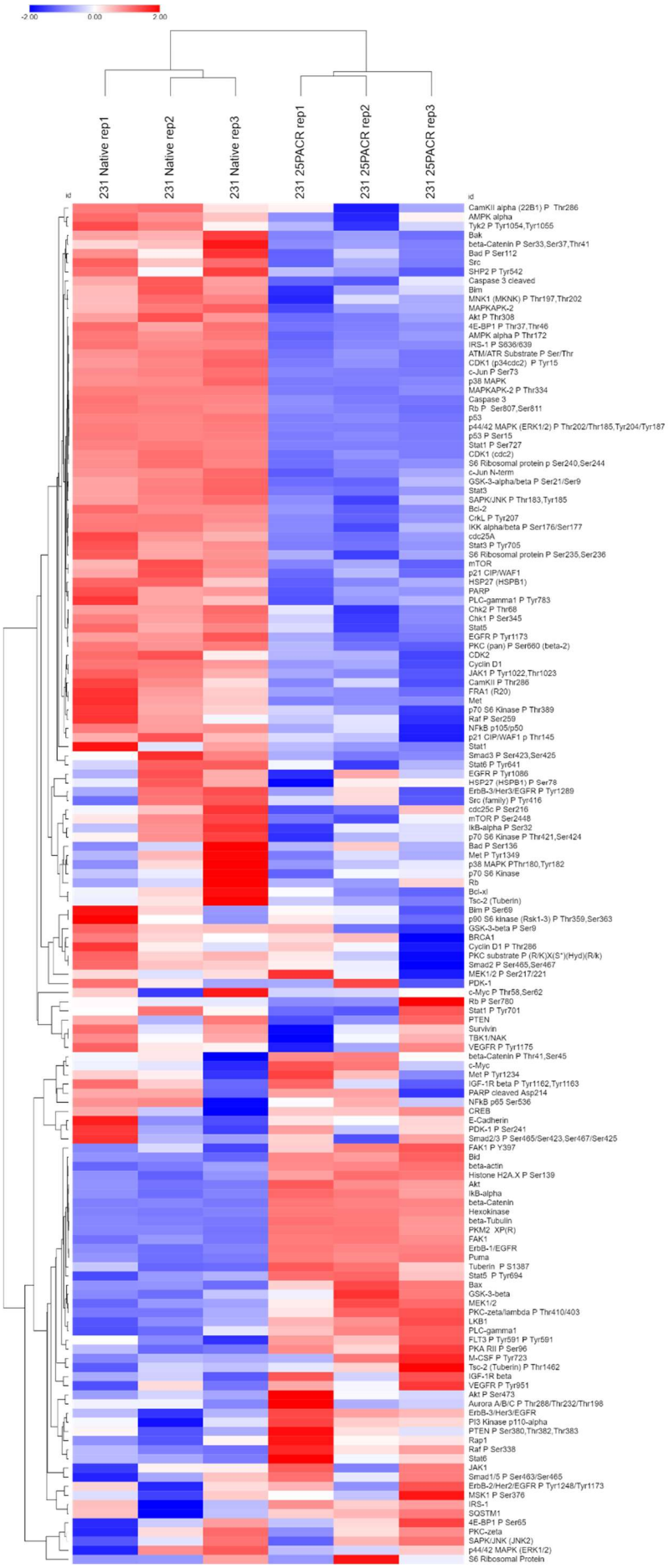

Figure 4.1: Hierarchical clustering analysis of changes in protein and phosphoprotein levels upon acquirement of taxane resistance.

Levels of proteins and phosphoproteins in whole cell lysates were determined by RPPA. Normalized intensity values were standardized as Z-scores and subjected to hierarchical

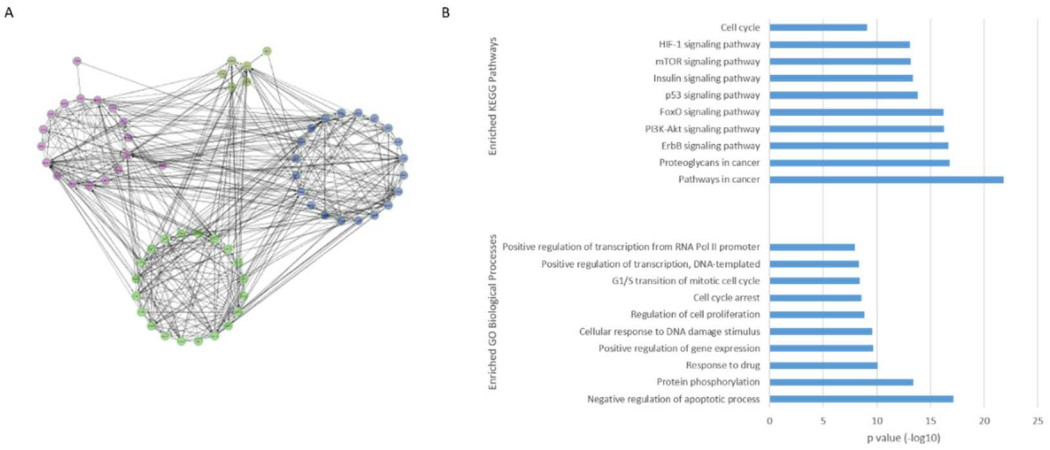

Figure 4.2: Functional annotation analysis of differentially expressed proteins identified via comparison of MDA-MB-231 25PACR and parental MDA-MB-231 (A) Functional interaction (FI) networks for 97 target antigens was visualised using Cytoscape Reactome FIViz. Four interconnecting modules were identified. Interconnecting lines show direction attribute values: --> activating/catalysing; --| inhibition; solid line for complexes or inputs; --- for predicted FIs. (B) Functionally enriched KEGG pathways and GO Biological Processes were identified and the top 10 statistically significant pathways ($p<0.05$) selected.

Nineteen of the statistically changed antigens also exhibited a log2 fold change of ≥ ± 0.58 (Figure 4.3). Twelve antigens (SQSTM1, β-actin, PKM2, β-tubulin, Bid, Hexokinase II, β-catenin, EGFR, Puma, Iκβ-α, β-Tuberin (pThr1462) and E-cadherin) were upregulated (red bars on graph). Downregulated antigens included MAPKAPK2 (pThr344), STAT1 (pS727), Caspase 3, p53 (pS15), ERK1/2 (pThr202), Rb (pS780), p21 CIP/WAP and cdc25a (blue bars on graph).

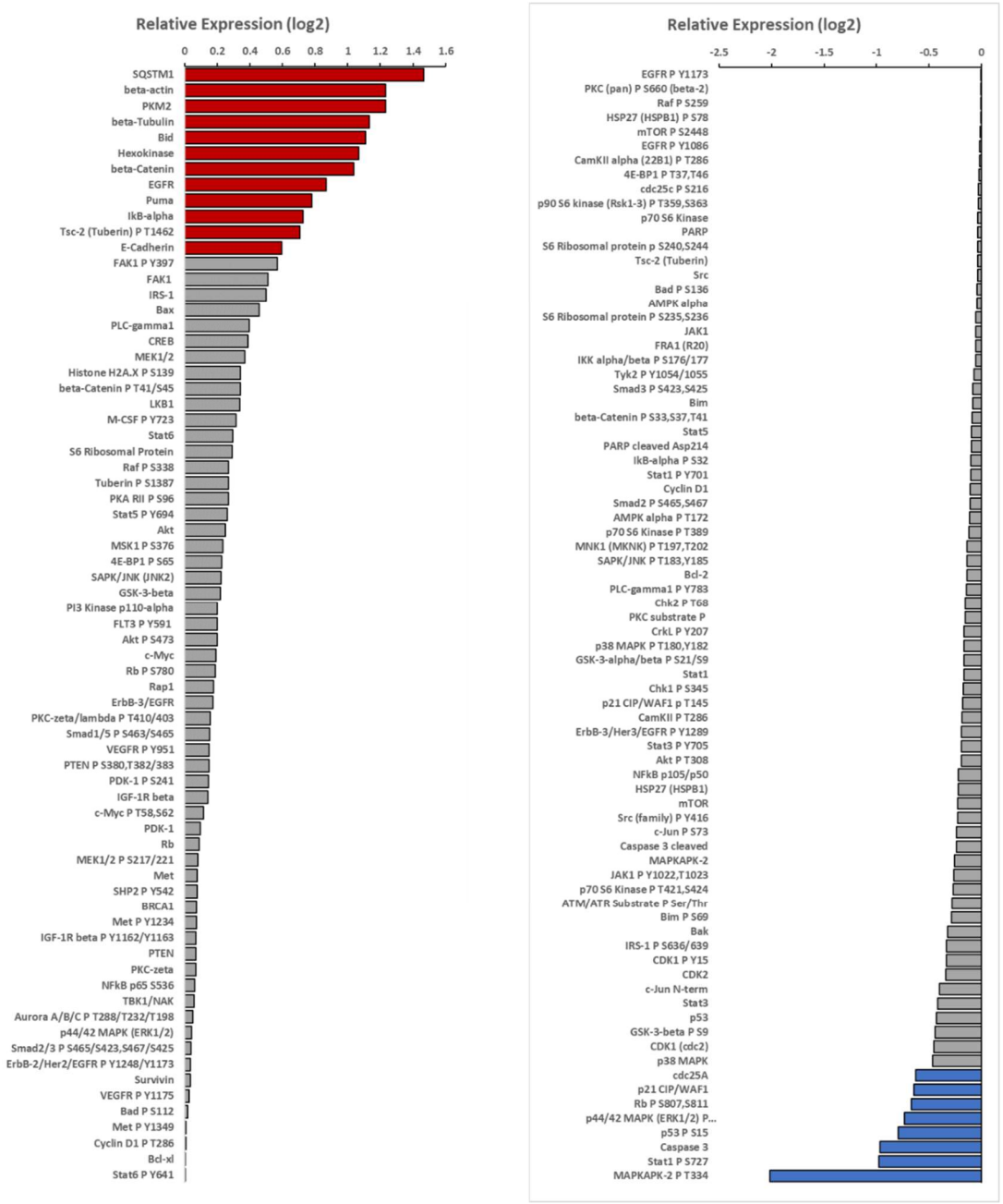

Figure 4.3: Reverse Protein Phase Array (RPPA) analysis results. The graphs present the fold-change in expression between parental MDA-MB-231 and taxane resistant MDA-MB-231 25PACR cells. Each bar shows the log2 of the relative fold change. Red bars signify significantly upregulated antigens, blue bars significantly downregulated antigens (log2 fold change ≥ ± 0.58, p≤ 0.05).

Functional interaction analysis of the significantly differentially expressed proteins revealed enrichment of the apoptotic response. Overexpression of β-tubulin (log2FC=1.13; p=1.12E^{-5}) was observed in the paclitaxel resistant cell line, MDA-MB-231 25PACR, compared to the parental cell line, a documented mechanism of resistance to taxanes. The overexpression of the βIII-tubulin in particular has been associated with taxane resistance in breast cancer. Significant downregulation of Caspase 3 (log2FC=-0.96773; p=1.59E^{-10}) was noted in the paclitaxel-resistant MDA-MB-231 25PACR cell line compared to the parental cell line, suggesting inhibition of the apoptotic process. Significant down-regulation of the phosphorylated forms of RB1 (log2FC=-0.629; p=3.44E^{-5}) and TP53 (log2FC=-0.579; p=0.0002), key proteins in the cell cycle, were also observed in the resistant cell line. Additionally, hexokinase-2 (HK2), a key enzyme in glucose metabolism and considered to play a role in the regulation of the apoptotic cascade by preventing induction of Bax and Bad, was found to be significantly overexpressed (log2FC=1.067; p=1.06E^{-5}) in the paclitaxel resistant cell line. However, neither of these pro-apoptotic proteins demonstrated significant change in the MDA-MB-231 25PACR cell line relative to the parental line. Furthermore, expression of the pro-apoptotic proteins BID (log2FC=1.108; p=0.001) and PUMA (log2FC=1.716; p=0.002) were found to be significantly upregulated in the resistant cell line.

SQSTM1/p62 was identified as being the most overexpressed antigen in the taxane resistant MDA-MB-231 25PACR cell line (log2FC=1.467; p=0.00022) by RPPA. This multifunctional protein, first identified as an adaptor of autophagy, is also involved in mitotic transit through CDK1, and signalling through MAPK and NF-κB. Total and activated CDK1 were found to be statistically significantly downregulated in MDA-MB-231 25PACR (p=0.0005 and p=0.0003 respectively) but, with log2 FC values of -0.454 and -0.337, did not achieve the fold cut off of log2 ± 0.58 which had been applied to this analysis. NF-κB p105 differential expression reached significance of p=0.0002 but also did not reach log2 FC cut off. PKM2 acts in concert with EGFR and β-catenin promoting expression of target genes such as cyclin D1 (CCND1). Both EGFR (p=0.0006) and β-catenin (p=2.86E^{-6}) were significantly overexpressed in MDA-MB-

231 25PACR cells by RPPA. The expression of p21CIP/WAF, a cell cycle inhibitory protein, was downregulated in MDA-MB-231 25PACR cells ($p=6.84E^{-5}$). It was anticipated that a reduction in expression of this protein would translate in to an upregulation of the cyclin kinases, CDK1 and CDK2. However both antigens were found to be downregulated although again not reaching the log2FC limit set for the analysis.

Functional interaction analysis also identified the dysregulation of the ErB2 and PI3K-Akt pathways in the MDA-MB-231 25PACR cell line. Although overexpression of total EGFR was demonstrated in the taxane resistant cell line there was no significant change in its activated phosphorylated form. Total p38 MAPK ($p=4.04E^{-7}$) and its downstream target phospho-MAPKAPK2 T334 ($p=6.54E^{-7}$) were both also significantly downregulated. A trend towards upregulation of total Akt was observed but with no change in either of the phospho-Akt antigens. Total FAK ($p=1.21E^{-6}$) and phospho-FAK Y397 ($p=0.001$) were also found to be significantly upregulated in MDA-MB-231 25PACR cells although not reaching the threshold of fold change applied. A schematic diagram summarising the observed protein changes and their interactions are shown in Figure 4.4.

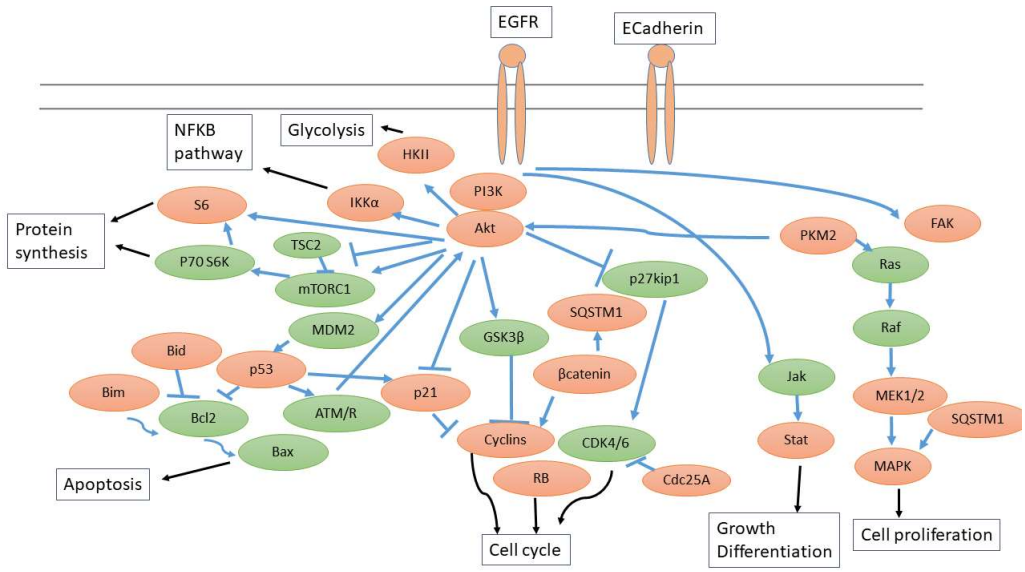

Figure 4.4: Schematic representation of pathway changes identified by RPPA. Proteins identified as dysregulated in MDA-MB-231 25PACR are shown in orange, other pathway members in green. Blue arrows represent positive regulation and headed-arrows represent negative regulation.

4.2.2 Targeted exome sequencing of the isogenic taxane-resistant cell lines

The parental and taxane resistant isogenic cell lines were first screened for genomic alterations which could potentially be associated with the resistant phenotype using MSK-IMPACT™ (Memorial Sloan Kettering-Integrated Mutation Profiling of Actionable Cancer Targets) panel assay. This was performed in collaboration with Dr Melanie Spears (OICR, Toronto, Canada). DNA from the parental and resistant isogenic cell lines was sequenced using the MSK-IMPACT™ platform, a capture based next generation sequencing (NGS) assay which is capable of identifying copy number alterations (CNA), protein-coding mutations and selected promoter mutations in 468 cancer-associated genes. Predictions for pathogenicity was also performed as part of the analysis.

Copy number alterations profiled differences between the parental and resistant cell lines, but also clearly demonstrated the differences between the MDA-MB-231 and MCF7 cell lines (Figure 4.5). Amplification of *RECQL4* was the only common copy

number alteration observed in all cell lines. Several copy number gains associated with resistance in the MDA-MB-231 25PACR cell line resided on chromosome 5, which included genes associated with the PI3K-Akt pathway such as *FGFR1*, *PIK3R1*, *IL7R* and *FLT4*. This cell line also had an area of loss on chromosome 22 which included *MAPK1*, *CHEK2, NF2 and EP300.* The copy number profile of the docetaxel resistant MDA-MB-231 25DOCR was very similar to the parental cell line, with only one areas of CNA which could be attributed to docetaxel resistance. Copy number loss on chromosome X, which included *AR*, *ATRX*, *BTK* and *STAG2,* was detected in MDA-MB-231 25DOCR only. The isogenic cell line MCF7 25PACR demonstrated several copy number alterations acquired during exposure to paclitaxel. Areas of loss were found on chromosomes 6 and 9, and areas of gain at chromosomes 12, 14 and 16. Genes mapped to the areas of loss at chromosome 6 included *ESR1*, *IFNGR1* and *LATS2*, down-regulation of which have been associated with acquired taxane resistance.

Using the latest version of the human genome as reference, somatic mutations were identified in the isogenic cell lines (Figure 4.6). Seventeen mutations were identified in the resistant cell line MDA-MB-231 25PACR and 18 mutations in the docetaxel-resistant MDA-MB-231 25DOCR cell line (Table 4.1). These mutations were all also observed in the parental cell line with the exception of the following identified in both resistant cell lines: the missense mutation, STK19 (p.S145W) and a splice site mutation in NOTCH4 (p.X1380*). A missense mutation in SETD2 (D324Y) was also identified in MDA-MB-231 25PACR cells. Similarly, the majority of the twelve mutations identified in the paclitaxel resistant MCF7 25 PACR cell line were also observed in the MCF7 parental cell line (Table 4.2). It was noted that the activating PIK3CA mutation, pE545K, was carried by both the parental and resistant isogenic MCF7 cell line. Four mutations were observed in MCF7 25PACR cells alone; a missense mutation in MAP3K13 (p.D380N), a silent mutation in PLCG2 (p.T378T) and nonsense mutations in MET (p.S470*) and FLT1 (p.S195*). The functional impact of mutations unique to the resistant cell lines were further investigated through interrogation of the COSMIC (Catalogue of Somatic Mutations in Cancer) database

(www.cancer.sanger.co.uk/cancer) and TCGA dataset via www.cbioportal.org. It is predicted that the nonsense mutations identified in MET and FLT1 are likely to be pathogenic in nature. The somatic mutation in MET occurs in the conserved SEMA domain of the extracellular portion of the receptor. The SEMA domain is necessary for the dimerisation and activation of the receptor, which leads to initiation of downstream signalling via PI3K-Akt and Ras/MAPK signalling. The impact of mutations on the SEMA domain and their role in cancer is not well defined, however it is likely that the mutation would affect the binding dynamics of the receptor. FLT1, the gene which encodes VEGFR1, also carried a nonsense mutation in the ligand binding site of the receptor. Two isoforms of VEGFR1 are encoded by FLT1; a membrane bound form and a soluble form. Again, there is little in the curated databases or literature about the effect of FLT1 mutation. However, VEGFR1 plays a critical role in physiological and pathogenic angiogenesis, with loss of VEGFR1 expression associated with poor prognosis in breast cancer (242, 243). It is plausible that mutation of the immunoglobulin domain may result in reduced expression of VEGFR, suggesting a role in taxane resistance. However, as none of the identified mutations had been previously described, it seemed unlikely that the genomic changes observed in the isogenic cell lines could be directly associated with the chemoresistant phenotype observed.

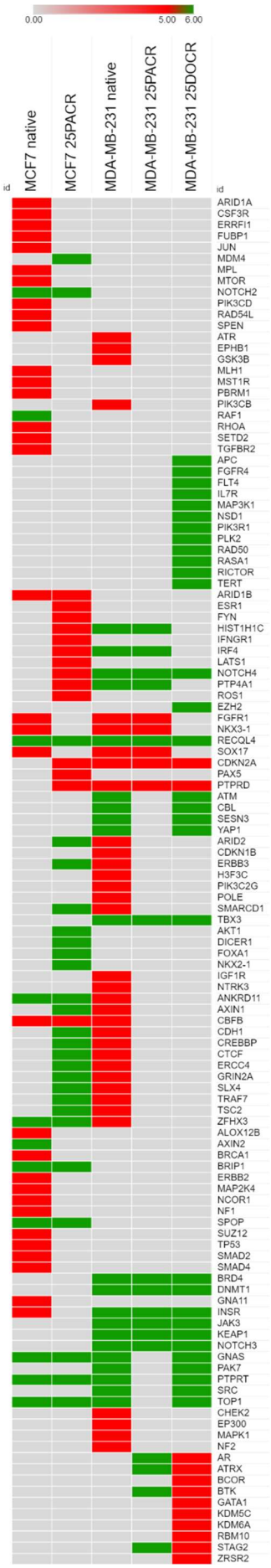

Figure 4.5: Copy number alterations in taxane resistant isogenic cell lines.

Summary of the genes that showed copy number alteration in resistant cells compared to parental cell lines by targeted exome sequencing. Each row represents an individual gene, arranged in chromosomal order. Columns represent each cell line. Green = gain; red = loss; grey = no change observed.

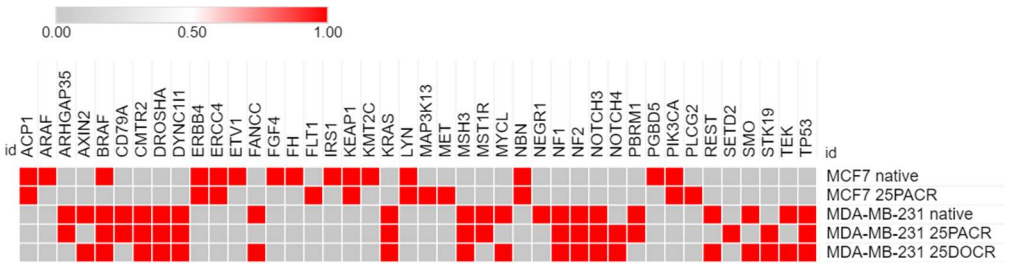

Figure 4.6: Summary of observed gene mutations in the taxane resistant isogenic cell line series. Brick plot of somatic mutations of frequently mutated genes identified by MSK-IMPACT targeted exome sequencing. Each column represents an individual gene, rows are per cell line. Red=somatic mutation; grey=no observed change

To understand the function of all mutated genes identified, gene ontology (GO) functional enrichment analysis was conducted using the online bioinformatics resource, DAVID (Database for Annotation, Visualisation and Integration Discovery) (241). The knowledgebase behind this tool serves to agglomerate gene/protein identifiers with their annotations from public resources, such as NCBI, Ensembl, Gene Ontology and KEGG, to identify statistically significant enriched terms. GO Biological Processes enriched in the mutated genes included the following terms: regulation of transcription (GO:0006351), MAPK cascade (GO:0000165); regulation of cell proliferation (GO:0008285 and GO:0008284); negative regulation of apoptotic process (GO:0043066); positive regulation of RNA polymerase II promoter (GO:0045944) and positive regulation of phosphatidylinositol 3-kinase activity (GO:0045944). Functional interaction of the pathways were visualised using the Cytoscape STRING module. The identified genes were not members of a single pathway, instead mapping via TP53 to a number of inter-linking signalling pathways such as MAPK, Wnt, Hippo and Notch (Figure 4.7).

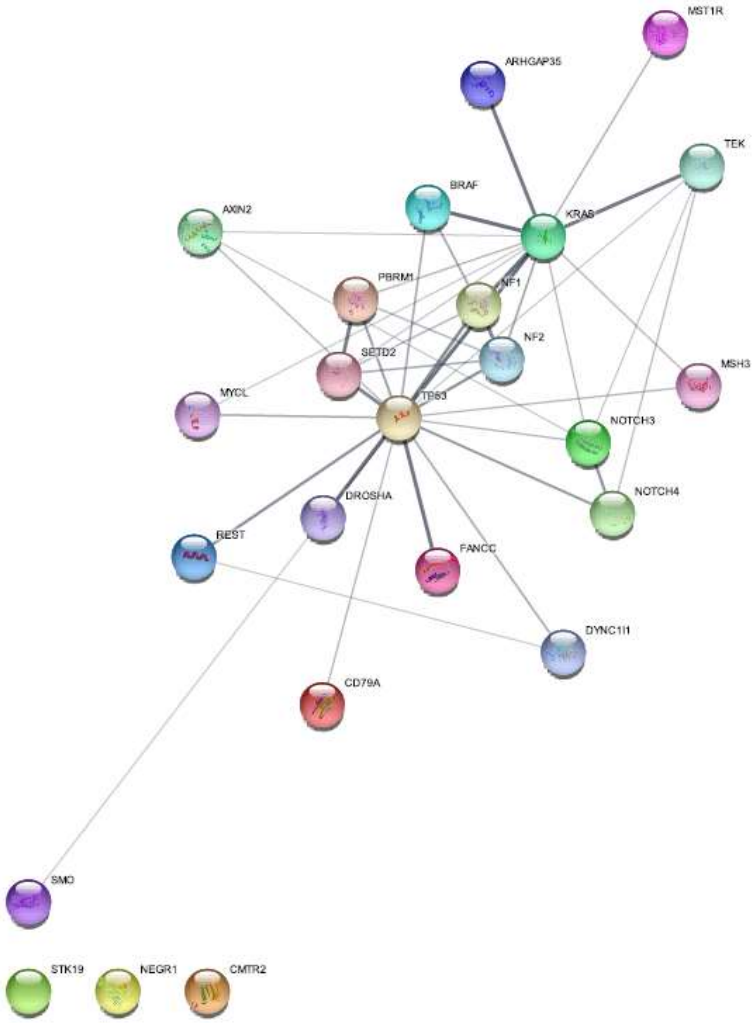

Figure 4.7: Functional interaction network of mutated genes identified by MSK-IMPACT analysis of MDA-MB-231 and MCF7 taxane resistant cell line models. Interactions were visualised using Cytoscape STRING network module.

Table 4.1: MSK-Impact™ assay for human cancer genes for MDA-MB-231 parental and isogenic taxane resistant cell lines

Sample	Chr	Pos.	Ref	Var	Gene ID	Mutation Type; effect	AA change
MDA-MB-231 parent	1	40363463	C	T	MYCL	Missense Mutation; Passenger	p.E256K
MDA-MB-231 parent	1	72400838	T	G	NEGR1	Silent; Passenger	p.T111T
MDA-MB-231 parent	3	49939843	G	T	MST1R	Missense Mutation; Passenger	p.F400L
MDA-MB-231 parent	3	52685790	T	C	PBRM1	Missense Mutation; Passenger	p.I228V
MDA-MB-231 parent	4	57797845	G	C	REST	Missense Mutation; Passenger	p.D941H
MDA-MB-231 parent	5	31526458	G	A	DROSHA	Silent; Passenger	p.P194P
MDA-MB-231 parent	5	80109433	G	A	MSH3	Missense Mutation; Likely pathogenic	p.G896R
MDA-MB-231 parent	7	95709774	C	A	DYNC1I1	Missense Mutation; Passenger	p.R601S

MDA-MB-231 parent	7	128829039	G	GGCT	SMO	In Frame Ins; Potentially pathogenic	p.L23dup
MDA-MB-231 parent	7	140481417	C	A	BRAF	Missense Mutation; Likely pathogenic	p.G464V
MDA-MB-231 parent	9	27197430	G	C	TEK	Missense Mutation; Passenger	p.R581T
MDA-MB-231 parent	9	97897664	C	T	FANCC	Silent; Passenger	p.L269L
MDA-MB-231 parent	12	25398281	C	T	KRAS	Missense Mutation; Likely pathogenic	p.G13D
MDA-MB-231 parent	16	71318544	C	CA	CMTR2	Frame Shift Ins; Likely pathogenic	p.C427Lfs*2
MDA-MB-231 parent	17	7577099	C	T	TP53	Missense Mutation; Likely pathogenic	p.R280K
MDA-MB-231 parent	17	29541474	T	TC	NF1	Frame Shift_ Ins; Likely pathogenic	p.T467Hfs*3
MDA-MB-231 parent	17	63533189	G	A	AXIN2	Splice Region; Passenger	
MDA-MB-231 parent	19	15300174	T	A	NOTCH3	Missense Mutation; Likely pathogenic	p.T368S

MDA-MB-231 parent	19	42383297	G	A	CD79A	Missense Mutation; Likely pathogenic	p.C106Y
MDA-MB-231 parent	19	47425394	G	A	ARHGAP35	Silent; Passenger	p.K1154K
MDA-MB-231 parent	22	30057209	G	T	NF2	Nonsense Mutation; Likely pathogenic	p.E231*
MDA-MB-231 25PACR	3	47165156	C	A	SETD2	Missense Mutation; Passenger	p.D324Y
MDA-MB-231 25PACR	3	49939843	G	T	MST1R	Missense Mutation; Passenger	p.F400L
MDA-MB-231 25PACR	3	52685790	T	C	PBRM1	Missense Mutation; Passenger	p.I228V
MDA-MB-231 25PACR	5	31526458	G	A	DROSHA	Silent; Passenger	p.P194P
MDA-MB-231 25PACR	5	80109433	G	A	MSH3	Missense Mutation; Likely pathogenic	p.G896R
MDA-MB-231 25PACR	6	31940401	C	G	STK19	Missense Mutation; Passenger	p.S145W
MDA-MB-231 25PACR	6	32168893	C	A	NOTCH4	Splice Site; Passenger	p.X1380_splice

MDA-MB-231 25PACR	7	95709774	C	A	DYNC1I1	Missense Mutation; Passenger	p.R601S
MDA-MB-231 25PACR	7	140481417	C	A	BRAF	Missense Mutation; Likely pathogenic	p.G464V
MDA-MB-231 25PACR	12	25398281	C	T	KRAS	Missense Mutation; Likely pathogenic	p.G13D
MDA-MB-231 25PACR	16	71318544	C	CA	CMTR2	Frame Shift Ins; Likely pathogenic	p.C427Lfs*2
MDA-MB-231 25PACR	17	7577099	C	T	TP53	Missense Mutation; Likely pathogenic	p.R280K
MDA-MB-231 25PACR	17	29541474	T	TC	NF1	Frame_ Shift Ins; Likely pathogenic	p.T467Hfs*3
MDA-MB-231 25PACR	19	15300174	T	A	NOTCH3	Missense Mutation; Likely pathogenic	p.T368S
MDA-MB-231 25PACR	19	42383297	G	A	CD79A	Missense Mutation; Likely pathogenic	p.C106Y
MDA-MB-231 25PACR	19	47425394	G	A	ARHGAP35	Silent; Passenger	p.K1154K
MDA-MB-231 25DOCR	1	40363463	C	T	MYCL	Missense Mutation; Passenger	p.E256K

MDA-MB-231 25DOCR	4	57797845	G	C	REST	Missense Mutation; Passenger	p.D941H
MDA-MB-231 25DOCR	5	31526458	G	A	DROSHA	Silent; Passenger	p.P194P
MDA-MB-231 25DOCR	5	80109433	G	A	MSH3	Missense Mutation; Likely pathogenic	p.G896R
MDA-MB-231 25DOCR	6	31940401	C	G	STK19	Missense Mutation; Passenger	p.S145W
MDA-MB-231 25DOCR	6	32168893	C	A	NOTCH4	Splice Site; Passenger	p.X1380_splice
MDA-MB-231 25DOCR	7	95709774	C	A	DYNC1I1	Missense Mutation; Passenger	p.R601S
MDA-MB-231 25DOCR	7	128829039	G	GGCT	SMO	In Frame Ins; Potentially pathogenic	p.L23dup
MDA-MB-231 25DOCR	7	140481417	C	A	BRAF	Missense Mutation; Likely pathogenic	p.G464V
MDA-MB-231 25DOCR	9	27197430	G	C	TEK	Missense Mutation; Passenger	p.R581T
MDA-MB-231 25DOCR	9	97897664	C	T	FANCC	Silent; Passenger	p.L269L

MDA-MB-231 25DOCR	12	25398281	C	T	KRAS	Missense Mutation; Likely pathogenic	p.G13D
MDA-MB-231 25DOCR	16	71318544	C	CA	CMTR2	Frame Shift Ins; Likely pathogenic; Likely pathogenic	p.C427L fs*2
MDA-MB-231 25DOCR	17	7577099	C	T	TP53	Missense Mutation; Likely pathogenic	p.R280K
MDA-MB-231 25DOCR	17	29541474	T	TC	NF1	Frame Shift Ins; Likely pathogenic	p.T467H fs*3
MDA-MB-231 25DOCR	17	63533189	G	A	AXIN2	Splice Region; Passenger	
MDA-MB-231 25DOCR	19	15300174	T	A	NOTCH3	Missense Mutation; Likely pathogenic	p.T368S
MDA-MB-231 25DOCR	22	30057209	G	T	NF2	Nonsense Mutation; Likely pathogenic	p.E231*

Highlighted in red are the mutations shared by MDA-MB-231 and the isogenic taxane-resistant cell lines MDA-MB-231 25PACR and MDA-MB-231 25DOCR cell lines compared to the reference genome; in black are the mutations unique to either. The impact of the mutation on each protein are shown in column titled 'AA change' where: Alanine(A); Arginine(R); Asparagine(N); Aspartic Acid(D); Cysteine(C); Glutamic Acid(E); Glutamine(Q); Glycine(G); Histidine(H); Isoleucine(I); Leucine(L); Lysine(K); Methionine(M); Phenylalanine(F); Proline(P); Serine(S); Threonine(T); Tryptophan(W); Tyrosine(Y); Valine(V)

Table 4.2: MSK-Impact™ assay for human cancer genes for MCF7 parental and MCF7 25PACR taxane resistant cell lines

Sample	Chr	Pos.	Ref.	Var.	Gene ID	Mutation Type	AA change
MCF7 parent	1	230459353	G	A	PGBD5	Missense Mutation; Passenger	p.H396Y
MCF7 parent	1	241661129	C	T	FH	Silent; Passenger	p.*511*
MCF7 parent	2	277002	C	T	ACP1	Nonsense Mutation; Passenger	p.Q106*
MCF7 parent	2	212248542	T	C	ERBB4	Missense Mutation; Passenger	p.Y1242C
MCF7 parent	2	227660008	C	T	IRS1	Silent; Passenger	p.V1149V
MCF7 parent	2	227662476	G	A	IRS1	Missense Mutation; Passenger	p.R327C
MCF7 parent	3	178936091	G	A	PIK3CA	Missense Mutation; Likely pathogenic	p.E545K
MCF7 parent	7	13975527	C	A	ETV1	Splice Region; Passenger	

MCF7 parent	7	140507806	A	G	BRAF	Missense Mutation; Passenger	p.L222S
MCF7 parent	7	151879490	T	C	KMT2C	Missense Mutation; Passenger	p.M1819V
MCF7 parent	8	56911984	G	A	LYN	Silent; Passenger	p.K404K
MCF7 parent	8	90976658	G	T	NBN	Missense Mutation; Passenger	p.P325H
MCF7 parent	8	90994994	G	A	NBN	Nonsense Mutation; Likely pathogenic	p.R43*
MCF7 parent	11	69589541	G	A	FGF4	Silent; Passenger	p.I104I
MCF7 parent	16	14041636	G	C	ERCC4	Missense Mutation; Passenger	p.S728T
MCF7 parent	19	10602447	C	T	KEAP1	Silent; Passenger	p.V377V
MCF7 parent	X	47426492	C	T	ARAF	Missense Mutation; Passenger	p.R279C
MCF7 25PACR	2	277002	C	T	ACP1	Nonsense Mutation; Passenger	p.Q106*

MCF7 25PACR	2	212248542	T	C	ERBB4	Missense Mutation; Passenger	p.Y1242C
MCF7 25PACR	3	178936091	G	A	PIK3CA	Missense Mutation; Likely pathogenic	p.E545K
MCF7 25PACR	3	185167815	G	A	MAP3K13	Missense Mutation; Passenger	p.D380N
MCF7 25PACR	7	116380020	C	G	MET	Nonsense Mutation; Likely pathogenic	p.S470*
MCF7 25PACR	8	56911984	G	A	LYN	Silent; Passenger	p.K404K
MCF7 25PACR	8	90976658	G	T	NBN	Missense Mutation; Passenger	p.P325H
MCF7 25PACR	8	90994994	G	A	NBN	Nonsense Mutation; Likely pathogenic	p.R43*
MCF7 25PACR	13	29008287	G	T	FLT1	Nonsense Mutation; Likely pathogenic	p.S195*
MCF7 25PACR	16	14041636	G	C	ERCC4	Missense Mutation; Passenger	p.S728T

MCF7 25PACR	16	81929473	C	A	PLCG2	Silent; Passenger	p.T378T
MCF7 25PACR	19	10602447	C	T	KEAP1	Silent; Passenger	p.V377V

Highlighted in red are the mutations shared by both MCF7 and MCF7 25PACR cell lines compared to the reference genome, while in black are the mutations unique to either. The impact of the mutation on each protein are shown in column titled 'AA change' where: Alanine(A); Arginine(R); Asparagine(N); Aspartic Acid(D); Cysteine(C); Glutamic Acid(E); Glutamine(Q); Glycine(G); Histidine(H); Isoleucine(I); Leucine(L); Lysine(K); Methionine(M); Phenylalanine(F); Proline(P); Serine(S); Threonine(T); Tryptophan(W); Tyrosine(Y); Valine(V)

4.2.3 Transcriptomic profiling of taxane resistant cell lines using Nanostring® technology

To expand and complement the results from the RPPA, transcriptomic profiles of all paired isogenic taxane resistant cell lines were characterised by gene expression analysis utilising the Nanostring platform. The PanCancer Pathway panel was selected for its broad coverage of signalling pathways but also as it encompassed half of the targets analysed with the reverse phase protein array. Paired analyses was performed between parental and resistant cell lines to quantify differentially expressed genes (DEGs) after taxane resistance had been established. All resistant cell lines were assessed with three replicates for each group prepared.

Preliminary analysis investigated the similarity between the taxane sensitive parental cell line and the derived taxane resistant isogenic cell line. Unsupervised bidirectional hierarchical clustering of the log2 normalised data revealed sample repeat clustering at the first level of the dendogram, and cell line clustering above that, with the triple negative MDA-MB-231 cell lines clustered separately from the ER+ MCF7 cell lines (Figure 4.8). It was noted that the paclitaxel resistant MDA-MB-231 25PACR cell line demonstrated less similarity to the parental cell line, MDA-MB-231, than the docetaxel resistant cell line MDA-MB-231 25DOCR. This suggested that the two taxanes (paclitaxel and docetaxel) may confer chemoresistance by inducing changes in different genes.

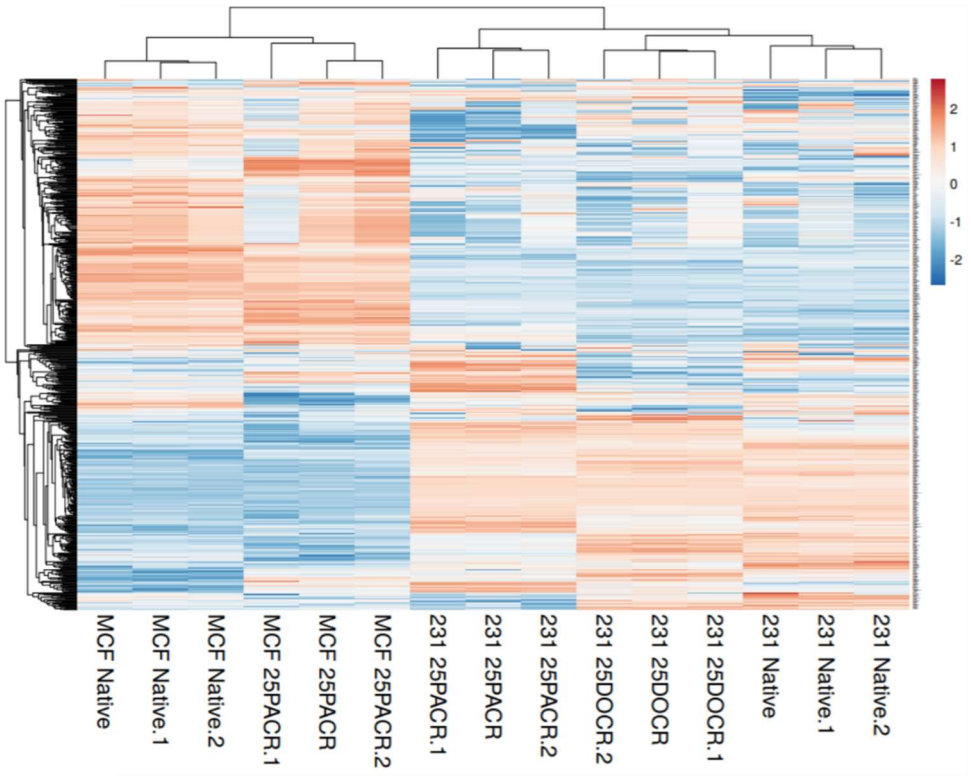

Figure 4.8: Expression of cancer associated pathway mRNAs are altered in taxane resistant cell lines compared to native parental lines. Unsupervised hierarchical clustering of 730 mRNAs which feature on the PanCancer Pathway Nanostring panel from taxane resistant MDA-MB-231 and MCF7 isogenic cell lines and their respective parental control cell lines. Log 2 mean centred heatmap of all genes for each code set are depicted. Columns represent individual biological samples, rows represent individual mRNA transcripts. Red represents higher relative expression and blue lower relative expression. Unit variance scaling is applied to rows. Both rows and columns are clustered using Pearson correlation distance, average linkage performed and the heatmap drawn in Clustvis (244).

Differential expression analysis was performed using the nSolver v 4.0 advance analysis software and comparisons between all taxane resistant isogenic cell lines with their parental cell line were made. The nSolver software was used to calculate log2 ratios to describe the fold change observed with associated p-values for each mRNA. Differentially expressed genes (DEGs) were identified by applying cut-off thresholds of ± 0.58 log2-ratio and a p-value ≤ 0.05.

Analysis of the PanCancer Pathway code set for each isogenic/parental cell line comparison showed that the acquisition of taxane resistance resulted in a change in

expression levels of between 20% - 30% of the total mRNA of the PanCancer Pathway code set for each isogenic cell line comparison. The expression of 198 genes in the PanCancer pathway panel were significantly differentially regulated ($p \leq 0.05$, log2 ratio $\geq \pm 0.58$) between the paclitaxel resistant isogenic cell line MDA-MB-231 25PACR and the parental MDA-MB-231 cell line (Table 4.3). The majority of these were found to be upregulated (118; 60%) upon acquisition of paclitaxel resistance, whereas 80 (40%) were down-regulated. The comparison of the docetaxel resistant MDA-MB-231 25DOCR cell lines with the parental cell line revealed a total of 141 differentially expressed genes across the same panel. This comparison revealed a similar division with 57% (80) of the genes being upregulated and 43% (61) downregulated. Finally analysis of MCF7 25PACR compared with its parental counterpart, MCF7, revealed 161 differentially expressed genes. Of these differentially expressed genes, 76 were upregulated (47%) in the taxane resistant isogenic cell line compared to the parental MCF7 cell line, whereas 85 genes (53%) were downregulated.

Table 4.3: Differentially expressed genes from PanCancer Pathway codeset in taxane resistant cell lines

	MDA-MB-231 25PACR	MDA-MB-231 25DOCR	MCF7 25PACR
Upregulated	118	80	76
Down-regulated	80	61	85

Comparison of native parental cell lines and taxane resistant isogenic cell lines. A threshold of 0.58 log2 fold change, p≤0.05 was applied to the normalised values.

The distribution of calculated fold change (log 2 resistant/parental) and the results for each individual differential expression analysis are shown in volcano plots with the fold change (log2 ratio) and the p value displayed on the x and y axes respectively (Figure 4.9A-C). The mRNAs that fell below the threshold were excluded from further analyses. To identify those genes which were commonly dysregulated in the taxane resistant cell lines, Venn diagrams were employed to visualise the overlap between the cell lines (Figure 4.9D). Of these, 74 mRNA were commonly altered in MDA-MB-231 25PACR and MDA-MB-231 25DOCR cell lines, 63 mRNA between MDA-MB-231 25PACR and MCF7 25PACR and 41 mRNA between MDA-MB-231 25DOCR and MCF7 25PACR.

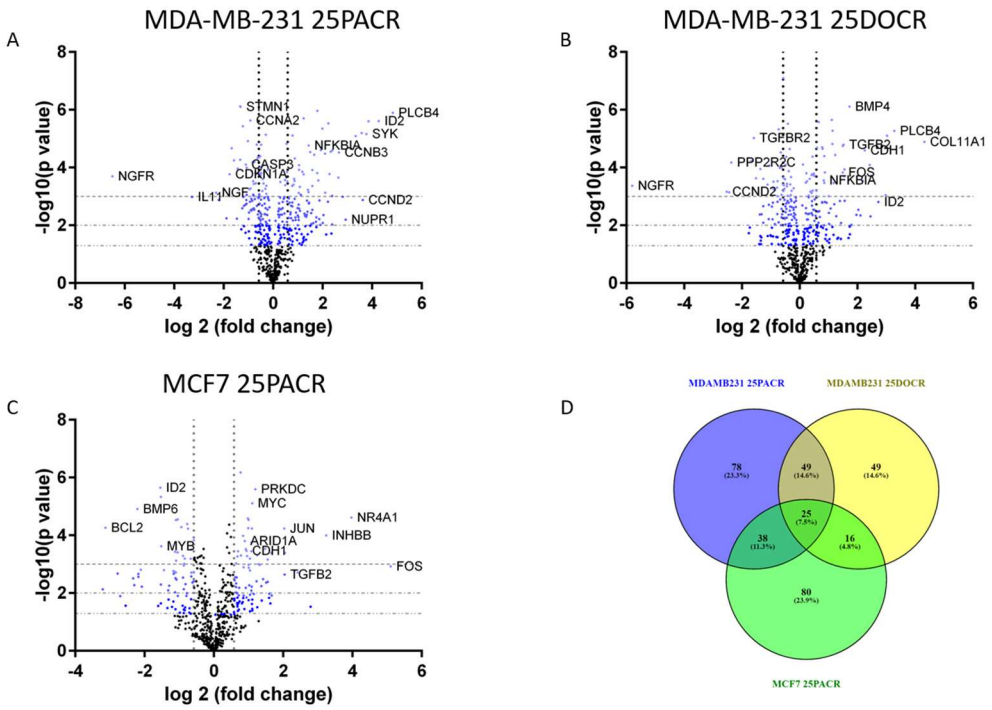

Figure 4.9: Differential gene expression associated with taxane resistance. The volcano plots display each mRNA log10 (p-value) and log2 fold change for resistant vs. parental cells: (A) MDA-MB-231 25PACR, (B) MDA-MB-231 25DOCR and (C) MCF7 25PACR. Ascending vertical dotted lines represent $p<0.05$, $p<0.01$ and $p<0.001$ respectively. Those mRNA with a log2 fold change of ± 0.58 and statistically significant are coloured blue. Volcano plots were created using GraphPad Prism (D) Venn diagram showing overlapping differentially expressed genes between MDA-MB-231 25PACR, MDA-MB-231 25DOCR and MCF7 25PACR taxane resistant cell lines. Venn diagrams were created using the online tool Venny 2.1 (245)

Supervised hierarchical clustering of the differentially expressed mRNA confirmed consistent expression across the cell line replicates (Figure 4.10). However, clustering highlighted clear differences between the MDA-MB-231 and MCF7 cell lines, emphasising the diversity was greater between cell lines than between paclitaxel resistant and parental cell lines.

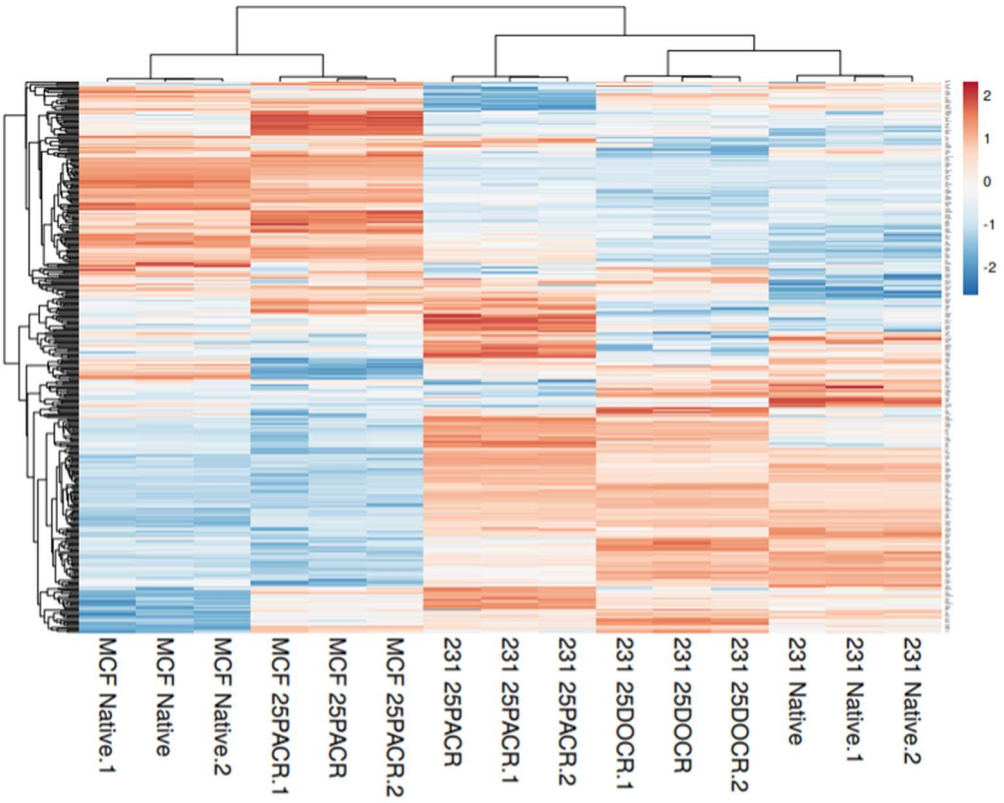

Figure 4.10: Supervised hierarchical clustering of genes from the Nanostring PanCancer Pathway codeset in taxane resistant isogenic cell lines. Log 2 mean centred supervised hierarchical clustered heatmap of all differentially expressed genes (log 2 FC ≥ ±0.58; p value ≤0.05) of the PanCancer Pathway panel. Columns represent individual biological samples, rows represent individual mRNA transcripts. Red represents higher relative expression and blue lower relative expression. Unit variance scaling is applied to rows. Both rows and columns are clustered using Pearson correlation distance, average linkage performed and the heatmap drawn in Clustvis (244)

Of the 74 genes identified as being differentially expressed in the two MDA-MB-231 taxane resistance models, 63 mRNA shared directionality of change. Of these, 49 mRNA were overexpressed and 14 mRNA downregulated in the MDA-MB-231 resistant cell lines. An FI network was created of interconnecting genes and clustering modules were filtered for clusters with nodes ≥ 10, and four modules were obtained (Figure 4.11). GO enrichment analysis revealed that the FI network were statistically significantly enriched for biological processes including: regulation of transcription from RNA polymerase II, regulation of apoptotic process and regulation of signalling receptor activity. Enriched pathways included cytokine-cytokine receptor interaction

and PI3K-Akt signalling (module 1; Figure 4.11A), transcriptional misregulation of cancer (module 2; Figure 4.11B), MAPK signalling (module 3; Figure 4.11C) and PI3K-Akt signalling (module 4; Figure 4.11D).

A

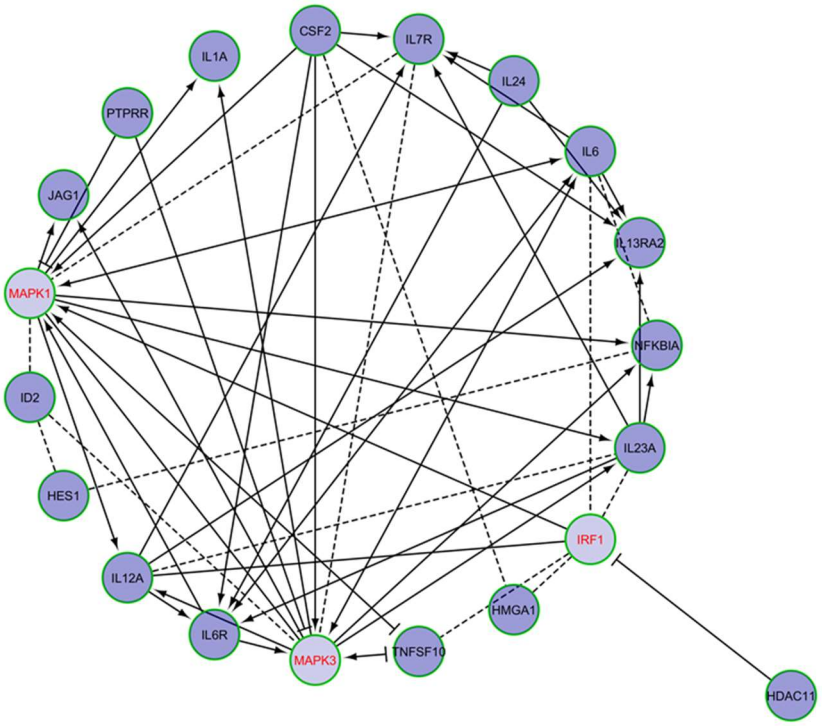
CSF2
IL7R
IL1A
IL24
PTPRR
IL6
JAG1
IL13RA2
MAPK1
NFKBIA
ID2
IL23A
HES1
IRF1
IL12A
HMGA1
IL6R
MAPK3
TNFSF10
HDAC11

B

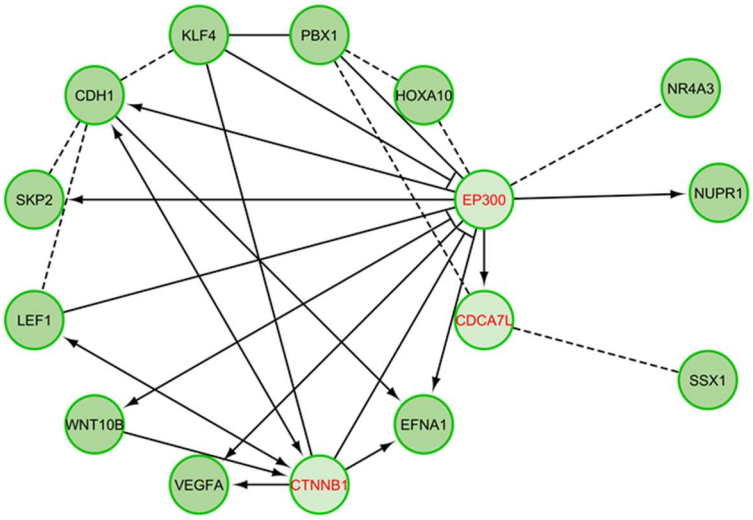
KLF4
PBX1
CDH1
HOXA10
NR4A3
SKP2
EP300
NUPR1
LEF1
CDCA7L
SSX1
WNT10B
EFNA1
VEGFA
CTNNB1

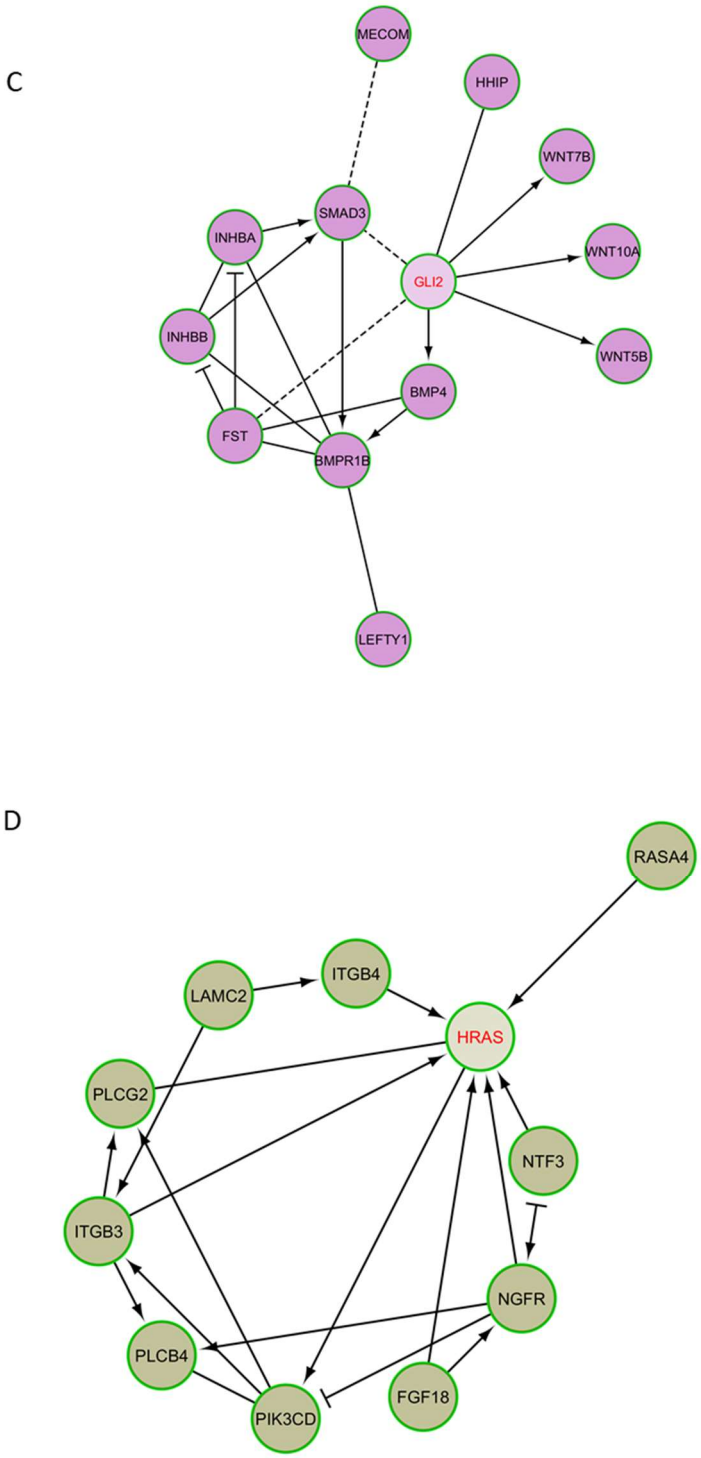

Figure 4.11; Enrichment analysis of DEGs from both MDA-MB-231 taxane resistant cell line models. Functional interaction (FI) networks for 65 target genes was visualised using Cytosape Reacomte FIViz. Four modules were identified of ≥ 10 nodes: (A) Module 1 the most significant cluster with 17 nodes (B) module 2 (C) module 3 and (D) module 4. Linker genes are shown in red. Interconnecting lines show direction attribute values: --> activating/catalysing; --| inhibition; solid line for complexes or inputs; --- for predicted FIs.

Due to the inability to produce a stable docetaxel resistant MCF7 cell line, analysis was limited to enrichment analysis for those 161 DEGs identified in the paclitaxel resistant MCF7 25PACR cell line. Again an FI network of an interconnecting set of modules was created in Cytoscape, eight of which were composed of ≥ 10 nodes. GO enrichment of the FI network identified significant association to regulation of cell proliferation, regulation of transcription and MAPK cascade. Pathway enrichment analysis of the most significant module consisting of 51 nodes, identified associations with transcriptional misregulation of cancer, cell cycle and Notch signalling pathway (Figure 4.12A). The second most significant module of 35 nodes was enriched for Ras signalling, Rap signalling and PI3-Akt signalling pathways (Figure 4.12B). Module 3 was associated with the cell cycle and apoptosis (Figure 4.12C) and module 4 with the MAPK signalling pathway (Figure 4.12D). The remaining modules were associated with focal adhesion (Figure 4.12E) and the TGFβ signalling pathway (Figure 4.12F).

A

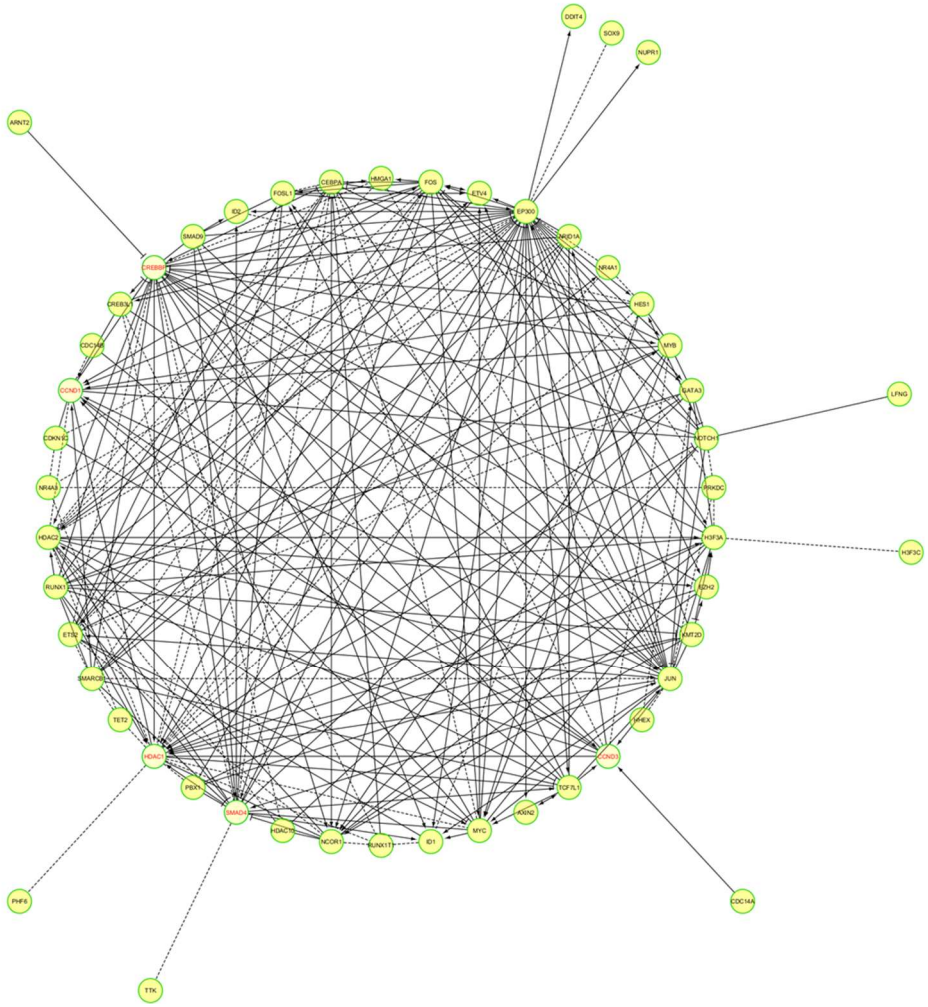
DDIT4
SOX9
NUPR1
ARNT2
FOSL1
CEBPA
HMGA1
FOS
LETV1
EP300
IDS
SMAD6
CREBBP
NKD1A
NR4A1
CREB3L1
HES1
CDC14B
MYB
CCND1
GATA3
LFNG
CDKN1C
HDTCH
NR4A3
PRKDC
HDAC2
H3F3A
H3F3C
RUNX1
EZH2
ETS2
KMT2D
SMARCB1
JUN
TET2
PHEX
HDAC1
CCND3
PBX1
TCF7L1
SMAD4
KDM2
HDAC10
NCOR1
RUNX1T1
ID1
MYC
PHF6
CDC14A
TTK

B

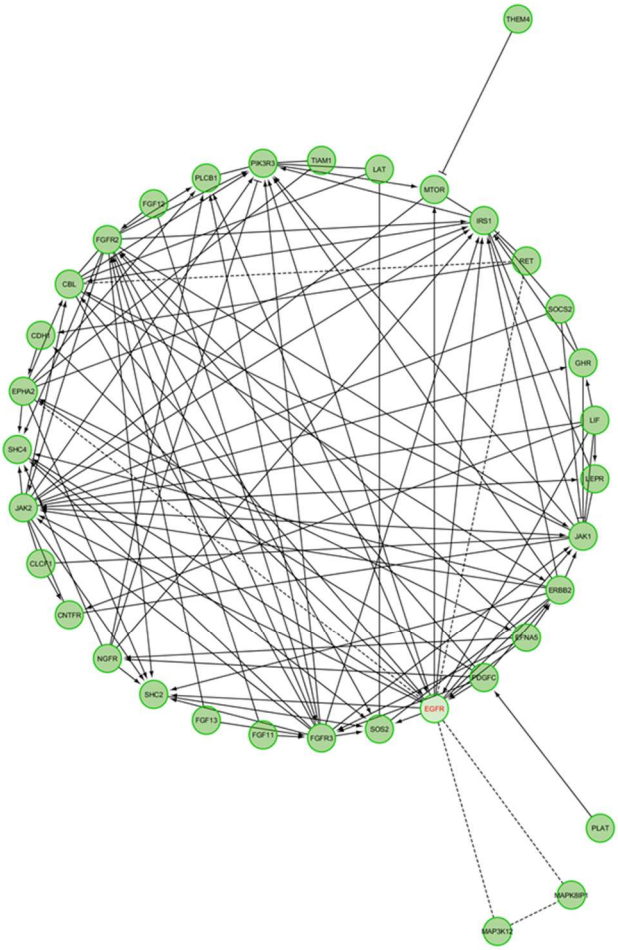
THEM4
PIK3R3
TIAM1
LAT
PLCB1
MTOR
FGF12
IRS1
FGFR2
RET
CBL
SOCS2
CDH1
GHR
EPHA2
LIF
SHC4
LEPR
JAK2
JAK1
CLCF1
ERBB2
CNTFR
IFNA5
NGFR
PDGFC
SHC2
EGFR
FGF13
SOS2
FGF11
FGFR3
PLAT
MAPK8IP1
MAP3K12

C

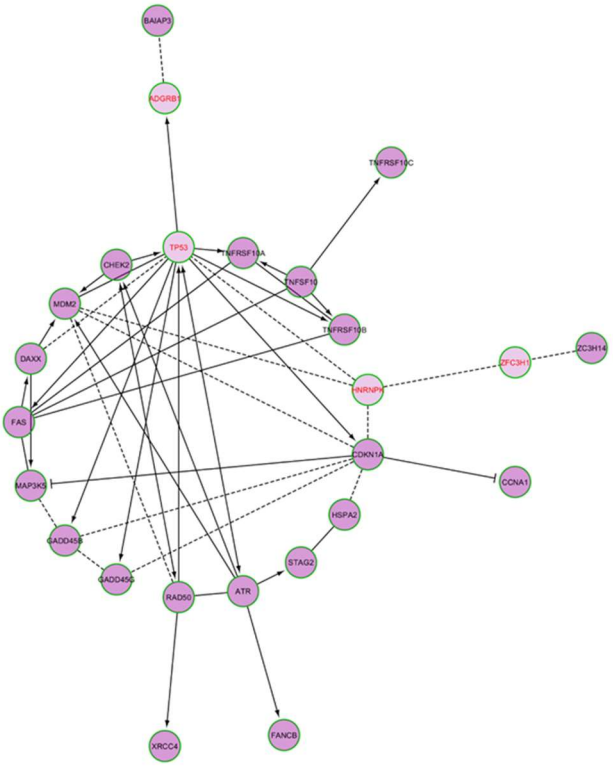
BAIAP3
ADGRB1
TNFRSF10C
TP53
CHEK2
TNFRSF10A
TNFSF10
MDM2
TNFRSF10B
DAXX
ZFC3H1
ZC3H14
HNRNPK
FAS
CDKN1A
CCNA1
MAP3K5
HSPA2
GADD45B
STAG2
GADD45G
RAD50
ATR
XRCC4
FANCB

D

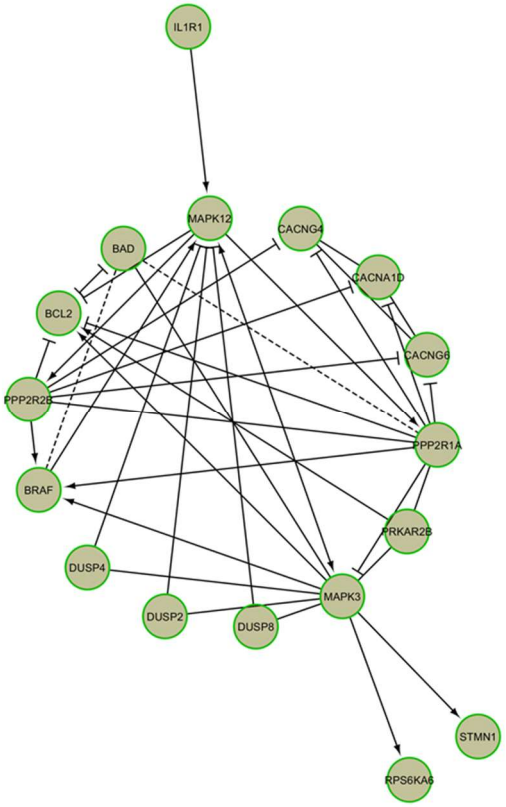
IL1R1
MAPK12
CACNG4
BAD
CACNA1D
BCL2
CACNG8
PPP2R2B
PPP2R1A
BRAF
PRKAR2B
DUSP4
MAPK3
DUSP2
DUSP8
STMN1
RPS6KA6

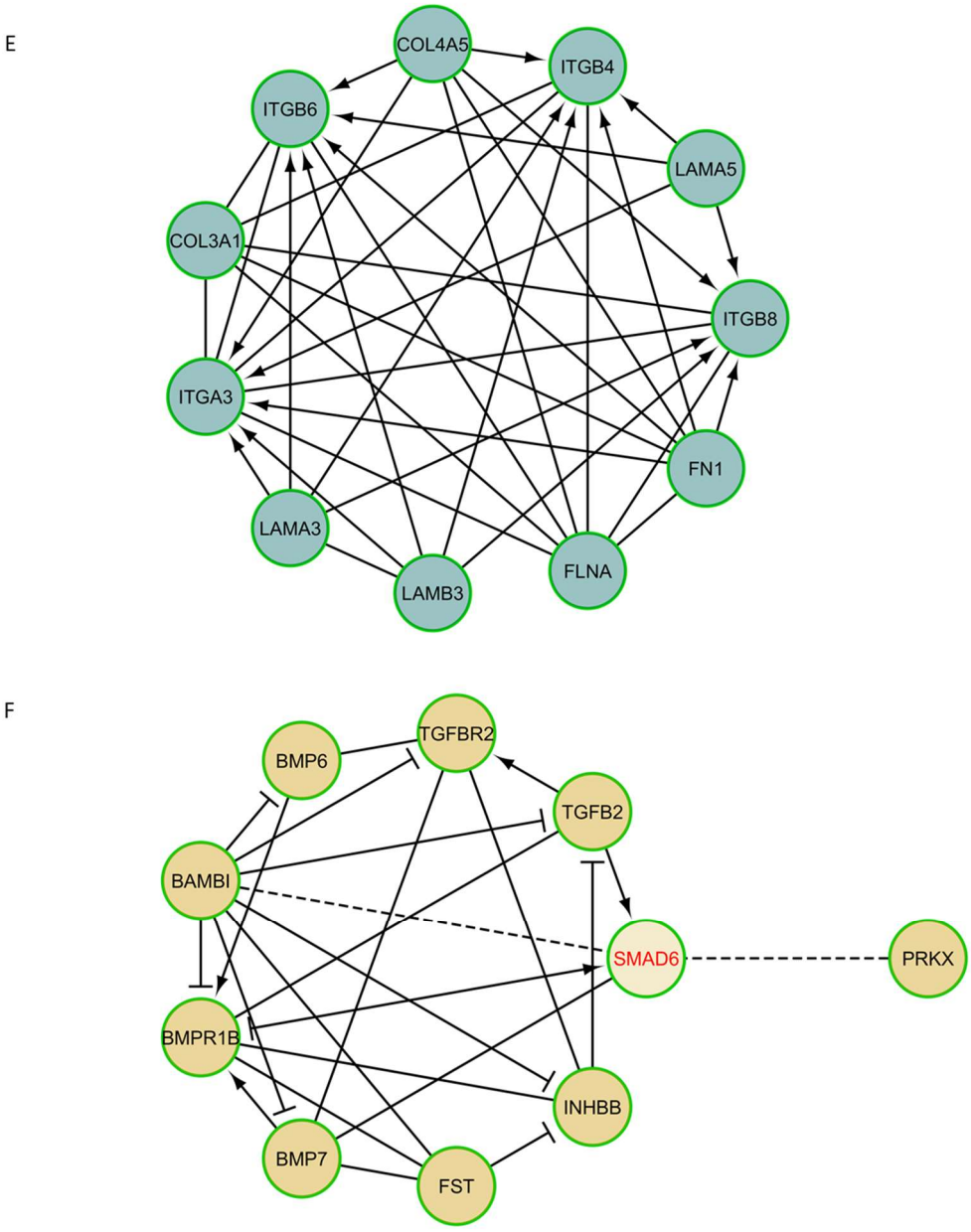

Figure 4.12: Enrichment analysis of DEGs from MCF7 25PACR taxane resistant cell line model. Functional interaction (FI) networks for 161 target genes was visualised using Cytosape Reacomte FIViz. Six interconnecting modules were identified of ≥ 10 nodes: (A) Module 1 the most significant cluster with 51 nodes; (B) module 2 contained 35 nodes; (C) 25 nodes were visualised in module 3; (D) module 4 with 17 nodes; (E) module 5 with 11 nodes and (F) module 6 with 10 nodes. Linker genes are shown in red. Interconnecting lines show direction attribute values: --> activating/catalysing; --| inhibition; solid line for complexes or inputs; --- for predicted FIs.

Despite all three chemoresistant cell lines demonstrating similar *in vitro* profiles with regard to proliferation, cell cycle and apoptosis it was evident that only a small number of genes were commonly dysregulated across all isogenic cell lines (Figure 4.9C). Of the 23 mRNAs dysregulated in all three resistant cell lines, 15 were found to share directionality in change. Nine mRNAs were shown to have consistent upregulation across all three chemoresistant cell lines: (*NUPR1, PBX1, HES1, CDH1, ITGB4, NR4A1, BMPR1B, WNT7B,* and *INHBB*) and 6 mRNAs consistently downregulated (*CCNA1, BCL2, TNFSF10, HIST1H3H, HMGA1* and *NGFR*) (Table 4.4).

Table 4.4: List of the common statistically significant differentially expressed genes derived from the Nanostring PanCancer Pathway codeset in the taxane resistant cell lines.

Probe name	MDA-MB-231 25PACR		MDA-MB-231 25DOCR		MCF7 25PACR		Pathway
	Log2FC	Pvalue	Log2FC	Pvalue	Log2FC	Pvalue	
CDH1	3.36	0.0007	3.92	4.81 E-6	0.89	0.0008	Driver gene
NUPR1	2.84	0.0036	2.42	0.0019	0.79	0.0197	Transcriptional misregulation
PBX1	2.25	0.0002	0.95	0.0011	1.23	0.0012	Transcriptional misregulation; positive regulation of transcription from RNA Pol II promoter
HES1	1.84	0.006	2.06	0.0031	1.99	0.0004	Notch signalling; positive regulation of transcription from RNA Pol II promoter
JAG2	1.72	0.0115	1.76	0.0182	0.58	0.0071	Notch signalling
ITGB4	1.4	0.0004	0.73	0.0024	0.72	0.0007	PI3K-Akt signalling

NR4A3	1.37	0.0018	0.96	0.0369	1.32	0.0194	PI3K-Akt signalling; MAPK signalling; positive regulation of transcription from RNA Pol II promoter
BMPR1B	1.34	0.0018	1.57	0.0002	2.27	0.0015	TGFβ signalling; positive regulation of transcription from RNA Pol II promoter
WNT7B	1.31	0.0064	0.87	0.0101	0.62	0.0374	Hippo Hedgehog; WNT signalling
INHBB	0.96	0.0019	1.41	0.0015	3.18	8.11 E-5	TGFβ signalling
BCL2	-1.0	0.0034	-0.6	0.0443	-3.18	3.94 E-5	Driver gene; Cell cycle and apoptosis; PI3K- Akt pathway
TNFSF10	-1.2	0.0022	-0.93	0.0018	-3.28	0.008	Cell cycle; apoptosis

HIST1H3H	-1.46	1 E-6	-0.74	2.25 E-6	-1	1.11 E-5	Driver gene; Transcriptional misregulation
HMGA1	-1.61	1.4 E-5	-1.02	0.0003	-0.93	0.0059	Chromatin modification; positive regulation of transcription from RNA Pol II promoter
NGFR	-7.4	0.0038	-5.82	0.0009	-1.8	0.0388	Transcriptional misregulation; PI3K- Akt pathway; RAS signalling

FC = fold change

An FI network of those 23 mRNA was created in Cytoscape (Figure 4.13A) and enrichment analysis for KEGG pathways and GO biological processes associated with the mRNA performed. Due to the small number of mRNA identified as being commonly changed in all three resistant cell lines, linker genes were included in the enrichment analysis. KEGG pathway enrichment analyses included pathways in cancer (p=4.74E-11), TGF-β signalling (p=4.18E-7) and PI3-Akt signalling (p=4.96E-6) (Figure 4.13B) with GO biological processes highlighting changes in regulation of transcription by RNA polymerase II promoter and regulation of apoptosis (Figure 4.13C).

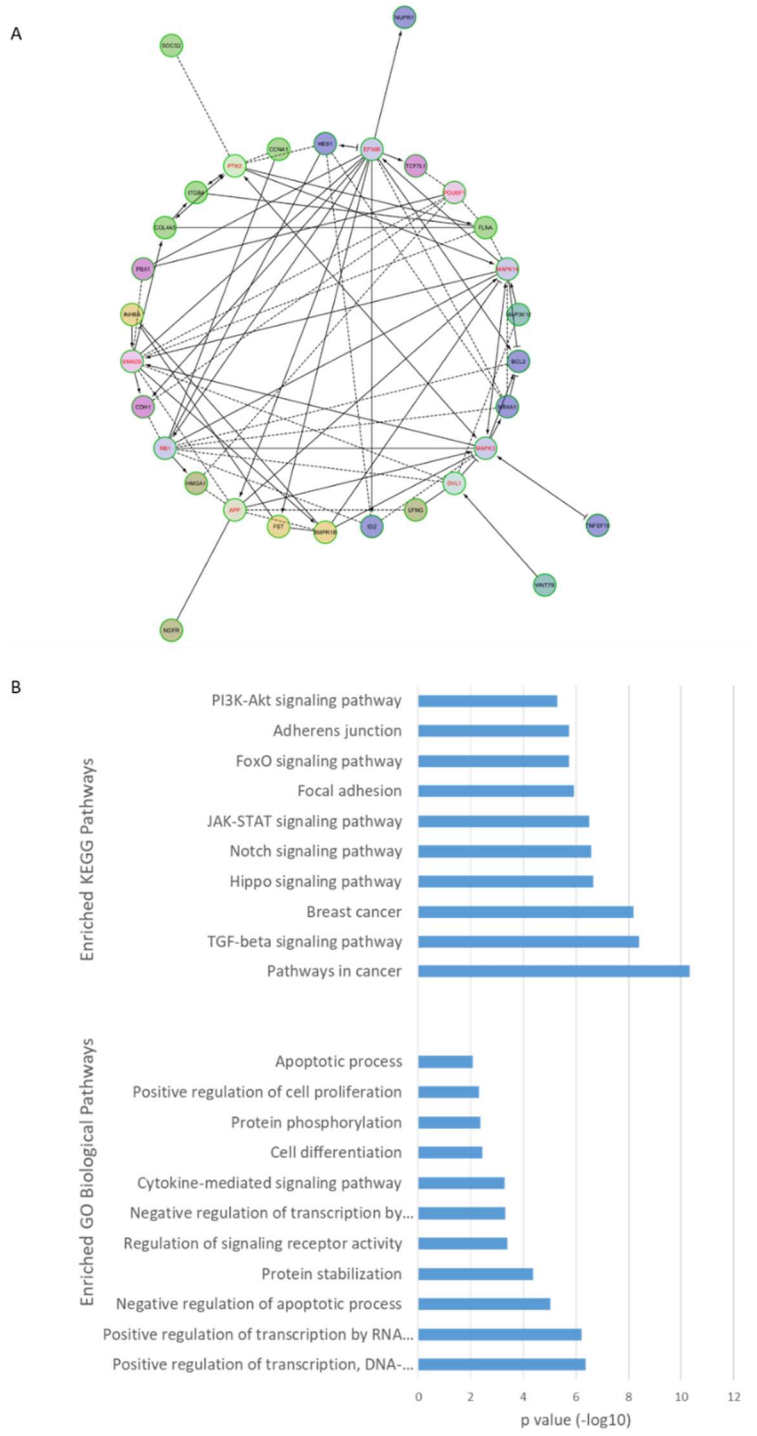

Figure 4.13: Enrichment analysis of commonly dysregulated taxane resistance associated DEGs from Nanostring PanCancer pathway code set. (A) Functional interaction (FI) network constructed for 23 target mRNA clustered in to four modules (shown in different colours). Linker genes are shown in red. Overrepresentation analysis of (B) KEGG pathways and (C) Gene Ontology Biological Processes. Bars indicate p values shown as – log10.

4.2.4 Validation of the dysregulated pathways as identified by RPPA and Nanostring

Cytoscape analysis of both proteomic and transcriptomic data indicated dysregulation of the MAPK and PI3K-Akt signalling pathways, amongst others. To understand the role of these pathways in taxane resistance, the expression of some key proteins involved were quantified by Western blotting. Included in the panels are lysates for the later derivations of the resistant cell lines (Figure 4.14).

Upregulation of EGFR had been observed in the paclitaxel resistant cell line, MDA-MB-231 25PACR, while performing the initial characterisation of the taxane resistant cell lines. However the anticipated activation of the PI3K-Akt pathway via Akt1 phosphorylation was not observed in any of the resistant cell lines. Upregulation of total FAK and the activated form was noted in the both the resistant MDA-MB-231 cell lines, although it appeared down-regulated in the MCF7 25PACR cell line. Activation of p44/42 MAPK was absent in both of the MDA-MB231 docetaxel resistant isogenic cell lines, as well as the MDA-MB-231 50PACR resistant cell line. In all of these lines, an increase in total p44/42 MAPK could be seen. This pattern was mimicked in the MCF7 paclitaxel resistant series. Finally, a reduction in p38 MAPK protein was seen in all resistant cell lines.

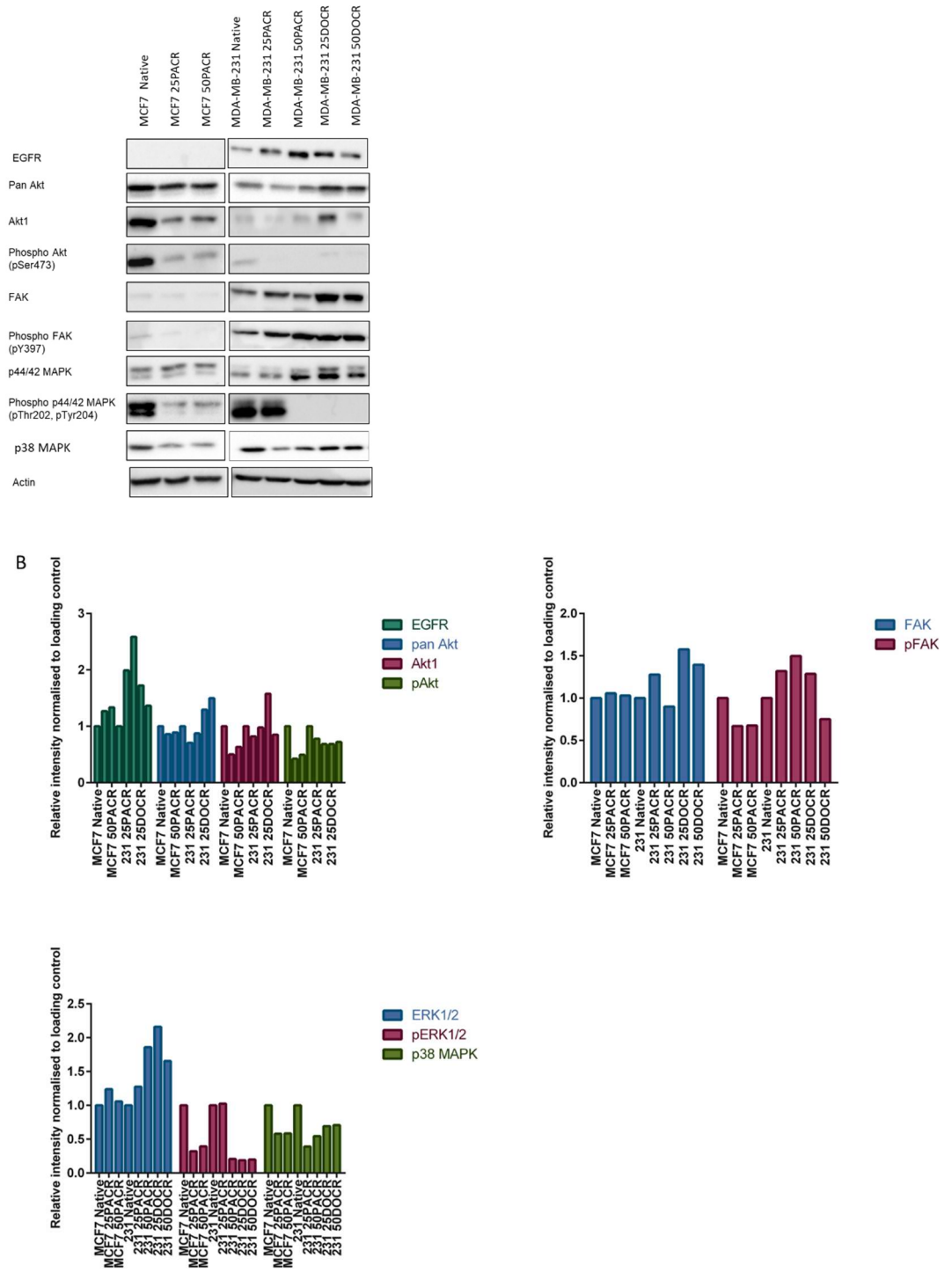

Figure 4.14: EGFR and PI3K-Akt signalling pathway proteins in MCF7 and MDA-MB-231 parental and taxane resistant isogenic cell lines. (A) Whole cell lysates were separated by SDS-PAGE (B) Expression of proteins relative to parental cell line after normalisation to loading control (n=1)

4.3 Discussion

Acquired or innate taxane resistance represents a major clinical challenge in the treatment of breast cancer. For these patients, treatment options are limited and the outcome is poor. Identification of pathways involved in the development of taxane resistance may, therefore, lead to the development of novel therapeutic approaches. The aim of this chapter was to further characterise the taxane-resistant cell line models derived for this thesis through a multi-omic approach, with focus on the mutational, transcriptomic and proteomic profiles in order to hypothesise mechanisms of chemoresistance. Together the results from each analysis pointed to dysregulation of cell cycle associated processes, and of the PI3K-Akt and MAPK pathways.

Cancer associated signalling pathways were profiled by RPPA with a panel of 150 validated target-specific antibodies. The capacity of RPPA technology to profile changes in expression and activation of proteins at this scale has provided a viable means of analysing the proteome. RPPA has become a powerful tool for the investigation of disease mechanism and increasingly to determine deregulated signalling networks in cancer (239, 240) and has been utilised by the Cancer Genome Atlas group to characterise a broad range of cancers (246).

Hierarchical clustering and functional interaction analysis of the differentially expressed antigens revealed enrichment of the PI3K-Akt signalling and ErbB2 signalling pathways. An absence of HER2 and an increase in expression of EGFR was observed in the paclitaxel resistant cell line when compared to the parental cell line, an observation that agreed with results from Chapter 3 which gave confidence in the RPPA process. Downstream from EGFR, FAK and its activated form were also both found to be statistically significantly upregulated. FAK overexpression is significantly associated with the development of malignancy in various cancers, including breast cancer and is often found to be upregulated in triple negative breast cancer (247-249). FAK is a cytosolic tyrosine kinase canonically activated by matrix and integrin receptors controlling cell motility(250). Phosphorylation at Tyrosine 397 is an

indicator of activation and has also been associated with poor prognosis and outcome in breast cancer patients (251). However the molecular mechanisms responsible for this overexpression have not been elucidated. Although the usefulness of FAK as a prognostic biomarker has yet to be evaluated, it has gained interest as a novel druggable target for the treatment of a variety of cancers. A recent study by Osterman et al indicated FAK activation sustained intrinsic and acquired cisplatin resistance in ovarian cancer via a Wnt/β-catenin/myc 'stemness' pathway. Hyperactivation of β-catenin-dependent Wnt signalling has been associated with poor prognosis in breast cancer patients(252), with Wnt signalling playing a crucial role in tumorogenesis and chemoresistance(253). β-catenin was also found to overexpressed in the MDA-MB-231 25PACR cell line along with SQSTM1/p62 and PKM2. SQSTM1/p62 was the most upregulated antigen in the panel analysed by RPPA. First identified as an autophagy adaptor and regulated by β-catenin, this multifunctional protein also plays an important role as a signalling hub. Over expression of SQSTM1 has been found to significantly correlate with increased risk of distant metastasis and poor outcome in patients with triple negative breast cancer (254). Additionally a study by Yan et al (255) suggested a role for elevated SQSTM1 expression in cisplatin-resistance in ovarian cells. SQSTM1/p62 has also been found to be a regulator of p38 MAP kinase (p38MAPK) (256). However the associated activation of p38MAPK and AKT was not observed by RPPA, an observation which was subsequently confirmed by Western blotting. Its role as a mediator of cell cycle mitotic transition through CDK1 is also of interest, given the ability of the resistant cell lines to overcome G2/M arrest that is typical of the effects of taxanes. PKM2 has also been implicated in the activation of the MAPK, Akt and FAK pathways. This protein was identified as being critical for cancer-specific aerobic glycolysis known as the Warburg effect (257) with a role in transcriptional regulation leading to EMT (258). Overexpression of β-tubulin was unsurprising given the microtubule binding mechanism of paclitaxel (234). Studies have shown that overexpression of β-tubulin promotes cancer development and induces EMT (186) and is postulated to be a marker of resistance (183, 259).

Analysis by RPPA was limited to the comparison of the paclitaxel resistant MDA-MB-231 25PACR cell line and the parental MDA-MB-231 cell line and, as it was not possible to repeat this experiment further in to my studies, the results must be viewed as potentially only attributable to the triple negative breast cancer cell line. Overall the changes found were modest, with only a small subset of statistically significant alterations identified with associated fold change above a threshold of 1.5. Despite the success of RPPA as a method for sensitive, high-throughput screening of a multitude of targets, its limitations lie with the specificity and sensitivity of the antibodies used, in particular for the identification of proteins with post-translational modifications, such as phosphorylation(260). In this study, it was clear that there was a skew towards downregulation of the phosphorylated proteins and those changes which were identified as being significantly changed, were judged with caution. To achieve a comprehensive evaluation of the taxane resistant proteome, mass spectrometry based proteomic profiling and expansion of the sample set to include all of the resistant cell lines may offer a more encompassing view.

Large scale genomic sequencing projects, curated by sites such as COSMIC (261), have led to the identification of thousands of mutations in cancer cells, delivering great insight in to the mutational landscape of cancer development and progression. With concurrent development of targeted antibody and small molecule therapies, the combination of both aspects have helped the drive towards precision medicine in the treatment of cancer (262, 263). This technology has also been employed to aid the discovery of mechanisms which underlie acquired resistance, primarily through the ability to perform paired sequencing of pre- and post-treatment samples to identify novel mutations of acquired resistance. A study by Juric *et al* identified that PTEN mutations were responsible for acquired resistant to apelisisb through comparison of pre- and post-treatment biopsies from a PI3KCA-mutated breast cancer patient (264). To enable precision medicine in cancer patients, targeted exome sequencing panels have been developed which focus on actionable targets. With the aim of this thesis being the identification of mechanisms of acquired taxane resistance in breast cancer, exome sequencing by MSK-IMPACT™ was then employed to characterise the

genomic landscape of the panel of the isogenic taxane resistant cell lines. This paired analysis highlighted the high degree of similarity between the parental and resistant cell lines in terms of the shared number and type of mutations (Figures 4.4 and 4.5). This study unveiled very few resistance-phenotype specific mutations, none of which were shared by the taxane-resistant MDA-MB-231 and MCF7 cell lines.

A total of 17 mutations were found in the MDA-MB-231 25PACR cell line, 18 in the MDA-MB-231 25DOCR. All but five were also found in the parental cell line. Both isogenic taxane resistant MDA-MB-231 cell lines carried missense mutations in *STK19* and a splice site mutation in *NOTCH4*, both of which were classed as passenger mutations. *STK19* is a serine/threonine kinase which has been found to act as a regulator of *NRAS* activity and has been associated with melanoma (265). The role of *STK19* in breast cancer or chemoresistance has not been evaluated. *NOTCH4* is a member of the highly conserved Notch signalling pathway which plays a role in the regulation of tissue homeostasis (266). Its dysfunction has been implicated in cancer progression(267) and mutation of *NOTCH4* has also been implicated in chemoresistance of triple negative breast cancer (268). MDA-MB-231 25PACR also carried a further passenger missense mutation in *SETD2*. *SETD2* encodes a methyltransferease known to be responsible for histone H3 methylation (269) and is involved in a number of cellular processes including transcriptional regulation and DNA damage repair (270, 271).

The cell line, MCF7 25PACR, was found to carry four mutations not seen in the parental cell line. Two of these were classed as passenger mutations. A missense mutation was found in the oncogene *MAP3K13*, which encodes a kinase that phosphorylates and activates *MAP2K7* and subsequently the JNK signalling pathway (207). The second passenger mutation was a silent mutation found in *PLCG2*, which encodes phospholipase C, a protein with a regulatory role in cancer. Two nonsense mutations with likely pathogenic consequences were identified in MCF7 25PACR cells. The first of these was identified in the proto-oncogene *MET* and a second in *FLT1*, which encodes VEGFR. Ontology analysis of the observed mutated genes

revealed their association with regulation of transcription, regulation of cell proliferation and negative regulation of the apoptotic process. Further work is required to understand the functional impact of these mutations in taxane-resistant breast cancer cells.

Gene expression analysis was performed using Nanostring® technology using the Pancancer Pathway panel which focused on canonical cancer pathways and offered a degree of overlap with the targets of the RPPA assay. Unsupervised hierarchical clustering of the isogenic cell lines demonstrated clear delineation of the cell line subtypes, with the parental and resistant cell line samples for each cell line clustering at the primary level of the dendogram. Functional interaction analysis of the differentially expressed genes revealed a number of enriched pathways and biological processes. Among these, transcriptional regulation of cancer pathway was enriched for all paired comparisons between parental and resistant cell lines, which had also been identified as enriched from the RPPA and targeted exome sequencing analyses. Six of the 23 mRNA consistently differentially expressed between all three of the taxane resistant cell lines were related to this pathway: *NUPR1*, *BAIAP3*, *PBX1*, *HIST1H3H*, *CCNA1* and *NGFR.* Of these genes, two in particular are of interest in the context of biomarkers of taxane resistance. *NUPR1,* a transcriptional regulator, has been observed to be overexpressed in a number of malignancies, and also to be associated with chemoresistance(272-274). Recent studies have suggested that *NUPR1* plays a diverse role in the cell, and is implicated in migration, invasion and regulation of autophagy (275). A study in MDA-MB-231 cells also demonstrated a complex interplay forming a NUPR1-PI3K/Akt-p21 axis that serves to enhance chemoresistance in breast cancer (272). It is therefore believed that NUPR1 regulates chemotherapeutic resistance by mediating anti-apoptotic activity and autophagy (276). *PBX1*, consistently upregulated in the taxane resistant breast cancer cell lines, is over-expressed in a variety of solid tumours including ovarian, oesophageal and breast cancer (277-279). Overexpression in breast cancer has been found to correlate with poor prognosis (280). A study in platinum-resistant ovarian cancer cells found that silencing of *PBX1* resensitised the cells to treatment (277). Together these results

suggest that *NUPR1* and *PBX1* are possible candidates as markers of response to taxanes. Future work to investigate whether *NUPR1* or *PBX1* siRNA knockdown would result in a return to taxane sensitivity in the isogenic cell lines is required. Oncogenic transcription factors such as PBX1 are not viable as direct druggable targets as their action is mediated by protein-DNA binding interaction, rather than enzymatic activity. Instead disruption of the binding interaction or of the target genes themselves might offer a means of targeting these genes. As PBX1 modulates CDK inhibitors such as p21 and p27, it is reasonable to suggest that use of these compounds in the context of reversal of taxane resistance would offer a successful treatment option to chemoresistance. Further investigation in to druggable binding partners for *NUPR1* and *PBX1* would also be merited.

In summary this chapter aimed to investigate the pathways influenced by the acquisition of taxane resistance in the isogenic breast cancer cell line models using a multi-omic data-driven approach. A limitation of the platforms used in this thesis was that, due to their focussed nature, attempts to deduce direct correlations proved difficult. A broader approach to both proteomic and transcriptomic analysis may have provided more robust associations and a wider view of changes induced in response to acquired taxane resistance. However, functional interaction analysis of the observed differential changes indicated a high degree of commonality across methods, suggesting that this multi-omic approach had been successful in identifying pathway changes which could be associated with resistance.

Due to time constraints, further investigation of all differentially expressed pathways was not possible within the time-frame of this thesis and the decision to focus on pathways consistently identified by all –omics platforms was made. However, further investigation of other key signalling pathways with associations to chemoresistance, such as those of the JAK/STAT or TGF-β pathway which play critical roles in tumour growth and migration, remain of interest for future analysis (281) (282).

The observation that deregulation of the PI3K-Akt signalling pathway was associated with taxane resistance in the isogenic cell lines was an attractive option for further

investigation. The PI3K-Akt pathway, which is frequently dysregulated in cancer, is recognised as being a key link to chemoresistance through its association with upstream and downstream partners which induce a pro-survival signal. The pathway is highly complex and exerts its effects through synergy with other cellular mechanisms resulting in modulation of cell proliferation, the cell cycle and apoptosis. These biological processes were also observed to be altered in the isogenic cell lines, and may therefore suggest a potential route for the treatment of taxane resistance in breast cancer. The development of inhibitors of the PI3K-Akt pathway and of kinases regulating the cell cycle has increased in recent years, with treatments reaching clinical trial. An investigation of PI3K-Akt and cyclin dependent kinases as therapeutic targets for the treatment of taxane resistant breast cancer is discussed in Chapter 5.

5. IDENTIFICATION OF SMALL MOLECULE KINASE INHIBITORS TARGETING DYSREGULATED TAXANE RESISTANCE ASSOCIATED PATHWAYS

5.1 Introduction

Standard of care treatment for breast cancer includes surgery, radiotherapy, endocrine and targeted therapy, chemotherapy, or a combination of these (136). Chemotherapy may be offered in both the adjuvant and neoadjuvant setting. Anthracyclines and taxanes are the most effective and widely used chemotherapeutic agents for treating invasive breast cancer (283-285). However, their use as first-line therapies for early breast cancer has led to an increase in resistance and subsequent treatment options are limited. The identification and development of novel treatment regimens for those patients is therefore of paramount importance. The drive to identify novel clinical strategies has been aided by efforts to identify mechanisms which drive chemoresistance, but a definitive approach has not yet been successfully identified and the development of novel anti-cancer drugs targeted to treatment of these chemoresistant tumours remains an unmet need.

Strategies for rational drug discovery in recent years have tended to be centred on high-throughput screening of compound libraries. Targeting of mechanistic compound libraries has been a successful approach in identifying candidate therapies for the treatment of a range of diseases, particularly when combined with well-defined preclinical models. The results of chapter 4 indicated that deregulation of the PI3K-Akt pathway and the cell cycle are associated with the development of the taxane resistant phenotype. Targeted inhibition of protein kinases which play an integral part as regulators of these pathways has gained increasing interest as a promising strategy in the development of novel chemotherapeutics with several inhibitors already reaching clinical trial (112, 286).

The PI3K pathway plays a key role in many cellular processes including cell proliferation, survival, migration and apoptosis (287) and is dysregulated in cancer (288). Activation of the PI3K pathway is observed in approximately 70% of all breast cancer cases with the *PI3KCA* gene frequently mutated (226, 289). Consequently, the development of inhibitors of the PI3K pathway as a treatment for cancer has gained momentum in recent years, many of which are now in clinical trial (112, 113). Progression of the cell cycle is controlled by serine/threonine cyclin-dependent kinases (CDKs), which are critical players in the control of cell cycle progression and transcription. The CDK family, which encompasses 21 kinases, have diverse cellular functions. CDK1, CDK2, CDK4 and CDK6 play key roles in the regulation of the cell cycle, complexing with cyclins to tightly synchronise the cell cycle (290), whereas CDK7, CDK8 and CDK9 have been identified as playing key roles in gene transcription (291). Due to the dysregulation of the CDK family in cancer (4, 127, 127), targeting of CDKs has emerged as a promising strategy in the treatment of many cancer types and great efforts have been made in the development of pan-CDK and CDK-specific inhibitors (292). The development of CDK-specific inhibitors against the CDK4/CDK6 axis, targeting cell proliferation, has been particularly successful with palbociclib approved for use in the treatment of advanced ER+ breast cancer (134). However, its use in the treatment of triple negative breast cancer has been unsuccessful with resistance to single-agent CDK4/6 inhibition (135). Triple negative breast cancer is a complex, heterogeneous disease, suggesting that combination therapies which target more than one pathway, might offer a more sustained and effective response.

This chapter describes a mechanistic approach to identifying novel inhibitors of taxane resistant breast cancer. Here I discuss the screening of a small molecule kinase library centred on compounds which target the deregulated PI3K pathway and cell cycle of the taxane resistant isogenic cell lines. The activity and mechanism of action of a select group of compounds were explored, along with an assessment of drug combinations to identify potentially synergistic co-therapy regimens. The results indicate the potential for use of PI3K and CDK inhibitors in the treatment of chemorefractory breast cancer.

5.2 Results

5.2.1 OICR Small Molecule Kinase Screen

To identify potential novel small molecule kinase inhibitors with activity against taxane resistance, a pharmacological screen of 89 compounds active against kinases directed against deregulated pathways identified in chapter 4 was performed. Compounds were selected from the OICR Tool Kit library, a Mechanism of Action collection of 560 kinases with known biological targets which have reached the clinical stage of development or are marketed therapeutics. The inhibitors were chosen to broadly target the PI3K/Akt/mTOR pathway and the cell cycle (Figure 5.1), with particular focus on the cyclin kinases which act as regulators of the cell cycle and transcription via RNA polymerase II.

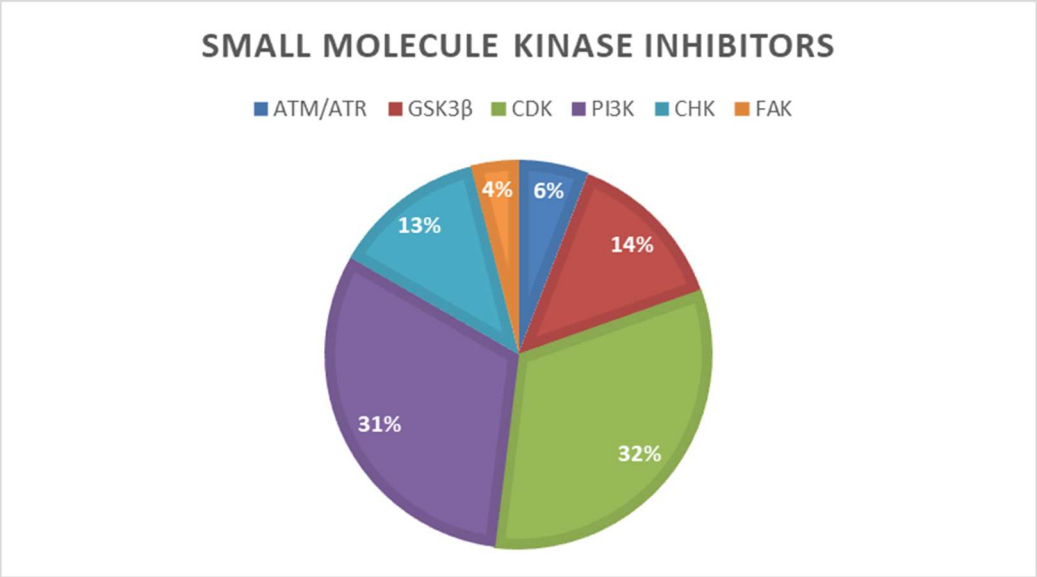

Figure 5.1: Small molecule kinase inhibitors of the PI3K-Akt pathway and cell cycle selected for screen

To assess the in vitro anti-proliferative effects of the selected kinases on the MDA-MB-231 isogenic taxane resistant cell lines, MDA-MB-231 25PACR and MDA-MB-231 25DOCR, and the parental MDA-MB-231 cells, high-throughput screens were performed. The cells were incubated for 72 hrs with a 12-point concentration curve over a range of 0.026 μM - 10 μM before cell viability was assessed. A single data point was collected for each treatment. Positive hits were defined as those compounds achieving 50% cell death at a kinase inhibitor concentration of < 5μM in at least one of the taxane resistant cell lines (Figure 5.2). Twenty eight of the 89 compounds screened fulfilled this criteria, all of which were directed towards PI3K, CDK and Chk family members (Table 5.1). A literature search identified 18 of these inhibitors as being clinically relevant and already approved for testing in clinical trials. The inhibitors directed against GSK3β and FAK in this screen did not inhibit taxane resistance in the MDA-MB-231 isogenic cell lines, even at the highest dose of the drugs tested. Similarly, the ATM/ATR inhibitors did not achieve 50% cell kill in the tested cell lines, and were discounted from further investigation. Of the 10 Chk inhibitors tested, half of the compounds were observed to reach the criteria set out for defining screen 'hits'. Of these inhibitors, only MK-8766 has been approved for use in clinical trials.

The most potent inhibitors of the taxane resistant cell lines were those that targeted the PI3K and CDK pathways. Overall, pan-CDK inhibitors had a greater anti-proliferative effect on the chemoresistant cell lines than specific inhibitors such as palbociclib and abemaciclib, inhibitors of CDK4/6, which did not reach 50% kill at the highest concentration tested.

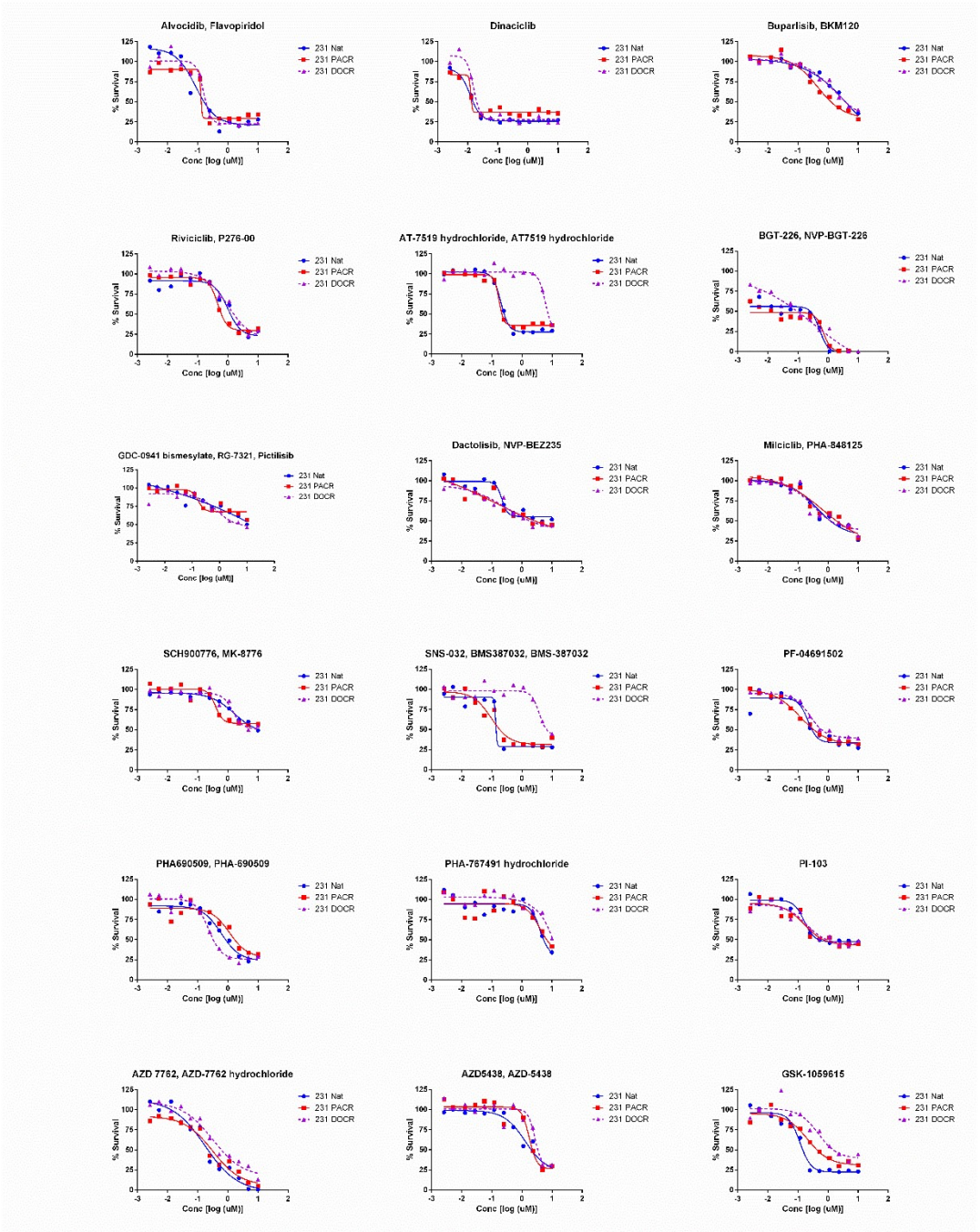
Alvocidib, Flavopiridol
Dinaciclib
Buparlisib, BKM120
Riviciclib, P276-00
AT-7519 hydrochloride, AT7519 hydrochloride
BGT-226, NVP-BGT-226
GDC-0941 bismesylate, RG-7321, Pictilisib
Dactolisib, NVP-BEZ235
Milciclib, PHA-848125
SCH900776, MK-8776
SNS-032, BMS387032, BMS-387032
PF-04691502
PHA690509, PHA-690509
PHA-767491 hydrochloride
PI-103
AZD 7762, AZD-7762 hydrochloride
AZD5438, AZD-5438
GSK-1059615
231 Nat
231 PACR
231 DOCR
% Survival
Conc [log (uM)]

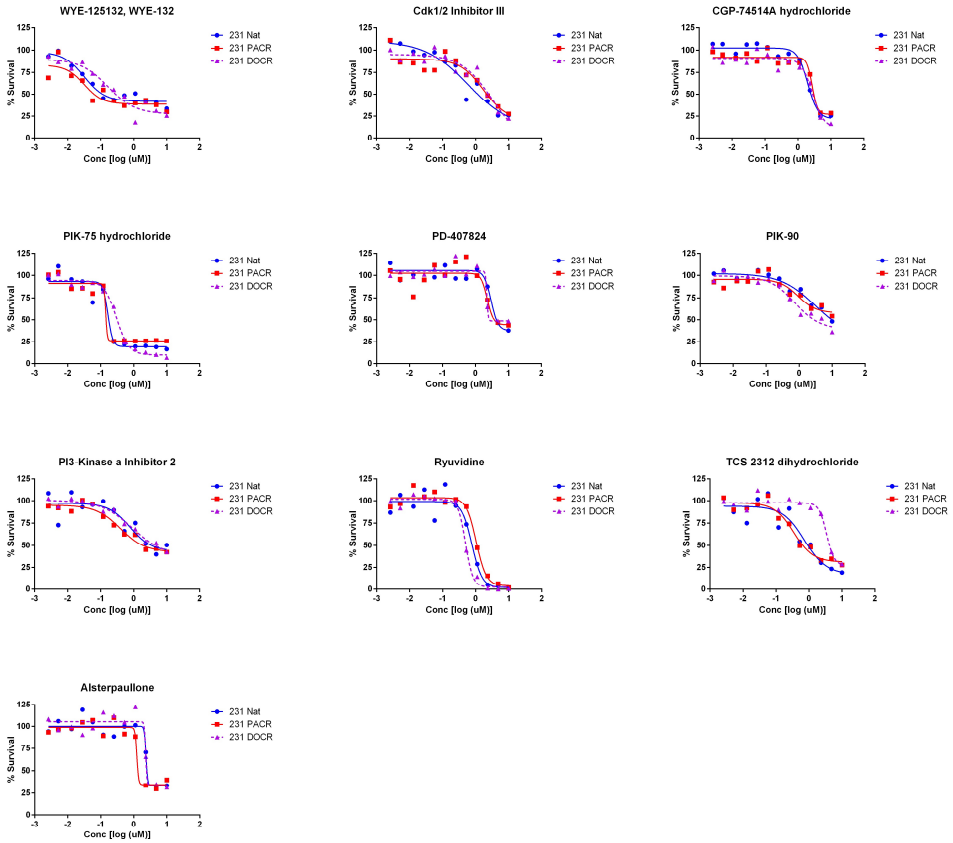

Figure 5.2: Dose response curves for small molecule kinase screen compounds with potency of <5 µM in MDA-MB-231 taxane resistant cells. Cells were plated at 1000-1200 cells per well in a 384 well plate and exposed to a 12-point concentration curve ranging from 0.026 µM - 10 µM. Cell viability was determined 72hr later by CellTitre-Go™ assay. Each data point represents a single value for each treatment condition, normalised to vehicle and positive controls.

Table 5.1: Small molecule kinase inhibitors with activity against MDA-MB-231 taxane resistant isogenic cell line series of <5 µM.

Compound	MDA-MB-231 Native IC_{50} (µM)	MDA-MB-231 25PACR IC_{50} (µM)	MDA-MB-231 25DOCR IC_{50} (µM)	Target	Development
Alvocidib/Flavopiridol	0.086	0.127	0.158	CDK1,CDK2,CDK4,CDK6, CDK9; GSK3β	Phase III
Dinaciclib/SCH-727965	0.012	0.013	0.016	CDK1, CDK2, CDK5, CDK9	Phase III
Buparlisib/BKM120	4.889	0.455	1.589	PI3K	Phase II/III
Riviciclib/P276-00	0.997	0.466	0.999	CDK1, CDK2, CDK4, CDK6, CDK9	Phase II
AT-7519 hydrochloride	0.1998	0.174	5.973	CDK1, CDK2, CDK4, CDK6, CDK9	Phase II
BGT-226/NVP-BGT226	0.521	0.693	0.327	PI3K, mTOR	Phase II
Pictilisib/ GDC-0941	3.582	0.232	0.385	PI3K	Phase II
Dactolisib/NVP-BEZ235	0.218	0.134	0.304	PI3K, mTOR	Phase II

Milciclib/PHA-848125	0.424	0.679	0.314	CDK2, CDK1, CDK4, CDK5, CDK7	Phase II
MK-8776/SCH900776	1.628	0.394	1.458	CHK1, Chk2	Phase II
SNS-032	0.135	0.097	3.73	CDK2, CDK7, CDK9	Phase I/II
PF-04691502	0.215	0.12	0.25	PI3K, mTOR	Discontinued - Phase I
PHA690509	0.603	1.134	0.228	CDK2	Phase I
PHA-767491/CAY-10572	4.001	3.979	N/A	CDC7, CDK9	Phase I
PI-103	0.16	0.159	0.188	PI3K, mTOR	Phase I
AZD7762	0.174	0.311	0.313	CHK1, CHK2	Discontinued - Phase I
AZD5438	1.284	1.764	2.706	CDK1, CDK2, CDK9	Discontinued - Phase I
GSK-1059615/GSK-615	0.117	0.212	0.47	PI3K, mTOR	Discontinued - Phase I
WYE-125132/WYE-132	0.032	0.032	0.167	mTORC1, mTORC2, PI3K	Preclinical
Cdk1/2 Inhibitor III	0.609	1.743	3.184	CDK1, CDK2	Tool compound
CGP-74514A hydrochloride	1.988	2.703	2.736	CDK1	Tool compound

PD-407824	2.996	2.288	2.225	CHK1, WEE1	Tool compound
PI3-Kinaseα Inhibitor 2	0.781	0.403	0.942	PI3K	Tool compound
PIK-75 hydrochloride	0.166	0.142	0.303	PI3K	Tool compound
PIK-90	3.214	0.946	0.751	PI3Ka	Tool compound
Ryuvidine	0.777	1.047	0.495	CDK4/Cyclin D1	Tool compound
TCS 2312 dihydrochloride	0.743	0.35	3.439	CHK1	Tool compound
Alsterpaullone	2.35	1.238	2.299	CDK1, CDK2, CDK5, GSK3β	No development reported

5.2.2 Validation of small molecule kinase hits

The small molecule kinase inhibitor screen was performed as a high-throughput assessment of compound activity and, as such, was limited to a single point per concentration for each inhibitor. To validate the results from the screen, a secondary screen was performed which included the taxane resistant MCF7 isogenic cell lines. Three PI3K inhibitors were included: BYL719 (alpelisib), BKM120 (buparlisib) and a tool compound, PIK75. Although PIK75 did not pass the selection criteria from the high-throughput screen, a preliminary experiment had identified its activity at nanomolar concentrations. Three cyclin kinase inhibitors were selected for testing:

dinaciclib, alvocidib and SNS-032. All compounds with the exception of PIK75 have been approved for testing in clinical trials.

5.2.2.1 PI3K inhibitors

To determine if all of the taxane resistant cell lines models had similar levels of sensitivity to the PI3K inhibitors, an assessment of the IC_{50} for each compound was performed. Cells were exposed to an 8 point semi-log concentration curve ranging from 0.3 nM to 1µM for 72hrs before proliferation was assessed using a CCK8 assay. All experiments were performed in triplicate. The IC_{50} for each cell line was calculated using GraphPad and statistical significance of response of isogenic resistant cell line compared to its parental cell line assessed (Figure 5.3). The IC_{50} values for all tested cell lines were found to be in accordance with the preliminary high-throughput screen (Table 5.2). Overall, the MCF7 cell line and the paclitaxel-resistant MCF7 25PACR cell line were more sensitive to the three PI3K inhibitors tested in the sub-study.

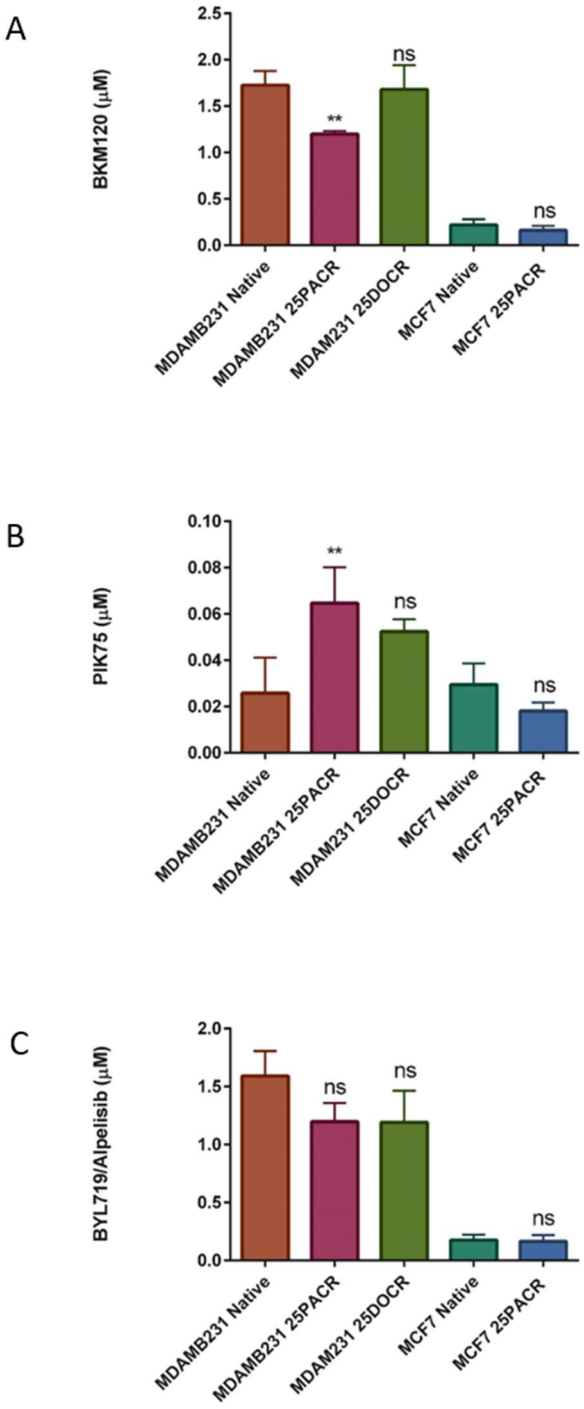

Figure 5.3: Half maximum inhibitory concentrations (IC50) for selected PI3K inhibitors. 96 well plates were seeded with 5000 cells/well for each cell line and after 24hrs treated with increasing doses of (A) BKM120, (B) PIK75 or (C) BYL719/Alpelisib for 72hrs. CCK-8 assays were then performed and data analysed using GraphPad Prism 6 software. Results are expressed as mean IC50 ± SEM of three independent experiments performed in triplicate for each cell line. Statistical significance was determined by one-way ANOVA using the Tukey multiple comparison test. ** $p<0.01$, ns – non significant.

Table 5.2: Half-maximal inhibitory concentration (IC50) values of selected PI3K inhibitors

	BKM-120 (µM ± SEM)	PIK-75 (µM ± SEM)	BYL719/Alpelisib (µM ± SEM)
MDA-MB-231 Native	1.726 ± 0.088	0.026 ± 0.009	1.591 ± 0.123
MDA-MB-231 25PACR	1.198 ± 0.02 (0.69)	0.065 ± 0.009 (2.5)	1.198 ± 0.09 (0.75)
MDA-MB-231 25DOCR	1.681 ± 0.149 (0.97)	0.052 ± 0.003 (2)	1.191 ± 0.193 (0.75)
MCF7 Native	0.220 ± 0.035	0.029 ± 0.003	0.177 ± 0.026
MCF 25PACR	0.161 ± 0.028 (0.73)	0.018 ± 0.002 (0.62)	0.164 ± 0.032 (0.92)

Cells were plated at 5000 cells per well in a 96 well plate and exposed to drug concentrations ranging from 0.3 to 3000nM. Cell viability was determined 72hr later by Cell Counting Kit-8 (CCK-8) assay. Results show the mean of biological replicate experiments (n=3, with 3 technical replicates for each treatment condition) in micromolar concentrations. Resistance factors are shown in parentheses and represents resistant IC_{50}/parental IC_{50}.

To assess BKM120-induced effects in downstream signalling pathways, and to evaluate predictive biomarkers of response to treatment, protein lysates from parental MDA-MB-231 cell line and paclitaxel-resistant MDA-MB-231 25PACR treated with BKM120 and analysed by RPPA. Raw fluorescence intensity values were normalised and standardised by Z-score transformation. The heat map in Figure 5.4 displays the unsupervised hierarchical clustering analysis of the relative enrichment of 150 proteins and phosphoproteins (red, up-regulated; blue, down-regulated). Down regulation of key elements of the PI3K-Akt pathway were observed in both MDA-MB-231 and MDA-MB-231 25PACR after treatment with 1 µM BKM120 for 48

hrs, including PI3K p110α. These proteins included total and pAkt S473, pS6 S240, p4EPB1 S65 and p70S6K. Reduced expression of pAkt S473 and pS6 S240 was confirmed by western blotting (Figure 5.5). The expression of the MAPK pathway proteins MEK1/2 and ERK1/2 were also downregulated, when it was anticipated that compensatory upregulation might have been observed. However, although downregulation of expression of pERK1/2 in a concentration dependent manner was confirmed by western blotting in the MDA-MB-231 cell line, a similar effect was not observed in the paclitaxel resistant MDA-MB-231 25PACR cells.

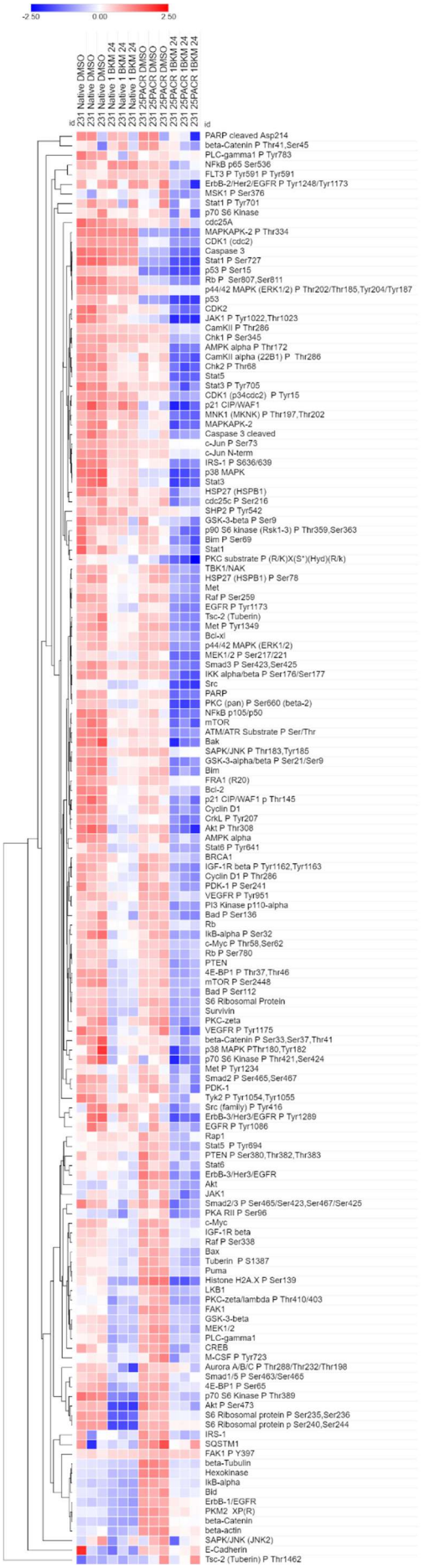

Figure 5.4: Unsupervised hierarchical clustering of changes in protein and phosphoproteins associated with BKM120 treatment. MDA-MB-231 and MDA-MB-231 25PACR cells were treated with 1µM BKM120 for 48 hrs, lysed and analysed by reverse phase protein array. Normalized intensity values were standardized as Z-scores and subjected to hierarchical clustering analysis. Heat maps display the relative enrichment of proteins or phosphoproteins (red, up-regulated; blue, down-regulated).

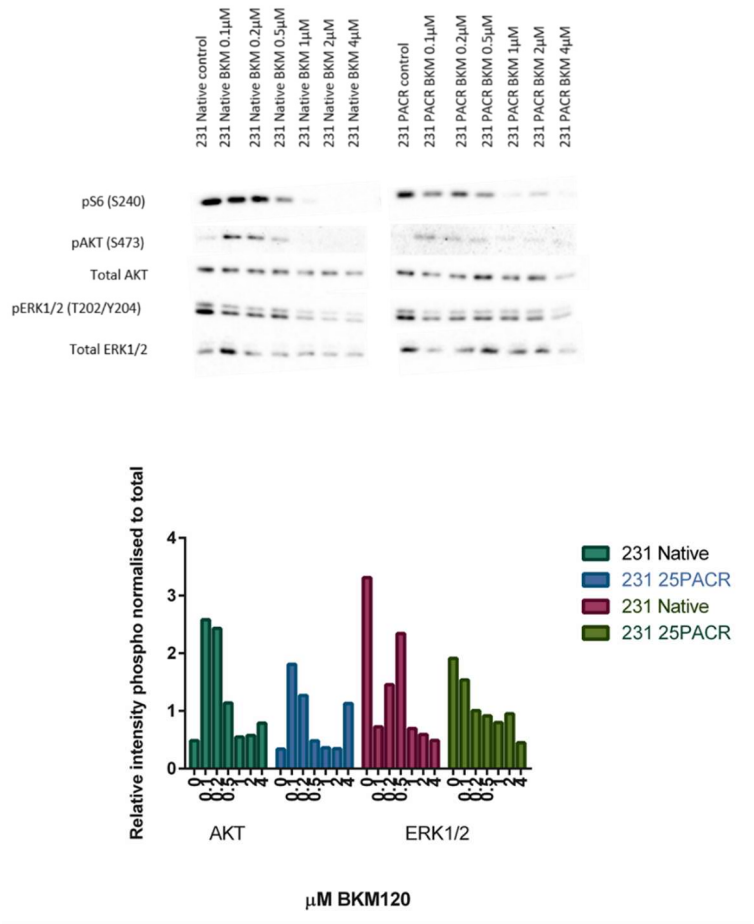

Figure 5.5: Western blot analysis of PI3-Akt pathway associated proteins and phoshoproteins in MDA-MB-231 and MDA-MB-231 25PACR cells treated with BKM120. Whole cell lysates of parental and taxane-resistant MDA-MB-231PACR were collected under the indicated conditions. The proteins were separated by SDS-PAGE and probed for pS6 S240, pAkt (S473), total Akt, pERK1/2 (T202/Y204) and total ERK1/2. Quantitative analysis of the relative intensity of phosphoprotein to total protein was performed (n=1)

5.2.2.1 Validation of CDK Inhibitors

The potency of the selected cyclin-dependent kinase inhibitors identified in the small molecule kinase screen were confirmed in proliferation assays of all isogenic cell lines (Figure 5.6). The cyclin-dependent kinase inhibitors alvoicidib and dinaciclib had potent activity against all tested cell lines with observed IC_{50}s in the range of 0.012 µM – 0.225 µM and 0.006 µM – 0.052 µM respectively (Table 5.3). SNS-032 also inhibited the proliferation of MDA-MB-231 and MDA-MB-231 25PACR cells at a similar level. However, the IC_{50} for MDA-MB-231 25DOCR cell line at 6.185 µM was 22-fold greater than the IC_{50} of the parental cell line (0.272 µM), suggesting that the docetaxel-resistant MDA-MB-231 cell line was cross-resistant to this compound. Given the overlapping targets for each of the selected inhibitors, it was therefore interesting to note the apparent resistance of MDA-MB-231 25DOCR to SNS-032, which has potency to CDK2, CDK7 and CDK9, which was not seen with the other selected cyclin inhibitors.

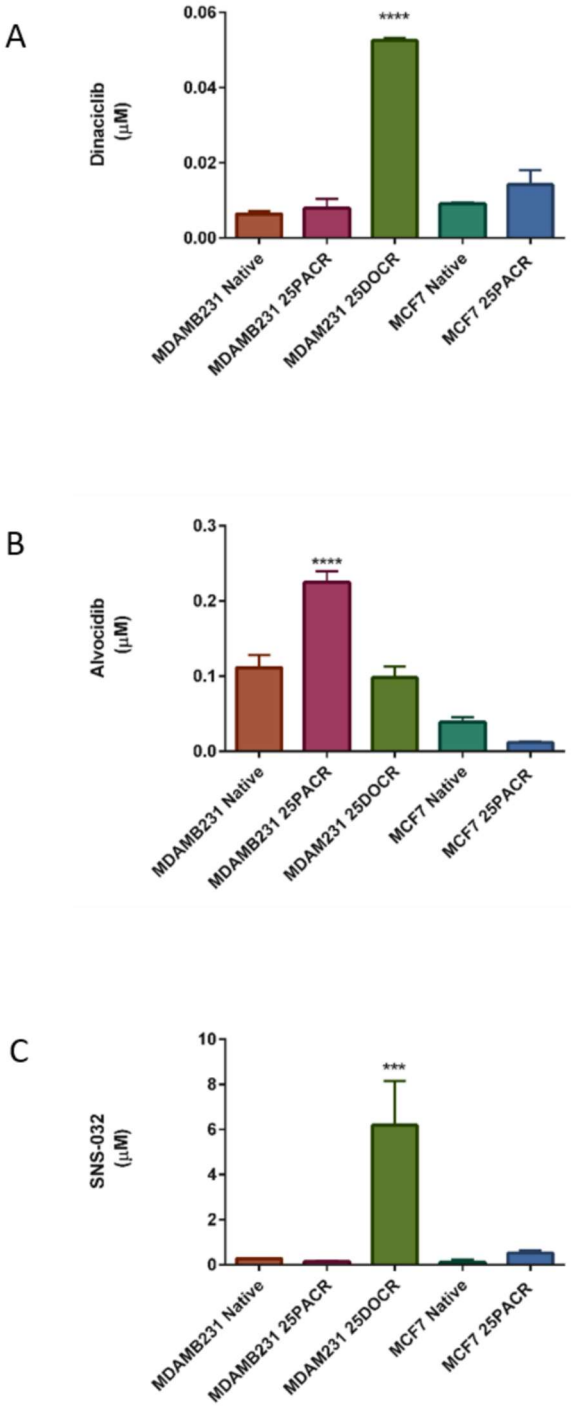

Figure 5.6: Half maximum inhibitory concentrations (IC50) for selected CDK inhibitors. 96 well plates were seeded with 5000 cells/well for each cell line and after 24hrs treated with increasing doses of (A) Dinaciclib, (B) Alvocidib or (C) SNS-032 for 72hrs. CCK-8 assays were then performed and data analysed using GraphPad Prism 6 software. Results are expressed as mean IC50 ± SEM of three independent experiments performed in triplicate for each cell line. Statistical significance was determined by one-way ANOVA using the Tukey multiple comparison test. * $p<0.05$, ** $p<0.01$, ns – non significant.

Table 5.3: Half-maximal inhibitory concentration (IC50) values of selected CDK inhibitors

	Alvocidib (µM ± SEM)	Dinaciclib (µM ± SEM)	SNS-032 (µM ± SEM)
MDA-MB-231 Native	0.112 ± 0.009	0.006 ± 0.001	0.272 ± 0.016
MDA-MB-231 25PACR	0.225 ± 0.011 (0.49)	0.008 ± 0.001 (1.33)	0.139 ± 0.015 (0.51)
MDA-MB-231 25DOCR	0.098 ± 0.009 (0.875)	0.052 ± 0.0004 (8.67)	6.185 ± 1.132 (22.7)
MCF7 Native	0.039 ± 0.004	0.009 ± 0.002	0.123 ± 0.065
MCF 25PACR	0.012 ± 0.001 (0.31)	0.025 ± 0.009 (2.78)	0.524 ± 0.078 (4.26)

Cells were plated at 5000 cells per well in a 96 well plate and exposed to drug concentrations ranging from 0.3 to 3000nM. Cell viability was determined 72hr later by Cell Counting Kit-8 (CCK-8) assay. Results show the mean of biological replicate experiments (n=3, with 3 technical replicates for each treatment condition) in micromolar concentrations. Resistance factors are shown in parentheses and represents resistant IC_{50}/parental IC_{50}.

5.2.3 Dinaciclib induces deregulation of the cell cycle

To better define the underlying mechanism by which dinaciclib caused a decrease in cell proliferation, an assessment of apoptosis and the effects on the cell cycle were determined. Induction of apoptosis was observed in the isogenic MDA-MB-231 cell lines by assessment of caspase 3/7 activity (Figure 5.7). This confirmed caspase activation in the MDA-MB-231 isogenic cell lines with a concentration dependent increase in the relative apoptotic index for all three MDA-MB-231 cell lines in the series. However, a statistically significant increase ($p<0.05$) was only observed with the parental MDA-MB-231 cell line and the docetaxel resistant line, MDA-MB-231

25DOCR, at two of the tested concentrations; 100 and 300 nM dinaciclib. The observed increase in apoptosis in MDA-MB-231 25PACR cells was not found to be statistically significant at any of the tested concentrations.

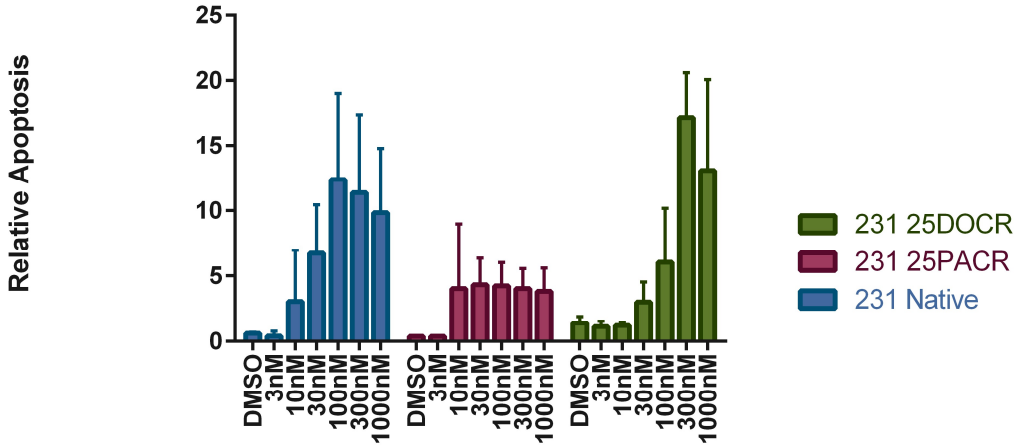

Figure 5.7: Dinaciclib induces caspase 3/7 activity in the MDA-MB-231 isogenic cell lines. Cell lines were seeded in 96 well plates with 5000 cells/well for each cell line. After 24hrs the media was replaced with media containing a six-point dose range of dinaciclib or 0.1% DMSO and 1nM Caspase-3/7 reagent. Plates were imaged in an Incucyte® Zoom for 72 hours, acquiring 4 phase contrast and 'green' channel images per well every 3 hours. Images were analysed by Incucyte® software and results expressed as apoptotic index ± SEM of two independent experiments performed in triplicate for each cell line. Statistical significance was determined by two-way ANOVA using the Tukey multiple comparison test (* $p<0.05$).

Analysis of the effects of dinaciclib inferred it had the ability to alter cancer cell progression through the cell cycle although consistency of effect was not observed across the cell line models. Accumulation of cells in the G2/M phase of the cell cycle was observed at dinaciclib concentrations of 100 nM and above in the native parental MDA-MB-231 cell line (Figure 5.8A). This was accompanied with a corresponding increase in the S-phase population. Results for both of the MDA-MB-231 isogenic taxane resistant cell lines were less clear. Exposure of MDA-MB-231 25PACR cells to dinaciclib revealed an increase in the percentage of cells in the S phase of the cell cycle, with a corresponding decrease in cells in G2/M (Figure 5.8B). Dinaciclib did not appear to exert an overt effect on the cell cycle of MDA-MB-231 25DOCR, with a slight increase in the G0/G1 phase and accompanying reduced S phase population (Figure

5.8C). Dinaciclib treatment was found to block the cell cycle at the G2/M phase resulting in a reduced S-phase population in the MCF7 native and taxane resistant MCF7 cell lines (Figure 5.8D & E). Significant increase in MCF7 native parental cells at the G2/M phase was observed after 24 hr treatment with 10 nM dinaciclib with 54% of the cell population arresting at this phase compared to 17% of cells treated with 0.1% DMSO vehicle control. This was maintained in all of the higher concentrations tested.

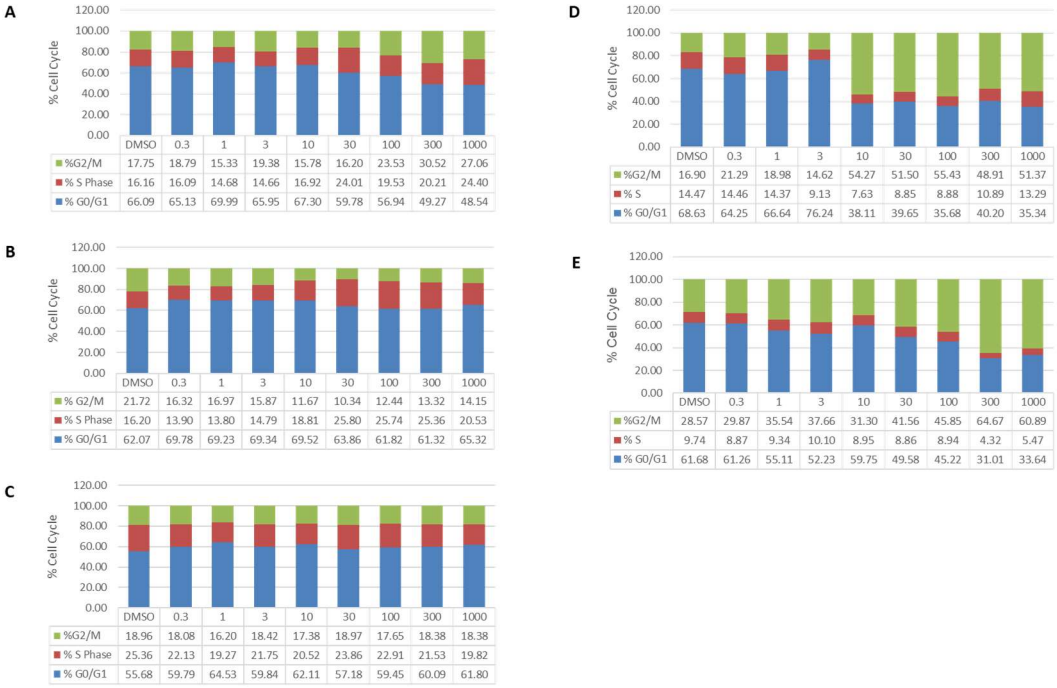

Figure 5.8: Cell cycle distribution in (A) MDA-MB-231 parental, (B) MDA-MB-231 25PACR (C) MDA-MB-231 25DOCR (D) MCF7 parental and (E) MCF7 25PACR upon exposure to dinaciclib. Asynchronously growing cell lines were seeded in 96 well optical bottom plates with 2500 cells/well for each cell line. After 24 hrs the media was replaced with media containing an eight-point dilution series of dinaciclib or 0.1% DMSO as appropriate. After a further 24 hrs cells were fixed with 4% paraformaldehyde before staining with Hoescht 33342. Six images per well were acquired using an ImageXpress Micro XLS widefield microscope. Images were quantified using the Cell Cycle application for MetaXpress software. Results expressed as normalised mean confluence ± SEM of three independent experiments performed in triplicate for each cell line.

Next I aimed to understand the molecular mediators of cell growth inhibition and apoptotic effects induced by dinaciclib. To achieve this the taxane resistant cell lines and the parental cell lines were treated with two concentrations of dinaciclib for 4, 8, 12 and 24 hrs before their lysates were assessed by western blotting (Figure 5.9). The phosphorylation levels of pRB S807/S811, a protein with a central role in the cell cycle and apoptosis and a downstream target of CDK2, was significantly decreased in all of the cell lines in a concentration and time dependent manner. This effect was also observed with cyclin B1 expression in all cell lines except MDA-MB-231 25DOCR cells. Cyclin B1 plays an important role in the activation of CDK1, a driver of G2/M transition in the cell cycle and its consistent expression in MDA-MB-231 25DOCR correlates with the seemingly unchanged cell cycle observed in Figure 5.8C. PLK1, another modulator of CDK1, was downregulated in a time dependent manner in the parental and MDA-MB-231 25PACR cell line, but not to the same degree in MDA-MB-231 25DOCR.

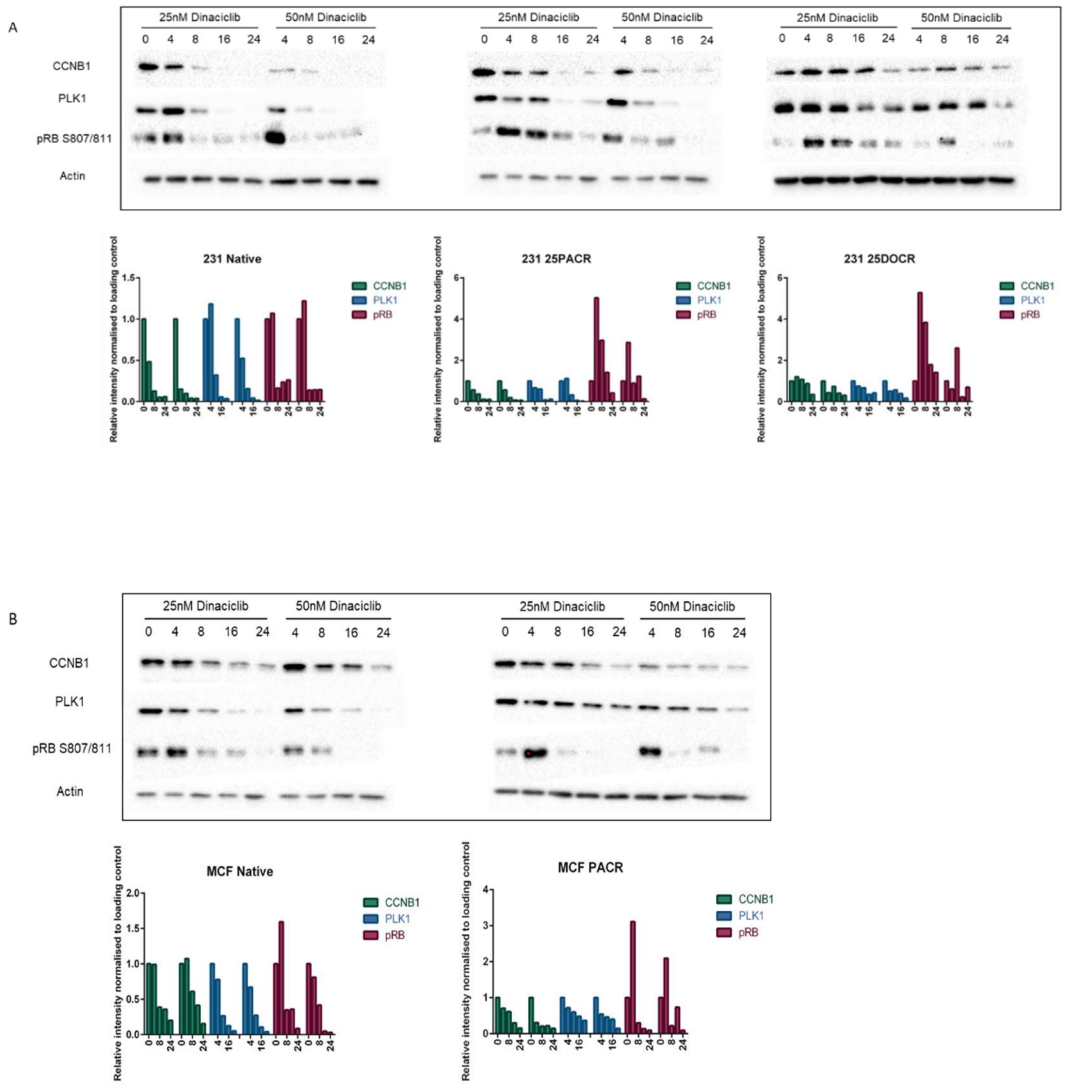

Figure 5.9: Assessment of downstream targets of dinaciclib. Whole cell lysates of (A) parental and taxane-resistant MDA-MB-231PACR and MDA-MB-231 25DOCR and (B) parental MCF7 and paclitaxel-resistant MCF7 25PACR were collected under the indicated conditions. The proteins were separated by SDS-PAGE and probed for CCNB1, PLK1, pRB S807/811 and actin (n=1) and quantitative analysis of their relative intensity to time 0 after normalisation to loading controls performed.

5.2.4 Assessment of combinatorial effect of dinaciclib with select chemotherapy agents

In an effort to overcome resistance sometimes associated with monotherapy leading to treatment failure, the combination of two or more therapeutic treatments to increase treatment efficacy has increasingly become a standard in cancer treatment (293). As dinaciclib had resulted in a reduction in CDK1 expression in MDA-MB-231 25PACR and MCF7 25PACR cell lines and induction of G2/M arrest, I considered whether resensitisation to paclitaxel would occur. Secondly, as sensitivity to anthracyclines had been observed in MDA-MB-231 25PACR and MCF7 25PACR (Table 3.4), dinaciclib in combination with epirubicin was also evaluated.

To achieve this, cells were seeded in 96-well plates and a drug matrix of compounds applied. The drugs were added in semi-log concentration ranges; dinaciclib at 1, 3, 10, 30 and 100 nM and an eight-point concentration range for both taxanes and epirubicin from 0.3 – 1000 nM. Each drug matrix was performed in triplicate. After 72 hrs treatment, cell survival was assessed by CCK-8 assays. The viability for each combination was expressed as the ratio to the DMSO control and Synergyfinder® software (214) employed to identify the relationship between each combination using the Bliss independence reference model, which compares the observed versus predicted inhibition response.

The simultaneous addition of taxanes with dinaciclib resulted in a decrease in cell proliferation for all taxane-resistant cell lines (Figure 5.10A). The average Bliss δ scores of cell line response to the combination of the two drugs were -6.377 for MDA-MB-231 25PACR, -4.895 for MDA-MB-231 25DOCR and 0.762 for MCF7 25PACR indicating an additive effect for all cell lines (Figure 5.10B). However, these effects were modest and there was no apparent reversal in sensitivity to taxane.

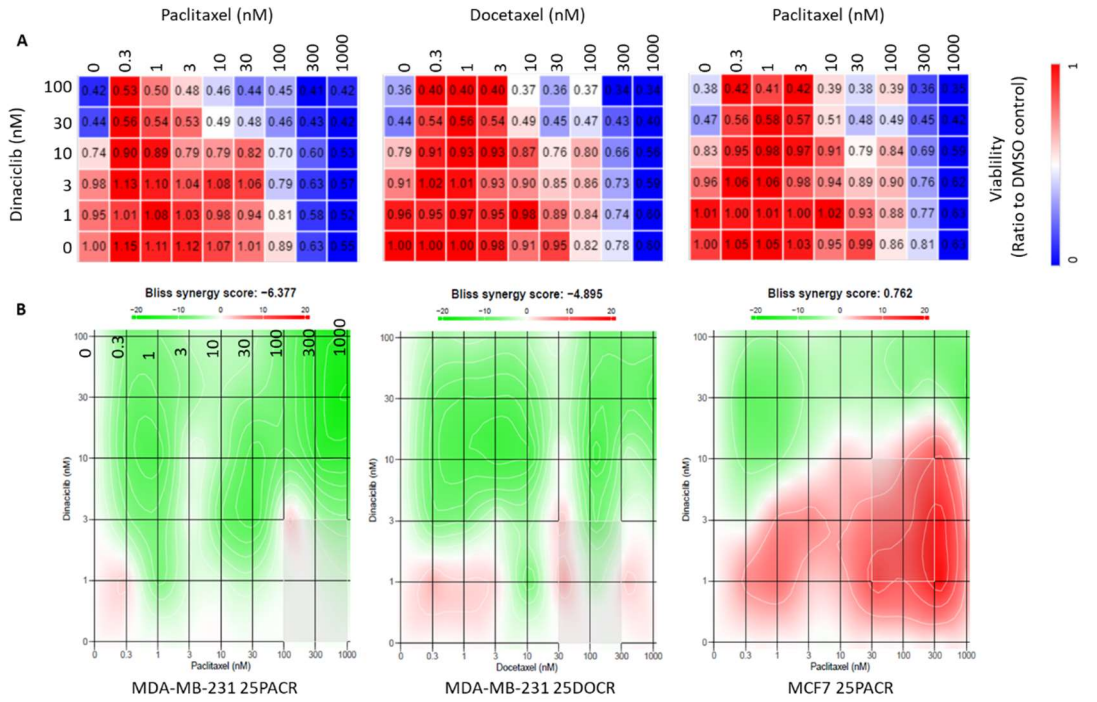

Figure 5.10: Combination of taxanes and dinaciclib induce an additive effect which reduces cell viability. MDA-MB-231 25PACR, MDA-MB-231 25DOCR and MCF7 25PACR cells were treated for 72 hrs with the indicated concentrations of dinaciclib in combination with either paclitaxel or docetaxel and cell viability assessed. The synergy score for each combination was calculated using Synergyfinder® software. Red and green areas represent synergy (synergy score greater than 10 and antagonsim less than -10). White rectangles indicate the maximum synergy area. (n=3)

The combination of dinaciclib and epirubicin was next compared. Again, an additive effect was observed for MDA-MB-231 25PACR with an average (and maximum) Synergyfinder® Bliss δ scores of -5.363 (8.42). Interestingly, given the observed resistance to epirubicin as assessed in chapter 3 (Table 3.4), a Bliss δ score of 5.508 (9.62) for MDA-MB-231 25DOCR was calculated, suggesting a trend towards synergy. Low levels of synergy were observed in the combination of 30nM dinaciclib with 20nM epirubicin. Similarly, MCF7 25PACR demonstrated an average Bliss δ score of 9.95 (21.84) which suggests a synergistic effect when dinaciclib was combined with epirubicin. A combination of 10nM dinaciclib and 10-100 nM epirubicin induced the optimum cell growth inhibition.

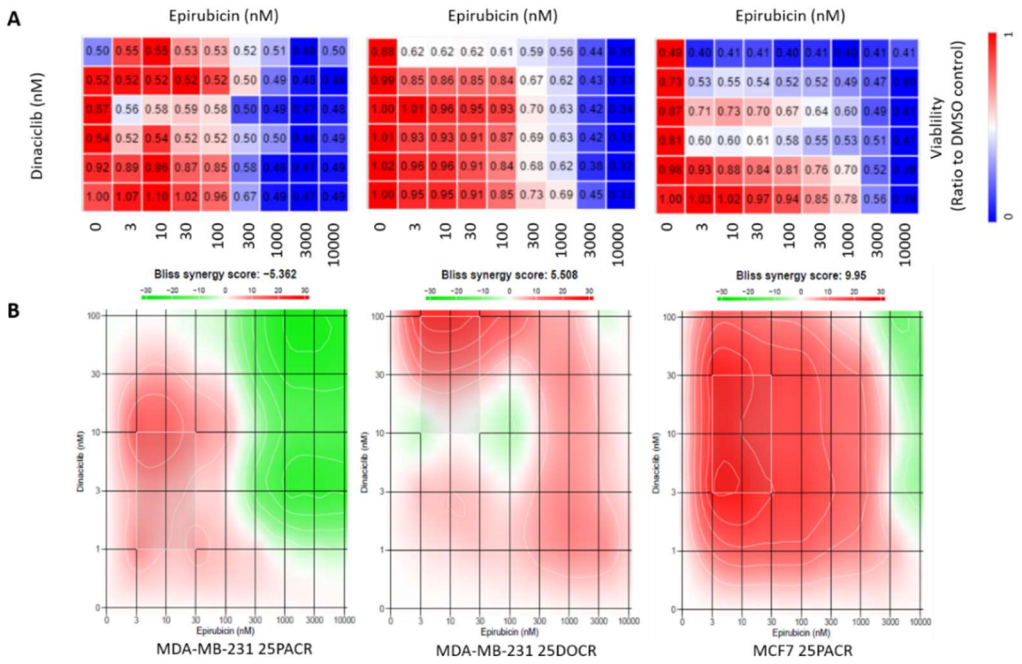

Figure 5.11: Combination of epirubicin and dinaciclib induce an additive effect in MDA-MB-231 taxane resistant cell lines and synergy in MCF7 25PACR. MDA-MB-231 25PACR, MDA-MB-231 25DOCR and MCF7 25PACR cells were treated for 72 hrs with the indicated concentrations of dinaciclib in combination with epirubicin and cell viability assessed. The average synergy score for each combination was calculated using Synergyfinder® software. Red areas represent synergy, antagonsim in green and white additive effects. White rectangles indicate the maximum synergy area. (n=3)

5.3 Discussion

Breast cancer patients with chemoresistant disease face an uncertain future, with few options available to them upon relapse. Despite significant advances in the diagnosis and treatment of the disease, drug resistance remains a major obstacle to effective therapy. It is therefore essential that novel treatments for chemoresistant disease are identified. Informed by the multi-omics results of the chapter 4, which identified deregulation of the PI3K/Akt pathway and the cell cycle, a conventional target-based approach to drug identification was taken with the screen focused on inhibitors of these pathways. Both pathways are integral to a number of hallmarks of cancer such as inhibition of apoptosis, uncontrolled cellular proliferation and survival (4). Pharmacological modulation of the PI3K pathway and cell cycle may therefore offer an important approach for the treatment of taxane resistant breast cancer.

The PI3K/Akt pathway controls many critical cellular roles including metabolism, growth, survival and proliferation through a signalling cascade via PI3K (294, 294). PI3Ks are divided into three classes, of which class I in particular has been implicated in the development of cancer, tumour growth and chemoresistance (100, 295). Activating mutations of the PI3KCA gene, which encodes the p110α catalytic subunit of class IA, is the second most frequently mutated in cancer (296) and, as such, has become an important target for drug discovery over the last two decades. BYL719 (alpelisib), a PIK3CA specific inhibitor (297) was approved for breast cancer treatment by the FDA in May 2019. Results from a phase I/II trial of alpelisib plus paclitaxel in locally recurrent or metastatic HER2 negative breast cancer indicated robust efficacy in patients with a mutation in PIK3CA (298). Its use in triple negative anthracycline-resistant breast cancer is currently being assessed in combination with paclitaxel (NCT04216472). Similarly, cell cycle deregulation where loss of Rb expression, amplification of CDKs and overexpression of cyclins in cancer are frequently observed (299) also offers an attractive option as potential druggable targets. The critical role of CDKs in regulating the cell cycle and transcription has led to the development of small molecule kinase inhibitors including pan-CDKi and CDK-specific compounds. Palbociclib, a specific CDK4/6 inhibitor, was the first CDK inhibitor approved by the

FDA for treatment of advanced hormone receptor positive breast cancer (300). Although reports of poor tolerability and resistance have been reported, targeting of these pathways remains of clinical interest and are still being actively pursued as viable therapeutic targets.

In this chapter I have shown that the taxane resistant isogenic cell line models can be effectively used to identify small molecule kinase inhibitors with activity in chemoresistant disease. Dose dependent survival changes were observed across the panel of small molecule kinase inhibitors using the MDA-MB-231 taxane resistant isogenic cell line, with approximately one third of the tested kinases reaching 50% cell death at clinically relevant concentrations. Inhibitors which targeted FAK, GSK3β and ATM/ATR were discounted from further study due to their lack of potency against the taxane resistant cell lines. However, their activity against taxane resistant disease cannot be fully discounted given the relatively small number of compounds screened and the single-pass aspect of the high-throughput screen. Overall, there was a strong bias to inhibitors which specifically targeted the class I PI3K family and those which targeted pan-CDK family members. A review of the results of the screen focused on those inhibitors which had already been approved for clinical trial. Of these, the most effective inhibitor of the MDA-MB-231 cell line series was dinaciclib, a CDK1, CDK2, CDK5 and CDK9 inhibitor (301) which had potency at nanomolar concentrations. Alvocidib, a pan class I inhibitor targeting CDK1, CDK2, CDK4 and CDK7 (302) was also highly effective against the taxane resistant cell lines. Of those inhibitors targeting the PI3K family, BKM120 (buparlisib) was the most potent clinically relevant of the inhibitors with use in over 80 clinical trials. BKM120 was first developed to treat head and neck carcinoma (303, 304) but has confirmed efficacy in a number of solid tumours and haematological malignancies (305).

The potency of these and other inhibitors were confirmed by extension to include MCF7 and the isogenic MCF7 25PACR cell line, again inducing strong dose dependent responses. As anticipated, the MCF7 parental and MCF7 25PACR cell lines were more sensitive to the effects to the PI3K inhibitors tested. These cell lines had been found

to be carriers of the activating PI3KCA mutation pE454K (Table 4.1), a mutation which enhances cellular proliferation, transformation and survival (306, 307). The increased sensitivity of the PI3KCA- mutated MCF7 cell lines to BKM120 was in agreement with published data from a phase 1b clinical trial of BKM120 with letrozole in ER+ HER2- breast cancer. Here they observed that those patients harbouring PI3KCA mutations, including pE545K, clinically benefited from PI3K inhibition (308). MDA-MB-231 25PACR was significantly more sensitive to BKM120 than the parental MDA-MB-231 cell line. Although targeted exome-sequencing of MDA-MB-231 25PACR did not reveal mutation in any of the assessed 'hot-spots', this does not exclude the possibility that a novel mutation has occurred which also renders this cell line more sensitive to the effects of BKM120. This finding suggests that whole-genome sequencing of the cell lines may be advantageous in this context.

Taking a proteomic approach to characterising the effects of BKM120 on the paclitaxel-resistant MDA-MB-231 cell line, attenuation of signal transduction downstream of PI3K was evident in both the parental and resistant cell lines, with downregulation of pAkt S473, pS6 S240 and p70S6K. Modulation of mTORC signalling and the reduction of S6 phosphorylation has been reported as being a key component of BKM120 treatment (309) an observation also confirmed in a RPPA analysis of samples from a recent phase II trial of BKM120 in metastatic breast cancer patients (310).

Although preclinical and clinical trial studies have indicated that the PI3K pathway is a viable drug target, poor drug tolerance and resistance have limited their development. Clinical trials with BKM120 have been hampered by the serious psychiatric side-effects reported by some patients (311) with the mood disorders attributed to the ability of BKM120 to cross the blood-brain barrier (312). The study by Garrido-Castro *et al* added to the evidence that BKM120 had no single-agent activity in unselected triple negative breast cancer (313). Whilst BKM120 may not be viable as an option for future clinical use, the screen identified other PI3K inhibitors with efficacy against the taxane resistant breast cancer cell lines which deserve

further investigation. BYL719 was also found to inhibit the proliferation of the taxane resistant cell lines with potent efficacy, again with greatest effect in the PI3KCA-mutated MCF7 isogenic cell lines. The SOLAR-1 and BYlieve trials have both reported improved progression free survival in PI3KCA -mutant hormone positive breast cancer patients with the PI3K inhibitor BYL719 (alpelisib) in combination with fulvestrant (116, 314) and highlights the clinical utility of this class of inhibitor. Further studies to investigate the mechanism of action of BYL719 in the taxane resistant cell lines are planned.

The final part of this chapter focused on the effects of the CDK inhibitor, dinaciclib, on the taxane resistant cell line models. With nanomolar potency across all cell lines, treatment with dinaciclib was found to induce apoptosis in a concentration dependent manner in the MDA-MB-231 taxane resistant isogenic cell lines. Cell cycle deregulation was observed in the MCF7 parental and paclitaxel-resistant derivate, MCF7 25PACR, with dinaciclib exposure resulting in accumulation in the G2/M phase. This effect was also demonstrated in the MDA-MB-231 parental cell line, agreeing with previously published observations (315). However, cell cycle effects were not consistent across the resistant cell lines with MDA-MB-231 25DOCR cells appearing to accumulate in the G0/G1 phase while the MDA-MB-231 25PACR cells accumulated in the S phase. A decrease in pRb S807/811 expression levels in all cell lines, as assessed by western blotting, suggested that CDK2 activity had been suppressed by dinaciclib. As mitosis is initiated by the activation of the cyclin B1-CDK1 complex (316), the downregulation of CCNB1 expression in response to dinancilb infers that CDK1 was also inactivated, which would result in the arrest of the taxane resistant cell lines in the G2/M phase of the cell cycle. Expression levels of PLK1, a modulator of the cylinB1-CDK1 complex, was downregulated in the isogenic MCF series, MDA-MB-231 parental and paclitaxel-resistant MDA-MB-231 25PACR cell lines. Expression changes of these CDK1 and CDK2 modulators in MDA-MB-231 25DOCR was considerably less marked and further experiments to define expression of other cell cycle checkpoint proteins are required to fully define the mechanism of action of dinaciclib in this cell line.

Overall dinaciclib, with potency for RB phosphorylation and nanomolar efficacy, is a promising pan-CDK inhibitor for further investigation in taxane resistant breast cancer. To further potentiate its activity, I considered whether a synergistic partner for combination therapy could be identified. Combinatorial targeting of multiple pathways is advantageous to the patient, with synergistic drug activity reducing the drug dose given resulting in less side-effects and an increase in treatment tolerability (293). Dinaciclib and taxane induced only additive effects, with no obvious return to a taxane-sensitive phenotype. A trend towards synergy did emerge with higher doses of paclitaxel in the examination of MCF7 25PACR which raises the possibility that the correct concentration range had not been explored. This cell line also showed promising synergy in combination with epirubicin with low nanomolar concentrations producing the greatest effect. However, while dinaciclib was generally well tolerated as a monotherapy (317, 318) its use in the clinic in combination has been less successful with a phase 1 clinical trial of dinaciclib with epirubicin in the treatment of metastatic triple negative breast cancer reporting no clinical benefit due to associated toxicities (319).

In conclusion, a rational mechanism of action approach to drug screening was successfully employed to identify inhibitors of taxane resistance in breast cancer and demonstrated their mechanisms of action. Few treatment options are available to those with taxane resistant disease, particularly those with triple negative disease, compounded further by inter- and intra-tumour heterogeneity. The results of this chapter suggests that the integration of transcriptomic and proteomic data with phenotypic response to small molecule kinases is a strategy which could be further exploited in this context. As the isogenic taxane-resistant cell line models have proved to be robust models for chemoresistant disease, their use in a screen of larger target-annotated reference compound libraries is merited, particularly with a view to devising combinatorial approaches which might offer patient benefit.

6. DISCUSSION AND CONCLUSION

6.1 Introduction

Breast cancer is the most commonly diagnosed cancer and leading cause of cancer-related death among women globally (9). Treatment of breast cancer is typically tailored according to the histopathological grade and stage and, increasingly, the molecular subtype of the tumour. Molecularly, breast cancer is a highly heterogeneous disease broadly divided into hormone/estrogen receptor positive (HR+/ER+), human epidermal receptor 2 positive (HER2+) or triple negative (ER-/PR-/HER2-) subtypes with treatments offered accordingly. Options for patients may include a combination of surgery, radiotherapy and systemic therapy, which includes hormone therapy, targeted therapy and chemotherapy. Taxanes are among the most active and widely used chemotherapy agents employed in the treatment of breast cancer, used either alone or in combination with other systemic therapies (218). The taxanes exert their effect by destabilising microtubules resulting in cell cycle arrest and cell death (221, 232). As with other cytotoxic cancer drugs, inherent or acquired resistance is frequently observed, leading to lack of efficacy or shorter responses to treatment (320). Taxane resistance therefore represents a major clinical challenge due to its contribution to therapeutic failure. Current treatment options for those with acquired taxane resistance are limited and the prognosis for patients is poor. Despite concerted efforts, the key molecular events driving chemoresistance remain unclear (321), and is further complicated by the clinical and cellular heterogeneity observed in breast cancer (41, 42). Multiple but independent mechanisms of acquired taxane resistance have been postulated, and include activation of signalling pathways, inhibition of apoptosis, increase in drug efflux and modification of cell cycle checkpoints (156, 219). However, an increased understanding of the mechanisms driving resistance to taxanes has the potential to improve therapeutic strategies benefiting patient management. The ability to identify molecular changes at transcriptomic and proteomic levels has been enhanced by the development of

high-throughput technologies accelerating tumour stratification, biomarker identification and the development of directed therapeutic strategies. Whilst the ideal sample cohort for studying the mechanisms of taxane resistance in breast cancer would be to compare patient samples taken before and after recurrence, the difficulty in attaining a specimen collection in sufficient quantities mean that other avenues must be pursued. One of the most common and successful *in vitro* approaches is the development of isogenic cell lines allowing the direct comparison of daughter to parental cell line, providing a controlled experimental system thus, reserving patient-derived material for subsequent validation of putative biomarkers of resistance.

The central aim of this thesis was therefore to identify mechanisms driving acquired taxane-resistance in breast cancer through the development and characterisation of isogenic preclinical cell line models, and to identify novel therapeutic strategies via a mechanism of action approach. Comprehensive transcriptomic and proteomic analyses revealed deregulation of cell cycle-associated pathways and the PI3K-Akt pathway in the taxane-resistant isogenic cell lines when compared to their respective parent cell lines. Additionally, a small molecule kinase screen revealed that inhibitors of these pathways demonstrated potent anti-proliferative activity in the isogenic cell lines, suggesting a potential novel chemotherapeutic approach for the treatment of taxane resistant breast cancer.

6.2 Summary of findings

Chapter 3 described the establishment isogenic cell line models of taxane-resistance in breast cancer by incremental exposure to either paclitaxel or docetaxel, and their subsequent characterisation. This work built on previous studies performed by our group where taxane-resistant ZR-75-1 and paclitaxel-resistant MDA-MB-231 (MDA-MB-231 25PACR) were developed through continuous exposure to incremental increases in dosage of taxane (220). To extend and complement this panel, a docetaxel-resistant cell line (MDA-MB-231 25DOCR) was derived from the master

stocks of parental MDA-MB-231 cells used in the initial study to ensure that any new cell line was truly isogenic in nature and could be used in comparative analyses. A paclitaxel-resistant MCF7 isogenic cell line was also established (MCF7 25PACR) although the ability to derive a stable docetaxel-resistant cell line proved impossible, despite repeated efforts. Similarly, I was unable to induce stable models of taxane-resistance in SK-BR-3 with either of the taxanes. Other groups have successfully established taxane-resistant cell line models for both MCF7 and SK-BR-3 (322-325) although it would appear that alternative methods such as pulse-treatment of drug or clonal selection were employed. To ensure consistency across all isogenic cell line models, these methods were not pursued in this thesis but may offer a means of establishing stable resistance in these cell lines, and should be considered for future work. Significant increases in IC_{50}s to taxanes were observed in the established isogenic cell lines confirming resistance had been established. Upregulation of P-glycoprotein at the protein level, and the observation that the taxane-resistant cell lines were cross-resistant to other chemotherapeutic agents, suggested that the resistance phenotype could be attributed to the upregulation of the MDR family of proteins. P-glycoprotein is a member of the ATP-binding cassette (ABC) transporter superfamily which acts to efflux a number of natural and cationic compounds, as well as chemotherapy drugs such as anthracyclines and taxanes (170). Overexpression of this family of proteins have been identified as a common mechanism of resistance in *in vitro* studies but has not been observed at the same level in the clinical setting (237, 326, 327). However, resensitisation to taxanes after siRNA knockdown of MDR1 did not occur and it was considered likely that alternative mechanisms of resistance were responsible for the chemoresistant phenotype observed in the established cell line models. Together with evidence that the taxanes did not induce cell cycle arrest or apoptosis in the taxane-resistant cell lines, it was concluded that robust models of chemoresistance had been established which were appropriate for further use in this study.

A comprehensive multi-omics analysis of the taxane-resistant cell lines and their parental cell lines to gain insight in to the drivers of taxane resistance was then

performed and described in chapter 4. Increasingly, this approach is taken to provide an accurate genomic and proteomic picture of cancer subtypes, with the aim of driving biomarker discovery and improving treatment selection for patients. A relatively small number of differential transcriptomic and proteomic changes were observed between the parental cell line and the daughter taxane-resistant cell lines, which was unsurprising given the isogenic nature of the cell line models. Functional interaction analysis of the significant differential changes observed in the transcriptome and proteome highlighted commonality in dysregulation of a select number of pathways across methodologies. Differential gene expression analysis of the MDA-MB-231 isogenic series and the MCF7 resistant cell line highlighted up-regulation of the PI3K-Akt pathway, JAK-STAT pathway and cytokine-cytokine receptor interaction, along with control of apoptosis and transcriptional regulation. Similarly, functional interaction analysis of differentially expressed proteins identified by RPPA also reinforced modulation of these pathways and biological processes. The combined analyses strongly indicated that deregulation of the PI3K-Akt signalling pathway and cell cycle, and of transcriptional regulation from RNA Polymerase II were central to the mechanisms of resistance in the isogenic cell lines derived for this study. These results are in accordance with previous reports of deregulation of these pathways in response to chemotherapy (221) and emphasises that resistance to taxanes is a result of complex interplay between multiple pathways.

Finally, a 'mechanism of action' kinase screen, informed by the results of chapter 4, resulted in identification of clinically relevant PI3K and cyclin-dependent kinase (CDK) inhibitors with nanomolar activity against the taxane resistant cell lines. The PI3K-Akt pathway has emerged as novel target for overcoming drug resistance (328) with dysregulation associated with breast cancer progression due to chemoresistance (329, 330). PI3KCA gene mutations are among the most frequently identified in cancer and are detected in 20-40% of breast tumours (100, 331). Three major hotspot mutations account for approximately 90% of all PI3KCA mutations, namely E542K and E545K which disrupt the helical domain and H1047R which affects the kinase domain of the p110α subunit (289, 332). The E545K activating mutation was observed in the

MCF7 parental and paclitaxel-resistant isogenic line by targeted-exome sequencing, which proved to be more susceptible to PI3K inhibition than the MDA-MB-231 isogenic series. The targeting of the cell cycle via inhibition of CDK has also gained clinical interest due to the critical role they play in cell cycle progression and transcription (290, 291), and a number of clinical trials exploring their impact in breast cancer have already taken place (134, 319). Functional assessment of the effects of dinaciclib demonstrated deregulation of the cell cycle and an increase in apoptosis, with deregulation of CDK1 activity suggested through inhibition of cyclin-B1 and PLK1. Finally, dinaciclib was shown to exert synergistic activity in the taxane-resistant cell lines when combined with epirubicin,

6.3 Future studies

The preclinical investigations explored in this thesis focused on *in vitro* characterisation of the taxane-resistant isogenic cell line and subsequent potency and selectivity of the PI3K and CDK inhibitors identified as part to the small molecule kinase screen.

Differential transcriptomic and proteomic expression analyses demonstrated clear differences between the parental and taxane-resistant cell lines, which deserve further investigation in to their potential as predictive markers of response to treatment. Due to the lack of publicly available breast cancer datasets with follow up data which include taxane treated only arms, it has proven difficult to ascertain their expression in resistant populations. Investigation of their expression in relation to recurrence and survival is merited, and it is hoped that access to a clinical dataset or to clinical material to assess expression to substantiate these findings can be achieved. A number of individual over-expressed genes identified by other studies as being of interest in the chemoresistance setting also deserve further examination, in particular *NUPR1* and *PBX1*. Experiments to define the effects of selective gene knockdown in the isogenic cell lines should be explored, in particular the impact on proliferation and potential resensitisation to taxanes.

One of the major limitations in drug development is the difficulty in translating the results of preclinical studies, typically performed in high-throughput two dimensional (2D) culture, to the clinic. Such cultures lack the heterogeneity seen in malignancy and do not account for the effects of the tumour microenvironment, both of which have a major impact on cancer development (333) To further the development of the candidate compounds, it is important to assess their efficacy in a three-dimensional (3D) setting, either *in vitro* or as xenografts. Preliminary studies establishing whether the taxane resistant cell lines have the ability to migrate and invade *in vitro* are necessary prior to establishment as xenografts. These characteristics may be investigated via simple scratch wound assays, and assessment of random migration of the taxane-resistant cell lines by invasion in to 3D extracellular matrices using basement membrane or collagen.

Murine models of cancer have historically dominated clinical research due to ease of breeding, and the availability of identical genetic strains of mice. Such models allow *in vivo* monitoring of tumour growth and drug toxicity, bridging the gap between 2D cell lines and living organs by taking in to account the interactions between cells and extracellular supporting matrix, which is lacking in 2D cell culture. Traditionally xenograft models are established by subcutaneous injection in to the flank of a mouse but a more clinically relevant model can be achieved through orthoptic injection, in the case of breast cancer to the mammary fat pad of the mouse. Future plans are to include both models to assess PI3K and CDK inhibitor efficacy *in vivo*, alone or in combination with other compounds, as potential therapeutic strategies for the treatment of chemoresistant disease.

Consideration must also be given to the possibility that establishment of the chemoresistant cell lines as xenografts may not be possible. Concurrent experiments to establish the taxane resistant cell lines as multicellular tumour spheroids and organoids as 3D co-culture systems are therefore also planned. High-throughput 96 well assays have been developed where cells are cultured along with cancer-associated fibroblasts, critical components of the breast stroma (334), in a non-

adherent environment allowing spheroids to form. Assays such as these are compatible with all of the technologies described in this thesis, allowing future investigation of the interplay of the microenvironment with the chemoresistant cell lines. Of particular interest is to establish whether the small molecule kinases identified retain their efficacy in a 3D-spheroid setting.

The ideal approach to studying chemoresistance is to utilise patient derived material, but the availability of paired tissue, before and after recurrence is limited. To extend this investigation of taxane resistance, the employment of patient-derived xenografts (PDX) models should also be explored. PDX models initially retain the architecture and stromal components of the primary tumour and are therefore considered to offer a more accurate representation of the tumour environment (335). Public availability of taxane resistant PDX models are limited but establishment of resistance through long-term exposure to taxanes *in vivo* should be possible. By employing this technique with a number of PDX models derived from chemo-naïve tumours, a panel of taxane resistant counterparts could be developed providing a rich resource of paired samples for further investigation.

The characterisation of the taxane-resistant cell line models via a multi-omics approach identified a number of differentially expressed druggable pathways, which could not be pursued in the time-frame of this thesis. The small molecule kinase screen performed as part of this thesis followed a mechanism of action approach and was thus limited to a selection of compounds targeting the PI3K-Akt and cell cycle via CDK inhibition. Further work where a more comprehensive approach to target screening is taken therefore has the potential to identify further inhibitors with selectivity for taxane resistance.

6.4 Conclusion

In this thesis I have successfully developed and characterised preclinical two novel isogenic models of taxane-resistant breast cancer cell lines. Through a combined transcriptomic and proteomic approach, I identified a number of deregulated pathways with the potential as therapeutic targets. It was clear that acquired taxane resistance is a result of a complex interplay of multiple molecular events, which requires further interrogation if the mechanisms driving resistance are to be defined. A focussed small molecule kinase screen identified inhibitors of PI3K and CDK as having potent activity against taxane resistance which merit further investigation as a strategy for treating patients with resistant disease.

Reference List

(1) Sung H, Ferlay J, Siegel RL, Laversanne M, Soerjomataram I, Jemal A, et al. Global Cancer Statistics 2020: GLOBOCAN Estimates of Incidence and Mortality Worldwide for 36 Cancers in 185 Countries. CA Cancer J Clin 2021;71:209-49.

(2) Steeg PS. Targeting metastasis. Nat Rev Cancer 2016;16:201-18.

(3) Hanahan D, Weinberg RA. The hallmarks of cancer. Cell 2000;100:57-70.

(4) Hanahan D, Weinberg RA. Hallmarks of cancer: the next generation. Cell 2011;144:646-74.

(5) Watson IR, Takahashi K, Futreal PA, Chin L. Emerging patterns of somatic mutations in cancer. Nat Rev Genet 2013;14:703-18.

(6) Martincorena I, Campbell PJ. Somatic mutation in cancer and normal cells. Science 2015;349:1483-9.

(7) Broustas CG, Lieberman HB. DNA damage response genes and the development of cancer metastasis. Radiat Res 2014;181:111-30.

(8) Hanahan D, Coussens LM. Accessories to the crime: functions of cells recruited to the tumor microenvironment. Cancer Cell 2012;21:309-22.

(9) Ferlay J, Colombet M, Soerjomataram I, Parkin DM, Pineros M, Znaor A, et al. Cancer statistics for the year 2020: An overview. Int J Cancer 2021.

(10) CRUK. https://www.cancerresearchuk.org/health-professional/cancer-statistics/statistics-by-cancer-type/breast-cancer/incidence-invasive. 2021.

(11) Torre LA, Siegel RL, Ward EM, Jemal A. Global Cancer Incidence and Mortality Rates and Trends--An Update. Cancer Epidemiol Biomarkers Prev 2016;25:16-27.

(12) Eccles SA, Aboagye EO, Ali S, Anderson AS, Armes J, Berditchevski F, et al. Critical research gaps and translational priorities for the successful prevention and treatment of breast cancer. Breast Cancer Res 2013;15:R92.

(13) McPherson K, Steel CM, Dixon JM. ABC of breast diseases. Breast cancer-epidemiology, risk factors, and genetics. BMJ 2000;321:624-8.

(14) Pharoah PD, Day NE, Duffy S, Easton DF, Ponder BA. Family history and the risk of breast cancer: a systematic review and meta-analysis. Int J Cancer 1997;71:800-9.

(15) Familial breast cancer: collaborative reanalysis of individual data from 52 epidemiological studies including 58,209 women with breast cancer and 101,986 women without the disease. Lancet 2001;358:1389-99.

(16) Miki Y, Swensen J, Shattuck-Eidens D, Futreal PA, Harshman K, Tavtigian S, et al. A strong candidate for the breast and ovarian cancer susceptibility gene BRCA1. Science 1994;266:66-71.

(17) Wooster R, Neuhausen SL, Mangion J, Quirk Y, Ford D, Collins N, et al. Localization of a breast cancer susceptibility gene, BRCA2, to chromosome 13q12-13. Science 1994;265:2088-90.

(18) Antoniou A, Pharoah PD, Narod S, Risch HA, Eyfjord JE, Hopper JL, et al. Average risks of breast and ovarian cancer associated with BRCA1 or BRCA2 mutations detected in case Series unselected for family history: a combined analysis of 22 studies. Am J Hum Genet 2003;72:1117-30.

(19) Parkin DM, Boyd L, Walker LC. 16. The fraction of cancer attributable to lifestyle and environmental factors in the UK in 2010. Br J Cancer 2011;105 Suppl 2:S77-S81.

(20) Wellings SR, Jensen HM. On the origin and progression of ductal carcinoma in the human breast. J Natl Cancer Inst 1973;50:1111-8.

(21) Wellings SR, Jensen HM, Marcum RG. An atlas of subgross pathology of the human breast with special reference to possible precancerous lesions. J Natl Cancer Inst 1975;55:231-73.

(22) Tavassoli FA DP. *Organization Classification of Tumors: Pathology and Genetics of Tumors of the Breast and Female Genital Organs.* WHO Classification of Tumours, 3rd Edition, Volume 4. 2021.

(23) CRUK. https://www.cancerresearchuk.org/about-cancer/breast-cancer/stages-types-grades/types/ductal-carcinoma-in-situ-dcis. 2021.

(24) Levi F, Randimbison L, Te VC, La VC. Invasive breast cancer following ductal and lobular carcinoma in situ of the breast. Int J Cancer 2005;116:820-3.

(25) Li CI, Malone KE, Saltzman BS, Daling JR. Risk of invasive breast carcinoma among women diagnosed with ductal carcinoma in situ and lobular carcinoma in situ, 1988-2001. Cancer 2006;106:2104-12.

(26) Duggal S, Robin J, Julian TB. Ductal carcinoma in situ: an overview. Expert Rev Anticancer Ther 2013;13:955-62.

(27) Li CI, Uribe DJ, Daling JR. Clinical characteristics of different histologic types of breast cancer. Br J Cancer 2005;93:1046-52.

(28) CRUK. https://www.cancerresearchuk.org/about-cancer/breast-cancer/stages-types-grades/types/lobular-carcinoma-in-situ-lcis. 2021.

(29) CRUK. https://www.cancerresearchuk.org/about-cancer/breast-cancer/stages-types-grades/types/invasive-lobular-breast-cancer. 2021.

(30) Lester SC, Bose S, Chen YY, Connolly JL, de Baca ME, Fitzgibbons PL, et al. Protocol for the examination of specimens from patients with invasive carcinoma of the breast. Arch Pathol Lab Med 2009;133:1515-38.

(31) BLOOM HJ, RICHARDSON WW. Histological grading and prognosis in breast cancer; a study of 1409 cases of which 359 have been followed for 15 years. Br J Cancer 1957;11:359-77.

(32) Frkovic-Grazio S, Bracko M. Long term prognostic value of Nottingham histological grade and its components in early (pT1N0M0) breast carcinoma. J Clin Pathol 2002;55:88-92.

(33) Edge SB, Compton CC. The American Joint Committee on Cancer: the 7th edition of the AJCC cancer staging manual and the future of TNM. Ann Surg Oncol 2010;17:1471-4.

(34) Greene FL, Sobin LH. A worldwide approach to the TNM staging system: collaborative efforts of the AJCC and UICC. J Surg Oncol 2009;99:269-72.

(35) Hortobagyi GN. Toward individualized breast cancer therapy: translating biological concepts to the bedside. Oncologist 2012;17:577-84.

(36) Hammond ME, Hayes DF, Dowsett M, Allred DC, Hagerty KL, Badve S, et al. American Society of Clinical Oncology/College of American Pathologists guideline recommendations for immunohistochemical testing of estrogen and progesterone receptors in breast cancer (unabridged version). Arch Pathol Lab Med 2010;134:e48-e72.

(37) Gown AM, Goldstein LC, Barry TS, Kussick SJ, Kandalaft PL, Kim PM, et al. High concordance between immunohistochemistry and fluorescence in situ hybridization testing for HER2 status in breast cancer requires a normalized IHC scoring system. Mod Pathol 2008;21:1271-7.

(38) Tvrdik D, Stanek L, Skalova H, Dundr P, Velenska Z, Povysil C. Comparison of the IHC, FISH, SISH and qPCR methods for the molecular diagnosis of breast cancer. Mol Med Rep 2012;6:439-43.

(39) Slamon DJ, Clark GM, Wong SG, Levin WJ, Ullrich A, McGuire WL. Human breast cancer: correlation of relapse and survival with amplification of the HER-2/neu oncogene. Science 1987;235:177-82.

(40) Perou CM, Jeffrey SS, van de Rijn M, Rees CA, Eisen MB, Ross DT, et al. Distinctive gene expression patterns in human mammary epithelial cells and breast cancers. Proc Natl Acad Sci U S A 1999;96:9212-7.

(41) Sorlie T, Perou CM, Tibshirani R, Aas T, Geisler S, Johnsen H, et al. Gene expression patterns of breast carcinomas distinguish tumor subclasses with clinical implications. Proc Natl Acad Sci U S A 2001;98:10869-74.

(42) Perou CM, Sorlie T, Eisen MB, van de Rijn M, Jeffrey SS, Rees CA, et al. Molecular portraits of human breast tumours. Nature 2000;406:747-52.

(43) Perou CM. Molecular stratification of triple-negative breast cancers. Oncologist 2011;16 Suppl 1:61-70.

(44) Prat A, Parker JS, Karginova O, Fan C, Livasy C, Herschkowitz JI, et al. Phenotypic and molecular characterization of the claudin-low intrinsic subtype of breast cancer. Breast Cancer Res 2010;12:R68.

(45) Moasser MM. The oncogene HER2: its signaling and transforming functions and its role in human cancer pathogenesis. Oncogene 2007;26:6469-87.

(46) Baselga J, Swain SM. Novel anticancer targets: revisiting ERBB2 and discovering ERBB3. Nat Rev Cancer 2009;9:463-75.

(47) de Ruijter TC, Veeck J, de Hoon JP, van EM, Tjan-Heijnen VC. Characteristics of triple-negative breast cancer. J Cancer Res Clin Oncol 2011;137:183-92.

(48) Burstein MD, Tsimelzon A, Poage GM, Covington KR, Contreras A, Fuqua SA, et al. Comprehensive genomic analysis identifies novel subtypes and targets of triple-negative breast cancer. Clin Cancer Res 2015;21:1688-98.

(49) Lehmann BD, Colaprico A, Silva TC, Chen J, An H, Ban Y, et al. Multi-omics analysis identifies therapeutic vulnerabilities in triple-negative breast cancer subtypes. Nat Commun 2021;12:6276.

(50) Morris GJ, Naidu S, Topham AK, Guiles F, Xu Y, McCue P, et al. Differences in breast carcinoma characteristics in newly diagnosed African-American and Caucasian patients: a single-institution compilation compared with the National Cancer Institute's Surveillance, Epidemiology, and End Results database. Cancer 2007;110:876-84.

(51) Bianchini G, Balko JM, Mayer IA, Sanders ME, Gianni L. Triple-negative breast cancer: challenges and opportunities of a heterogeneous disease. Nat Rev Clin Oncol 2016;13:674-90.

(52) Kriegsmann M, Endris V, Wolf T, Pfarr N, Stenzinger A, Loibl S, et al. Mutational profiles in triple-negative breast cancer defined by ultradeep multigene sequencing show high rates of PI3K pathway alterations and clinically relevant entity subgroup specific differences. Oncotarget 2014;5:9952-65.

(53) Shah SP, Roth A, Goya R, Oloumi A, Ha G, Zhao Y, et al. The clonal and mutational evolution spectrum of primary triple-negative breast cancers. Nature 2012;486:395-9.

(54) Dent R, Trudeau M, Pritchard KI, Hanna WM, Kahn HK, Sawka CA, et al. Triple-negative breast cancer: clinical features and patterns of recurrence. Clin Cancer Res 2007;13:4429-34.

(55) Liedtke C, Mazouni C, Hess KR, Andre F, Tordai A, Mejia JA, et al. Response to neoadjuvant therapy and long-term survival in patients with triple-negative breast cancer. J Clin Oncol 2008;26:1275-81.

(56) Filipits M, Rudas M, Jakesz R, Dubsky P, Fitzal F, Singer CF, et al. A new molecular predictor of distant recurrence in ER-positive, HER2-negative breast cancer adds independent information to conventional clinical risk factors. Clin Cancer Res 2011;17:6012-20.

(57) Paik S, Shak S, Tang G, Kim C, Baker J, Cronin M, et al. A multigene assay to predict recurrence of tamoxifen-treated, node-negative breast cancer. N Engl J Med 2004;351:2817-26.

(58) van 't Veer LJ, Dai H, van de Vijver MJ, He YD, Hart AA, Mao M, et al. Gene expression profiling predicts clinical outcome of breast cancer. Nature 2002;415:530-6.

(59) Parker JS, Mullins M, Cheang MC, Leung S, Voduc D, Vickery T, et al. Supervised risk predictor of breast cancer based on intrinsic subtypes. J Clin Oncol 2009;27:1160-7.

(60) Karam A. Update on breast cancer surgery approaches. Curr Opin Obstet Gynecol 2013;25:74-80.

(61) Matsen CB, Neumayer LA. Breast cancer: a review for the general surgeon. JAMA Surg 2013;148:971-9.

(62) Kummel S, Holtschmidt J, Loibl S. Surgical treatment of primary breast cancer in the neoadjuvant setting. Br J Surg 2014;101:912-24.

(63) Berveiller P, Mir O, Veyrie N, Barranger E. The sentinel-node concept: a dramatic improvement in breast-cancer surgery. Lancet Oncol 2010;11:906.

(64) Rebbeck TR, Friebel T, Lynch HT, Neuhausen SL, van ', V, Garber JE, et al. Bilateral prophylactic mastectomy reduces breast cancer risk in BRCA1 and BRCA2 mutation carriers: the PROSE Study Group. J Clin Oncol 2004;22:1055-62.

(65) Kunkler I. Radiotherapy for breast cancer. N Engl J Med 2002;346:862-4.

(66) Roos WP, Kaina B. DNA damage-induced cell death: from specific DNA lesions to the DNA damage response and apoptosis. Cancer Lett 2013;332:237-48.

(67) Clarke M, Collins R, Darby S, Davies C, Elphinstone P, Evans V, et al. Effects of radiotherapy and of differences in the extent of surgery for early breast cancer on local recurrence and 15-year survival: an overview of the randomised trials. Lancet 2005;366:2087-106.

(68) NICE guidelines. https://www.nice.org.uk/guidance/ng101/chapter/Recommendations#radiotherapy. 2021.

(69) Favourable and unfavourable effects on long-term survival of radiotherapy for early breast cancer: an overview of the randomised trials. Early Breast Cancer Trialists' Collaborative Group. Lancet 2000;355:1757-70.

(70) Nelson LR, Bulun SE. Estrogen production and action. J Am Acad Dermatol 2001;45:S116-S124.

(71) Saha RS, Vadlamudi RK. Role of estrogen receptor signaling in breast cancer metastasis. Int J Breast Cancer 2012;2012:654698.

(72) Caldon CE, Sergio CM, Schutte J, Boersma MN, Sutherland RL, Carroll JS, et al. Estrogen regulation of cyclin E2 requires cyclin D1 but not c-Myc. Mol Cell Biol 2009;29:4623-39.

(73) Doisneau-Sixou SF, Sergio CM, Carroll JS, Hui R, Musgrove EA, Sutherland RL. Estrogen and antiestrogen regulation of cell cycle progression in breast cancer cells. Endocr Relat Cancer 2003;10:179-86.

(74) Shiau AK, Barstad D, Loria PM, Cheng L, Kushner PJ, Agard DA, et al. The structural basis of estrogen receptor/coactivator recognition and the antagonism of this interaction by tamoxifen. Cell 1998;95:927-37.

(75) Cole MP, Jones CT, Todd ID. A new anti-oestrogenic agent in late breast cancer. An early clinical appraisal of ICI46474. Br J Cancer 1971;25:270-5.

(76) Jordan VC. Tamoxifen: a most unlikely pioneering medicine. Nat Rev Drug Discov 2003;2:205-13.

(77) Osborne CK, Zhao H, Fuqua SA. Selective estrogen receptor modulators: structure, function, and clinical use. J Clin Oncol 2000;18:3172-86.

(78) Stewart HJ, Prescott RJ, Forrest AP. Scottish adjuvant tamoxifen trial: a randomized study updated to 15 years. J Natl Cancer Inst 2001;93:456-62.

(79) Fisher B, Jeong JH, Bryant J, Anderson S, Dignam J, Fisher ER, et al. Treatment of lymph-node-negative, oestrogen-receptor-positive breast cancer: long-term findings from National Surgical Adjuvant Breast and Bowel Project randomised clinical trials. Lancet 2004;364:858-68.

(80) Gray RG RDHKeal. aTTom: Long-term effects of continuing adjuvant tamoxifen to 10 years versus stopping at 5 years in 6,953 women with early breast cancer**.** J Clin Oncol 31 (suppl):5-5. 2013.

(81) Davies C, Pan H, Godwin J, Gray R, Arriagada R, Raina V, et al. Long-term effects of continuing adjuvant tamoxifen to 10 years versus stopping at 5 years after diagnosis of oestrogen receptor-positive breast cancer: ATLAS, a randomised trial. Lancet 2013;381:805-16.

(82) Long X, Nephew KP. Fulvestrant (ICI 182,780)-dependent interacting proteins mediate immobilization and degradation of estrogen receptor-alpha. J Biol Chem 2006;281:9607-15.

(83) Miller WR. Aromatase inhibitors and breast cancer. Minerva Endocrinol 2006;31:27-46.

(84) Bonneterre J, Buzdar A, Nabholtz JM, Robertson JF, Thurlimann B, von EM, et al. Anastrozole is superior to tamoxifen as first-line therapy in hormone receptor positive advanced breast carcinoma. Cancer 2001;92:2247-58.

(85) Paridaens RJ, Dirix LY, Beex LV, Nooij M, Cameron DA, Cufer T, et al. Phase III study comparing exemestane with tamoxifen as first-line hormonal treatment of metastatic breast cancer in postmenopausal women: the European Organisation for Research and Treatment of Cancer Breast Cancer Cooperative Group. J Clin Oncol 2008;26:4883-90.

(86) Zhang J, Yang PL, Gray NS. Targeting cancer with small molecule kinase inhibitors. Nat Rev Cancer 2009;9:28-39.

(87) Yarden Y, Sliwkowski MX. Untangling the ErbB signalling network. Nat Rev Mol Cell Biol 2001;2:127-37.

(88) Faber AC, Li D, Song Y, Liang MC, Yeap BY, Bronson RT, et al. Differential induction of apoptosis in HER2 and EGFR addicted cancers following PI3K inhibition. Proc Natl Acad Sci U S A 2009;106:19503-8.

(89) Segovia-Mendoza M, Gonzalez-Gonzalez ME, Barrera D, Diaz L, Garcia-Becerra R. Efficacy and mechanism of action of the tyrosine kinase inhibitors gefitinib, lapatinib and neratinib in the treatment of HER2-positive breast cancer: preclinical and clinical evidence. Am J Cancer Res 2015;5:2531-61.

(90) Dent S, Oyan B, Honig A, Mano M, Howell S. HER2-targeted therapy in breast cancer: a systematic review of neoadjuvant trials. Cancer Treat Rev 2013;39:622-31.

(91) McArthur HL, Hudis CA. Trastuzumab: a picky partner? Clin Cancer Res 2009;15:6311-3.

(92) Collignon J, Jerusalem G. [Will targeted therapies replace chemotherapy?]. Rev Med Liege 2012;67 Spec No:29-36.

(93) Higgins MJ, Baselga J. Targeted therapies for breast cancer. J Clin Invest 2011;121:3797-803.

(94) EBCTCG Trastuzumab for early-stage, HER2-positive breast cancer: a meta-analysis of 13864 women in seven randomised trials. Lancet Oncol 2021;22:1139-50.

(95) Wissner A, Mansour TS. The development of HKI-272 and related compounds for the treatment of cancer. Arch Pharm (Weinheim) 2008;341:465-77.

(96) Paul B, Trovato JA, Thompson J. Lapatinib: a dual tyrosine kinase inhibitor for metastatic breast cancer. Am J Health Syst Pharm 2008;65:1703-10.

(97) Saini KS, Azim HA, Jr., Metzger-Filho O, Loi S, Sotiriou C, de AE, et al. Beyond trastuzumab: new treatment options for HER2-positive breast cancer. Breast 2011;20 Suppl 3:S20-S27.

(98) Kondapalli L, Soltani K, Lacouture ME. The promise of molecular targeted therapies: protein kinase inhibitors in the treatment of cutaneous malignancies. J Am Acad Dermatol 2005;53:291-302.

(99) Engelman JA. Targeting PI3K signalling in cancer: opportunities, challenges and limitations. Nat Rev Cancer 2009;9:550-62.

(100) Zhao L, Vogt PK. Class I PI3K in oncogenic cellular transformation. Oncogene 2008;27:5486-96.

(101) Thorpe LM, Yuzugullu H, Zhao JJ. PI3K in cancer: divergent roles of isoforms, modes of activation and therapeutic targeting. Nat Rev Cancer 2015;15:7-24.

(102) Fruman DA, Chiu H, Hopkins BD, Bagrodia S, Cantley LC, Abraham RT. The PI3K Pathway in Human Disease. Cell 2017;170:605-35.

(103) Manning BD, Cantley LC. AKT/PKB signaling: navigating downstream. Cell 2007;129:1261-74.

(104) Carracedo A, Pandolfi PP. The PTEN-PI3K pathway: of feedbacks and cross-talks. Oncogene 2008;27:5527-41.

(105) Fresno Vara JA, Casado E, de CJ, Cejas P, Belda-Iniesta C, Gonzalez-Baron M. PI3K/Akt signalling pathway and cancer. Cancer Treat Rev 2004;30:193-204.

(106) Liu P, Cheng H, Roberts TM, Zhao JJ. Targeting the phosphoinositide 3-kinase pathway in cancer. Nat Rev Drug Discov 2009;8:627-44.

(107) Samuels Y, Wang Z, Bardelli A, Silliman N, Ptak J, Szabo S, et al. High frequency of mutations of the PIK3CA gene in human cancers. Science 2004;304:554.

(108) Bachman KE, Argani P, Samuels Y, Silliman N, Ptak J, Szabo S, et al. The PIK3CA gene is mutated with high frequency in human breast cancers. Cancer Biol Ther 2004;3:772-5.

(109) Stemke-Hale K, Gonzalez-Angulo AM, Lluch A, Neve RM, Kuo WL, Davies M, et al. An integrative genomic and proteomic analysis of PIK3CA, PTEN, and AKT mutations in breast cancer. Cancer Res 2008;68:6084-91.

(110) Saal LH, Holm K, Maurer M, Memeo L, Su T, Wang X, et al. PIK3CA mutations correlate with hormone receptors, node metastasis, and ERBB2, and are

MUTUALLY EXCLUSIVE WITH PTEN LOSS IN HUMAN BREAST CARCINOMA. CANCER RES 2005;65:2554-9.

(111) ZHAO JJ, CHENG H, JIA S, WANG L, GJOERUP OV, MIKAMI A, ET AL. THE P110ALPHA ISOFORM OF PI3K IS ESSENTIAL FOR PROPER GROWTH FACTOR SIGNALING AND ONCOGENIC TRANSFORMATION. PROC NATL ACAD SCI U S A 2006;103:16296-300.

(112) MENG D, HE W, ZHANG Y, LIANG Z, ZHENG J, ZHANG X, ET AL. DEVELOPMENT OF PI3K INHIBITORS: ADVANCES IN CLINICAL TRIALS AND NEW STRATEGIES (REVIEW). PHARMACOL RES 2021;105900.

(113) YANG J, NIE J, MA X, WEI Y, PENG Y, WEI X. TARGETING PI3K IN CANCER: MECHANISMS AND ADVANCES IN CLINICAL TRIALS. MOL CANCER 2019;18:26.

(114) RAGON BK, KANTARJIAN H, JABBOUR E, RAVANDI F, CORTES J, BORTHAKUR G, ET AL. BUPARLISIB, A PI3K INHIBITOR, DEMONSTRATES ACCEPTABLE TOLERABILITY AND PRELIMINARY ACTIVITY IN A PHASE I TRIAL OF PATIENTS WITH ADVANCED LEUKEMIAS. AM J HEMATOL 2017;92:7-11.

(115) ANDRE F, CIRUELOS E, RUBOVSZKY G, CAMPONE M, LOIBL S, RUGO HS, ET AL. ALPELISIB FOR PIK3CA-MUTATED, HORMONE RECEPTOR-POSITIVE ADVANCED BREAST CANCER. N ENGL J MED 2019;380:1929-40.

(116) ANDRE F, CIRUELOS EM, JURIC D, LOIBL S, CAMPONE M, MAYER IA, ET AL. ALPELISIB PLUS FULVESTRANT FOR PIK3CA-MUTATED, HORMONE RECEPTOR-POSITIVE, HUMAN EPIDERMAL GROWTH FACTOR RECEPTOR-2-NEGATIVE ADVANCED BREAST CANCER: FINAL OVERALL SURVIVAL RESULTS FROM SOLAR-1. ANN ONCOL 2021;32:208-17.

(117) BASELGA J. TARGETING THE PHOSPHOINOSITIDE-3 (PI3) KINASE PATHWAY IN BREAST CANCER. ONCOLOGIST 2011;16 SUPPL 1:12-9.

(118) BOWER JJ, VANCE LD, PSIODA M, SMITH-ROE SL, SIMPSON DA, IBRAHIM JG, ET AL. PATTERNS OF CELL CYCLE CHECKPOINT DEREGULATION ASSOCIATED WITH INTRINSIC MOLECULAR SUBTYPES OF HUMAN BREAST CANCER CELLS. NPJ BREAST CANCER 2017;3:9.

(119) Dominguez-Brauer C, Thu KL, Mason JM, Blaser H, Bray MR, Mak TW. Targeting Mitosis in Cancer: Emerging Strategies. Mol Cell 2015;60:524-36.

(120) Asghar U, Witkiewicz AK, Turner NC, Knudsen ES. The history and future of targeting cyclin-dependent kinases in cancer therapy. Nat Rev Drug Discov 2015;14:130-46.

(121) Sherr CJ, Roberts JM. Living with or without cyclins and cyclin-dependent kinases. Genes Dev 2004;18:2699-711.

(122) Schafer KA. The cell cycle: a review. Vet Pathol 1998;35:461-78.

(123) Malumbres M, Barbacid M. To cycle or not to cycle: a critical decision in cancer. Nat Rev Cancer 2001;1:222-31.

(124) Malumbres M, Barbacid M. Mammalian cyclin-dependent kinases. Trends Biochem Sci 2005;30:630-41.

(125) Ravikumar G, Ananthamurthy A. Cyclin D1 expression in ductal carcinoma of the breast and its correlation with other prognostic parameters. J Cancer Res Ther 2014;10:671-5.

(126) Arnold A, Papanikolaou A. Cyclin D1 in breast cancer pathogenesis. J Clin Oncol 2005;23:4215-24.

(127) Malumbres M, Barbacid M. Cell cycle, CDKs and cancer: a changing paradigm. Nat Rev Cancer 2009;9:153-66.

(128) Nahta R, Takahashi T, Ueno NT, Hung MC, Esteva FJ. P27(kip1) down-regulation is associated with trastuzumab resistance in breast cancer cells. Cancer Res 2004;64:3981-6.

(129) Berton S, Cusan M, Segatto I, Citron F, D'Andrea S, Benevol S, et al. Loss of p27(kip1) increases genomic instability and induces radio-resistance in luminal breast cancer cells. Sci Rep 2017;7:595.

(130) Floros KV, Jacob S, Kurupi R, Fairchild CK, Hu B, Puchalapalli M, et al. Targeting transcription of MCL-1 sensitizes HER2-amplified breast cancers to HER2 inhibitors. Cell Death Dis 2021;12:179.

(131) Johnson SF, Cruz C, Greifenberg AK, Dust S, Stover DG, Chi D, et al. CDK12 Inhibition Reverses De Novo and Acquired PARP Inhibitor Resistance in BRCA Wild-Type and Mutated Models of Triple-Negative Breast Cancer. Cell Rep 2016;17:2367-81.

(132) Musgrove EA, Caldon CE, Barraclough J, Stone A, Sutherland RL. Cyclin D as a therapeutic target in cancer. Nat Rev Cancer 2011;11:558-72.

(133) Dickson C, Fantl V, Gillett C, Brookes S, Bartek J, Smith R, et al. Amplification of chromosome band 11q13 and a role for cyclin D1 in human breast cancer. Cancer Lett 1995;90:43-50.

(134) Beaver JA, Amiri-Kordestani L, Charlab R, Chen W, Palmby T, Tilley A, et al. FDA Approval: Palbociclib for the Treatment of Postmenopausal Patients with Estrogen Receptor-Positive, HER2-Negative Metastatic Breast Cancer. Clin Cancer Res 2015;21:4760-6.

(135) DeMichele A, Clark AS, Tan KS, Heitjan DF, Gramlich K, Gallagher M, et al. CDK 4/6 inhibitor palbociclib (PD0332991) in Rb+ advanced breast cancer: phase II activity, safety, and predictive biomarker assessment. Clin Cancer Res 2015;21:995-1001.

(136) Waks AG, Winer EP. Breast Cancer Treatment: A Review. JAMA 2019;321:288-300.

(137) Tanaka S, Iwamoto M, Kimura K, Matsunami N, Morishima H, Yoshidome K, et al. Phase II Study of Neoadjuvant Anthracycline-Based Regimens Combined With Nanoparticle Albumin-Bound Paclitaxel and Trastuzumab for Human Epidermal Growth Factor Receptor 2-Positive Operable Breast Cancer. Clin Breast Cancer 2015;15:191-6.

(138) Gonzalez-Neira A. Pharmacogenetics of chemotherapy efficacy in breast cancer. Pharmacogenomics 2012;13:677-90.

(139) Poole CJ, Earl HM, Hiller L, Dunn JA, Bathers S, Grieve RJ, et al. Epirubicin and cyclophosphamide, methotrexate, and fluorouracil as adjuvant therapy for early breast cancer. N Engl J Med 2006;355:1851-62.

(140) Oronsky BT, Reid T, Knox SJ, Scicinski JJ. The scarlet letter of alkylation: a mini review of selective alkylating agents. Transl Oncol 2012;5:226-9.

(141) NICE guidelines; https://www.nice.org.uk/guidance/CG80/chapter/1-Guidance#chemotherapy. 2017.

(142) Miles DW. Recent advances in systemic therapy. When HER2 is not the target: advances in the treatment of HER2-negative metastatic breast cancer. Breast Cancer Res 2009;11:208.

(143) Miles DW. Recent advances in systemic therapy. When HER2 is not the target: advances in the treatment of HER2-negative metastatic breast cancer. Breast Cancer Res 2009;11:208.

(144) Bear HD, Anderson S, Brown A, Smith R, Mamounas EP, Fisher B, et al. The effect on tumor response of adding sequential preoperative docetaxel to preoperative doxorubicin and cyclophosphamide: preliminary results from National Surgical Adjuvant Breast and Bowel Project Protocol B-27. J Clin Oncol 2003;21:4165-74.

(145) Wang H, Mao Y, Zhou N, Hu T, Hsieh TS, Liu LF. Atp-bound topoisomerase ii as a target for antitumor drugs. J Biol Chem 2001;276:15990-5.

(146) Jacobson MD. Reactive oxygen species and programmed cell death. Trends Biochem Sci 1996;21:83-6.

(147) Rowinsky EK, Onetto N, Canetta RM, Arbuck SG. Taxol: the first of the taxanes, an important new class of antitumor agents. Semin Oncol 1992;19:646-62.

(148) Schiff PB, Horwitz SB. Taxol stabilizes microtubules in mouse fibroblast cells. Proc Natl Acad Sci U S A 1980;77:1561-5.

(149) Schiff PB, Fant J, Horwitz SB. Promotion of microtubule assembly in vitro by taxol. Nature 1979;277:665-7.

(150) Willson ML, Burke L, Ferguson T, Ghersi D, Nowak AK, Wilcken N. Taxanes for adjuvant treatment of early breast cancer. Cochrane Database Syst Rev 2019;9:CD004421.

(151) Sharifi-Rad J, Bahukhandi A, Dhyani P, Sati P, Capanoglu E, Docea AO, et al. Therapeutic Potential of Neoechinulins and Their Derivatives: An Overview of the Molecular Mechanisms Behind Pharmacological Activities. Front Nutr 2021;8:664197.

(152) Emadi A, Jones RJ, Brodsky RA. Cyclophosphamide and cancer: golden anniversary. Nat Rev Clin Oncol 2009;6:638-47.

(153) Frederiks CN, Lam SW, Guchelaar HJ, Boven E. Genetic polymorphisms and paclitaxel- or docetaxel-induced toxicities: A systematic review. Cancer Treat Rev 2015;41:935-50.

(154) Kus T, Aktas G, Kalender ME, Demiryurek AT, Ulasli M, Oztuzcu S, et al. Polymorphism of CYP3A4 and ABCB1 genes increase the risk of neuropathy in breast cancer patients treated with paclitaxel and docetaxel. Onco Targets Ther 2016;9:5073-80.

(155) Rochette L, Guenancia C, Gudjoncik A, Hachet O, Zeller M, Cottin Y, et al. Anthracyclines/trastuzumab: new aspects of cardiotoxicity and molecular mechanisms. Trends Pharmacol Sci 2015;36:326-48.

(156) Longley DB, Johnston PG. Molecular mechanisms of drug resistance. J Pathol 2005;205:275-92.

(157) Cree IA, Charlton P. Molecular chess? Hallmarks of anti-cancer drug resistance. BMC Cancer 2017;17:10.

(158) Konieczkowski DJ, Johannessen CM, Garraway LA. A Convergence-Based Framework for Cancer Drug Resistance. Cancer Cell 2018;33:801-15.

(159) Wani MC, Taylor HL, Wall ME, Coggon P, McPhail AT. Plant antitumor agents. VI. The isolation and structure of taxol, a novel antileukemic and antitumor agent from Taxus brevifolia. J Am Chem Soc 1971;93:2325-7.

(160) Trudeau ME. Docetaxel: a review of its pharmacology and clinical activity. Can J Oncol 1996;6:443-57.

(161) Schiff PB, Fant J, Horwitz SB. Promotion of microtubule assembly in vitro by taxol. Nature 1979;277:665-7.

(162) Nicolaou KC, Yang Z, Liu JJ, Ueno H, Nantermet PG, Guy RK, et al. Total synthesis of taxol. Nature 1994;367:630-4.

(163) Kavallaris M. Microtubules and resistance to tubulin-binding agents. Nat Rev Cancer 2010;10:194-204.

(164) Altmann KH. Microtubule-stabilizing agents: a growing class of important anticancer drugs. Curr Opin Chem Biol 2001;5:424-31.

(165) Dumontet C, Jordan MA, Lee FF. Ixabepilone: targeting betaIII-tubulin expression in taxane-resistant malignancies. Mol Cancer Ther 2009;8:17-25.

(166) Manfredi JJ, Parness J, Horwitz SB. Taxol binds to cellular microtubules. J Cell Biol 1982;94:688-96.

(167) Ganansia-Leymarie V, Bischoff P, Bergerat JP, Holl V. Signal transduction pathways of taxanes-induced apoptosis. Curr Med Chem Anticancer Agents 2003;3:291-306.

(168) McGrogan BT, Gilmartin B, Carney DN, McCann A. Taxanes, microtubules and chemoresistant breast cancer. Biochim Biophys Acta 2008;1785:96-132.

(169) Li W, Zhu W, Lv C, Qu H, Xu K, Li H, et al. Low-dose paclitaxel downregulates MYC proto-oncogene bHLH transcription factor expression in colorectal carcinoma cells. Oncol Lett 2018;15:1881-7.

(170) Ramachandra M, Ambudkar SV, Chen D, Hrycyna CA, Dey S, Gottesman MM, et al. Human P-glycoprotein exhibits reduced affinity for substrates during a catalytic transition state. Biochemistry 1998;37:5010-9.

(171) Pusztai L. Markers predicting clinical benefit in breast cancer from microtubule-targeting agents. Ann Oncol 2007;18 Suppl 12:xii15-xii20.

(172) Fletcher JI, Haber M, Henderson MJ, Norris MD. ABC transporters in cancer: more than just drug efflux pumps. Nat Rev Cancer 2010;10:147-56.

(173) Gottesman MM, Fojo T, Bates SE. Multidrug resistance in cancer: role of ATP-dependent transporters. Nat Rev Cancer 2002;2:48-58.

(174) van EM, Boosman RJ, Schinkel AH, Huitema ADR, Beijnen JH. Cytochrome P450 3A4, 3A5, and 2C8 expression in breast, prostate, lung, endometrial, and ovarian tumors: relevance for resistance to taxanes. Cancer Chemother Pharmacol 2019;84:487-99.

(175) Thelen K, Dressman JB. Cytochrome P450-mediated metabolism in the human gut wall. J Pharm Pharmacol 2009;61:541-58.

(176) Oyama T, Kagawa N, Kunugita N, Kitagawa K, Ogawa M, Yamaguchi T, et al. Expression of cytochrome P450 in tumor tissues and its association with cancer development. Front Biosci 2004;9:1967-76.

(177) van EM, Boosman RJ, Schinkel AH, Huitema ADR, Beijnen JH. Cytochrome P450 3A4, 3A5, and 2C8 expression in breast, prostate, lung, endometrial, and ovarian tumors: relevance for resistance to taxanes. Cancer Chemother Pharmacol 2019;84:487-99.

(178) Hendrikx JJ, Lagas JS, Song JY, Rosing H, Schellens JH, Beijnen JH, et al. Ritonavir inhibits intratumoral docetaxel metabolism and enhances docetaxel antitumor activity in an immunocompetent mouse breast cancer model. Int J Cancer 2016;138:758-69.

(179) Savas U, Griffin KJ, Johnson EF. Molecular mechanisms of cytochrome P-450 induction by xenobiotics: An expanded role for nuclear hormone receptors. Mol Pharmacol 1999;56:851-7.

(180) Sakurai K, Enomoto K, Matsuo S, Amano S, Shiono M. CYP3A4 expression to predict treatment response to docetaxel for metastasis and recurrence of primary breast cancer. Surg Today 2011;41:674-9.

(181) Miyoshi Y, Taguchi T, Kim SJ, Tamaki Y, Noguchi S. Prediction of response to docetaxel by immunohistochemical analysis of CYP3A4 expression in human breast cancers. Breast Cancer 2005;12:11-5.

(182) Miyoshi Y, Ando A, Takamura Y, Taguchi T, Tamaki Y, Noguchi S. Prediction of response to docetaxel by CYP3A4 mRNA expression in breast cancer tissues. Int J Cancer 2002;97:129-32.

(183) Hasegawa S, Miyoshi Y, Egawa C, Ishitobi M, Taguchi T, Tamaki Y, et al. Prediction of response to docetaxel by quantitative analysis of class I and III beta-tubulin isotype mRNA expression in human breast cancers. Clin Cancer Res 2003;9:2992-7.

(184) Nami B, Wang Z. Genetics and Expression Profile of the Tubulin Gene Superfamily in Breast Cancer Subtypes and Its Relation to Taxane Resistance. Cancers (Basel) 2018;10.

(185) Kamath K, Wilson L, Cabral F, Jordan MA. BetaIII-tubulin induces paclitaxel resistance in association with reduced effects on microtubule dynamic instability. J Biol Chem 2005;280:12902-7.

(186) Lebok P, Ozturk M, Heilenkotter U, Jaenicke F, Muller V, Paluchowski P, et al. High levels of class III b-tubulin expression are associated with aggressive tumor features in breast cancer. Oncol Lett 2016;11:1987-94.

(187) Giannakakou P, Gussio R, Nogales E, Downing KH, Zaharevitz D, Bollbuck B, et al. A common pharmacophore for epothilone and taxanes: molecular basis for drug resistance conferred by tubulin mutations in human cancer cells. Proc Natl Acad Sci U S A 2000;97:2904-9.

(188) Berrieman HK, Lind MJ, Cawkwell L. Do beta-tubulin mutations have a role in resistance to chemotherapy? Lancet Oncol 2004;5:158-64.

(189) Prosser SL, Pelletier L. Mitotic spindle assembly in animal cells: a fine balancing act. Nat Rev Mol Cell Biol 2017;18:187-201.

(190) Honore S, Pasquier E, Braguer D. Understanding microtubule dynamics for improved cancer therapy. Cell Mol Life Sci 2005;62:3039-56.

(191) Dehmelt L, Halpain S. The MAP2/Tau family of microtubule-associated proteins. Genome Biol 2005;6:204.

(192) Zhang CC, Yang JM, White E, Murphy M, Levine A, Hait WN. The role of MAP4 expression in the sensitivity to paclitaxel and resistance to vinca alkaloids in p53 mutant cells. Oncogene 1998;16:1617-24.

(193) Irshad S, Gillett C, Pinder SE, A'hern RP, Dowsett M, Ellis IO, et al. Assessment of microtubule-associated protein (MAP)-Tau expression as a predictive and prognostic marker in TACT; a trial assessing substitution of sequential docetaxel for FEC as adjuvant chemotherapy for early breast cancer. Breast Cancer Res Treat 2014;144:331-41.

(194) Rodrigues-Ferreira S, Nehlig A, Moindjie H, Monchecourt C, Seiler C, Marangoni E, et al. Improving breast cancer sensitivity to paclitaxel by increasing aneuploidy. Proc Natl Acad Sci U S A 2019;116:23691-7.

(195) Brattsand G. Correlation of oncoprotein 18/stathmin expression in human breast cancer with established prognostic factors. Br J Cancer 2000;83:311-8.

(196) Alli E, Yang JM, Ford JM, Hait WN. Reversal of stathmin-mediated resistance to paclitaxel and vinblastine in human breast carcinoma cells. Mol Pharmacol 2007;71:1233-40.

(197) Thornton BR, Toczyski DP. Securin and B-cyclin/CDK are the only essential targets of the APC. Nat Cell Biol 2003;5:1090-4.

(198) McInnes C, Wyatt MD. PLK1 as an oncology target: current status and future potential. Drug Discov Today 2011;16:619-25.

(199) Sudo T, Nitta M, Saya H, Ueno NT. Dependence of paclitaxel sensitivity on a functional spindle assembly checkpoint. Cancer Res 2004;64:2502-8.

(200) Whitaker RH, Placzek WJ. Regulating the BCL2 Family to Improve Sensitivity to Microtubule Targeting Agents. Cells 2019;8.

(201) Fan W. Possible mechanisms of paclitaxel-induced apoptosis. Biochem Pharmacol 1999;57:1215-21.

(202) Campbell KJ, Tait SWG. Targeting BCL-2 regulated apoptosis in cancer. Open Biol 2018;8.

(203) Datta SR, Dudek H, Tao X, Masters S, Fu H, Gotoh Y, et al. Akt phosphorylation of BAD couples survival signals to the cell-intrinsic death machinery. Cell 1997;91:231-41.

(204) Lin A, Karin M. NF-kappaB in cancer: a marked target. Semin Cancer Biol 2003;13:107-14.

(205) Chuang SE, Yeh PY, Lu YS, Lai GM, Liao CM, Gao M, et al. Basal levels and patterns of anticancer drug-induced activation of nuclear factor-kappaB (NF-kappaB),

AND ITS ATTENUATION BY TAMOXIFEN, DEXAMETHASONE, AND CURCUMIN IN CARCINOMA CELLS. BIOCHEM PHARMACOL 2002;63:1709-16.

(206) HUANG Y, FAN W. IKAPPAB KINASE ACTIVATION IS INVOLVED IN REGULATION OF PACLITAXEL-INDUCED APOPTOSIS IN HUMAN TUMOR CELL LINES. MOL PHARMACOL 2002;61:105-13.

(207) KESHET Y, SEGER R. THE MAP KINASE SIGNALING CASCADES: A SYSTEM OF HUNDREDS OF COMPONENTS REGULATES A DIVERSE ARRAY OF PHYSIOLOGICAL FUNCTIONS. METHODS MOL BIOL 2010;661:3-38.

(208) YAMAMOTO K, ICHIJO H, KORSMEYER SJ. BCL-2 IS PHOSPHORYLATED AND INACTIVATED BY AN ASK1/JUN N-TERMINAL PROTEIN KINASE PATHWAY NORMALLY ACTIVATED AT G(2)/M. MOL CELL BIOL 1999;19:8469-78.

(209) MCCUBREY JA, STEELMAN LS, CHAPPELL WH, ABRAMS SL, WONG EW, CHANG F, ET AL. ROLES OF THE RAF/MEK/ERK PATHWAY IN CELL GROWTH, MALIGNANT TRANSFORMATION AND DRUG RESISTANCE. BIOCHIM BIOPHYS ACTA 2007;1773:1263-84.

(210) BACUS SS, GUDKOV AV, LOWE M, LYASS L, YUNG Y, KOMAROV AP, ET AL. TAXOL-INDUCED APOPTOSIS DEPENDS ON MAP KINASE PATHWAYS (ERK AND P38) AND IS INDEPENDENT OF P53. ONCOGENE 2001;20:147-55.

(211) SOULE HD, VAZGUEZ J, LONG A, ALBERT S, BRENNAN M. A HUMAN CELL LINE FROM A PLEURAL EFFUSION DERIVED FROM A BREAST CARCINOMA. J NATL CANCER INST 1973;51:1409-16.

(212) CAILLEAU R, OLIVE M, CRUCIGER QV. LONG-TERM HUMAN BREAST CARCINOMA CELL LINES OF METASTATIC ORIGIN: PRELIMINARY CHARACTERIZATION. IN VITRO 1978;14:911-5.

(213) FOGH J, FOGH JM, ORFEO T. ONE HUNDRED AND TWENTY-SEVEN CULTURED HUMAN TUMOR CELL LINES PRODUCING TUMORS IN NUDE MICE. J NATL CANCER INST 1977;59:221-6.

(214) IANEVSKI A, GIRI AK, AITTOKALLIO T. SYNERGYFINDER 2.0: VISUAL ANALYTICS OF MULTI-DRUG COMBINATION SYNERGIES. NUCLEIC ACIDS RES 2020;48:W488-W493.

(215) Geiss GK, Bumgarner RE, Birditt B, Dahl T, Dowidar N, Dunaway DL, et al. Direct multiplexed measurement of gene expression with color-coded probe pairs. Nat Biotechnol 2008;26:317-25.

(216) Shannon P, Markiel A, Ozier O, Baliga NS, Wang JT, Ramage D, et al. Cytoscape: a software environment for integrated models of biomolecular interaction networks. Genome Res 2003;13:2498-504.

(217) Wu G, Feng X, Stein L. A human functional protein interaction network and its application to cancer data analysis. Genome Biol 2010;11:R53.

(218) Early Breast Cancer Trialists' Collaborative Group (EBCTCG). Effects of chemotherapy and hormonal therapy for early breast cancer on recurrence and 15-year survival: an overview of the randomised trials. The Lancet 2005;365:1687-717.

(219) Maloney SM, Hoover CA, Morejon-Lasso LV, Prosperi JR. Mechanisms of Taxane Resistance. Cancers (Basel) 2020;12.

(220) Kenicer J, Spears M, Lyttle N, Taylor KJ, Liao L, Cunningham CA, et al. Molecular characterisation of isogenic taxane resistant cell lines identify novel drivers of drug resistance. BMC Cancer 2014;14:762.

(221) Murray S, Briasoulis E, Linardou H, Bafaloukos D, Papadimitriou C. Taxane resistance in breast cancer: mechanisms, predictive biomarkers and circumvention strategies. Cancer Treat Rev 2012;38:890-903.

(222) Roninson IB, Chin JE, Choi KG, Gros P, Housman DE, Fojo A, et al. Isolation of human mdr DNA sequences amplified in multidrug-resistant KB carcinoma cells. Proc Natl Acad Sci U S A 1986;83:4538-42.

(223) Fojo AT, Ueda K, Slamon DJ, Poplack DG, Gottesman MM, Pastan I. Expression of a multidrug-resistance gene in human tumors and tissues. Proc Natl Acad Sci U S A 1987;84:265-9.

(224) Almendro V, Marusyk A, Polyak K. Cellular heterogeneity and molecular evolution in cancer. Annu Rev Pathol 2013;8:277-302.

(225) Gerlinger M, Rowan AJ, Horswell S, Math M, Larkin J, Endesfelder D, et al. Intratumor heterogeneity and branched evolution revealed by multiregion sequencing. N Engl J Med 2012;366:883-92.

(226) Lawrence MS, Stojanov P, Mermel CH, Robinson JT, Garraway LA, Golub TR, et al. Discovery and saturation analysis of cancer genes across 21 tumour types. Nature 2014;505:495-501.

(227) Dawson SJ, Rueda OM, Aparicio S, Caldas C. A new genome-driven integrated classification of breast cancer and its implications. EMBO J 2013;32:617-28.

(228) Jamal-Hanjani M, Quezada SA, Larkin J, Swanton C. Translational implications of tumor heterogeneity. Clin Cancer Res 2015;21:1258-66.

(229) Khan GN, Kim EJ, Shin TS, Lee SH. Heterogeneous Cell Types in Single-cell-derived Clones of MCF7 and MDA-MB-231 Cells. Anticancer Res 2017;37:2343-54.

(230) Martin-Pardillos A, Valls A, Bande VG, Hurtado BP, Pineiro CR, Guijarro PJ, et al. The role of clonal communication and heterogeneity in breast cancer. BMC Cancer 2019;19:666.

(231) Steed H, Sawyer MB. Pharmacology, pharmacokinetics and pharmacogenomics of paclitaxel. Pharmacogenomics 2007;8:803-15.

(232) Donaldson KL, Goolsby GL, Kiener PA, Wahl AF. Activation of p34cdc2 coincident with taxol-induced apoptosis. Cell Growth Differ 1994;5:1041-50.

(233) Herbst RS, Khuri FR. Mode of action of docetaxel - a basis for combination with novel anticancer agents. Cancer Treat Rev 2003;29:407-15.

(234) Derry WB, Wilson L, Jordan MA. Substoichiometric binding of taxol suppresses microtubule dynamics. Biochemistry 1995;34:2203-11.

(235) Jordan MA, Wendell K, Gardiner S, Derry WB, Copp H, Wilson L. Mitotic block induced in HeLa cells by low concentrations of paclitaxel (Taxol) results in abnormal mitotic exit and apoptotic cell death. Cancer Res 1996;56:816-25.

(236) Hill BT, Whelan RD, Shellard SA, McClean S, Hosking LK. Differential cytotoxic effects of docetaxel in a range of mammalian tumor cell lines and certain drug resistant sublines in vitro. Invest New Drugs 1994;12:169-82.

(237) Alvarez M, Paull K, Monks A, Hose C, Lee JS, Weinstein J, et al. Generation of a drug resistance profile by quantitation of mdr-1/P-glycoprotein in the cell lines of the National Cancer Institute Anticancer Drug Screen. J Clin Invest 1995;95:2205-14.

(238) Allemani C, Matsuda T, Di C, V, Harewood R, Matz M, Niksic M, et al. Global surveillance of trends in cancer survival 2000-14 (CONCORD-3): analysis of individual records for 37513025 patients diagnosed with one of 18 cancers from 322 population-based registries in 71 countries. Lancet 2018;391:1023-75.

(239) Macleod KG, Serrels B, Carragher NO. Reverse Phase Protein Arrays and Drug Discovery. Methods Mol Biol 2017;1647:153-69.

(240) Lu Y, Ling S, Hegde AM, Byers LA, Coombes K, Mills GB, et al. Using reverse-phase protein arrays as pharmacodynamic assays for functional proteomics, biomarker discovery, and drug development in cancer. Semin Oncol 2016;43:476-83.

(241) Huang dW, Sherman BT, Lempicki RA. Systematic and integrative analysis of large gene lists using DAVID bioinformatics resources. Nat Protoc 2009;4:44-57.

(242) Lebok P, Huber J, Burandt EC, Lebeau A, Marx AH, Terracciano L, et al. Loss of membranous VEGFR1 expression is associated with an adverse phenotype and shortened survival in breast cancer. Mol Med Rep 2016;14:1443-50.

(243) Schmidt M, Voelker HU, Kapp M, Dietl J, Kammerer U. Expression of VEGFR-1 (Flt-1) in breast cancer is associated with VEGF expression and with node-negative tumour stage. Anticancer Res 2008;28:1719-24.

(244) Metsalu T, Vilo J. ClustVis: a web tool for visualizing clustering of multivariate data using Principal Component Analysis and heatmap. Nucleic Acids Res 2015;43:W566-W570.

(245) Oliveros JC. VENNY. An interactive tool for comparing lists with Venn Diagrams. 2017.

(246) Li J, Lu Y, Akbani R, Ju Z, Roebuck PL, Liu W, et al. TCPA: a resource for cancer functional proteomics data. Nat Methods 2013;10:1046-7.

(247) Yom CK, Noh DY, Kim WH, Kim HS. Clinical significance of high focal adhesion kinase gene copy number and overexpression in invasive breast cancer. Breast Cancer Res Treat 2011;128:647-55.

(248) Lahlou H, Sanguin-Gendreau V, Zuo D, Cardiff RD, McLean GW, Frame MC, et al. Mammary epithelial-specific disruption of the focal adhesion kinase blocks mammary tumor progression. Proc Natl Acad Sci U S A 2007;104:20302-7.

(249) Glenisson M, Vacher S, Callens C, Susini A, Cizeron-Clairac G, Le SR, et al. Identification of new candidate therapeutic target genes in triple-negative breast cancer. Genes Cancer 2012;3:63-70.

(250) Mitra SK, Hanson DA, Schlaepfer DD. Focal adhesion kinase: in command and control of cell motility. Nat Rev Mol Cell Biol 2005;6:56-68.

(251) Andisha NM, McMillan DC, Gujam FJA, Roseweir A, Edwards J. The relationship between phosphorylation status of focal adhesion kinases, molecular subtypes, tumour microenvironment and survival in patients with primary operable ductal breast cancer. Cell Signal 2019;60:91-9.

(252) Khramtsov AI, Khramtsova GF, Tretiakova M, Huo D, Olopade OI, Goss KH. Wnt/beta-catenin pathway activation is enriched in basal-like breast cancers and predicts poor outcome. Am J Pathol 2010;176:2911-20.

(253) Anastas JN, Moon RT. WNT signalling pathways as therapeutic targets in cancer. Nat Rev Cancer 2013;13:11-26.

(254) Luo RZ, Yuan ZY, Li M, Xi SY, Fu J, He J. Accumulation of p62 is associated with poor prognosis in patients with triple-negative breast cancer. Onco Targets Ther 2013;6:883-8.

(255) Yan XY, Zhang Y, Zhang JJ, Zhang LC, Liu YN, Wu Y, et al. p62/SQSTM1 as an oncotarget mediates cisplatin resistance through activating RIP1-NF-κB pathway in human ovarian cancer cells. Cancer Sci 2017;108:1405-13.

(256) Sudo T, Maruyama M, Osada H. p62 functions as a p38 MAP kinase regulator. Biochem Biophys Res Commun 2000;269:521-5.

(257) Christofk HR, Vander Heiden MG, Harris MH, Ramanathan A, Gerszten RE, Wei R, et al. The M2 splice isoform of pyruvate kinase is important for cancer metabolism and tumour growth. Nature 2008;452:230-3.

(258) Xiao H, Zhang L, Chen Y, Zhou C, Wang X, Wang D, et al. PKM2 Promotes Breast Cancer Progression by Regulating Epithelial Mesenchymal Transition. Anal Cell Pathol (Amst) 2020;2020:8396023.

(259) Seve P, Dumontet C. Is class III beta-tubulin a predictive factor in patients receiving tubulin-binding agents? Lancet Oncol 2008;9:168-75.

(260) Pierobon M, Wulfkuhle J, Liotta L, Petricoin E. Application of molecular technologies for phosphoproteomic analysis of clinical samples. Oncogene 2015;34:805-14.

(261) Forbes SA, Bindal N, Bamford S, Cole C, Kok CY, Beare D, et al. COSMIC: mining complete cancer genomes in the Catalogue of Somatic Mutations in Cancer. Nucleic Acids Res 2011;39:D945-D950.

(262) De RW, Claes B, Bernasconi D, De SJ, Biesmans B, Fountzilas G, et al. Effects of KRAS, BRAF, NRAS, and PIK3CA mutations on the efficacy of cetuximab plus chemotherapy in chemotherapy-refractory metastatic colorectal cancer: a retrospective consortium analysis. Lancet Oncol 2010;11:753-62.

(263) Morabito A, Piccirillo MC, Falasconi F, De FG, Del GA, Bryce J, et al. Vandetanib (ZD6474), a dual inhibitor of vascular endothelial growth factor receptor (VEGFR) and epidermal growth factor receptor (EGFR) tyrosine kinases: current status and future directions. Oncologist 2009;14:378-90.

(264) Juric D, Castel P, Griffith M, Griffith OL, Won HH, Ellis H, et al. Convergent loss of PTEN leads to clinical resistance to a PI(3)Ka inhibitor. Nature 2015;518:240-4.

(265) Yin C, Zhu B, Zhang T, Liu T, Chen S, Liu Y, et al. Pharmacological Targeting of STK19 Inhibits Oncogenic NRAS-Driven Melanomagenesis. Cell 2019;176:1113-27.

(266) Bray SJ. Notch signalling: a simple pathway becomes complex. Nat Rev Mol Cell Biol 2006;7:678-89.

(267) Radtke F, Raj K. The role of Notch in tumorigenesis: oncogene or tumour suppressor? Nat Rev Cancer 2003;3:756-67.

(268) Zhou L, Wang D, Sheng D, Xu J, Chen W, Qin Y, et al. NOTCH4 maintains quiescent mesenchymal-like breast cancer stem cells via transcriptionally activating SLUG and GAS1 in triple-negative breast cancer. Theranostics 2020;10:2405-21.

(269) Edmunds JW, Mahadevan LC, Clayton AL. Dynamic histone H3 methylation during gene induction: HYPB/Setd2 mediates all H3K36 trimethylation. EMBO J 2008;27:406-20.

(270) Strahl BD, Grant PA, Briggs SD, Sun ZW, Bone JR, Caldwell JA, et al. Set2 is a nucleosomal histone H3-selective methyltransferase that mediates transcriptional repression. Mol Cell Biol 2002;22:1298-306.

(271) Kanu N, Gronroos E, Martinez P, Burrell RA, Yi G, X, Bartkova J, et al. SETD2 loss-of-function promotes renal cancer branched evolution through replication stress and impaired DNA repair. Oncogene 2015;34:5699-708.

(272) Vincent AJ, Ren S, Harris LG, Devine DJ, Samant RS, Fodstad O, et al. Cytoplasmic translocation of p21 mediates NUPR1-induced chemoresistance: NUPR1 and p21 in chemoresistance. FEBS Lett 2012;586:3429-34.

(273) Murphy A, Costa M. Nuclear protein 1 imparts oncogenic potential and chemotherapeutic resistance in cancer. Cancer Lett 2020;494:132-41.

(274) Wang L, Sun J, Yin Y, Sun Y, Ma J, Zhou R, et al. Transcriptional coregualtor NUPR1 maintains tamoxifen resistance in breast cancer cells. Cell Death Dis 2021;12:149.

(275) Mu Y, Yan X, Li D, Zhao D, Wang L, Wang X, et al. NUPR1 maintains autolysosomal efflux by activating SNAP25 transcription in cancer cells. Autophagy 2018;14:654-70.

(276) Wang L, Sun J, Yin Y, Sun Y, Ma J, Zhou R, et al. Transcriptional coregualtor NUPR1 maintains tamoxifen resistance in breast cancer cells. Cell Death Dis 2021;12:149.

(277) Jung JG, Shih IM, Park JT, Gerry E, Kim TH, Ayhan A, et al. Ovarian Cancer Chemoresistance Relies on the Stem Cell Reprogramming Factor PBX1. Cancer Res 2016;76:6351-61.

(278) Yu D, Ma Y, Feng C, Ma Z, Guo J, Chen H, et al. PBX1 Increases the Radiosensitivity of Oesophageal Squamous Cancer by Targeting of STAT3. Pathol Oncol Res 2020;26:2161-8.

(279) Magnani L, Ballantyne EB, Zhang X, Lupien M. PBX1 genomic pioneer function drives ERa signaling underlying progression in breast cancer. PLoS Genet 2011;7:e1002368.

(280) Ao X, Ding W, Ge H, Zhang Y, Ding D, Liu Y. PBX1 is a valuable prognostic biomarker for patients with breast cancer. Exp Ther Med 2020;20:385-94.

(281) Quintas-Cardama A, Verstovsek S. Molecular pathways: Jak/STAT pathway: mutations, inhibitors, and resistance. Clin Cancer Res 2013;19:1933-40.

(282) Hao Y, Baker D, Ten DP. TGF-b-Mediated Epithelial-Mesenchymal Transition and Cancer Metastasis. Int J Mol Sci 2019;20.

(283) Wu J, Li S, Jia W, Su F. Response and prognosis of taxanes and anthracyclines neoadjuvant chemotherapy in patients with triple-negative breast cancer. J Cancer Res Clin Oncol 2011;137:1505-10.

(284) NCCN. NCCN Clinical Practice Guidelines in Oncology: Breast Cancer,version 2; http://www.nccn.com/. 2011.

(285) Piccart M. The role of taxanes in the adjuvant treatment of early stage breast cancer. Breast Cancer Res Treat 2003;79 Suppl 1:S25-S34.

(286) Ferguson FM, Gray NS. Kinase inhibitors: the road ahead. Nat Rev Drug Discov 2018;17:353-77.

(287) Vivanco I, Sawyers CL. The phosphatidylinositol 3-Kinase AKT pathway in human cancer. Nat Rev Cancer 2002;2:489-501.

(288) Liu JJ, Ho JY, Lee HW, Baik MW, Kim O, Choi YJ, et al. Inhibition of Phosphatidylinositol 3-kinase (PI3K) Signaling Synergistically Potentiates Antitumor Efficacy of Paclitaxel and Overcomes Paclitaxel-Mediated Resistance in Cervical Cancer. Int J Mol Sci 2019;20.

(289) Comprehensive molecular portraits of human breast tumours. Nature 2012;490:61-70.

(290) Woo RA, Poon RY. Cyclin-dependent kinases and S phase control in mammalian cells. Cell Cycle 2003;2:316-24.

(291) Loyer P, Trembley JH, Katona R, Kidd VJ, Lahti JM. Role of CDK/cyclin complexes in transcription and RNA splicing. Cell Signal 2005;17:1033-51.

(292) Zhong L, Li Y, Xiong L, Wang W, Wu M, Yuan T, et al. Small molecules in targeted cancer therapy: advances, challenges, and future perspectives. Signal Transduct Target Ther 2021;6:201.

(293) Bayat MR, Homayouni TS, Baluch N, Morgatskaya E, Kumar S, Das B, et al. Combination therapy in combating cancer. Oncotarget 2017;8:38022-43.

(294) Engelman JA, Luo J, Cantley LC. The evolution of phosphatidylinositol 3-kinases as regulators of growth and metabolism. Nat Rev Genet 2006;7:606-19.

(295) Dornan GL, Burke JE. Molecular Mechanisms of Human Disease Mediated by Oncogenic and Primary Immunodeficiency Mutations in Class IA Phosphoinositide 3-Kinases. Front Immunol 2018;9:575.

(296) Clarke PA, Workman P. Phosphatidylinositide-3-kinase inhibitors: addressing questions of isoform selectivity and pharmacodynamic/predictive biomarkers in early clinical trials. J Clin Oncol 2012;30:331-3.

(297) Fritsch C, Huang A, Chatenay-Rivauday C, Schnell C, Reddy A, Liu M, et al. Characterization of the novel and specific PI3Kα inhibitor NVP-BYL719 and development of the patient stratification strategy for clinical trials. Mol Cancer Ther 2014;13:1117-29.

(298) Sharma P, Abramson VG, O'Dea A, Nye L, Mayer I, Pathak HB, et al. Clinical and Biomarker Results from Phase I/II Study of PI3K Inhibitor Alpelisib plus Nab-paclitaxel in HER2-Negative Metastatic Breast Cancer. Clin Cancer Res 2021;27:3896-904.

(299) Malumbres M, Carnero A. Cell cycle deregulation: a common motif in cancer. Prog Cell Cycle Res 2003;5:5-18.

(300) Finn RS, Aleshin A, Slamon DJ. Targeting the cyclin-dependent kinases (CDK) 4/6 in estrogen receptor-positive breast cancers. Breast Cancer Res 2016;18:17.

(301) Parry D, Guzi T, Shanahan F, Davis N, Prabhavalkar D, Wiswell D, et al. Dinaciclib (SCH 727965), a novel and potent cyclin-dependent kinase inhibitor. Mol Cancer Ther 2010;9:2344-53.

(302) De Azevedo WFJ, Mueller-Dieckmann HJ, Schulze-Gahmen U, Worland PJ, Sausville E, Kim SH. Structural basis for specificity and potency of a flavonoid inhibitor of human CDK2, a cell cycle kinase. Proc Natl Acad Sci U S A 1996;93:2735-40.

(303) Patel V, Senderowicz AM, Pinto D, Jr., Igishi T, Raffeld M, Quintanilla-Martinez L, et al. Flavopiridol, a novel cyclin-dependent kinase inhibitor, suppresses the growth of head and neck squamous cell carcinomas by inducing apoptosis. J Clin Invest 1998;102:1674-81.

(304) Zheng Y, Yang J, Qian J, Zhang L, Lu Y, Li H, et al. Novel phosphatidylinositol 3-kinase inhibitor NVP-BKM120 induces apoptosis in myeloma cells and shows synergistic anti-myeloma activity with dexamethasone. J Mol Med (Berl) 2012;90:695-706.

(305) Xing J, Yang J, Gu Y, Yi J. Research update on the anticancer effects of buparlisib. Oncol Lett 2021;21:266.

(306) Bader AG, Kang S, Vogt PK. Cancer-specific mutations in PIK3CA are oncogenic in vivo. Proc Natl Acad Sci U S A 2006;103:1475-9.

(307) Zhao JJ, Liu Z, Wang L, Shin E, Loda MF, Roberts TM. The oncogenic properties of mutant p110alpha and p110beta phosphatidylinositol 3-kinases in human mammary epithelial cells. Proc Natl Acad Sci U S A 2005;102:18443-8.

(308) Mayer IA, Abramson VG, Formisano L, Balko JM, Estrada MV, Sanders ME, et al. A Phase Ib Study of Alpelisib (BYL719), a PI3Ka-Specific Inhibitor, with Letrozole in ER+/. Clin Cancer Res 2017;23:26-34.

(309) Elkabets M, Vora S, Juric D, Morse N, Mino-Kenudson M, Muranen T, et al. mTORC1 inhibition is required for sensitivity to PI3K p110a inhibitors in PIK3CA-mutant breast cancer. Sci Transl Med 2013;5:196ra99.

(310) Garrido-Castro AC, Saura C, Barroso-Sousa R, Guo H, Ciruelos E, Bermejo B, et al. Phase 2 study of buparlisib (BKM120), a pan-class I PI3K inhibitor, in patients with metastatic triple-negative breast cancer. Breast Cancer Res 2020;22:120.

(311) Di LA, Johnston S, Lee KS, Ciruelos E, Lonning PE, Janni W, et al. Buparlisib plus fulvestrant in postmenopausal women with hormone-receptor-positive, HER2-negative, advanced breast cancer progressing on or after mTOR inhibition (BELLE-3): a randomised, double-blind, placebo-controlled, phase 3 trial. Lancet Oncol 2018;19:87-100.

(312) Nanni P, Nicoletti G, Palladini A, Croci S, Murgo A, Ianzano ML, et al. Multiorgan metastasis of human HER-2+ breast cancer in Rag2-/-;Il2rg-/- mice and treatment with PI3K inhibitor. PLoS One 2012;7:e39626.

(313) Rodon J, Brana I, Siu LL, De Jonge MJ, Homji N, Mills D, et al. Phase I dose-escalation and -expansion study of buparlisib (BKM120), an oral pan-Class I PI3K inhibitor, in patients with advanced solid tumors. Invest New Drugs 2014;32:670-81.

(314) Turner S, Chia S, Kanakamedala H, Hsu WC, Park J, Chandiwana D, et al. Effectiveness of Alpelisib + Fulvestrant Compared with Real-World Standard Treatment Among Patients with HR+, HER2-, PIK3CA-Mutated Breast Cancer. Oncologist 2021;26:e1133-e1142.

(315) Rajput S, Khera N, Guo Z, Hoog J, Li S, Ma CX. Inhibition of cyclin dependent kinase 9 by dinaciclib suppresses cyclin B1 expression and tumor growth in triple negative breast cancer. Oncotarget 2016;7:56864-75.

(316) Nigg EA. Mitotic kinases as regulators of cell division and its checkpoints. Nat Rev Mol Cell Biol 2001;2:21-32.

(317) Mita MM, Joy AA, Mita A, Sankhala K, Jou YM, Zhang D, et al. Randomized phase II trial of the cyclin-dependent kinase inhibitor dinaciclib (MK-7965) versus capecitabine in patients with advanced breast cancer. Clin Breast Cancer 2014;14:169-76.

(318) Nemunaitis JJ, Small KA, Kirschmeier P, Zhang D, Zhu Y, Jou YM, et al. A first-in-human, phase 1, dose-escalation study of dinaciclib, a novel cyclin-dependent kinase inhibitor, administered weekly in subjects with advanced malignancies. J Transl Med 2013;11:259.

(319) Mitri Z, Karakas C, Wei C, Briones B, Simmons H, Ibrahim N, et al. A phase 1 study with dose expansion of the CDK inhibitor dinaciclib (SCH 727965) in combination with epirubicin in patients with metastatic triple negative breast cancer. Invest New Drugs 2015;33:890-4.

(320) Paridaens R, Biganzoli L, Bruning P, Klijn JG, Gamucci T, Houston S, et al. Paclitaxel versus doxorubicin as first-line single-agent chemotherapy for metastatic breast cancer: a European Organization for Research and Treatment of Cancer Randomized Study with cross-over. J Clin Oncol 2000;18:724-33.

(321) Bonnefoi H, Piccart M, Bogaerts J, Mauriac L, Fumoleau P, Brain E, et al. TP53 status for prediction of sensitivity to taxane versus non-taxane neoadjuvant chemotherapy in breast cancer (EORTC 10994/BIG 1-00): a randomised phase 3 trial. Lancet Oncol 2011;12:527-39.

(322) Nemcova-Furstova V, Kopperova D, Balusikova K, Ehrlichova M, Brynychova V, Vaclavikova R, et al. Characterization of acquired paclitaxel resistance of breast cancer cells and involvement of ABC transporters. Toxicol Appl Pharmacol 2016;310:215-28.

(323) Kars MD, Iseri OD, Gunduz U, Ural AU, Arpaci F, Molnar J. Development of rational in vitro models for drug resistance in breast cancer and modulation of MDR by selected compounds. Anticancer Res 2006;26:4559-68.

(324) Villeneuve DJ, Hembruff SL, Veitch Z, Cecchetto M, Dew WA, Parissenti AM. cDNA microarray analysis of isogenic paclitaxel- and doxorubicin-resistant breast tumor cell lines reveals distinct drug-specific genetic signatures of resistance. Breast Cancer Res Treat 2006;96:17-39.

(325) Pavlikova N, Bartonova I, Dincakova L, Halada P, Kovar J. Differentially expressed proteins in human breast cancer cells sensitive and resistant to paclitaxel. Int J Oncol 2014;45:822-30.

(326) Hegewisch-Becker S, Staib F, Loning T, Pichlmeier U, Kroger N, Reymann A, et al. No evidence of significant activity of the multidrug resistance gene product in primary human breast cancer. Ann Oncol 1998;9:85-93.

(327) Faneyte IF, Kristel PM, van de Vijver MJ. Determining MDR1/P-glycoprotein expression in breast cancer. Int J Cancer 2001;93:114-22.

(328) Verret B, Cortes J, Bachelot T, Andre F, Arnedos M. Efficacy of PI3K inhibitors in advanced breast cancer. Ann Oncol 2019;30:x12-x20.

(329) Guerrero-Zotano A, Mayer IA, Arteaga CL. PI3K/AKT/mTOR: role in breast cancer progression, drug resistance, and treatment. Cancer Metastasis Rev 2016;35:515-24.

(330) Berns K, Horlings HM, Hennessy BT, Madiredjo M, Hijmans EM, Beelen K, et al. A functional genetic approach identifies the PI3K pathway as a major determinant of trastuzumab resistance in breast cancer. Cancer Cell 2007;12:395-402.

(331) Comprehensive molecular portraits of human breast tumours. Nature 2012;490:61-70.

(332) Stephens PJ, Tarpey PS, Davies H, Van LP, Greenman C, Wedge DC, et al. The landscape of cancer genes and mutational processes in breast cancer. Nature 2012;486:400-4.

(333) Ostman A, Augsten M. Cancer-associated fibroblasts and tumor growth--bystanders turning into key players. Curr Opin Genet Dev 2009;19:67-73.

(334) Wiseman BS, Werb Z. Stromal effects on mammary gland development and breast cancer. Science 2002;296:1046-9.

(335) Tentler JJ, Tan AC, Weekes CD, Jimeno A, Leong S, Pitts TM, et al. Patient-derived tumour xenografts as models for oncology drug development. Nat Rev Clin Oncol 2012;9:338-50.